Crustal Deformation of the Yellowstone Volcanic Field From Precise Measurements of Temporal Gravity Changes and Supplementary Leveling and GPS Data

Dr. sc. techn. Felix Arnet

Zürich, 1996

Diss ETH No. 11388

Crustal Deformation of the Yellowstone Volcanic Field From Precise Measurements of Temporal Gravity Changes and Supplementary Leveling and GPS Data

A dissertation submitted to the
SWISS FEDERAL INSTITUTE OF TECHNOLOGY ZURICH
for the degree of
Doctor of Technical Sciences

presented by
Felix Karl Arnet
Dipl. Verm. Ing. ETH
born November 28, 1965
from Kriens LU

accepted on the recommendation of
Prof. Dr. H.-G. Kahle, examiner
Prof. Dr. E.E. Klingelé, co-examiner
Prof. Dr. R.B.Smith, co-examiner

Zurich 1996

Institut für Geodäsie und Photogrammetrie
Eidg. Technische Hochschule Zürich
ETH Hönggerberg
8093 Zürich

ISBN 3-906513-79-3

Table of Contents

Abstract

The Yellowstone caldera in north-west of Wyoming, U.S.A, shows high rates of height and gravity changes. The height changes were monitored by precise leveling, which was first conducted in 1923 and re-measured every few years since 1975. Gravity measurements were first carried out in 1977 and repeated almost annually since 1983. Both measuring types were concentrated on a line crossing the northern part of the caldera. A GPS network was installed additionally in 1987. It covers the whole national park region and was re-measured every second year. The measurements showed, that the Caldera experienced an uplift of up to 0.8 m from 1923 to 1984. Since 1984, the trend reversed and the heights decreased up to 14 cm. The gravity values along the same line changed up to -60 ± 12 µgal (1 µgal = 10^{-8} m s^{-2}) from 1977 to 1986. Until 1993, the gravity increased again up to $+60 \pm 12$ µgal. The GPS results showed within the bounds of accuracy the same height changes as the precision leveling. In addition, horizontal displacements of up to 3 cm towards the middle of the caldera were observed. Furthermore, it showed that the area of downshift expands partly considerably over the borders of the Yellowstone caldera. The factor between the height and gravity changes is a value that can be used to detect mass changes at depth. This value varies strongly from year to year. Over longer time spans, it converges towards the free-air gravity gradient of -0.3 mgal/m, where no mass changes occur. Finite element modeling shows, that the earth's crust in the Yellowstone National Park does not behave like an ideal elastic material. The horizontal displacements are significantly smaller than expected from the height changes. This is explained by the geology heavily disturbed by a lot of fault zones.

Zusammenfassung

Die Yellowstone Caldera im Nordwesten von Wyoming, U.S.A., wies hohe Raten von Höhen- und Schwereänderungen auf. Höhenänderungen wurden mittels Präzisionsnivellement 1923 und alle paar Jahre seit 1975 festgestellt. Schweremessungen wurden erstmals 1977 durchgeführt und ab 1983 mit wenigen Ausnahmen jedes Jahr. Beide Messmethoden wurden dabei vor allem auf einer Linie, die im nördlichen Teil die Caldera durchquert, konzentriert. 1987 wurde zusätzlich ein GPS-Netz eingerichtet, das sich über den ganzen Yellowstone National Park erstreckt und alle zwei Jahre nachgemessen wurde. Die Messungen ergaben, dass sich die Caldera entlang der nördlichen Linie von 1923 bis 1984 um bis zu 0.8 m hob. Seither senkte sie sich wieder, bis 1993 um bis 14 cm. Die Schwerewerte entlang derselben Linie änderten sich von 1977 bis 1986 um bis zu -60 ± 12 µgal (1 µgal = 10^{-8} m s^{-2}). Bis 1993 erhöhte sich die Schwere wieder um bis zu $+65 \pm 12$ µgal. Die GPS-Resultate zeigten innerhalb der Genauigkeit die gleichen Höhenänderung wie das Präzisionsnivellement. Zusätzlich wurden horizontale Verschiebungen um bis zu 3 cm in Richtung Calderamitte beobachtet und festgestellt, dass sich das Senkungsgebiet zum Teil deutlich über die Yellowstone Caldera ausbreitete. Der Faktor zwischen Höhen- und Schwereänderungen ist ein Mass für die Grösse der Massenänderungen im Untergrund. Dieser variiert stark zwischen den einzelnen Jahren. Über längere Zeiträume nähert er sich dem Freiluftschweregradienten von -0.3 mgal/m an, in denen keine Massenänderungen auftreten. Finite Element Modellierungen zeigten, dass sich die Erdkruste im Yellowstone National Park nicht wie ideales elastisches Material verhielt. Die Horizontalverschiebungen waren deutlich kleiner als von den Höhenänderungen her erwartet wurde. Dies wird auf die stark gestörte Geologie mit vielen Verwerfungen zurückgeführt.

1. Introduction

The Yellowstone caldera is located in the central part of the Yellowstone National Park in north-western Wyoming, USA (fig.1.1 and 1.2). It is an active silicic volcanic system that exhibits very high heat flow (exceeding 1500 mWm^{-2}), widespread earthquake activity and high rates of modern crustal deformation (Smith and Brail, 1994; Christiansen, 1984). The Yellowstone caldera is thought to be the product of a mantle heat source, i.e. a plume, hotspot or a zone of anomalous mantle upwelling. The silicic volcanic system started in the Snake River Plain in Idaho and moves with a velocity of about 4.5 cm/a towards north-east. The signs of the latest three eruptions of this hot spot are still visible at Yellowstone. They included giant, catastrophic explosions 2 Ma, 1.2 Ma and 0.6 ma ago and belong to the largest natural events, which have happened on the earth (the volume of eruption 0.6 ma ago was about 1000 km^3 (Christiansen, 1984).
From 1923 to 1984, the caldera experienced an uplift of up to 0.8 m, measured by precise leveling, followed by a subsidence until 1993 of up to 14 cm. It was expected, that, parallel to the height changes, also measurable gravity changes occurred in the Yellowstone Caldera. The two changes are primarily related by the free-air gravity gradient (-0.3086 mgal/m, 1 mgal = 10^{-5} ms^{-2}). Deviations from this relationship are due to mass movements. Several other scientific programs emphasize the relation between height and gravity changes : in volcanoes (Hawaiian volcanoes (Johnson, 1992, 1995), Poas and other central American volcanoes (Rymer and Brown, 1987), Italian volcanic fields (Berrino et al., 1992, 1993)), this approach can give information about mass intrusions. Other precise gravity networks were installed in seismic active zones and in geothermal fields in Italy (Marson et al (1981, 1988)). Other precise gravity networks were installed near fault zones in southern California (Whitcomb et al., 1980) to examine earthquake related tectonic problems. Furthermore, the relation between height and gravity changes can provide the flexural rigidity of the earth's lithosphere in areas of post-glacial rebound (Eastern Canada (Lambert) and in Fennoscandinavia (Kiviniemi, 1977)).
In the Yellowstone area, the main goal in measuring gravity and height changes simultaneously is to obtain information about the deformation associated with the Yellowstone volcanic system. The gravity changes were determined across a precise gravity network with 200 stations. It was installed by the University of Utah in 1977 (Evoy, 1978), coincident with the leveling network and covers the entire Yellowstone Plateau. The gravity network was re-observed in 1983, 1987, 1991, and 1993. Additional re-observations emphasized two caldera-crossing lines in 1979, 1986, 1988, 1989, and 1990. Height changes were determined by precise leveling with campaigns covering the

whole Yellowstone National Park in 1923, 1975 to 1977, and 1987. Furthermore, one caldera crossing line has been measured annually from 1986 to 1993 (Meertens et al, 1994). In 1987, a GPS network of about 40 points was established along the leveling lines as well as in the backcountry areas of the Yellowstone Plateau. Repetitive measurements of this network were carried out in 1989, 1991 and 1993. In addition to height changes, GPS measurements also provide information on horizontal displacements.

Using a combination of the gravity and height measurements, it is possible to estimate mass movements of the crust when they are sufficiently large. Additional information from the seismic velocity distribution of the Yellowstone region and density-velocity relationships allow an estimate of the density distribution under the Yellowstone caldera. This outline shows, that modeling crustal deformations involve high precision techniques of geodesy as well as geophysics and therefore it is one of the major bridges between these two disciplines.

In some areas like GPS, leveling and seismic velocity, the results of other scientific projects can be used directly for this thesis. In other methods, like gravity, which is the main task of this thesis, a great deal of research has been done to optimize the results of the measurements. The calibration of the systematic errors of the gravity meters has made it necessary to develop new techniques. Another important goal was to develop a theory and to construct a model to test for mass movements due to suspected magmatic and hydrothermal fluids associated with Yellowstone's active silicic volcanism - though, the gravity changes in the Yellowstone caldera during the time with precision gravity measurements may not be large enough to obtain significant results for mass movements underneath the caldera.

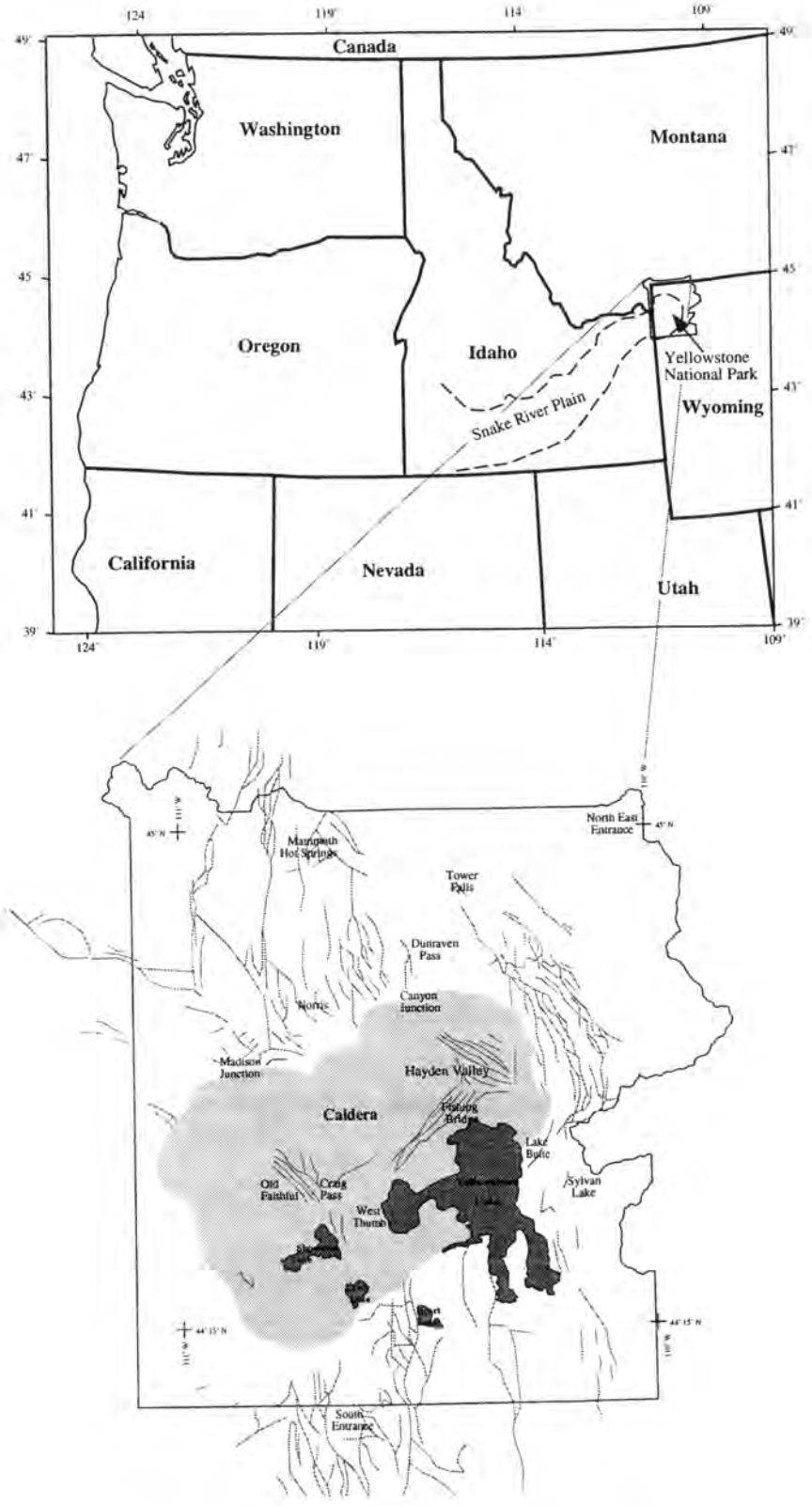

Fig 1.1 : Top : Map of northwestern USA, showing the location of the Yellowstone National Park. The Yellowstone hot spot moved along the Snake River Plain during the last 15 Ma. Bottom : locale map of the Yellowstone National Park showing selected geographic features and faults.

2. Gravity

The Yellowstone precision gravity network was established coincidentally with the precision leveling net and first measured in 1977 (Evoy, 1978). Originally, It was planned to replace the time-consuming and expensive precise leveling by gravity measurements, assuming that the height and gravity changes are related by the free-air gradient. In 1984, about 40 stations in backcountry area with access by boat and helicopter were added with a total of about 200 stations now in the network. Additional measurements of the entire network have been carried out in 1983, 1987 and 1991. Further, the stations in the vicinity of the caldera were measured in 1986 and 1989, the backcountry stations in 1989 and the line from Canyon Junction to Sylvan Lake in 1979 and yearly from 1986 to 1991 (see fig. 1.1).
It turned out that the gravity measurements are not precise enough and that there are too many blunders in the results to calculate height changes at the same accuracy as first order leveling. Furthermore, the assumption that the height and gravity changes are related by the free-air gradient is not valid. Mass movements can also effect the relation of the height and gravity changes.
Gravity measurements used in the Yellowstone Gravity studies were carried out using up to three LaCoste&Romberg gravimeters, models D and G, simultaneously. The data were corrected for earth tides and drift using ladder looping methods, followed by network distributions of error by a least-squares method. In order to tie the data from different gravimeters in different field campaigns, the mean error for each instrument was estimated by a least-squares adjustment producing. They were about ±10 mgal.
From 1977 to 1983, the overall gravity field decreased over the whole caldera by up to -70 µgal. Since 1986, this trend dramatically changed and is increasing again.

2.1 Gravity Measurement Methods

Gravity measurements are influenced by time-dependent variations of the instruments in the measuring device, called drift. Due to uncontrollable events, also tares ("jumps") or first order offsets can occur in the drift curves. Therefore, the sequence of the measured points should be chosen in a manner to have a measure of these non-gravitational influences. A basic rule is to measure at a base station at least every four hours, producing a loop to other stations. Using this method, not too many measurements are lost if a tare occurs. This rule becomes less important if several instruments are used at the same time and if multiple measurements at a point are carried out in different loops. In the Yellowstone campaigns several different loop methods were applied :

Simple Loops (fig. 2.1):
In this method, gravity stations are occupied along a line, beginning with a base station, that is re-measured at least every four hours.

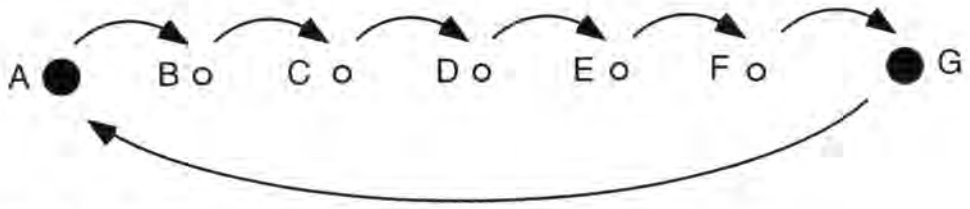

Fig. 2.1 : Simple loop

Ladder Loops (fig 2.2):
As in simple loops, in ladder loops the stations are measured along a line with a return to a base station every four hours. In addition, on the return leg to the base station, every station is reoccupied. This means, that the turning point of a loop is reached after a maximum of two hours.
Ladder loops are especially advisable, if the stations are distributed along a profile and every station is occupied twice (e.g. for control reasons). In this case it is faster than performing a single loop twice, where you pass every points four times, but measuring it just twice.

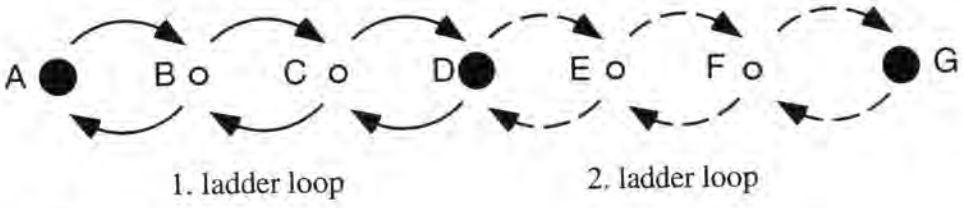

Fig. 2.2 : Ladder loop

Strengthened Ladder Loops (fig. 2.3):
If stations along a line are occupied more than twice (e.g. to increase the accuracy), it is advisable for statistical reasons not to measure the same combination of points in the same loop twice. Otherwise, if e.g. in fig. 2.3 loop 1 and loop 2 are each measured twice, the stations C and E are never measured within one loop, though they lie quite close together. It is better to add two ladder loops (3 and 4), where just every second station is measured, but a loop extending to more distant stations.

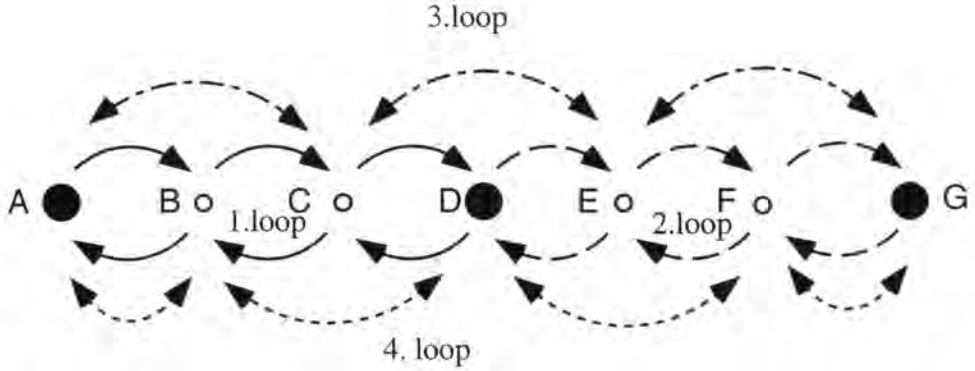

Fig. 2.3 : Strengthened ladder loop

2.2 Data Processing

Precision gravity data for the Yellowstone National Park gravity network for the period 1977 to 1993 was processed at the University of Utah over a ten years time span and the data were available in many different formats by Evoy(1977), Jackson(1983) and Hollis(1987). To simplify the data processing the entire data set was reformatted and put into a common form (see appendix B).

To reduce the field measurements for earth tides and instrument spring effects, the program 'dproduce' from the USGS was implemented in the program 'gravity' that allows computation of the gravity values of the stations by the least squares method (see Appendix B).

Basically, the program 'gravity' is an adjustment program by the least-squares method for gravity data. The observation equation for a measurement is :

(2.1) $$r_{sta} = r'_{sta} + v = g_{sta} + c_{0i} + c_{1i} \cdot t$$

with

r_{sta} : reading value at a station

r'_{sta} : reading at a station reduced by the gravity meter constants and earth tide (gravity observations).

v : residuals

g_{sta} : true gravity at the station

c_{0i} : offset between instrument i and base gravity value of the network

c_{1i} : linear drift constant of instrument i

t : time

The introduction of a quadratic form for the gravimeter drift, such as:

$$r'_{sta} + v = g_{sta} + c_{0i} + \underbrace{c_{1i} \cdot t + c_{2i} \cdot t^2}_{\text{gravimeter drift}}$$

was not used because it showed strong correlation (0.95 up to 1.00) between the linear term ($= c_1$) and the constant of the quadratic term ($= c_2$).

Taking all measurements together leads to a linear equation system for the unknowns **x** (the functional model):

(2.2) $\qquad \mathbf{r} + \mathbf{v} = A\mathbf{x} \qquad <=> \qquad \mathbf{v} = A\mathbf{x} - \mathbf{r}$

with

- **x** : vector of the unknowns (gravity, drift constants)
- A : normal equation matrix
- u : number of unknowns
- n : number of measurements

The dimension of x is u. The dimension of r and v is n, and the dimensions of A is n·u. For a statistical model it was assumed that all the measurements have a Gaussian distribution and that the measurements were uncorrelated. This assumption, however, is not totally correct because at least one of the randomly distributed errors has no Gaussian distribution. That is the error due to incorrect leveling of the instrument. It is more correct to assume that the angle between the leveled position and the true position v_a has some Gaussian distribution $p(v_a) = c\, e^{-dv_a^2}$ (if the instrument is adjusted correctly). But the gravity error v_g due to leveling error is a function of the cosine of the angle v_a , and for small angles it can be written as $v_g = c' v_a^2$ ($c' \approx 5$ µgal / pars^2). Therefore the distribution of this error is :

$$p(v_g) = \begin{cases} = 0 & , \text{if } v_g < 0 \\ = c\, e^{-\frac{d}{c'}} & , \text{if } v_g = 0 \\ = 2\, c\, e^{-\frac{d}{c'} v_g} & , \text{if } v_g > 0 \end{cases}$$

Although this seems to be one of the major possible errors, it is a special distribution that was not taken into account, because the adjustment of the data would be very difficult if not even impossible. Furthermore, that it is obvious from the distribution of the upper error, that all readings have an expected value slightly under the expected one without the error due to the leveling. However, because we measure only gravity differences, this offset cancels.
So the correlation matrix, Q_{rr}, and its inverse, the weight matrix P_{rr}, are :

(2.3) $$q_{r_i r_i} = \sigma^2_{ins} \qquad \text{or} \qquad p_{r_i r_i} = \frac{1}{\sigma^2_{ins}}$$

where σ_{ins} is the mean error of the instrument for the i^{th} measurement.
Because there are more measurements than unknowns, (2.2) represents an over-determined problem typically $n \approx 4u$ for every year of precision gravity observation. It can be solved after (A.3) of appendix A.
It seems very difficult to take the correct value for the mean error of the gravimeters. Therefore, it makes sense to make also an estimation for them a posteriori .

(2.4) $$\hat{\sigma}_{ins} = \sigma_{ins} \sqrt{\frac{\mathbf{v}_{ins}{}^T P \mathbf{v}_{ins}}{\sum_{ins} red(ins)}}$$

By introducing $\hat{\sigma}_{ins}$ (a posteriori) instead of σ_{ins} (a priori) in a new statistical model, the expected values of $\sqrt{\frac{v_s{}^T P v_s}{\sum_s red(s)}}$ will differ slightly from a t-distribution, but since there are much more observations than instruments, this difference should be negligible.
It is not necessary to know an approximate solution, because the observations are all linear equations. However, changing the mean error of an instrument to its a posteriori value will require several iterations (all without approximate solution).

2.2.1 Factors for Gravimeters

A calibration table is provided by the manufacturer with each gravity meter by the LaCoste&Romberg company. It shows the factor between the instrument units (i.u.) and the true relative gravity values. However, it has turned out, that these factors can be easily

$\pm 5 \cdot 10^{-4}$ different from the given value. To check whether there was an incorrect factor of a gravity meter, free factors for each gravimeter were calculated as :

(2.5) $$r'_{sta} + v = m_i\, g_{sta} + c_{0i} + c_{1i} \cdot t =$$
$$(m_0+dm)(g_0+dg) + (c_{00} + dc_0) + (c_{10} + dc_1)t = f(m,g,c_0,c_1)$$

Because this is no longer a linear problem, it was linearized by a Taylor series expansion about the origin :

(2.6) $$r'_{sta} + v = m_0 g_0 + c_{00} + c_{10}t + \frac{\partial f}{\partial m} dm + \frac{\partial f}{\partial g} dg + \frac{\partial f}{\partial c_0} dc_0 + \frac{\partial f}{\partial c_1} dc_1 + \text{t.o.h.o}$$

(t.o.h.o = terms of higher order, that are neglected)
After neglecting t.o.h.o (2.6) becomes

(2.7) $$v = g_0\, dm + m_0\, dg + dc_0 + dc_1 - (r - f_0)$$

This gives the functional model and the normal equation system. The statistical model stays the same as above.

2.2.2 Circular Error of the Gravimeters

The LaCoste & Romberg G gravimeters have circular errors depending on the position of the measuring screw. These errors are due to slight mechanical imperfections of the measuring screw and/or gear train. The model G meter has an expected circular error of less then 40 µgal (Valliant, 1991) with the period of the measuring screw, of about 72 mgal. Results of screw calibration of the instruments G461 and G264 showed that there can be three or even four maxima within one rotation.

2.2.2.1 Calibration with Two G-meters

The easiest possibility to calibrate the circular errors of an instrument is to have an absolute gravity calibration line with relatively small gravity differences between two points (3 to 5 mgal). Otherwise, the gaps between the data points will be too large to determine the circular error in a manner that can help to improve the measurements.
The results of the 1993 Yellowstone precise gravity campaign revealed significant offsets of the station values between the two instruments used, G264 and G461 (see fig. 3.5).

The mean internal errors (without the systematic circular error) of one measurement of the meters are about 8 µgal for G264 and 10.5 µgal for G461 a posteriori. So the accuracy of a measurement is less than the expected circular error. Because the signals of the gravity changes are also in the region of some 10's of µgal, it is desirable to know the systematic offsets. However, the problem is to calculate the systematic errors.
During one field campaign, the drift of an instrument, about 1 mgal, was small compared to the period of the circular error (≈ 72 mgal). Therefore the gravity offset between the instrument and the network was taken constant for one year as a good approximation. From this assumption follows that:

$$g_{base} = r_{base,i}(t_k) + g_{0,i}(t_k) + c(r_{base,i}(t_k)) = r_{base,i}(t_k) + g'_{0,i}(t_k) \tag{2.8}$$

$$g_a = r_{i1} + c(r_{i1}) + g'_{0,i}(t_k) = r_{j1} + c(r_{j1}) + g'_{0,j}(t_k) \tag{2.9}$$

with

g_{base}	: fixed gravity value of a base station
g	: gravity value of a station
c	: circular error
t_k	: time
i,j	: instrument names
$g_{0,i}(t_k)$	: gravity offset between instrument and gravity stations
$r_{base,i}$	: gravity value of instrument calculated from instrument tables

From that the difference between the two circular errors can be calculated :

$$c(r_{i1}) = c(r_{j1}) + \left[r_{j1} + g'_{0,j}(t_k) - r_{i1} - g'_{0,i}(t_k)\right] = c(r_{j1}) + \Delta(r_{i1}, t_k) \tag{2.10}$$

Note that c(r) is a rather small value (< 30 µgal) compared to the reading r and the offset g_0, so that the difference $r_{i1} - r_{j1}$ is approximately constant.
So during one campaign (at time t_k = constant, small drift of the instruments) the only information one can obtain about the circular errors is the difference between two different instruments.
However, if a second campaign (at time t_l) is measured again with the same two instruments, the offset of the instruments and the gravity network will be different and so

$$c(r_{i1}) = c(r_{j2}) + \Delta(r_{i1}, t_l) = c(r_j + \Delta r_j) + \Delta(r_{i1}, t_l) \tag{2.11}$$

with

$$\Delta r_j \approx \left[g'_{0,i}(t_k) - g'_{0,i}(t_l)\right] - \left[g'_{0,j}(t_k) - g'_{0,j}(t_l)\right]$$

(difference of the drifts between the two instruments from t_k to t_l)

$$c(r_{j1}) + \Delta(r_{i1}, t_k) = c(r_j + \Delta r_j) + \Delta(r_{i1}, t_k) \tag{2.12}$$

From equation (2.12) it is thus possible to calculate the circular errors of an instrument. It is desirable to have a rather large Δr_j ($\approx$ 10 mgal), because otherwise $c(r_j + \Delta r_j) - c(r_{j1})$ will be too small compared to the mean error of the difference $\Delta(r_{i1}, t_k) - \Delta(r_{i1}, t_k)$ ($\approx$ 10 mgal). So, if the drift of both instruments points in the same direction, it will be difficult or impossible to obtain reasonable results for the circular errors.

2.2.2.2 Calibration of a G-meter with a D-meter

The circular errors of a LaCoste&Romberg Type D gravimeter are less than 8 mgal and therefore much smaller than the ones of a G-meter. Furthermore, the period of the circular error is about 3.2 mgal. The mean error of a D-meter for a typical field campaign, with large gravity differences (> 10 mgal), is generally not smaller or even larger than the mean error of a G-meter and generally in Yellowstone campaigns is $\approx$ 14 µgal. So, the circular error of a D-meter is not significantly larger than other errors and was assumed to be zero. Based on this assumption the circular error of a G-meter can be directly calculated by the difference between the measurement of the G-meter and the one of the D-meter :

$$c(r_{i1}) = \Delta(r_{i1}, t_k) \tag{2.13}$$

2.2.2.3 Circular Error Model

With these formulas, the circular error can be determined at specific reading values. Because the values are not overdetermined, it is convenient to introduce a model for the circular error. It is in the nature of the problem to model it by a periodic function :

$$c(r_{sta}) = \sum_n a_n \sin\left(\frac{r_{sta}}{\lambda_n} + \varphi_n\right) \tag{2.14}$$

with :

r : reading

c(r) : circular error

n : periodic functions to model the error of an instrument
a_n : amplitude
λ_n : wavelength
φ_n : phase

Due to instrument specification, λ_n must be a factor of 72 instrument units (i.u.) for LaCoste&Romberg model G-meters. Therefore, $\lambda_n = \frac{72 \text{ i.u.}}{n}$.
So the observation equation for a measurement at the station i becomes :

$$r'_{sta} + v = m_i\, g_{sta} + c_{0i} + c_{1i} \cdot t + \sum_{n(i)} a_{ni} \sin\left(\frac{r_{sta}}{\lambda_{ni}} + \varphi_{ni}\right) \tag{2.15}$$

with the variables m_i, g_{sta}, c_{0i}, c_{1i}, a_{ni} and φ_{ni} (Definitions see (2.1),(2.5) and (2.14))
To test, whether the periodic error of the instrument is the published value of 72 i.u., λ_{ni} can also be introduced as variable. Again, linearization leads to the normal equation system. An advantage of this model for the circular error appears in the calibration with a D- Meter. Because the period of the circular error of the D-meter (≈ 3.2 mgal) is much smaller than the one of a G-Meter (≈ 72 mgal), the errors of the D-meter are smoothed and have less influence on the calibration curve for the G-meter.
The observation equation (2.15) represents the functional model, which is applied in the program 'gravity'. The statistical model in 'gravity' assumes, that all measurements are uncorrelated and have a Gaussian distribution.

2.3 Yellowstone Precision Gravity Measurements

2.3.1 Development of the Yellowstone Gravity Network

The first precision gravity marks were installed in the Yellowstone National Park in 1977 by the University of Utah (Evoy, 1978). 133 points were distributed along the roads of the whole park, coincident with leveling benchmarks. A higher concentration of stations was employed along the two caldera crossing lines from Canyon Junction to Fishing Bridge and from Madison to West Thumb, because they spanned the principal area of caldera deformation. These points form the backbone of the current network (see fig. 2.4), although only about 100 of them were still accessible in 1993. The other stations were lost mainly due to newly built roads, so that either the point itself was destroyed or the access by car was no longer possible.

Some new gravity stations were established at newly installed leveling benchmarks along the caldera lines from Canyon to Fishing Bridge (1987 and 1988) and from Madison to West Thumb (1989). In other areas along new roads without leveling benchmarks, some gravity stations were installed in 1991 (from Fishing Bridge to West Thumb, West Thumb to Shoshone Lake, and West Thumb to Lewis Lake).
In 1984, a backcountry network consisting of 32 stations accessed by helicopter or boat was established in the northeastern caldera and around Yellowstone Lake. Additional backcountry points were installed at most of the GPS stations mainly in 1987.
Because of the major interest to measure continuously gravity changes along the accessible roads of the Yellowstone National Park, it was necessary to establish new, save points along newly built or rebuilt roads before the old points were destroyed. An attempt to do thus was made along the road from Lake Butte to Sylvan Lake, where excenter points for the stations 37 mdc and 38 mdc were measured in 1993. Furthermore, a continuous record in the Hayden Valley was provided, although some of the points installed in 1977 lay on culverts or bridges and may be destroyed during planned road constructions. However, new gravity stations were installed close to most of these points in 1987 or 1988 coincident with new leveling benchmarks. Thus there is a substantial record of data, where old and new stations were measured in the same campaigns. By this method and assuming that the gravity differences between the respective stations remained constant (the stations lie within 100 m), the gravity values of the stations can be calculated for every campaign (see table C.2, app C)

2.3.2 Data Processing

The procedure for the adjustment of a gravity campaign is discussed here :
If there were several different gravimeters used in the campaign, first, one gravimeter was introduced with a mean error of 10 µgal and all the others with a mean error of 100 µgal to detect rough errors in the measurements with 100 µgal errors. There were no free factors introduced.
In order to find and to correct rough errors, one instrument was introduced with a mean error of 10 µgal, the others with 100 µgal. So it was easier to find coarse errors of the instruments with a high mean error. Coarse errors were corrected, or if not possible to correct them, they were marked in the result file so that they would not be used for further iterations. Then the gravimeter with the lowest mean error was changed and the procedure repeated. After this procedure was finished, all gravimeters were reintroduced with a mean error of 10 µgal. In further iterations, the mean errors of the instruments were allowed to change to the value the program found for them after the adjustment.

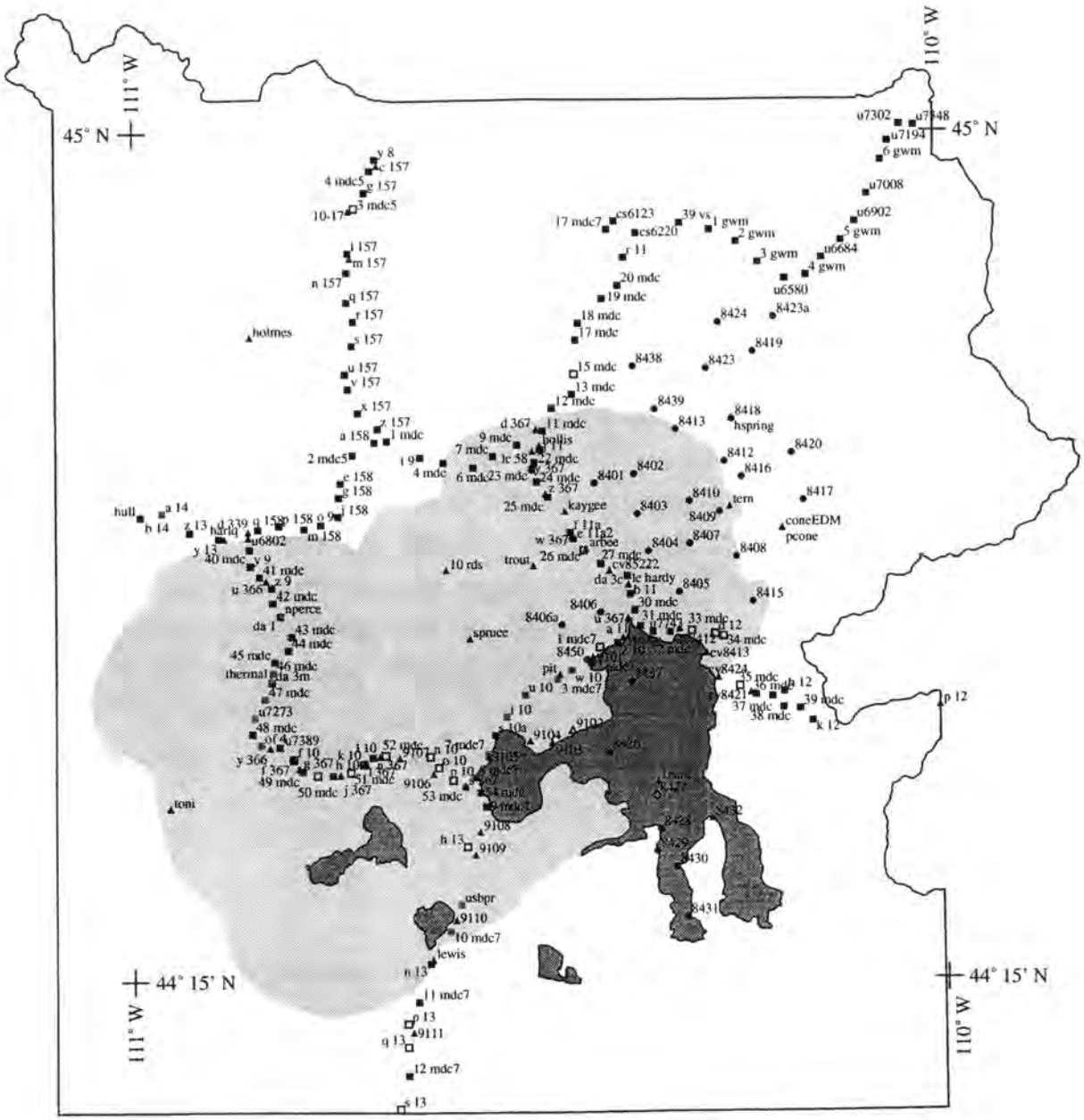

Symbols

installation :	1977	1984	1987-
status :			
o.k.	■	●	▲
unknown/instable	▪	•	▴
destroyed/no access	□	○	△

Fig 2.4 : Yellowstone Precision Gravity stations

Furthermore, rough errors were corrected or marked and wrongly marked errors reintroduced into the adjustment. Normally measurements with $\frac{v_i}{q_{v_i v_i}} > 3$ were removed except if the whole set of a day was bad so that it could be presumed that the mean error of the instrument was chosen too small. So all $\frac{\hat{\sigma}}{\sigma}$ of the whole set and all the instruments were 1. But still the measurements at stations that were used as base stations often showed $\frac{\hat{\sigma}_{sta}}{\sigma_{sta}} > 1.1$, so I surmise, that the mean errors could be generally chosen slightly too small and the mean errors of the stations, too. The difference of the mean errors of measurements at stations often measured and others indicates a correlation between the measurements. To be on the safe side of the size of the mean error of a station one can take either the mean error a priori if $\frac{\hat{\sigma}_{sta}}{\sigma_{sta}} < 1.0$, or the one a posteriori if $\frac{\hat{\sigma}_{sta}}{\sigma_{sta}} > 1.0$.

The values relative to the main base station, 11 mdc (near Canyon Junction), for all gravity campaigns are listed in table C.2 (app. C). Table C.3 (app. C) shows the measurements that were not used for the adjustment because they are assumed to have coarse errors.

2.3.3 Determination of the Absolute Factor of the Gravimeters

The U.S. geological Survey has established an absolute calibration line near San Jose, CA, (Jachens,1987) (table C.1, app. C). Its gravity range extends from 91 mgal less than the lowest to 85 mgal less than the highest gravity value of the Yellowstone precision gravity network. It covers about 215 mgal of the 300 mgal range or all stations except the ones from near Tower Falls to North East Entrance (18 stations), 4 stations nearest to Mammoth Hot Springs and 3 stations nearest to West Yellowstone.

The Californian base line has a start and an end point both observed with absolute gravity measurements and 6 stations in between, the values of which the USGS determined by measurements with LaCoste Romberg G Gravimeters. However, one relative station (HDB) on the line seems to have a wrong value. If the gravity value of this station is introduced as unknown in the adjustment, the value achieved is 40 µgal higher than the given one.

Two months before the 1987 Yellowstone gravity campaign, one ladder loop with the two LaCoste Romberg gravity meters G461 and G264 was performed along the USGS calibration line. The mean error for a measurement was calculated to be 14.5 µgal for

G264 and 12.5 µgal for G461. The factors determined for the instrument calibration tables are 1.000516 ± 0.000040 for G264 and 1.000726 ± 0.000034 for G461.
A second calibration campaign was accomplished three weeks after the 1991 Yellowstone campaign. Six ladder loops with G264 and two ladder loops with G461 were run on the line. Conversion factors of 1.000601 ± 0.000013 for G264 and 1.000173 ± 0.000023 for G461 were found. The mean error of a measurement for both instruments was about 10 µgal.
From these calibration tests it seems, that the correction factors between instrument units and gravity values change significantly between 1987 and 1991. The change in the instrument G461 is probably due to an unknown event in 1990, when the drift constant of this instrument changed by 70 mgal from one day to the next (see fig. 2.10). Unfortunately, it cannot be checked if factor actually changed on that specific day, because the mean error of a factor calculated out of the 1990 data is too large.
The instrument G461 was used during all Yellowstone gravity campaigns. So the factor for the calibration table of other instruments used during the campaigns can be calculated with G461 as reference.

2.3.4 Determination of Circular Errors of the Gravimeters

Comparison of the results of a gravity campaign adjusted for two good instruments (mean error ≈ 10 µgal), shows significant offsets between the gravity values found for a station, depending on the gravity value (fig. 2.5). As can be expected from the specification of the instrument, the offsets revealed a cyclic behavior. In order to reduce the systematic errors of the gravity meters, calibration offsets were modeled according to the method in chapter 2.2.2.
The instruments G461 and G264 were used during all the Yellowstone gravity campaigns from 1987 until 1993. In this time span, their drift constants shifted several mgal and additionally there was the large jump in 1990 with instrument G461. So it was possible to calculate a value for the circular errors of both instruments as described in chapter 2.2.2. Additionally, a separate campaign was carried out in 1994, designed especially to calibrate G264 and G461 against the LaCoste&Romberg gravimeter D16. For this special project independent stations were chosen from Dunraven Pass down to Tower Junction and from Mammoth Hot Springs to Norris Junction. The gravity differences between the stations were 3 to 5 mgal over a range of 200 mgal. This range is coincident with the one of the gravity campaigns except for some very high-elevation backcountry stations at Mt. Washburn and Mt. Holmes. There were very good measurements with both G-meters G461 (9 µgal mean error) and G264 (8 µgal) as well as with the D-meter D16 (12.5 µgal).

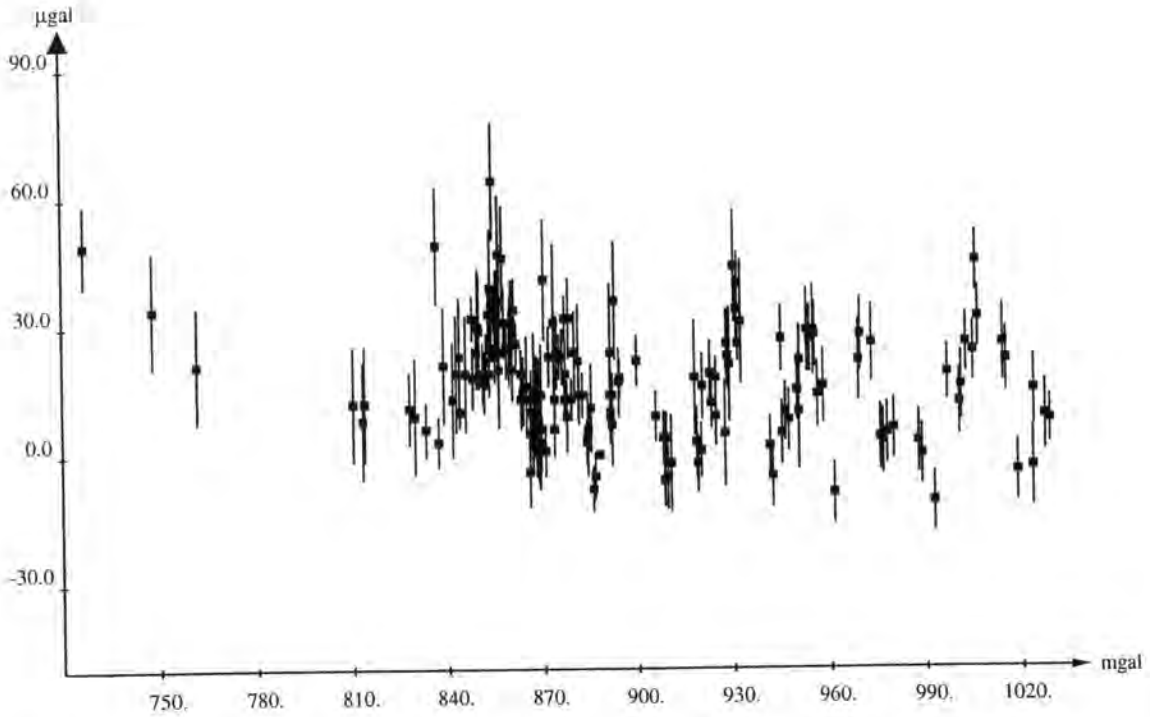

Fig. 2.5 Offset of the gravity values of the Yellowstone precision gravity net of for the instruments G264 and G461 adjusted independently in 1993. The vertical lines show the 1 σ error bars.

It was thus possible to compare the two proposed calibration methods of chapter 2.2.2.1 and 2.2.2.2 for consistency. The results do not differ significantly , as can be seen in figure 2.7.

Furthermore it was tested, whether the period of the error was actually 72 instrument units (i.u.). This test is very critical, because solutions for the amplitudes, wavelengths and phases are strongly dependent on the starting values introduced in the near solution. The most stable solutions are found with the data of 1993. Because the calibration factors for the two instruments G264 and G461 were nearly the same over the Yellowstone National Park (1.058 resp. 1.063) and there was no significant drift between the two instruments during the campaign, it is sufficient to check periods of the differences of circular errors of the two instruments. Even then, a stepwise procedure is required. In a first step, a wavelength of 72 i.u. must be introduced as fixed to get "good" starting values for the amplitude and phase. After finding a solution, the wavelength can be allowed to vary. The same procedure has to be done with all additional wavelengths introduced. The solutions are close to possible wavelengths of an interval of 72 i.u. (table 2.1) .

Frequency	λ [i.u]	σ_λ	**a** [µgal]	σ_a	φ [rad]	σ_φ
f[1]	71.14	1.7	7.30	0.8	-0.856	0.1
f[1]	72.46	1.7	7.93	0.9	-1.058	0.1
f[2]	36.53	0.7	-5.20	0.7	3.789	0.2
f[1]	71.01	2.4	5.35	0.9	-1.285	0.2
f[2]	35.78	0.6	-5.84	0.8	3.079	0.2
f[3]	24.09	0.2	8.48	0.7	1.873	0.1
f[1]	69.28	2.3	5.15	0.8	-1.265	0.2
f[2]	35.98	0.5	-6.63	0.8	3.169	0.1
f[3]	24.17	0.2	6.08	0.8	2.070	0.1
f[4]	17.82	0.1	6.99	0.7	0.793	0.1
f[1]	68.61	2.1	5.67	0.9	-1.370	0.2
f[2]	36.28	0.5	-7.03	0.8	3.268	0.1
f[3]	24.21	0.3	5.95	0.8	2.013	0.2
f[4]	17.80	0.1	6.51	0.8	0.867	0.1
f[5]	14.26	0.2	-2.72	0.7	2.685	0.3

Table 2.1 : Circular errors modeled for the differences between the two instruments G461 and G264 in 1993, with free wavelengths, and various numbers of frequencies.

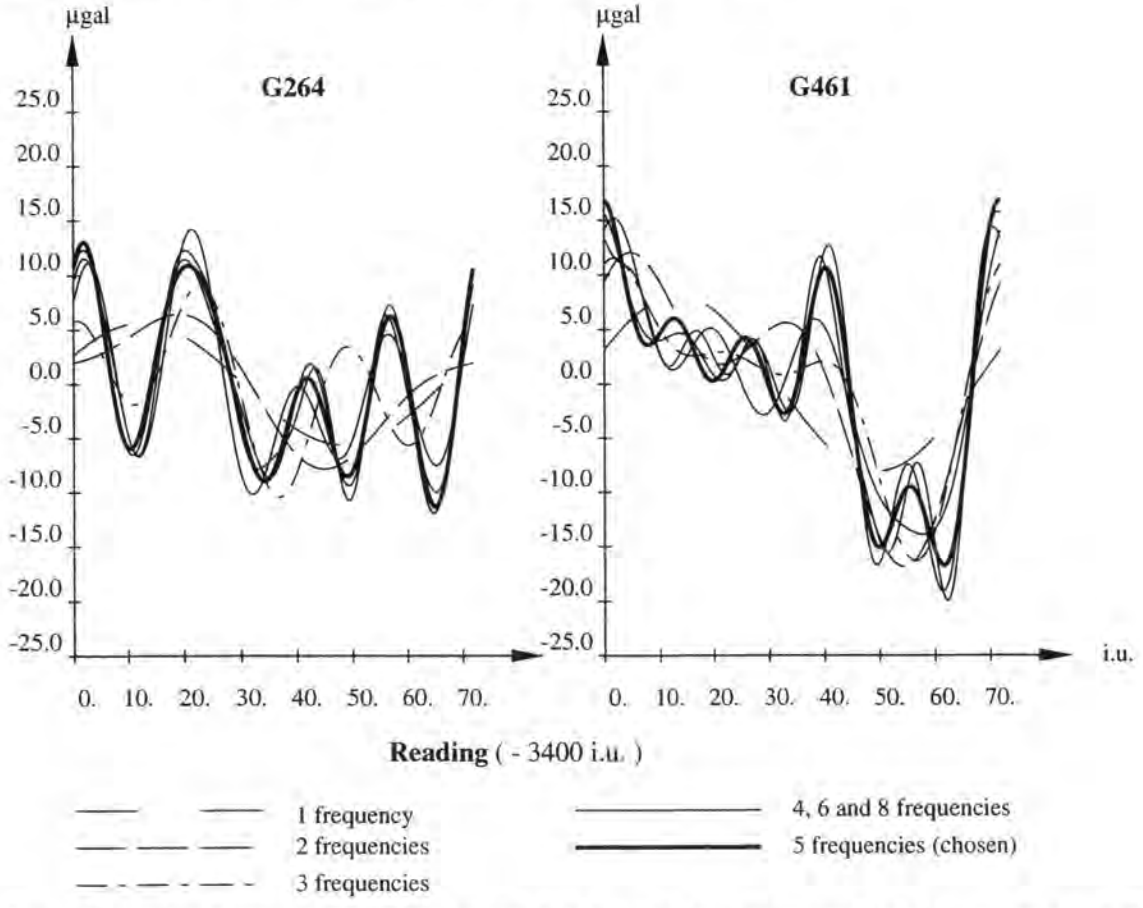

Fig. 2.6 Circular Errors of the gravity meters G264, and G461, calculated for different numbers of frequencies

In a next step one must decide, how many wavelengths should be introduced. If there are too few wavelengths, the circular error cannot be modeled in an accurate way, i.e., it is biased. On the other hand, if there are too many, the solutions tend to overoscillate in some parts of the curve. The solution for up to eight frequencies were calculated (see figure 2.6). Finally the solution with five wavelengths was taken as the model for the circular error (fig. 2.7, 2.8).

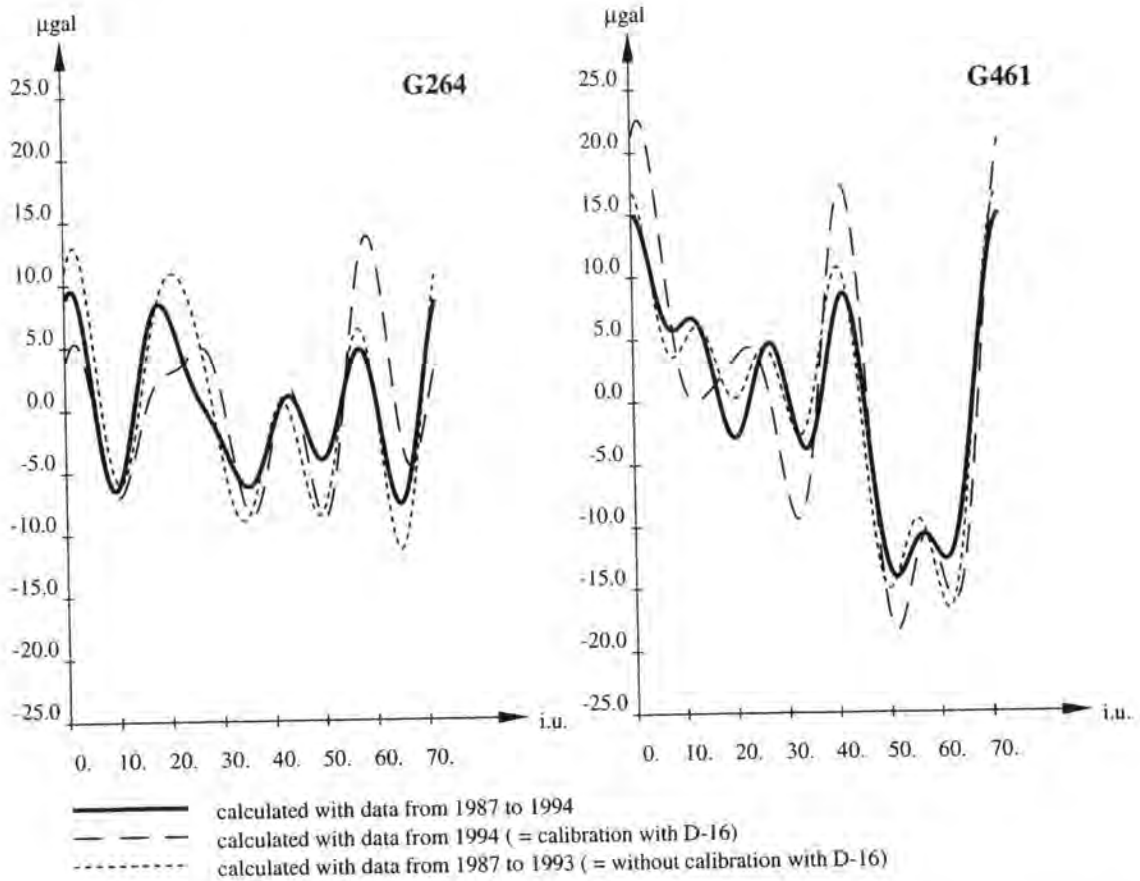

Fig. 2.7 Circular Errors of the gravity meters G264, and G461, calculated with different methods

2.3.5 Discussion of the Yellowstone Gravity Campaigns

All of the Yellowstone precision gravity data were reduced to fix a base station, 11 mdc at Canyon Junction, which was assigned with a value of 979888.130 mgal every year. This value was taken from an USGS calibration study (Carle et al, 1989), where the absolute gravity value for 11 mdc is given as above. This value is about 14 mgal higher than the value which would be expected from the measurements on the absolute gravity line near San Francisco (see Table 2.3). Because the main interest are the gravity changes, this difference does not matter for the further discussions.

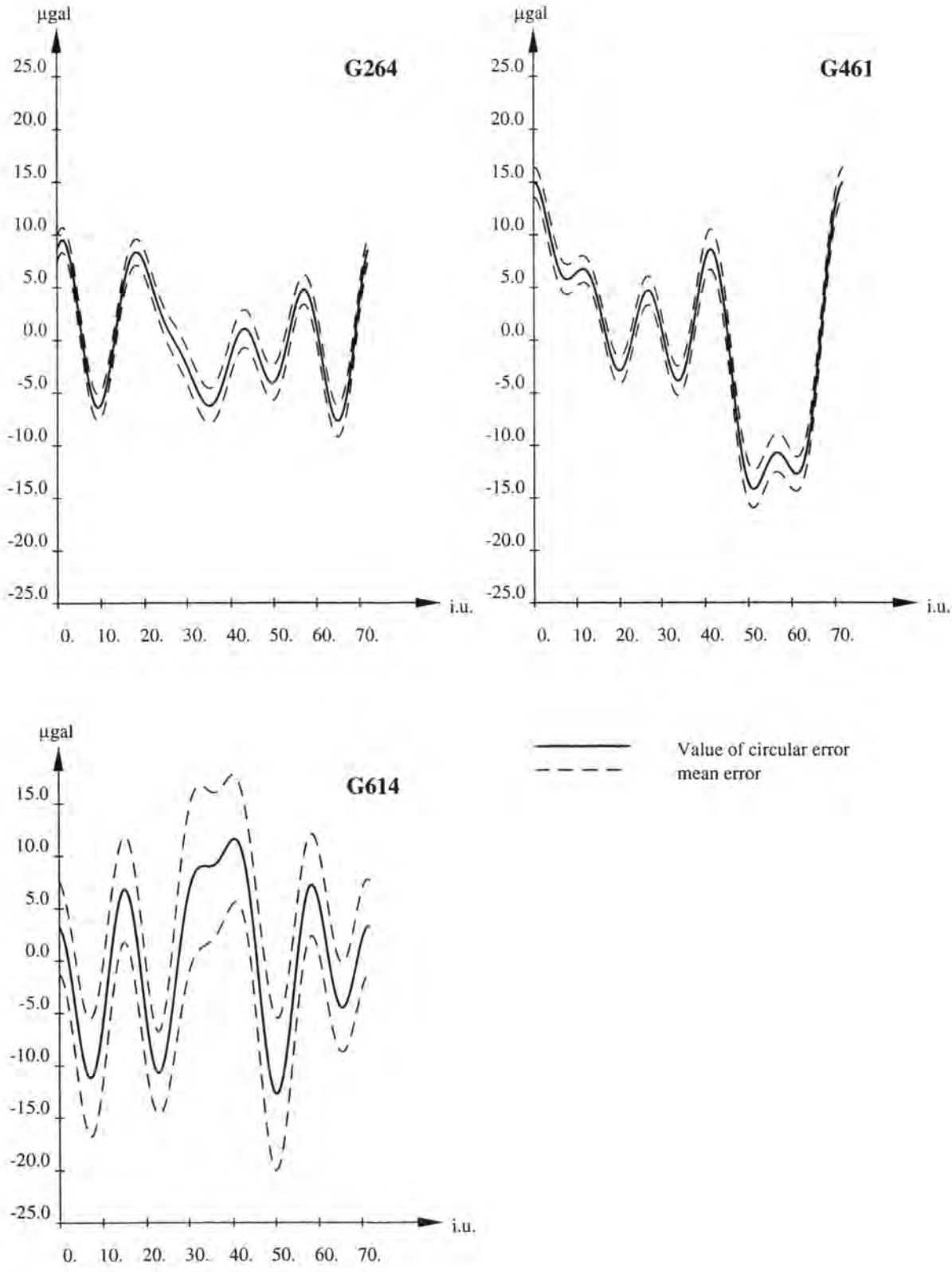

Fig 2.8 : Circular errors applied for the gravimeters G264, G461 and G614

year	base stations	# of stat.	Meas. Tech.	instrument	σ [μgal]	# of meas.	rem-oved	# of tares
1977	11 mdc,32 mdc, 40 mdc,54 mdc, a 158, cs6123	133	SL	G461 D 26	10.6 15.4	499 497	5 0	20 21
1979	11 mdc, z 10	28	SL	G461	19.9	175	4	2
1983	11 mdc,32 mdc, 40 mdc,54 mdc, a 158,cs6123	128	SL	G461 -July 8 July 8 - G614	43.9 15.6 27.3	179 347 552	4 6 8	1 3 22
1984	11 mdc,8450	45	SL	G461 G395	12.0 17.2	101 101	0 1	1 3
1986	11 mdc,40 mdc	51	SL	G461 G465	11.6 26.9	99 344	3 4	4 47
1987	11 mdc,30 mdc, 40 mdc,54 mdc, a 158,cs6123	143	LL	G461 G264 D 86	9.8 17.0 21.8	469 469 214	7 14 1	12 12 12
1988	11 mdc,u 367	47	LL	G461 G264	10.0 12.4	168 168	0 7	4 4
1989	11 mdc,u 367, 40 mdc, 54 mdc	99	LL	G461 G264	8.0 13.1	494 494	2 7	9 6
1990	11 mdc	46	LL	G461 G264	10.6 22.0	152 152	8 4	6 7
1991	11 mdc, u367, 40 mdc, s 367, a 158, cs6123	154	SLL	G461 G264 G839	44.9 9.4 20.8	282 695 493	120 1 11	8 15 43
1993	11 mdc, u 367, 40 mdc, s 367, a 158, cs6123	167	SLL	G461 G264	11.2 7.8	887 886	3 1	10 14
1994 (calib.)	11 mdc	58	LL	G461 G264 D 16	10.0 7.8 13.6	212 215 213	1 0 1	3 4 6

Table 2.2 : Some characteristics parameters of the Yellowstone gravity campaigns. **SL**: Simple Loops, **LL**: Ladder Loops, **SLL**: Strengthened Ladder Loops. σ: mean error of single measurement, **removed**: number of measurements with assumed rough errors. **tares**: changes in linear drift curve.

year	1987		1991	
instrument	G264	G461	G264	G461
expected constant of drift curve [mgal]	2740.6	2761.4	2733.0	2835.0
measured constant of drift curve [mgal]	2726.143	2746.978	2718.530	2821.487
difference [mgal]	14.5	14.4	14.5	13.5

Table 2.3 : Differences between San Francisco absolute gravity line and USGS Yellowstone gravity data base (used absolute gravity values : 11 mdc 979888.130 mgal, Station A in Menlo Park 979958.740 mgal)

Summary of the gravity campaign results (by year, see also table 2.2) :

1977 : Most of the stations were installed this year and measurements over the whole Park were carried out. The method applied was simple looping with base stations in 32 mdc (Fishing Bridge), 40 mdc (Madison Junction), 54 mdc (West Thumb), a 158 (Norris Junction) and cs6123 (Tower Junction). No connection measurements are available between a lot of neighbored points, especially between 49 mdc and 50 mdc near Old Faithful, p 158 and q 158 at Madison Junction, 7 mdc7 and 8 mdc7 near West Thumb and between r 11 and 17 mdc7 at Tower Falls. The data were good data with very few points removed ($\hat{\sigma}_{G461}$ = 10.6 µgal, $\hat{\sigma}_{D26}$ = 15.4 µgal).

1979 : This year, the measurements emphasized a caldera crossing profile from Canyon Junction to Sylvan Lake. A subbase was chosen in z 10 (at Lake Hotel), which is preferable to 32 mdc, and single loops were applied.
Some measurements removed. The data were slightly worse than 1977 but still good ($\hat{\sigma}_{G461}$ = 19.9 µgal).

1983 : This campaign was conducted over the entire National Park gravity network. Subbases were installed at 32 mdc (Fishing Bridge), 40 mdc (Madison Junction), 54 mdc (West Thumb), a 158 (Norris Junction) and cs6123 (Tower Junction). No direct connections exist between the points 40 mdc and q 158 at Madison Junction and a 158 and 1 mdc at Norris Junction. The single loop method was applied. Quite poor measurements especially at the beginning of the campaign with G461, but improved during the survey one day to another (July, 8 to July, 9). So I introduced two different mean errors for G461 ($\hat{\sigma}_{G461}$ = 43.9 µgal at the beginning and later 15.6 µgal). First few days the measurements of G614 were

done by electronic null and visual readings, which both seem to have about the same accuracy, but had a constant offset. But still the mean error $\hat{\sigma}_{G614}$ was ≈ 27.3 µgal.

Although the data are not very good, the circular error of the gravity meter G614 was determined, which was possible with the help of G461 (s. chapter 2.3.4 and fig 2.8).

Figures 2.9 : Measured lines at each campaign

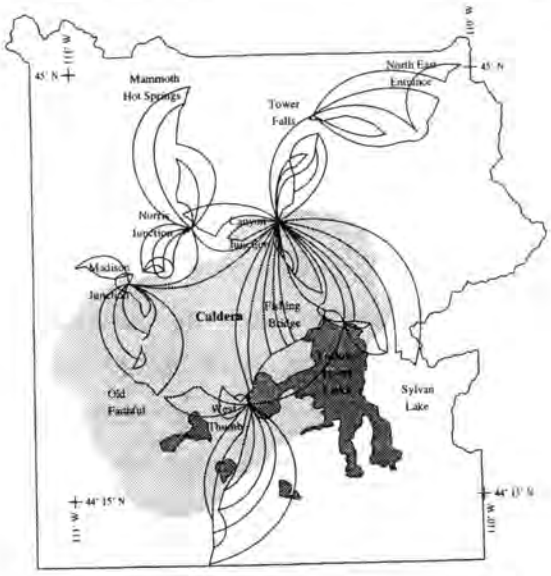

Fig. 2.9 a : Gravity loops 1977 (simple loops)

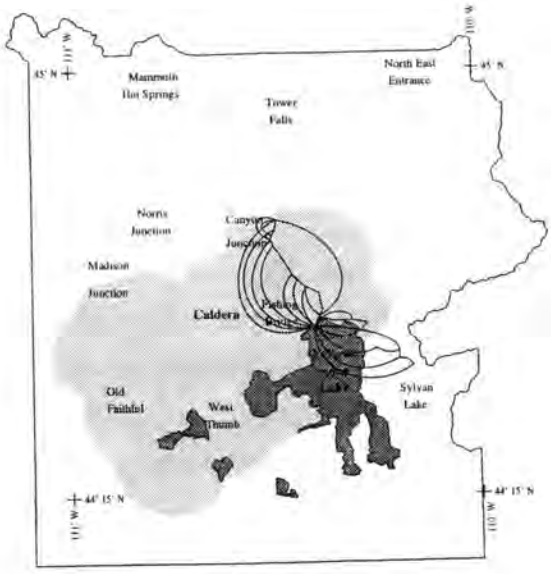

Fig. 2.9 b : Gravity loops 1979 (simple loops)

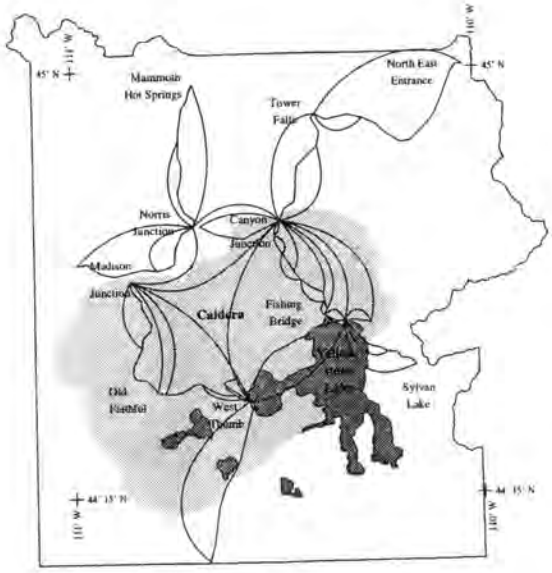

Fig. 2.9 c : Gravity loops 1983
(simple loops with unnecessary gaps)

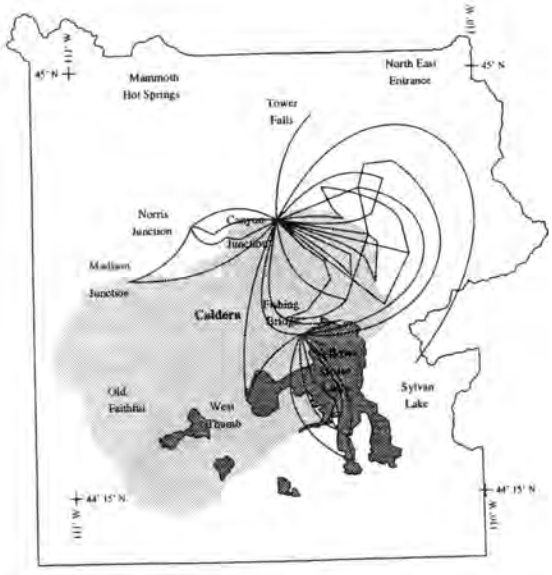

Fig. 2.9 d : Gravity loops 1984
(mainly backcountry points)

1984 : This was the first year of backcountry station measurements accessed by helicopter and boat with quite good results. Most of the stations were measured once with each gravimeter, so there were larger mean errors ($\hat{\sigma}_{G461}$ = 12.0 µgal, $\hat{\sigma}_{G395}$ = 17.2 µgal). For the measurements at the Yellowstone Lake, the Base 8450 was established at the Bridge Bay marina. Additionally, the line from Canyon Junction to Norris was measured.

1986 : The gravity profiles from Canyon Junction to Sylvan Lake and from Madison Junction to West Thumb were measured, again for a caldera crossing. A subbase was chosen in 40 mdc (Madison Junction) and simple loops were applied. Quite good measurements with some removed data ($\hat{\sigma}_{G461}$ = 11.6 µgal, $\hat{\sigma}_{G465}$ = 26.9 µgal).

1987 : This year there was again a campaign over the entire Yellowstone network. For the first time, the ladder loop method was applied. Subbases were measured in 30 mdc (Fishing Bridge), 40 mdc (Madison Junction), 54 mdc (West Thumb), a158 (Norris Junction) and cs6123 (Tower Junction). Gravity stations at quite a few newly installed leveling and GPS benchmarks in the Hayden Valley were added to the net. Good measurements of G461 and G264, and a little worse one with D86 which is very sensitive to high gravity changes and tares (E.E.Klingelé, personal communication).($\hat{\sigma}_{G461}$ = 9.8 µgal, $\hat{\sigma}_{G264}$ = 17.0 µgal, $\hat{\sigma}_{D26}$ = 21.8 µgal)

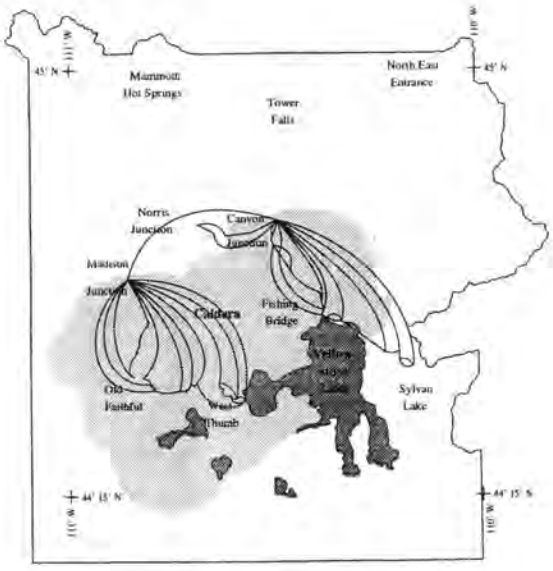

Fig. 2.9 e : Gravity loops 1986
(simple loops)

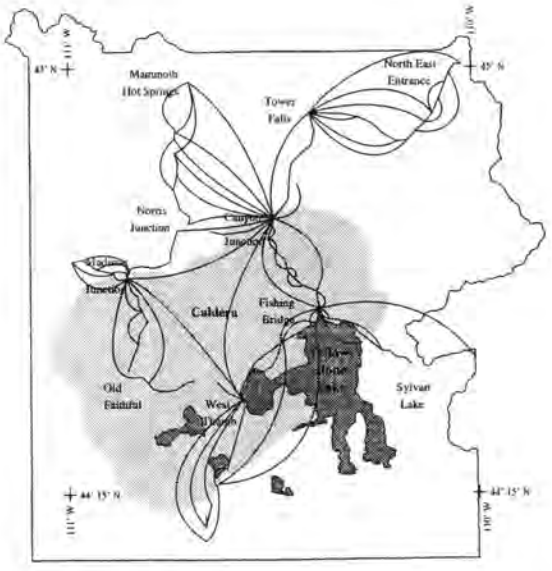

Fig. 2.9 f : Gravity loops 1987 (road points)
(ladder loops with some gaps)

1988: Ladder Loops were carried out along the caldera crossing line from Canyon Junction to Sylvan Lake. The subbase at Fishing Bridge was chosen at u 367. Very good measurements with G461 and G264 ($\hat{\sigma}_{G264} = 12.4$ µgal, $\hat{\sigma}_{G461} = 10.0$ µgal). However there were very strange drifts and jumps in the measurements with the borrowed USGS gravimeters G615 and G721, that were so bad they were not included in the main adjustment.

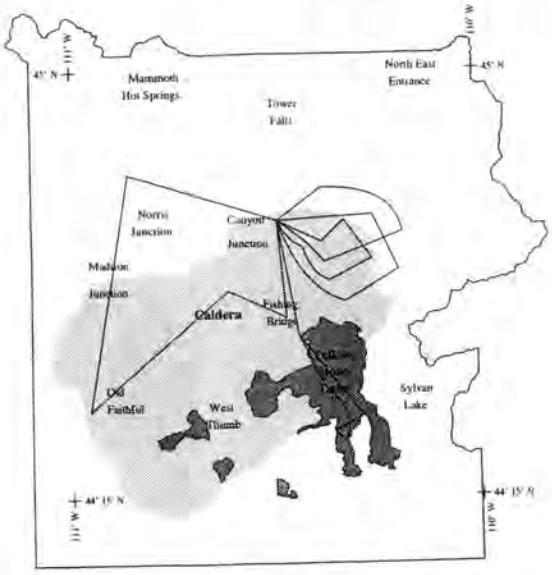

Fig. 2.9 g : Measuring lines 1987 (backcountry)

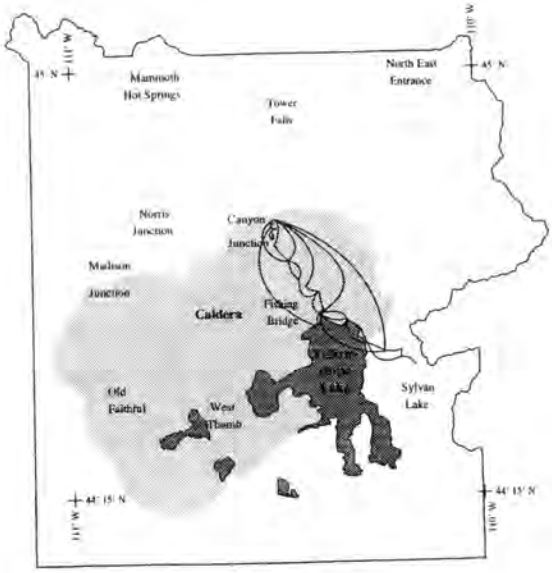

Fig. 2.9 h : Gravity measuring lines 1988 (ladder loops)

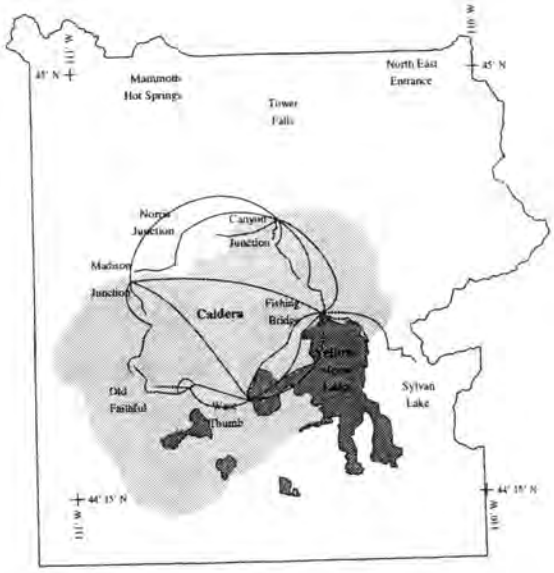

Fig. 2.9 i : Gravity loops 1989 (road points) (ladder loops with some unnecessary gaps)

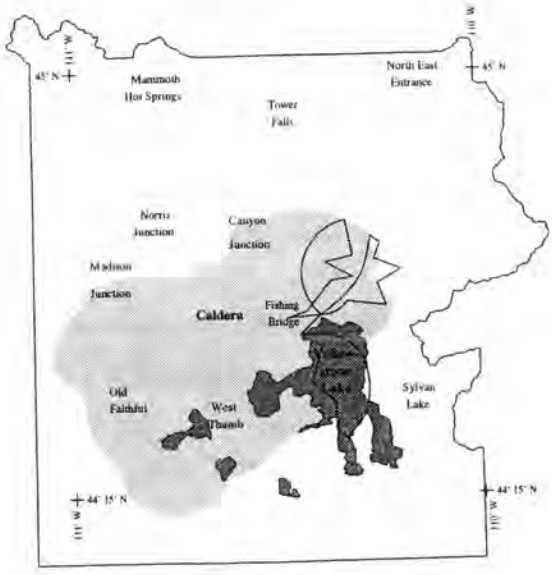

Fig. 2.9 j : Gravity loops 1989 (off road)

1989 : The road points measured this year were the ones on the loop from Canyon to Norris to Madison to West Thumb and back as well as the line from Fishing Bridge to Sylvan Lake. The subbases were in u 367, 40 mdc, 54 mdc and a 158. Ladder loops were applied, but the end points of the loops were not connected directly with the following points. Excellent measurements with a very low $\hat{\sigma}_{G461} = 8.0$ µgal for G461, $\hat{\sigma}_{G264} = 13.1$ µgal.

1990 : The campaign again emphasized the line from Canyon Junction to Sylvan Lake. No special subbase was chosen and ladder loops were carried out. A very large tare of +70 mgal occurred with the instrument G461. Quite good data with some removed measurements with both gravimeters ($\hat{\sigma}_{G461} = 10.6$ µgal, $\hat{\sigma}_{G264} = 22.0$ µgal).

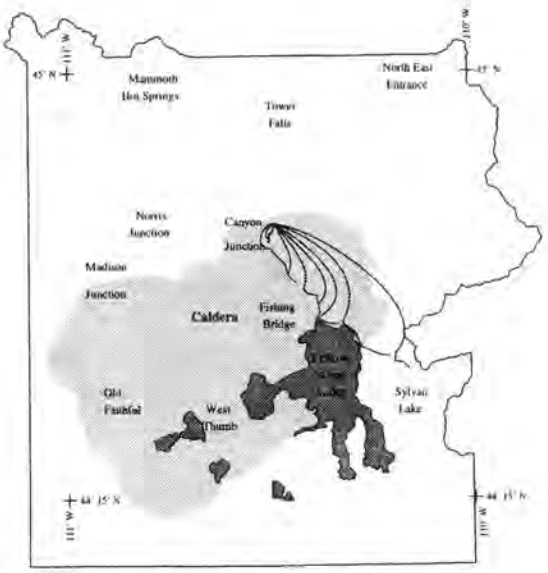

Fig. 2.9 1 : Yellowstone gravity measuring lines 1990
(ladder loops with unnecessary gaps)

1991 : The whole Yellowstone network was measured with strengthened ladder loops. Subbases were chosen in u 367, 40 mdc, s 367 (preferable to 54 mdc), a 158 and cs6123. The points at the Bridges in the Firehole River Valley and Hayden Valley were neglected. Very good measurements with G264, $\hat{\sigma}_{G264} = 9.4$ µgal. Enormous problems with G461 [1], ($\hat{\sigma}_{G461} = 44.9$ µgal and 40 % of removed measurements) and minor problems with G839 and the feedback system E839 ($\hat{\sigma}_{G839} = 20.8$ µgal, $\hat{\sigma}_{E839} = 18.6$ µgal).

(1) In spite of a revision of the instrument G461 by LaCoste Romberg during the gravity campaign, the problems with the instrument continued. So the instrument was shipped again to LaCoste Romberg after calibrating it on the USGS calibration line in Menlo Park (Ca). After two months of field checking the instrument, the problem finally identified : There was some corrosion in the wires of the thermal circuit of the instrument, so that the instrument heater would not work sometimes for five to ten minutes (personal communication Mr. Fett).

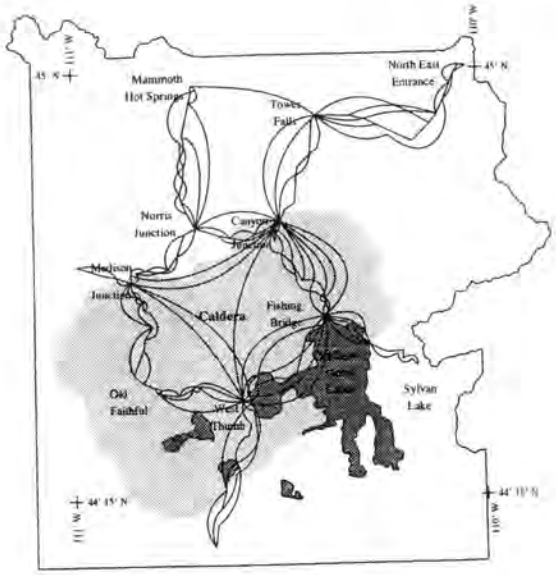

Fig. 2.9 m : Gravity loops 1991 (road points)
(strengthened ladder loops)

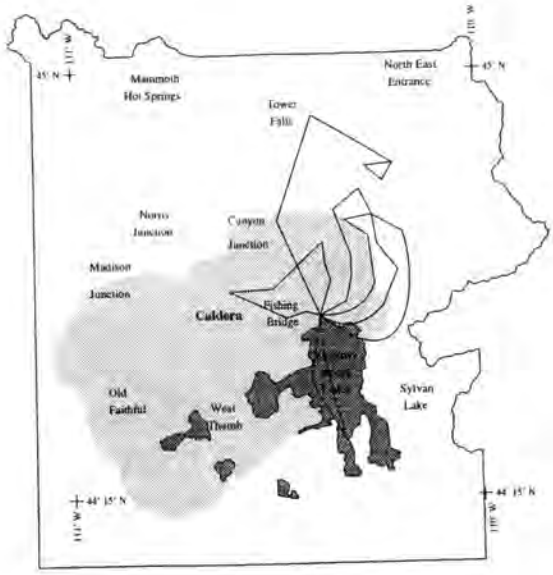

Fig. 2.9 n : Gravity loops 1991 (off road)

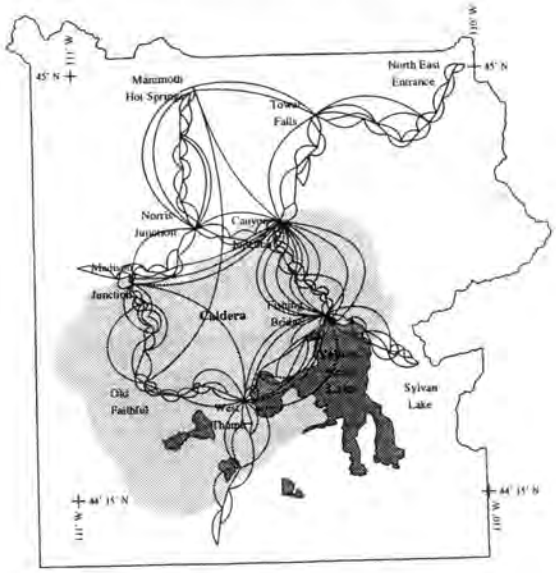

Fig. 2.9 o : Gravity loops 1993 (road points)
(strengthened ladder loops)

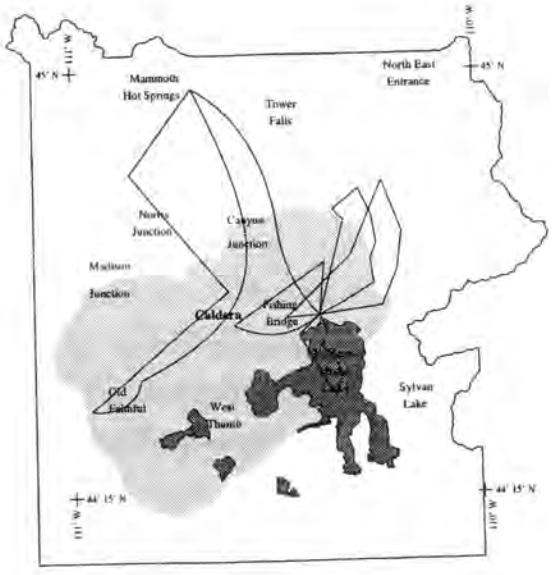

Fig. 2.9 p : Gravity loops 1993 (off road)

1993 : Again, the entire Yellowstone network was measured with strengthened ladder loops and the same base stations as in 1991. The points on the bridges in the Hayden Valley were measured in the early morning before the traffic increased. Very good measurements with both instruments G461 and G264 and hardly any removed data ($\hat{\sigma}_{G461}$ = 11.2 µgal, $\hat{\sigma}_{G264}$ = 7.8 µgal).

year	fixed instr.	fixed value	free instr.	free factor
1977	G461	1.000691	D26	1.000921 ± 0.000035
1983	G461	1.000691	G614	1.000037 ± 0.000043
1984	G461	1.000691	G395	1.000709 ± 0.000067
1986	G461	1.000691	G465	1.000291 ± 0.000260
1987	G461	1.000691	D86	0.999149 ± 0.000098
	G264	1.000488		
1988	G461	1.000691		
	G264	1.000488		
1989	G461	1.000691		
	G264	1.000488		
1990	G461	1.000691	until Sept. 11	
	G461	1.000144	after Sept. 13	
	G264	1.000488		
1991	G461	1.000144	E839	1.001341 ± 0.000408
	G264	1.000626	G839	1.000563 ± 0.000047
1993	G461	1.000144		
	G264	1.000626		

Table 2.5 : Scale Constants of Gravimeters

Figures 2.10 : Drift curves for each instrument and campaign. The drift curves were calculated after adjustment. The calculated values of the stations were introduced as fixed values. The plots show the improvements of all the measurements of an instrument, calculated with the fixed values for the gravity station. The scatter of the curve is an indication of the mean error of the instrument.

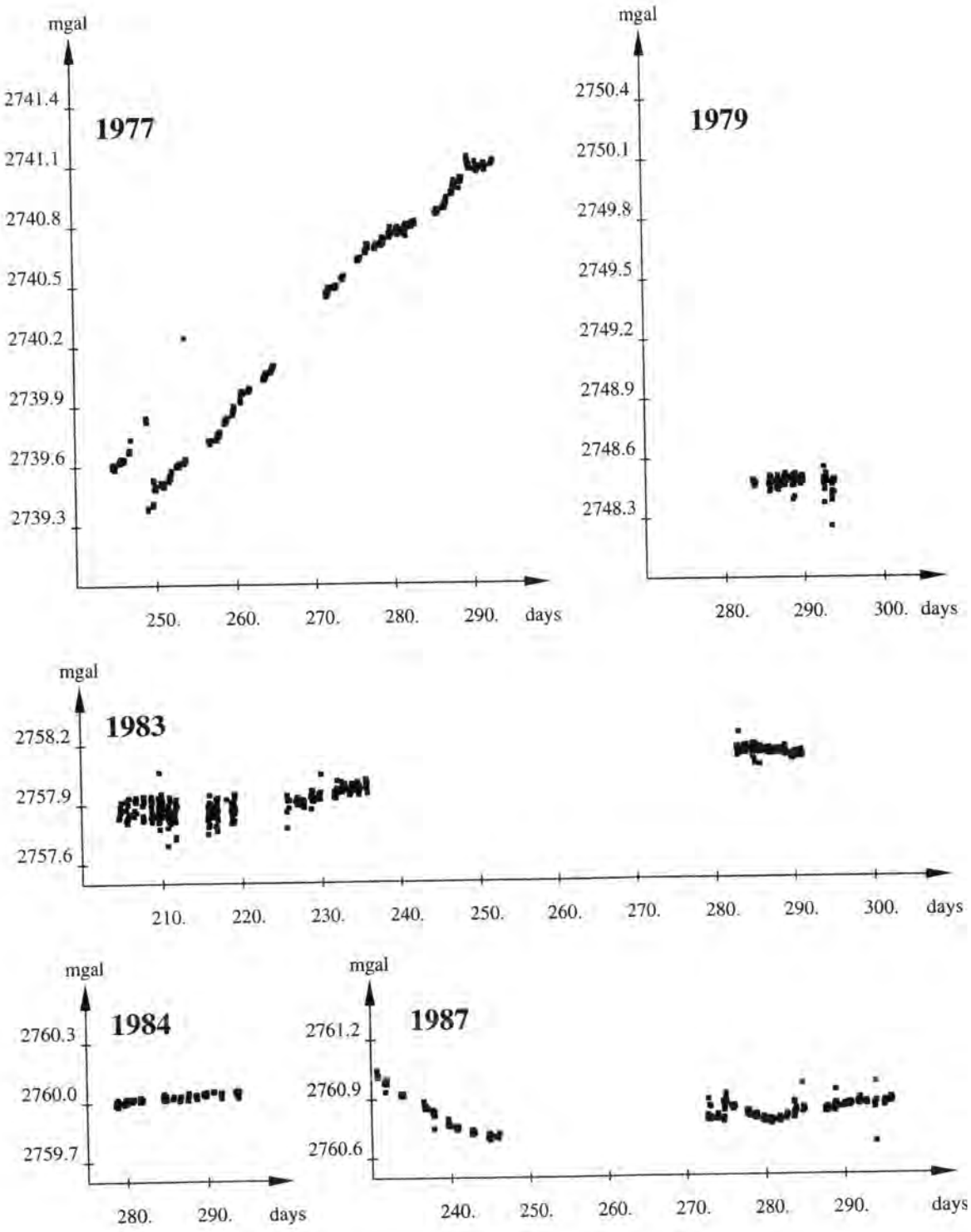

Fig. 2.10 a : Drift of gravity meter G461 in 1977, 1979, 1983, 1984 and 1987. The scatter of the data of 1983 show clearly the improvement of the measurements in the second half of the gravity campaign.

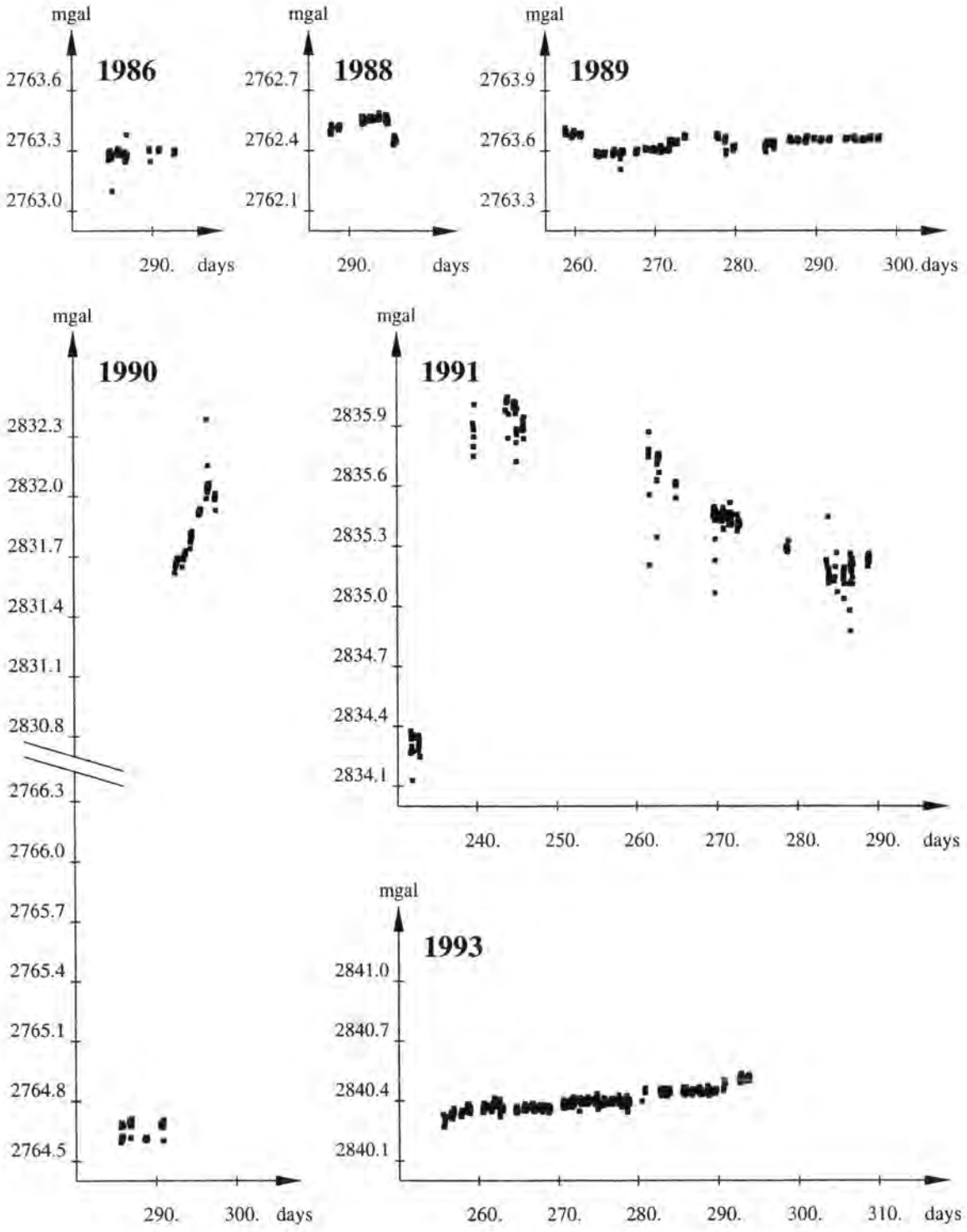

Fig. 2.10 b : Drift of gravity meter G461 in 1986, 1988, 1989, 1990, 1991 and 1993. The reason for the 70 mgal tare in 1990 is unknown. The large scatter in 1991 was due to corrosion of the heating circuit.

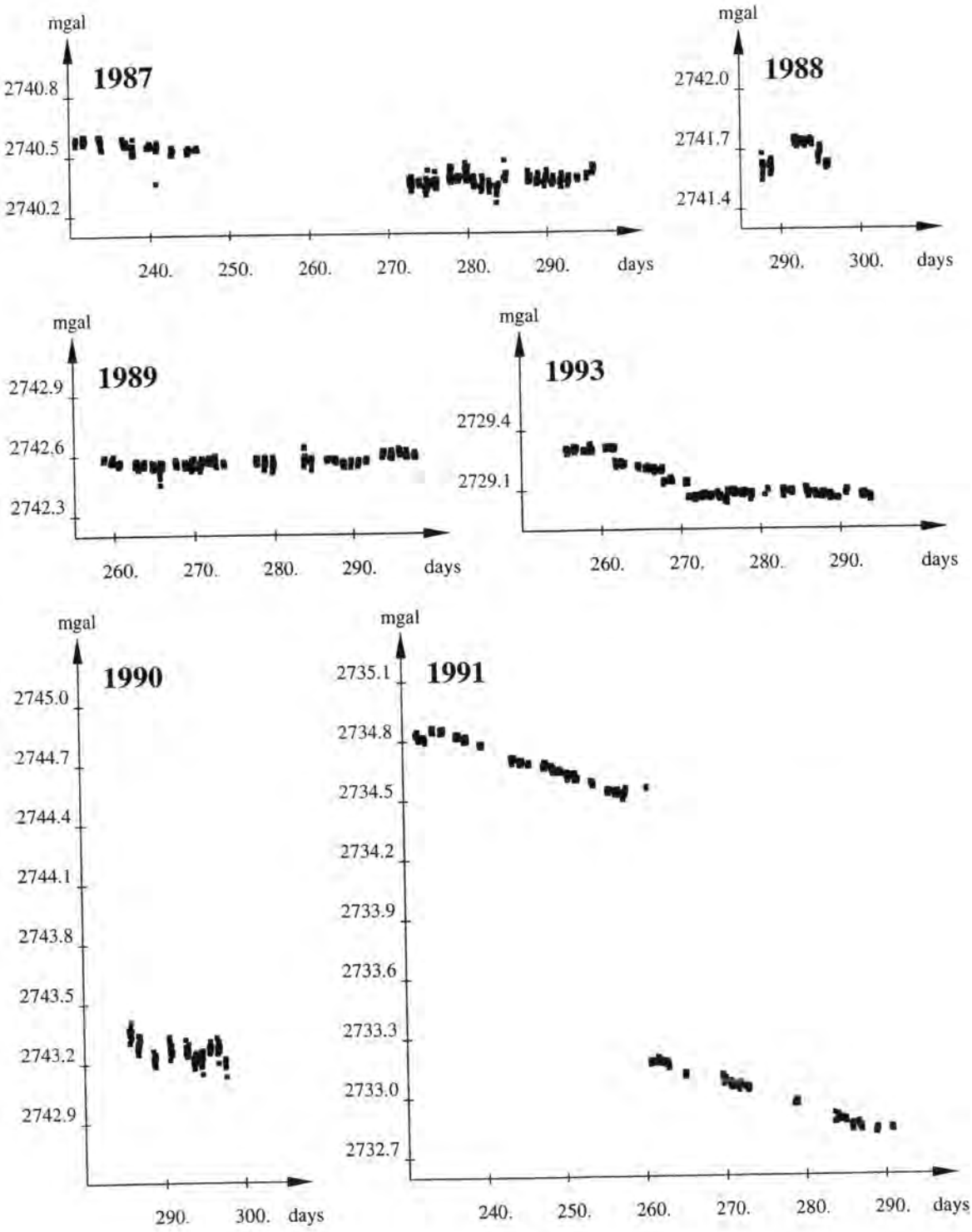

Fig. 2.10 c : Drift of gravity meter G264 from 1987 to 1993. The scatter of the data gets significantly smaller with time. The tare 1991 is due to a shock during transportation in its metallic suitcase.

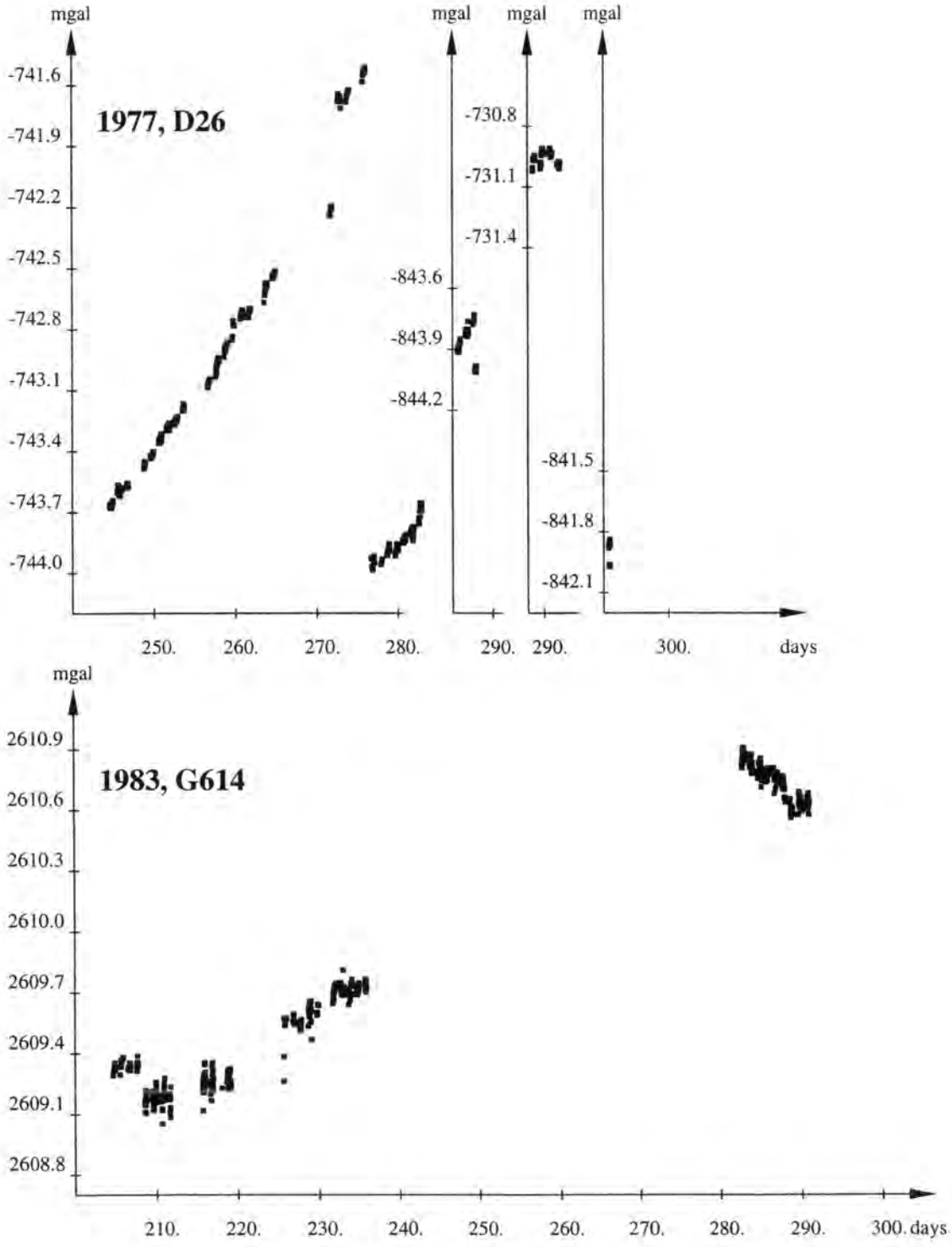

Fig. 2.10 d : Drift of gravity meter D26 in 1977 and G614 in 1983. The different gravity axis of D26 are due to re-adjustment of the measuring screw to be able to measure the entire Yellowstone gravity network.

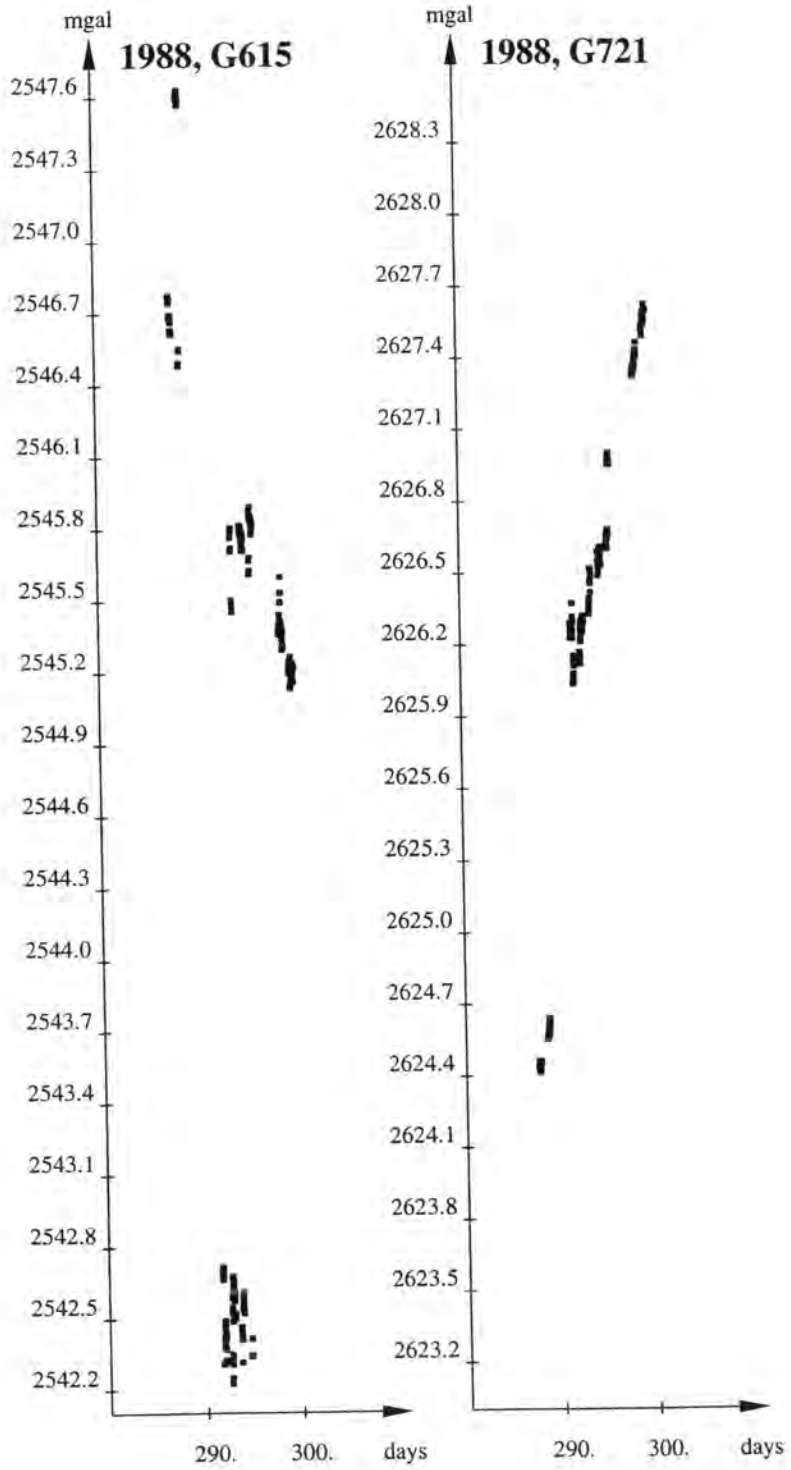

Fig. 2.10 e : Drift of gravity meter G615 and G721 in 1988. Both instruments show extremely high drift rates. Strange tares occurred with G615

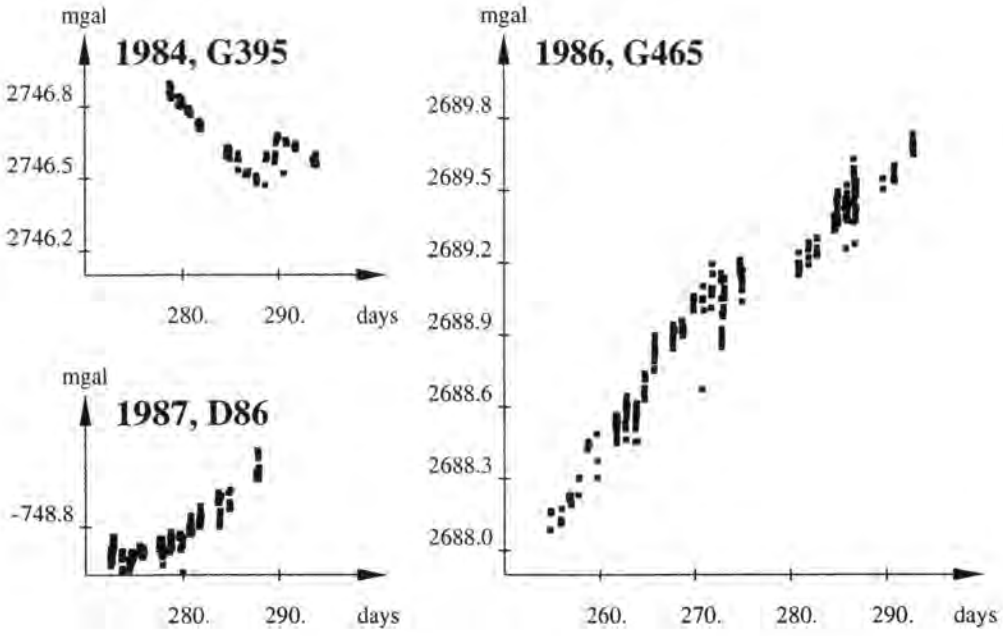

Fig. 2.10 f : Drift of gravity meters G395 in 1986, G465 in 1986, D86 in 1987

2.4 Observed Yellowstone Gravity Changes

All gravity data were reduced to the base station, 11 mdc, at Canyon Junction, that was assigned a value of 979888.130 mgal. (s. chapter 2.3.5, table 2.3)

Figures 2.11 : Gravity changes

1977 to 1979

There is a distinct gravity decrease between Canyon Junction and Fishing Bridge with a maximum of -58 ± 20 µgal at station 27 mdc. No significant change can be detected between Fishing Bridge and Sylvan Lake. So the gravity changes occurred within the Yellowstone caldera.

1977 to 1983

The trend of gravity decrease along the Canyon Junction to Fishing Bridge line continues and causes a maximal decrease of -52 ± 11 µgal at station 27 mdc.
There is also a similar gravity decrease across the southern caldera crossing line Madison Junction to West Thumb across the southern caldera, which has about the same amplitude (-57 ± 14 µgal at station l 10).

Outside the caldera there are some stations with large gravity changes. However, no significant trends were detected. A lot of these differences are probably due to the arrangement of the measurements, where some neighboring stations were measured in no loop simultaneously, so that the difference of the gravity changes between two adjacent stations was unreliable (e.g. near Madison junction, where there was no connection between the stations with the highest changes p 158, q 158, b 14 and the base station 40 mdc). Probably rough errors or blunders occurred at station t 9 (near Norris, -63 µgal, neighbored stations -15 and -30 µgal), 12 mdc (near Canyon), and l 157 (between Norris and Mammoth).

1977 to 1987

This discussion is short because the effect is a result of the changes between 1977 to 1983 and 1983 to 1987. The gravity decrease along the caldera crossing lines was not as large as it was between 1977 and 1983 and merely significant. All lines outside the caldera showed no significant changes.

1983 to 1987

During this period a measured gravity increase occurred over the caldera lines, which is not statistically significant (+17 ± 10 µgal) in f 11a (between Canyon Junction and Fishing Bridge); +32 ± 16 µgal in h 10 (between Madison Junction and West Thumb). Some of the rough errors appear mostly at the same stations as in the period from 1977 to 1983, but with opposite sign. This suggests that the measurements at these points were bad in 1983. This may be in connection with the instrument problems of that year.
A large gravity increase at station 6 gwm (near North East Entrance) occurred (60 µgal compared to +10 µgal in neighbored stations). This point is lying on a bridge, where a high water caused mass changes.
On all lines lying outside the caldera, no significant change was detected.

1984 to 1987

In 1984 the backcountry sites were the focus of the project. Because these stations were each just occupied once, using costly helicopter support, their mean errors are comparably large. There no significant changes are detectable.

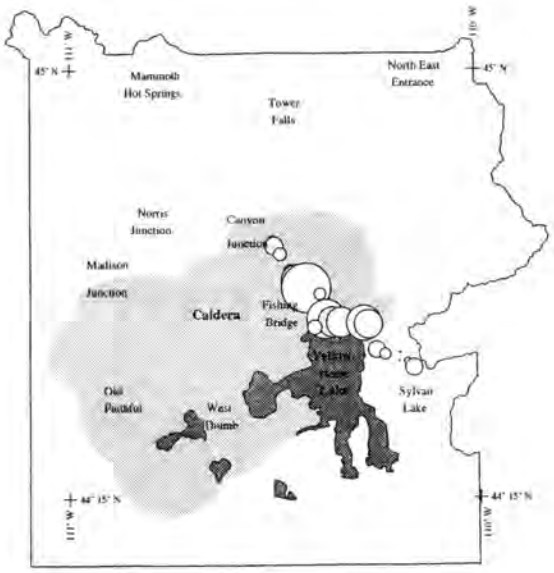

Fig. 2.11 a : Gravity changes from 1977 to 1979 decrease along northern caldera line

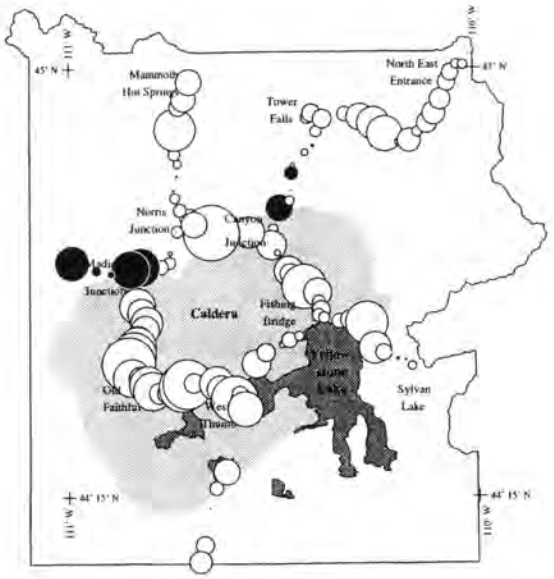

Fig.2.11 b : Gravity changes from 1977 to 1983 decrease all over Yellowstone caldera

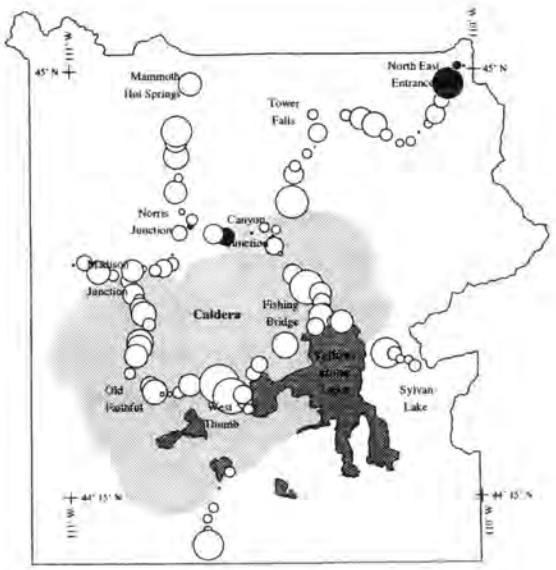

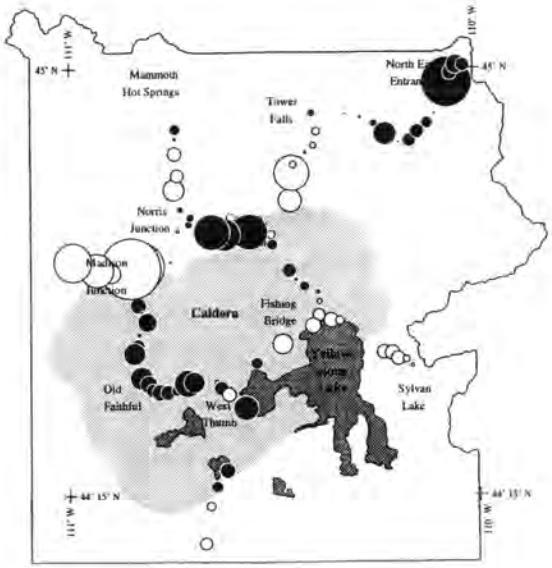

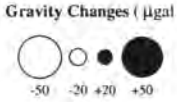

Fig. 2.11 c : Gravity changes from 1977 to 1987 : smaller signals due to change from gravity decrease to increase during this period

Fig.2.11 d : Gravity changes from 1983 to 1987: Slight gravity increase with some rough errors due to bad measurements 1983

1986 to 1987

During this period significant gravity increases occurred over the caldera crossing lines (+30 ±8 µgal in 27 mdc (between Canyon Junction and Fishing Bridge), +45 ± 25 µgal in 52 mdc near Craig Pass, +46 ± 22 µgal in 53 mdc in West Thumb).A rough error is in the data from 36 mdc to 39 mdc on the line from Fishing Bridge to Sylvan Lake in the year 1987, because compared to all data 1986, 1988, 1989, 1990 it shows an offset of about +30 µgal.

1987 to 1988

There seems to be a slight gravity decrease between Canyon Junction and Fishing Bridge.

1987 to 1989

These data also show a gravity decrease between Canyon Junction and Fishing Bridge, but there are several stations that showed a gravity increase, so again the result are considered as insignificant. More significant but still quite weak is the gravity decrease observed between Madison Junction and West Thumb (-35 ± 10 µgal in u7389, no gravity increases).
There are no significant changes in the backcountry stations (helicopter/boat).

1987 to 1990

There was no gravity change detected between Canyon Junction and Fishing Bridge. This may be due to the problems in the measurements of 1990.

1987 to 1991

There is a small but notable gravity increase (< 25 µgal) along the northern caldera crossing line except at station kaygee, which may be due to a rough error in the measurements in 1987. This increase was confirmed by most of the backcountry stations in this region, which also showed an increase (+50 ± 15 µgal in 8405 and 8408).
No significant gravity changes on any of the other gravity lines can be detected.

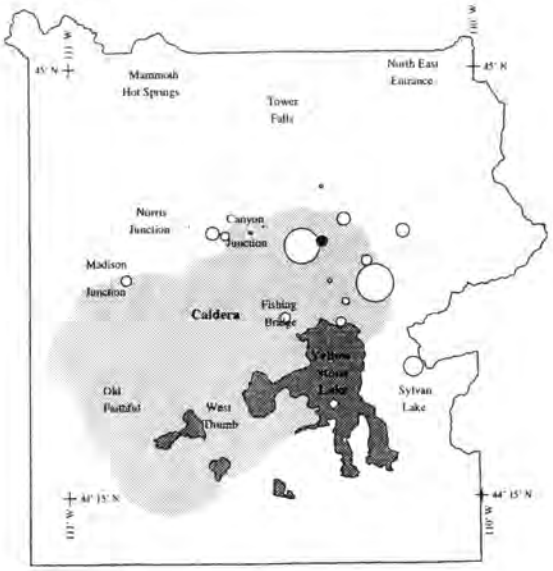

Fig. 2.11 e : Gravity changes from 1984 to 1987 :
First results of backcountry gravity changes

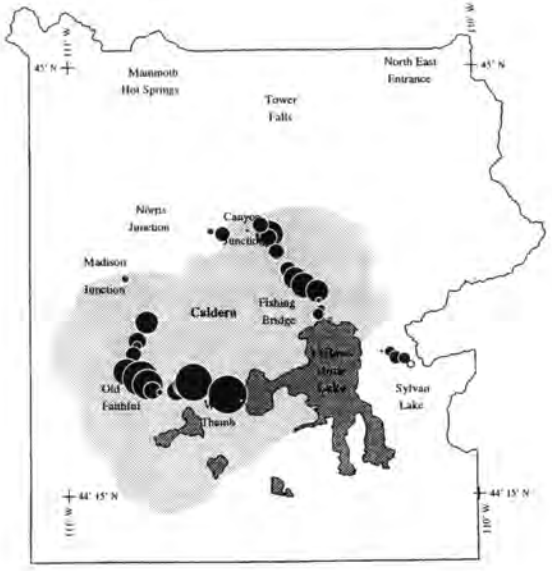

Fig.2.11 f : Gravity changes from 1986 to 1987
Significant gravity increase all over the caldera

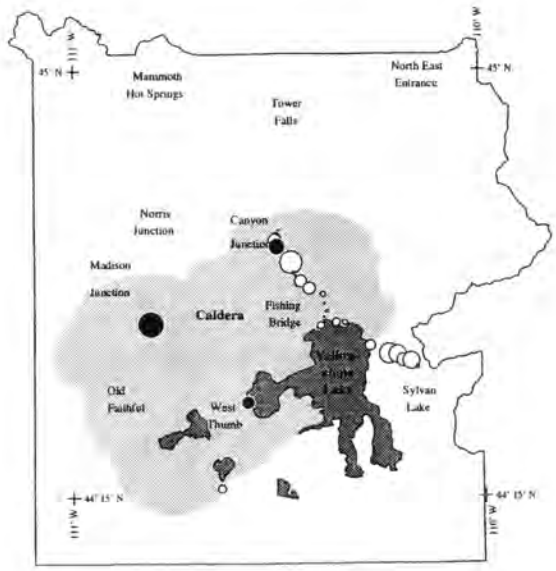

Fig. 2.11 g : Gravity changes from 1987 to 1988
no significant changes

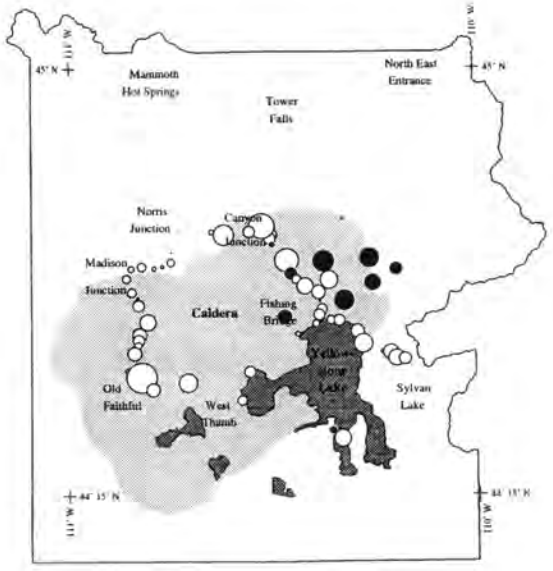

Fig.2.11 h : Gravity changes from 1987 to 1989
no clear trend detectable

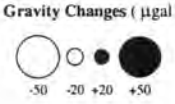

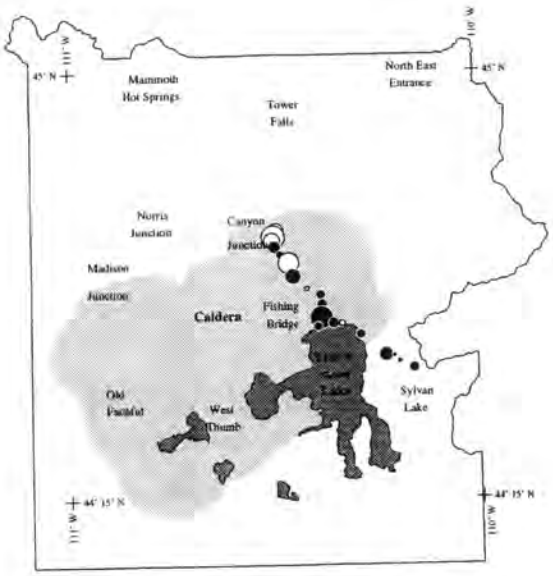

Fig. 2.11 i : Gravity changes from 1987 to 1990 still no significant change

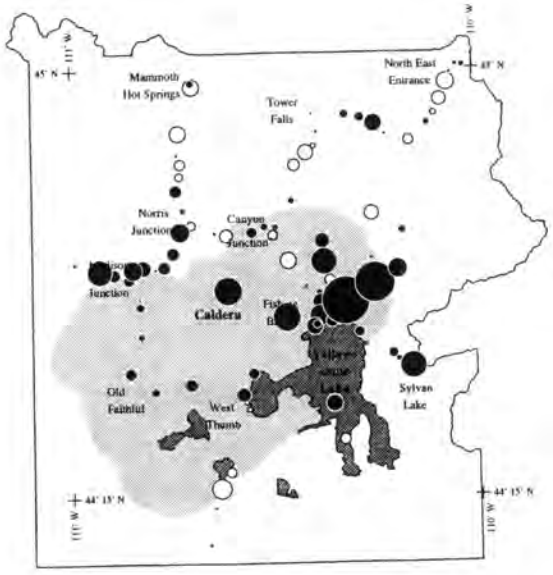

Fig.2.11 j : Gravity changes from 1987 to 1991 A trend towards gravity increase in the caldera

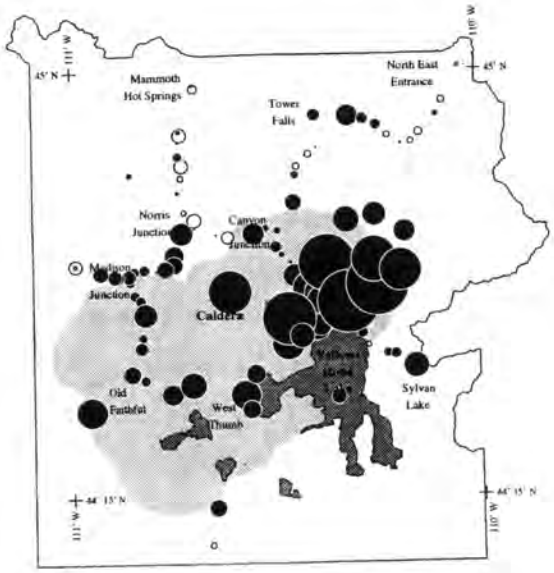

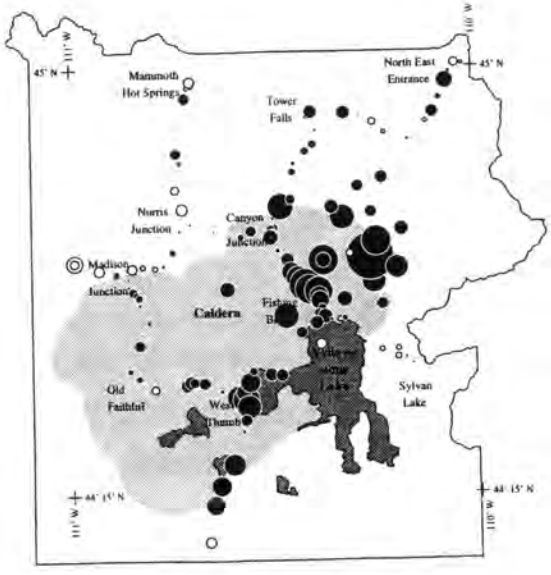

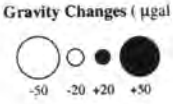

Fig. 2.11 k : Gravity changes from 1987 to 1993 : significant gravity increase in the caldera

Fig.2.11 l : Gravity changes from 1991 to 1993 increase; rather smooth data along lines with strengthened ladder loops in 1991 and 1993.

1987 to 1993

There was a significant gravity increase along the northern (< 45 µgal) as well as the southern (< 40 µgal) caldera crossing line. The backcountry stations around Fishing Bridge showed increases of up to 70 ± 20 µgal.
Outside the caldera, the changes were generally small and not significant.

1991 to 1993

In both campaigns, the strengthened ladder loop method was applied and at least one gravity meter was working very good. It shows, that gravity changes outside the caldera were small and hardly any rough errors occurred, while in the northern part of the caldera, there was a significant gravity increase (up to 35 ± 5 µgal along the road).

2.5 Summary

These results show two areas with large gravity changes inside the Yellowstone caldera : 1) in the north of Fishing Bridge, and 2) between Old Faithful and West Thumb.
There was a gravity decrease of up to -57 ± 15 µgal over the caldera between 1977 and 1983, probably with the highest changes at the begin of this period (1977 to 1979). This decrease may have continued until 1986.
From 1983 to 1987, it seems that there was a slight gravity increase, especially from 1986 to 1987 when there was a significant change of up to +30 ± 8 µgal. After that, from 1987 to 1991, the gravity seemed to be stable along this line, with a slight tendency towards increase. A very clear increase was measured from 1991 to 1993 (maximally +35 ± 5 µgal). From 1987 to 1989 gravity seems to have decreased along the southern caldera line (between Madison Junction and West Thumb), but no significant changes can be found on the same line from 1987 to 1991 and from 1987 to 1993 there was an increase like at the northern caldera line.
The lines outside the caldera showed no measurable changes. However, there were a lot of blunders in the results, especially during the first campaigns. They are mainly due to inefficient choice of loops (sometimes no ties between neighbored points). As the results from 1991 to 1993 show, these errors can be significantly reduced by applying the strengthened ladder loop method.

3. Other Geodetic and Geophysical Results

3.1 Yellowstone Precision Leveling

Gravity changes are mainly due to height changes . However, they are also influenced by mass changes. If the height changes are determined by an independent method, it is possible to interpret the two changes in a combined way. It is of particular interest to look at the factor between the gravity and the height changes and its value compared with the free-air gradient (-0.3086 mgal/m, see also chapter 4.2). The classic method to determine height changes is leveling. With precision leveling, an accuracy of ~ $\sqrt{D}$ mm can be achieved, where D is the leveled distance in km.

3.1.1 Overview

First precision leveling surveys over the whole Yellowstone National Park were done in 1923 and partly repeated in 1934 and 1960 (Pelton & Smith, 1982). From 1975 to 1977 the entire Yellowstone leveling net was re-surveyed and relative height changes of up to + 70 cm were discovered in the inner caldera lines from Canyon Junction to Fishing Bridge and from Madison Junction to West Thumb. Beginning in 1984, the line from Canyon Junction to Fishing Bridge to Lake Butte was re-leveled annually. In 1987 the whole network was re-measured. In 1986, the line from Madison Junction to West Thumb was re-leveled. The data show, that the heights along the northern caldera line increased from 1976 to 1984 by up to 120 mm, remained constant until 1985 and then decreased with a maximum velocity in 1987 ($\frac{\Delta h}{a} > -40$ mm) until 1993 (Dzurisin, 1990, and personal communication). The southern caldera line also showed a height increase from 1976 to 1986 ($\Delta h < 90$ mm) and a decrease from 1986 to 1987 ($\Delta h > -20$ mm).
Here only the data from 1975 to 1991 will be discussed. For a discussion of the previous data see Pelton and Smith (1982).

3.1.2 Introduction into Orthometric Heights

Because the equipotential surfaces of the Earth are not parallel, there is a theoretical offset of the height changes along a loop (see e.g. fig. 3.1 : leveling from A to B to C and back from C to A along the equipotential surface):

(3.1) $$\sum_{A}^{A} \Delta n \approx \oint dn \neq 0$$

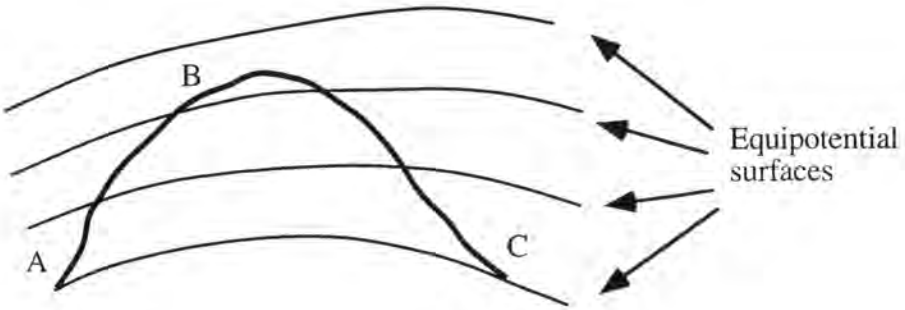

Fig. 3.1 : Non-parallel form of equipotential surfaces

This theoretical offset is avoided by calculating the potential change between two points instead of the height change :

(3.2) $$W_B - W_A = \int_A^B g\,dn \qquad \text{and} \qquad \oint g\,dn = 0 \approx \sum_A^A g\Delta n$$

In this formula, it is also necessary to know the absolute gravity along the leveling line. Furthermore, the geopotential number $C_A = W_A - W_0$ is defined, where W_0 is the potential at the geoid (≈ sea surface). An error estimate dC for the potential number C is, therefore,

(3.3) $$dC^2 = (\Delta n\, dg)^2 + (g\, d\Delta n)^2$$

Taking the potential difference of two neighbored leveling benchmarks, about 1 km apart and with the mean error mentioned above ($\sqrt{D}$ mm), a height difference of about 100 m and a gravity accuracy of about 1 mgal, then

$$dC^2 \approx (10^{-3}\ m^2s^{-2})^2 + (10^{-2}\ m^2s^{-2})^2$$

(with the same order as in the upper formula) and, therefore, it is clear, that almost all the error of the potential number arises from leveling.
The potential number C is not useful for common use because everybody can imagine a height, but not a potential. Therefore, C is normally converted to a dimension in meter.

There are three main heights achieved from C, the dynamic, the orthometric and the normal height. A more detailed discussion on these different heights is in e.g. Wirth, (1990).
The orthometric height h_P of a point P is defined as the length of the plumb line between P and the geoid (fig. 3.2). And so the formula

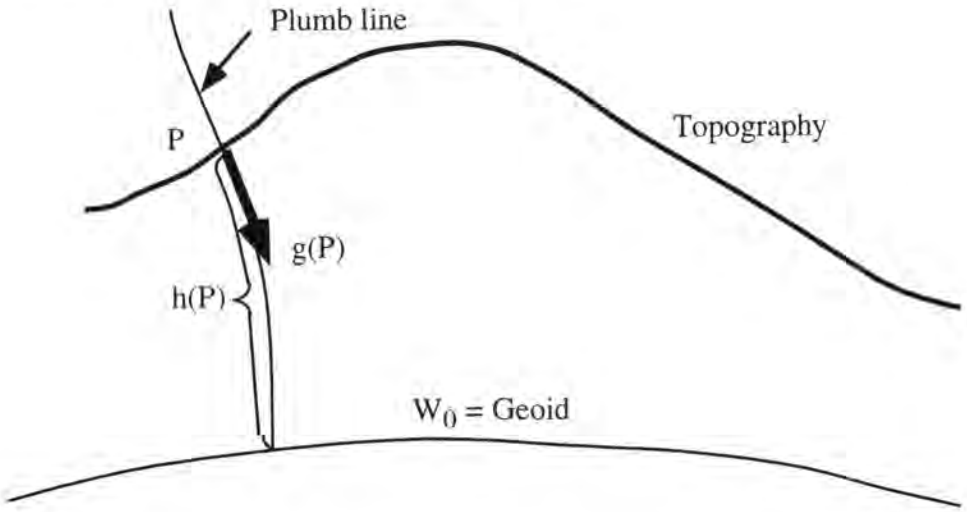

Fig. 3.2 : Orthometric height h measured along the line orthogonal to the equipotential surfaces from P to Q

(3.4) $$C(P) = \int_0^{h_P} g(z)dz \qquad \text{along the plumb line}$$

includes the orthometric height implicitly. To obtain h_P explicitly a mean gravity value $\bar{g}$ is defined,

(3.5) $$\bar{g} = \frac{1}{h_P} \int_0^{h_P} g(z)dz$$

and, therefore,

(3.6) $$C(P) = h_P\, \bar{g} \qquad \text{and} \qquad h_P = \frac{C(P)}{\bar{g}}$$

It is thus necessary to calculate $\bar{g}$. Generally it is sufficient to take the free-air gradient (-0.3087 mgal/m) and the effect of the Bouguer slab (0.1120 mgal/m) into account

$$(3.7) \qquad g(z) = g(h_P) + 0.3087\,(h_P - z)\,\frac{mgal}{m} - 2^{*}\,0.1120\,(h_P - z)\,\frac{mgal}{m}$$

$$= g(h_P) + 0.0848\,(h_P - z)\,\frac{mgal}{m}$$

Note that $g(h_P)$ is known and a density of 2.67 $\frac{g}{cm^3}$ is taken, as it is generally assumed for the crust, for the Bouguer slab. Using this approximation for the gravity will lead to Helmert orthometric heights and the integral for $\bar{g}$ becomes

$$\bar{g} = \frac{1}{h_P}\int_0^{h_P} g(h_P) + 0.0848\,(h_P - z)\,\frac{mgal}{m}\,dz$$

$$= g(h_P) + 0.0848\,\frac{h_P}{2}\,\frac{mgal}{m}$$

Giving the Helmert orthometric height h_P as :

$$(3.8) \qquad h_P = \frac{C(P)}{g(h_P) + 0.0424\,h_P\,\frac{mgal}{m}}$$

This equation involves h_P still on both sides. But after one or two iterations, with the leveled height of P as start value, h_P will be determined with sufficient accuracy.

For more accurate orthometric heights, also topographic corrections may be taken into account. Furthermore, if there was a large constant difference dg between the assumed gravity values used to calculate the potential number C and the true gravity values (but the relative gravity values were still accurate) then most of this offset in C will be canceled in the orthometric heights using again assumed gravity values. Let $\bar{g}'$, h' and C' be the assumed values, $\bar{g}$, h and C the true ones; all at the point P, as well as n the leveled height of P. Then $h' = \frac{C'}{\bar{g}'}$ and assuming the difference between the mean gravity $\bar{g}'$ and the gravity g' at P is calculated well enough, which is possible because it is not dependent on the absolute gravity

$$(3.9) \qquad h' = \frac{C + dg\,n}{\bar{g} + dg} = \frac{(C + dg\,n)\bar{g}}{(\bar{g} + dg)\bar{g}} = \frac{C}{\bar{g}} + \frac{dg(n - h)}{\bar{g} + dg} = h + corr.$$

h can also be approximated with

$$\frac{\sum g\, dn}{\bar{g}} \approx \frac{g_{h=\frac{n}{2}}}{\bar{g}} n$$

(in the corr.-term) and the difference between $g_{h=\frac{n}{2}}$ and $\bar{g}$ will not be larger then the difference of the gravity for the entire globe, which is about 1 percent. Thus an incorrect absolute gravity value of 100 mgal in the Yellowstone National Park, which lies at a mean height of about 2000 m, will affect the orthometric heights by 2 mm at most. But because we are only interested in the relative height differences, which are 1000 m at most, and the difference of any absolute gravity values is not larger then 0.3 percent, the effect due to an absolute error of the gravity values can be neglected (s. also table 3.3 for estimated absolute gravity difference of the Yellowstone gravity net).
The effect of neglecting the topography in the Helmert orthometric heights will mainly cancel when the height difference of the same point is taken at two different times :

$$(3.10) \qquad h_2 - h_1 = \frac{C_2}{\bar{g}_2} - \frac{C_1}{\bar{g}_1} = \frac{C_2}{\bar{g}_{2,H} + \frac{1}{h_2}\int_0^{h_2} g_{2,T}(z)dz} - \frac{C_1}{\bar{g}_{1,H} + \frac{1}{h_1}\int_0^{h_1} g_{1,T}(z)dz}$$

Approximation with the first two terms of Taylor series gives

$$\approx \frac{C_2}{\bar{g}_{2,H}} - \frac{C_1}{\bar{g}_{1,H}} - \frac{\int_0^{h_2} g_{2,T}(z)dz}{\bar{g}_2} + \frac{\int_0^{h_1} g_{1,T}(z)dz}{\bar{g}_1}$$

where the first two terms are the same as the height difference of the Helmert orthometric heights. The largest neglected terms are of the dimension $\frac{\int_0^h g_T(z)dz \int_0^h g_T(z)dz}{h\, g^2}$. The effect on gravity of the topography and mass anomalies will not be significantly larger than the effect of the Bouguer slab. It is assumed to be smaller then 200 mgal $\approx 2 \cdot 10^{-4}$ g at a height of 2000 m. Then these terms are about $4 \cdot 10^{-8}$ h or 0.1 mm at 2000 m. Additionally, they will mainly cancel because they are once taken positive and once negative. So the sum of these terms will be smaller then 0.1 mm.

If the topography did not change drastically between the two times of observations, then $g_{1,T}(z) \approx g_{2,T}(z+h_2-h_1)$ and the integral $\int_0^{h_1} g_{1,T}(z)dz \approx \int_{h_2-h_1}^{h_2} g_{2,T}(z)dz$. So the difference between the Helmert orthometric height difference and the real orthometric height difference becomes again, by approximation with the first two terms of Taylor series,

$$(3.11) \quad -\frac{\int_0^{h_2} g_{2,T}(z)dz}{\bar{g}_2} + \frac{\int_0^{h_1} g_{1,T}(z)dz}{\bar{g}_1} \approx -\frac{\int_0^{h_2-h_1} g_{2,T}(z)dz}{\bar{g}_2} + \frac{(\bar{g}_1-\bar{g}_2)\int_0^{h_1} g_{1,T}(z)dz}{\bar{g}_1^2}$$

Taking the same assumption as above, the first term on the right hand side is about $2 \cdot 10^{-4}(h_2-h_1)$. In the second term, $|\bar{g}_1-\bar{g}_2| < 0.1$ mgal if we take the results of Yellowstone National Park as reference and the value will be $< 10^{-7}$ m.

As a result we conclude that the difference between Helmert orthometric heights and exact orthometric heights is $< 2 \cdot 10^{-4} (h_2 - h_1)$.

Similar analyses as above show, that it is accurate enough for calculating height changes, just take the leveled height differences instead of the orthometric height differences. The more complicated method to compute orthometric heights makes only sense, if there is a loop leveled to adjust the theoretical closure offset due to the non-parallelity of the equipotential surfaces (eq. (3.1), fig. (3.1)).

Because some of the Yellowstone leveling data involve loops (1975 to 1975 and 1987), it is advisable to reduce all leveling data to orthometric heights, also the results of years, where just the line from Canyon Junction to Sylvan Lake was measured.

Furthermore, it is necessary to have orthometric heights to compare the leveled heights with the GPS heights and this may be even a more important reason to calculate orthometric heights.

3.1.3 Discussion of the Results

The height changes from 1976 to 1987, the two last periods of whole leveling network measurements, have a very similar form as the changes from 1923 to 1976 (see fig. 3.3). The entire caldera underwent uplift, with a maximum rate in the middle of the Hayden Valley of 10 mm/a. This value is not representative for the actual rate of height changes in the Yellowstone caldera, because measurements along the line from Canyon Junction - Fishing Bridge - Lake Butte show an increase of height until 1984, then rather abruptly reversed to subsidence. Unfortunately, no measurements are available north-east of the

Hayden Valley in the remote backcountry of the north-east caldera, where I assume crustal deformation must also be large, but access for leveling is not possible. There, the GPS stations established in 1987 will help to monitor the height changes. Outside the caldera only minor changes were found. Especially a small depression near Tower Falls of about -20 mm shall be mentioned here.

The line Canyon Junction - Fishing Bridge - Lake Butte (Table 1.1, app. C) shows uplift between 1976 and 1984 with a maximum rate of 20 mm/a. Until 1985, this value stayed constant and started to decrease afterwards with a rate of about -15 mm/a to -20 mm/a (fig. 3.5). The maximum velocity was approximately that of 1987 with up to -35 mm/a. From 1988 to 1993, the maximum changes seem to be every year about -15 to -20 mm.

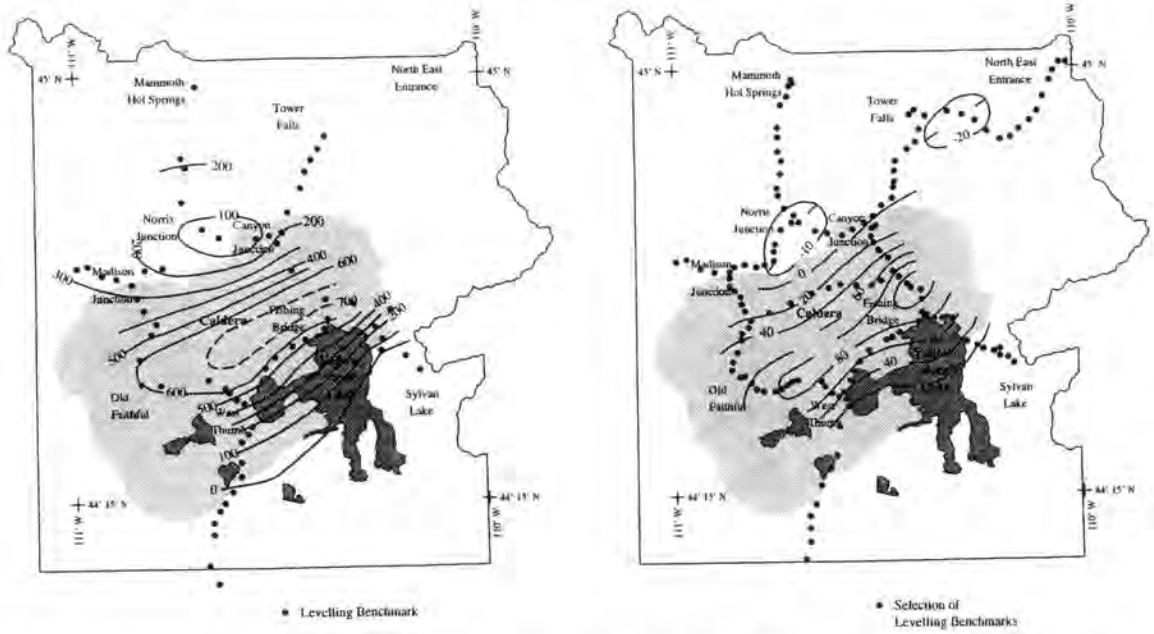

Fig. 3.3 : Yellowstone Height Changes from 1923 to 1976 (left side, after Pelton and Smith (1982)), and from 1976 to 1987 (in mm). Both distributions of height changes show basically the same pattern. In the period from 1976 to 1987, the height increase changed to subsidence in 1984.

A question is, why the caldera-wide of uplift, from 1976 to 1984, reverted to a subsidence. There seem to be several possible explanations. The first one is, that this change is connected with an earthquake swarm of magnitude 3.5 to 4.5 in the north-west of the Yellowstone National Park in 1985. Second was the effects of the Ms 7.5 Hebgen Lake earthquake in 1959. This last earthquake caused an immediate height change of 6 m just in the north-west of the border of the Yellowstone National Park. A trend of height decrease since 1923 in the Yellowstone caldera was possibly masked by fluidmechanical effects of this earthquake in the weak geological structure of the caldera. It may also be, that the hydrothermal pressure within the Yellowstone caldera became smaller due to

cooling of rhyolithic magma. This cooling may also include thermal contraction of the magma itself and of the overlying material. Another reason could be magmatic mass transfer (Fournier et al, 1990).

Nonetheless, it seems to be critical to expect, that the trend of the vertical movements did not change from 1923 to 1976, because geological features at the coastline of the Yellowstone Lake reveal, that trends changed several times since the latest ice age 10'000 years ago. Though, the amplitude of the changes from 1923 to 1976 with up to 13.5 mm/a were just slightly smaller than the contemporary changes.

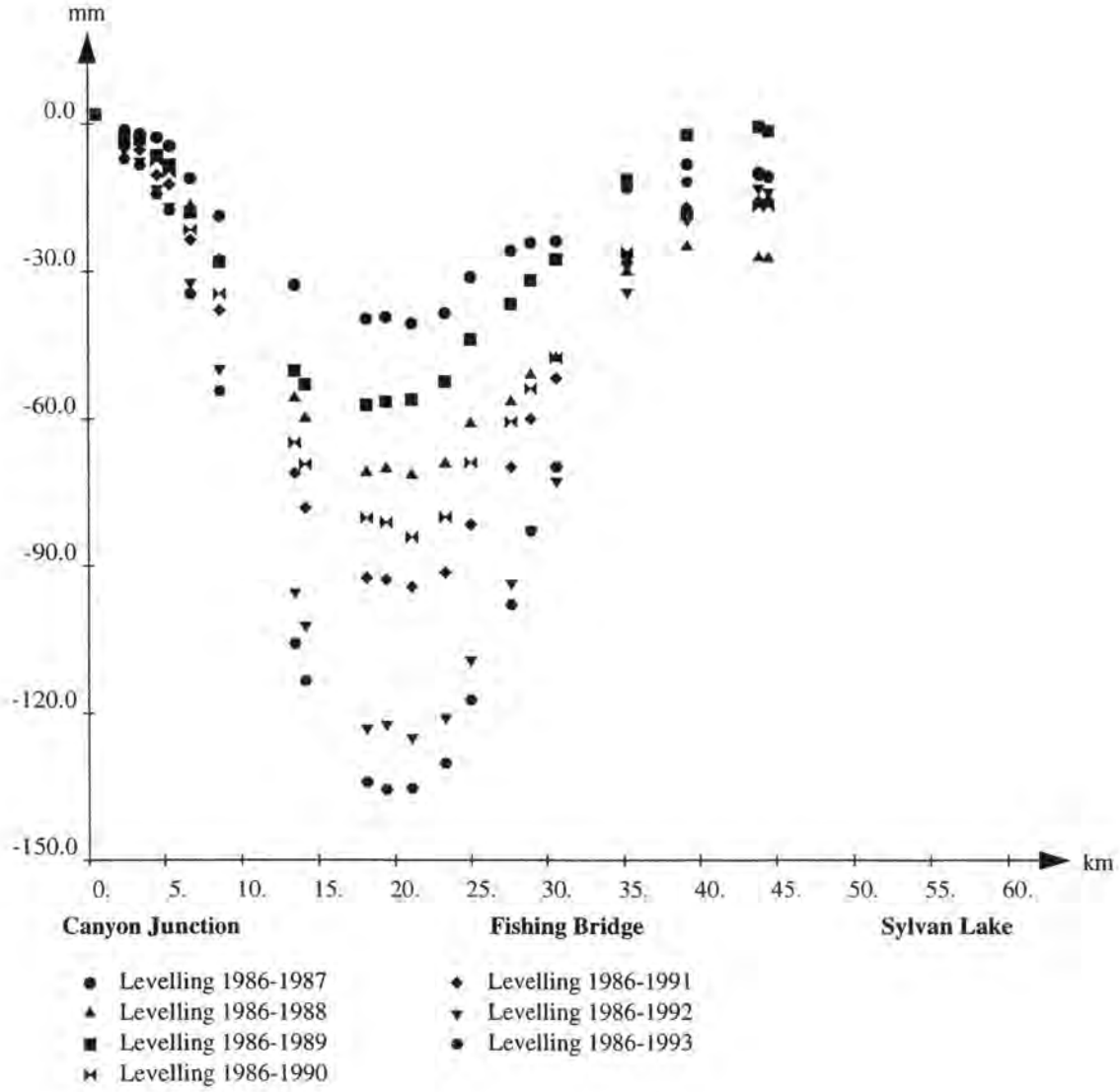

Fig. 3.5 : Height changes along the northern caldera crossing line from Canyon Junction to Fishing Bridge to Sylvan Lake from 1986 to 1993 (in mm). The highest rates were measured from 1986 to 1987 and from 1991 to 1992. The maximum mean error is less than 10 mm

3.2 Yellowstone GPS Data

Two major geodetic parameters, gravity and height, and the determination of their changes in the Yellowstone National Park region were the prospects of until now.
The purpose of GPS is to measure the distances between the stations of a network with high accuracy in a three dimensional system. So, additionally to height changes, GPS provides also horizontal displacements.
In 1987 a GPS network was installed in the Yellowstone National Park. 1989, 1991 and 1993 repetition measurements were performed. The data processing was done mainly by C. Meertens (1991) at the UNAVCO, Boulder CO, USA. Here a brief overview over the results shall be given.
The Yellowstone GPS net is part of a GPS network that extends from the Hebgen Lake Region (MT) down to the Grand Tetons (WY). It consists of almost 100 stations and about 50 of it lie within or close to the Yellowstone National Park (fig. 3.5).
In 1987 and 1989, the observation windows were about 6 hours a day. Each station was occupied at least for two to three days with Texas Instrument receivers 4100 in 1987, and by Trimble 4000SD and 4000SDT in 1987. In the 1991 and 1993 campaigns, the observation time was seven hours per day, except for some semi-permanent stations in backcountry regions with 15 hours observation times. Again, each station was occupied at least for two days. The receivers used were Trimble 4000SST in 1991 and Trimble 4000SSE in 1993.
The data reduction was done with the Bernese GPS software. The mean rms of the day-to-day scatter of the baselines are about $\sigma_H = \pm 0.7$ cm for the horizontal components and $\sigma_V = \pm 1.3$ cm for the vertical displacements.
From the GPS data, the height changes of the Yellowstone caldera since 1987 are clearly visible. It is about 2 to 3 cm/a for the period from 1987 to 1993 (fig. 3.6). The recognition of the decrease in south-east to north-west direction is more or less coincident with the one of the caldera. In the south-west to north-east direction, this may be the case as well. However, this extension is not very well determined, especially in the north eastern region.
Along with this decrease, there is a contraction towards the area with maximum height displacements. Additionally to that, there are significant displacements in the northern part of the Yellowstone National park in eastern direction. This shift may be in connection with the 1959 Hebgen Lake earthquake.

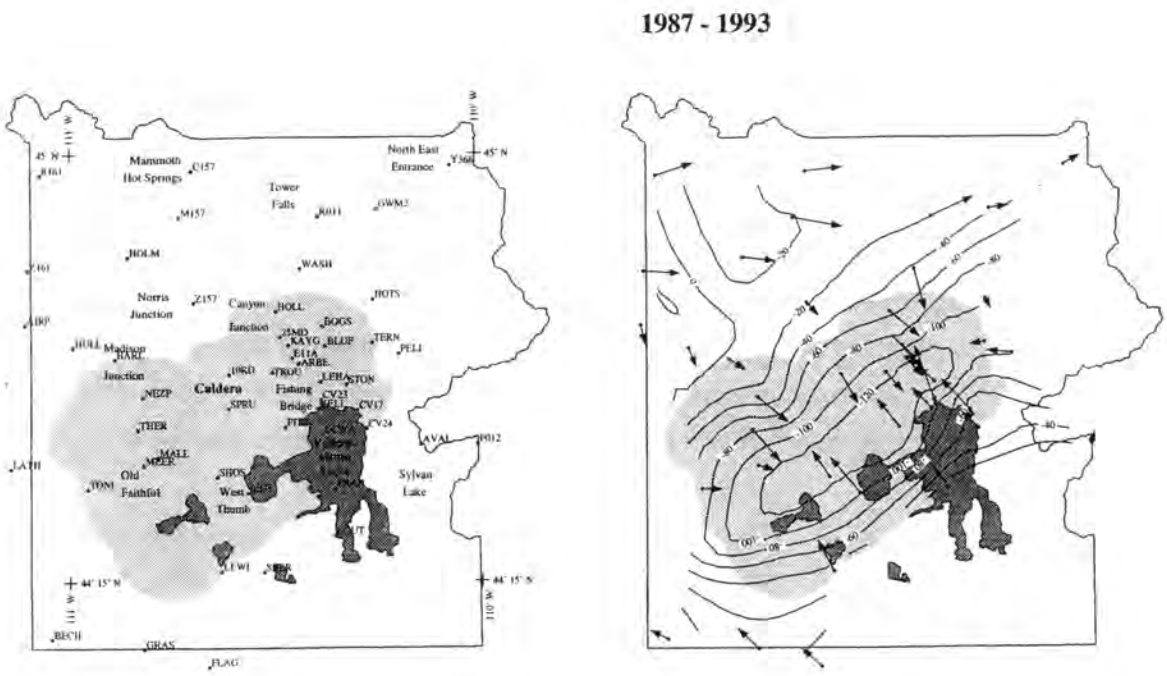

Fig 3.5 : Yellowstone GPS Stations

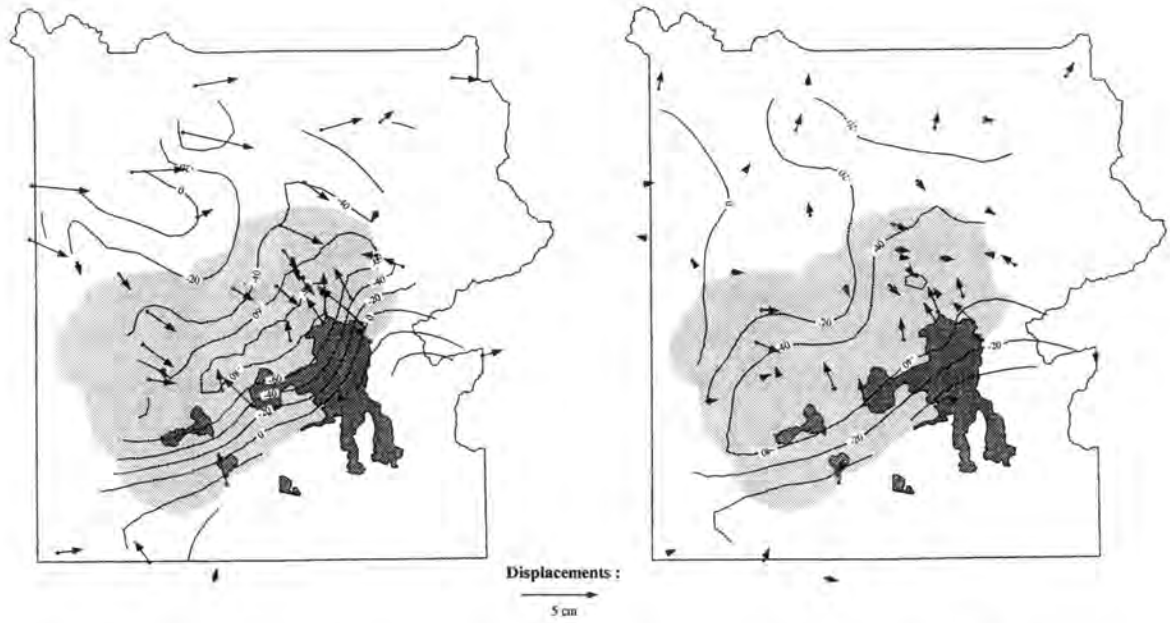

Fig 3.6 a - c : Yellowstone GPS changes, displacements relative to the station ARBE (Hayden Valley). Height changes in mm. The mean error of the displacements is ≈ 10 mm.

3.3 Yellowstone Regional Gravity Anomaly

The regional gravity field of the Yellowstone National Park presented here was taken from an USGS data base of 600 stations (Carle et al. 1991) which included the 200 precision gravity stations of the University of Utah. It shows a regional Bouguer anomaly of -60 mgal in of the Yellowstone caldera that extends beyond the rim of the caldera to the north. This is an indication that there exists a huge lack of mass in the Yellowstone caldera area compared to the surrounding mountains. This anomaly is partly due to the caldera filling material, but must also have additional causes, because the anomaly extends well over the caldera rim in the north-east.

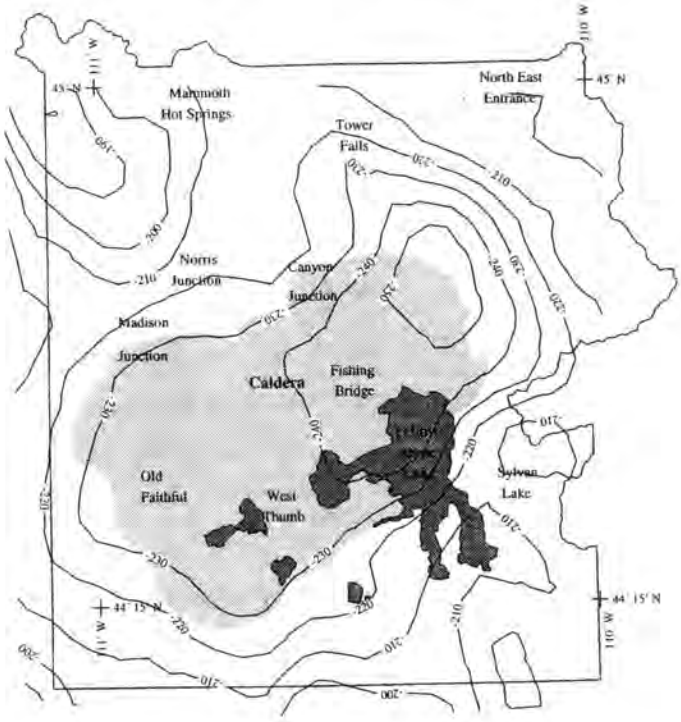

Fig. 3.7 Yellowstone Bouguer Anomaly. The enormous anomaly of -60 mgal compared with the surrounding regions in the Yellowstone caldera indicates a large density difference between the Rocky Mountains and the caldera filling material.

3.4 Earthquake Distribution and Seismic Velocity Models

The Yellowstone area is a seismic highly active zone. Because of the risk of seismic hazard, several seismic stations are distributed over the National Park. The local earthquakes recorded by these stations from 1973 to 1993 (fig 3.8) were processed by Miller (1994) to obtain a 3D model for the p-wave velocity and the s-wave velocity of the

Yellowstone region (fig. 3.9). Smith et al (1982) and Lehmann et al (1982) used a seismic profiling experiment to obtain a p-wave velocity model of the upper crust, extending well over the Yellowstone National Park (fig. 3.10)

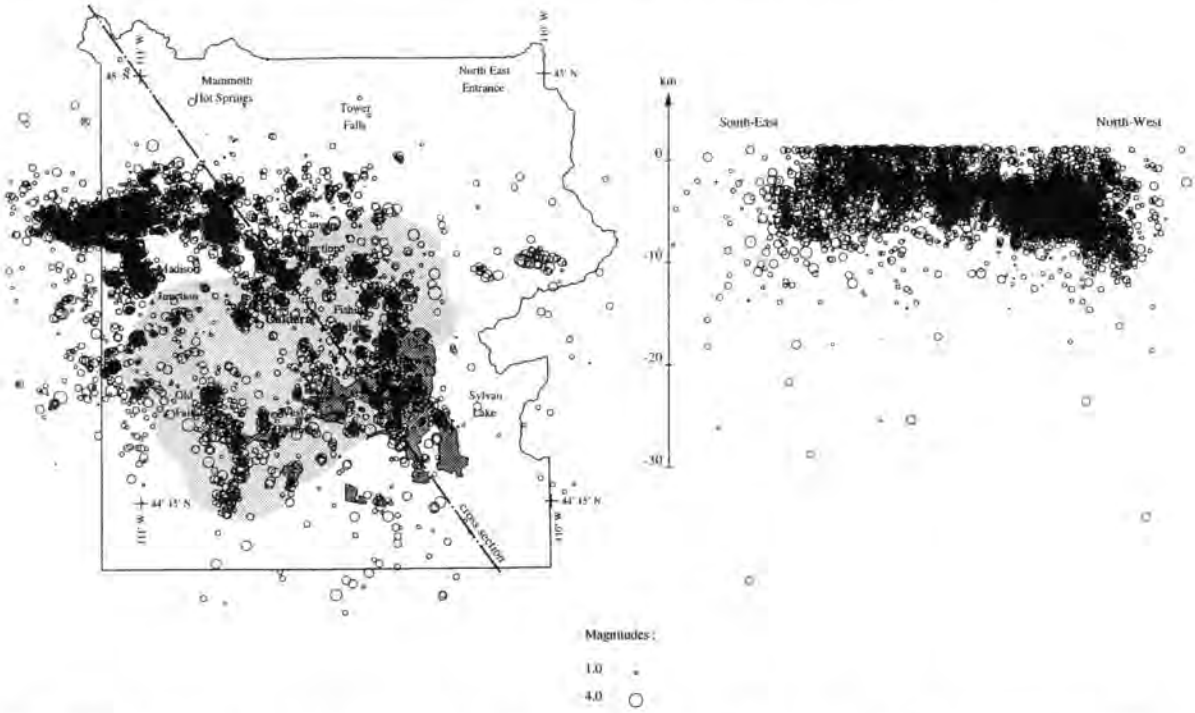

Fig. 3.8 Yellowstone Earthquake distribution from 1973 to 1993. Horizontal distribution and cross section from south-east to north-west. The swarm north-west of the Yellowstone caldera was measured mainly in 1985.

From the distribution of seismic p-wave velocity and gravity anomalies, a well constrained density model can be obtained by using velocity-density relationships such as Birch (1961), Woollard (1975), Kahle and Werner (1981) (s. chapter 4).

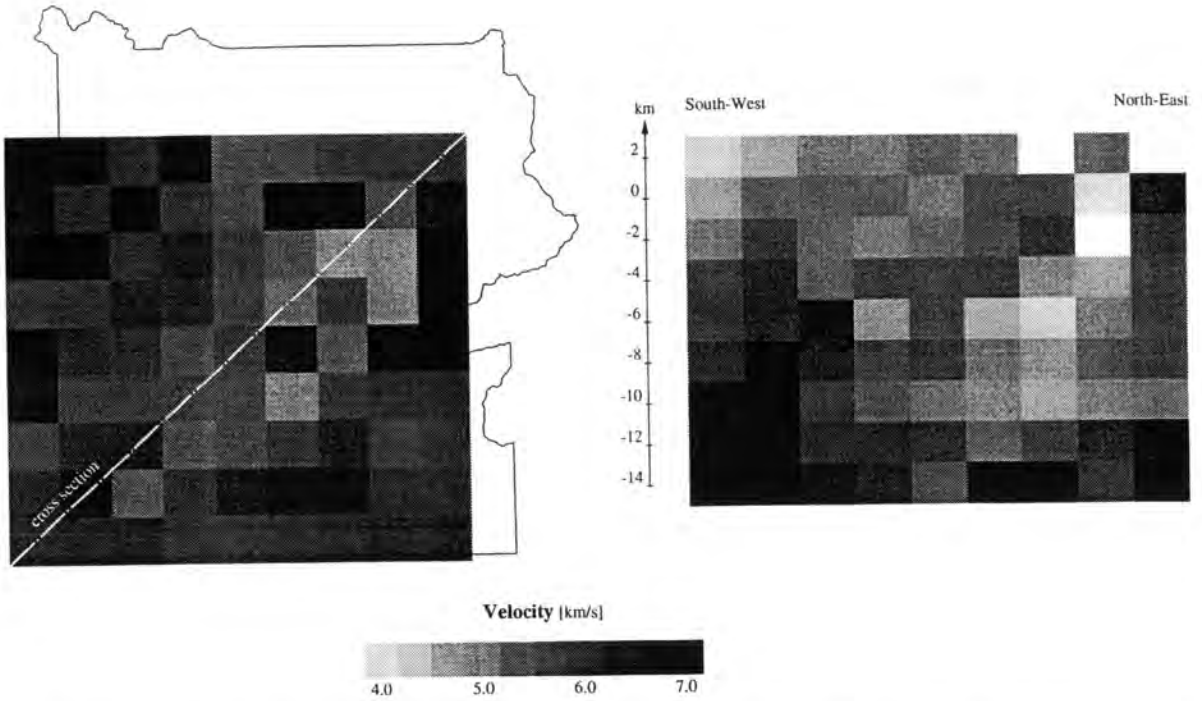

Fig. 3.9 Yellowstone p-wave velocity in a depth of 8 km and along a cross section from south-west to north east (after Miller 1994) show a velocity decrease within the Yellowstone caldera.

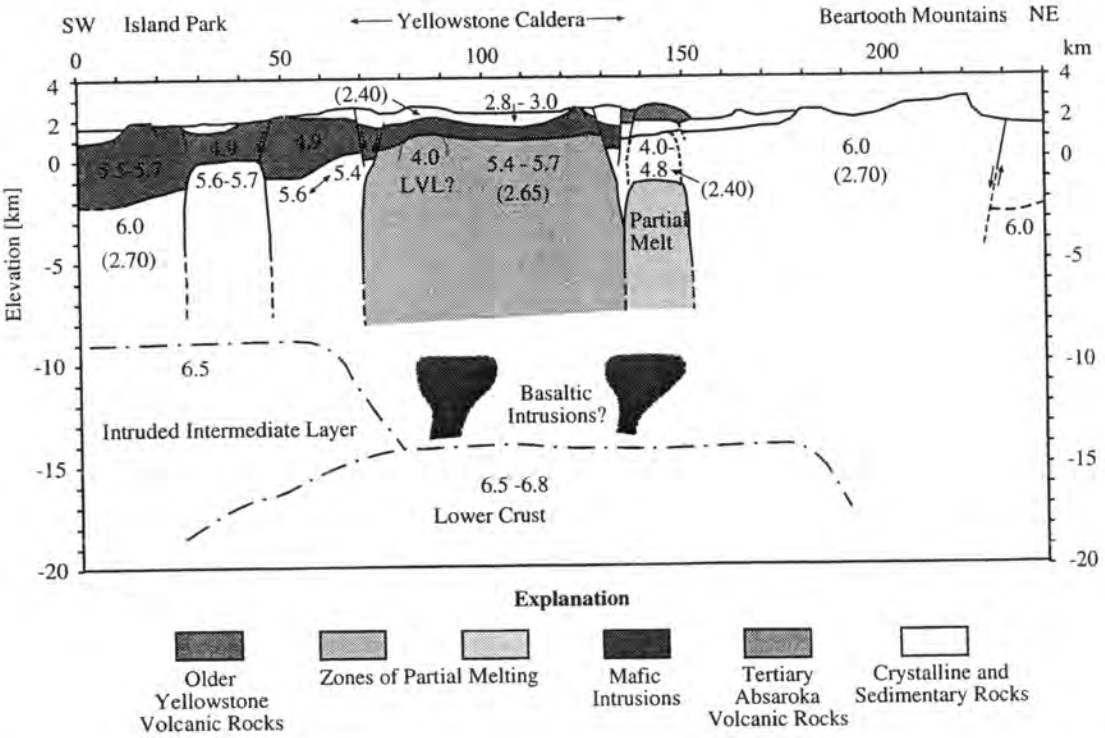

Fig. 3.10 Composite upper crustal p-wave velocity cross section for the Yellowstone volcanic plateau, interpreted from controlled source data (Schilly et al. (1982), Lehmann et al. (1982), Smith et al. (1982), Brokaw (1985))

4. Physical models

Up to this point in the thesis, the reductions of the gravity, leveling and GPS measurements were described and the results were shown for each method. The following chapters are concerned with the combined analysis of the three methods. The goal is to construct possible physical models, that fit the measured values.

4.1 Analysis of Changes in the Earth Potential Field and its Derivatives Due to Crustal Deformation

All following deductions will be made for three-dimensional problems. The formulations for two dimensions are similar and some special formulas are given for the two dimensional case.
The potential field of a point P or any derivative of it, f(P) can be written as a function of the form

$$(4.1) \qquad f(P) = \int_{V_A} \int \int G\rho(\mathbf{x})\, g(\mathbf{x} - \mathbf{x_P})\, dx\, dy\, dz = \int_{V_A} G\rho\, g(P)\, dV_A$$

with

G	: universal gravity constant
$\mathbf{x}$	: vector of a point (x, y, z)
$\rho(\mathbf{x})$	: density at a point $\mathbf{x}$
g	: function depending on f

For example, if f is the potential itself, then $g = \dfrac{1}{\sqrt{(x - x_P)^2 + (y - y_P)^2 + (z - z_P)^2}}$

The volume can be divided into a part, V_E, which does not move from time t_1 to t_2 and one which moves, V_M, in the same period. Furthermore, the index i corresponds to a value at time t_i. The integral V_M again can be divided into a part within the geoid, V_G, and the part of the topography, V_T.

$$(4.2) \qquad f(P) = \int_{V_A} G\rho g(P)\, dV_A = \int_{V_F} G\rho g(P)\, dV_F + \int_{V_M} G\rho g(P)\, dV_M$$

Furthermore, the normal gravity value at a point P is given by :

(4.3) $$g_0(P) = \int_{V_F} G\rho\, g(P)\, dV_F + c(P)$$

with c(P) a correction term depending on the regional field at P.
For a crustal movement within the volume V_M , from time t_1 to t_2

(4.4) $$\mathbf{x}_2 = \mathbf{x}_1 + \mathbf{d}(\mathbf{x}_1)$$

where **d** is the displacement vector. This movement leads to a change in the function f at a point P :

(4.5) $$f(P_2) - f(P_1) = \int_{V_{A_2}} G\rho_2 g(P_2)\, dV_{A_2} - \int_{V_{A_1}} G\rho_1 g(P_1)\, dV_{A_1} =$$

$$= \int_{V_F} G\rho_1 g(P_2)\, dV_F + \int_{V_{M_2}} G\rho_2 g(P_2)\, dV_{M_2}$$

$$- \int_{V_F} G\rho_1 g(P_1)\, dV_F - \int_{V_{M_1}} G\rho_1 g(P_1)\, dV_{M_1}$$

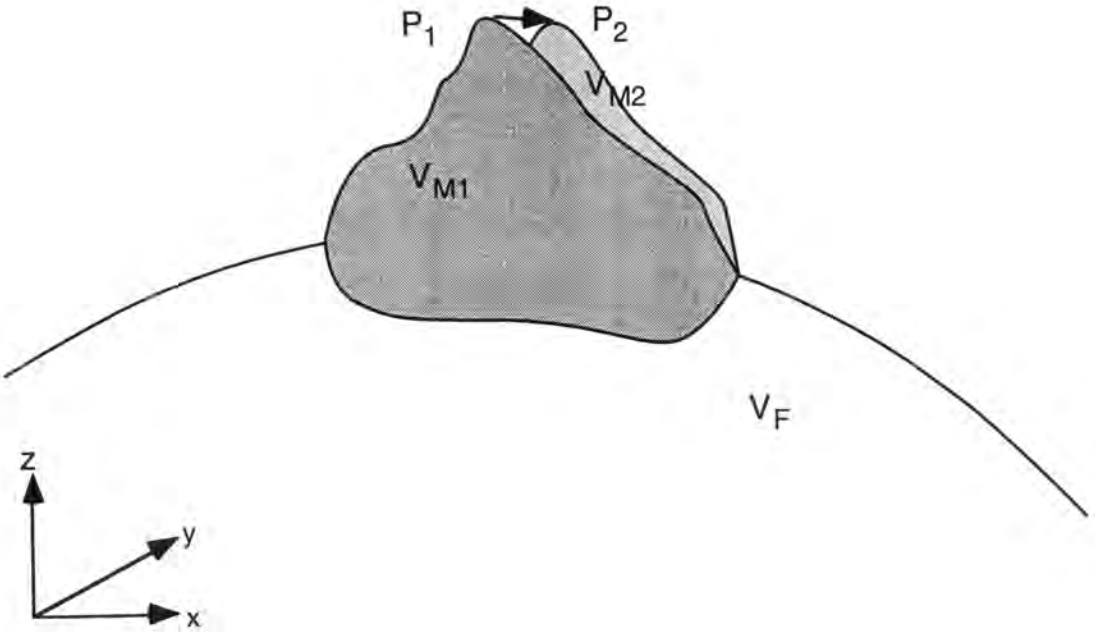

Fig. 4.1 : Deformation from t_1 to t_2

where the volume V_{M_2} is the transformed volume of V_{M_1}. Note, that the density in the integral over V_F remains constant and can be taken as ρ_1. Introducing (4.3) and assuming that $c(P_2) = c(P_1)$ (constant regional field) gives

$$(4.6)\quad f(P_2) - f(P_1) = g_0(P_2) - g_0(P_1) + \int_{V_{M_2}} G\rho_2 g(P_2)\, dV_{M_2} - \int_{V_{M_1}} G\rho_1 g(P_1)\, dV_{M_1}$$

The moving part shall be subdivided into flat faced polyhedrons of constant density. Within each polyhedron e there shall be a linear displacement **d**

$$(4.7)\qquad \mathbf{d}(\mathbf{x}) = \begin{pmatrix} d_x \\ d_y \\ d_z \end{pmatrix}_e = \begin{pmatrix} a_{xx}\,x + a_{xy}\,y + a_{xz}\,z + a_{x0} \\ a_{yx}\,x + a_{yy}\,y + a_{yz}\,z + a_{y0} \\ a_{zx}\,x + a_{zy}\,y + a_{zz}\,z + a_{z0} \end{pmatrix}_e$$

with a_{ij} = constant. Because of the law of conservation of mass it is

$$(4.8)\qquad \rho_2(\mathbf{x} + \mathbf{d}(\mathbf{x})) = \rho_2(\mathbf{y}) = \frac{\rho_1(\mathbf{x})}{|J_d|}$$

where $\mathbf{y} = \mathbf{x} + \mathbf{d}(\mathbf{x})$ and $|J_d|$ is the determinate of the Jacobi matrix defined as

$$(4.9)\quad J_d = \begin{pmatrix} \frac{\partial y_x}{\partial x_x} & \frac{\partial y_y}{\partial x_x} & \frac{\partial y_z}{\partial x_x} \\ \frac{\partial y_x}{\partial x_y} & \frac{\partial y_y}{\partial x_y} & \frac{\partial y_z}{\partial x_y} \\ \frac{\partial y_x}{\partial x_z} & \frac{\partial y_y}{\partial x_z} & \frac{\partial y_z}{\partial x_z} \end{pmatrix} = \begin{pmatrix} 1 + a_{xx} & a_{xy} & a_{xz} \\ a_{yx} & 1 + a_{yy} & a_{yz} \\ a_{zx} & a_{zy} & 1 + a_{zz} \end{pmatrix}$$

J_d is constant within one polyhedron and so, also due to mass conservation

$$(4.10)\qquad \rho_{e_2} = \rho_{e_1} \frac{V_{e_1}}{V_{e_2}}$$

where $V_{t,e}$ is the Volume of the polyhedron e at the time t.

Note, that until now just constant density and linear displacements were assumed, but not yet flat faced polyhedrons as elements e. However, the upper assumptions are only valid, if there is no mass diffusion like ground water transport within an element.

If these simplifications are correct, as it shall be assumed, and if the displacements are known, $f(P_2) - f(P_1)$ can be written as

$$(4.11)\quad f(P_2) - f(P_1) = g_0(P_2) - g_0(P_1) + \sum_e G\rho_{e_2} \int_{V_{e_2}} g(P_2)\, dV_{e_2} - G\rho_{e_1} \int_{V_{e_1}} g(P_1)\, dV_{e_1}$$

and introducing (4.10)

$$f(P_2) - f(P_1) = g_0(P_2) - g_0(P_1) + \sum_e G\rho_{e_1} \frac{V_{e_1}}{V_{e_2}} \int_{V_{e_2}} g(P_2)\, dV_{e_2} - G\rho_{e_1} \int_{V_{e_1}} g(P_1)\, dV_{e_1}$$

In the Yellowstone area we are mainly interested in gravity changes, which corresponds to

$$g = T_z = \frac{z}{\sqrt{x^2 + y^2 + z^2}}$$

Then the integrals over V_e can be solved without numerical integration, if V_e are flat faced polyhedrons of constant density by

$$(4.12)\quad T_z = \sum_{i=1}^{n} \sum_{k=1}^{m_i} \left(y_0 + \frac{z_0(c - ba)}{1 + b^2 + c^2} \right) P - z\ R$$

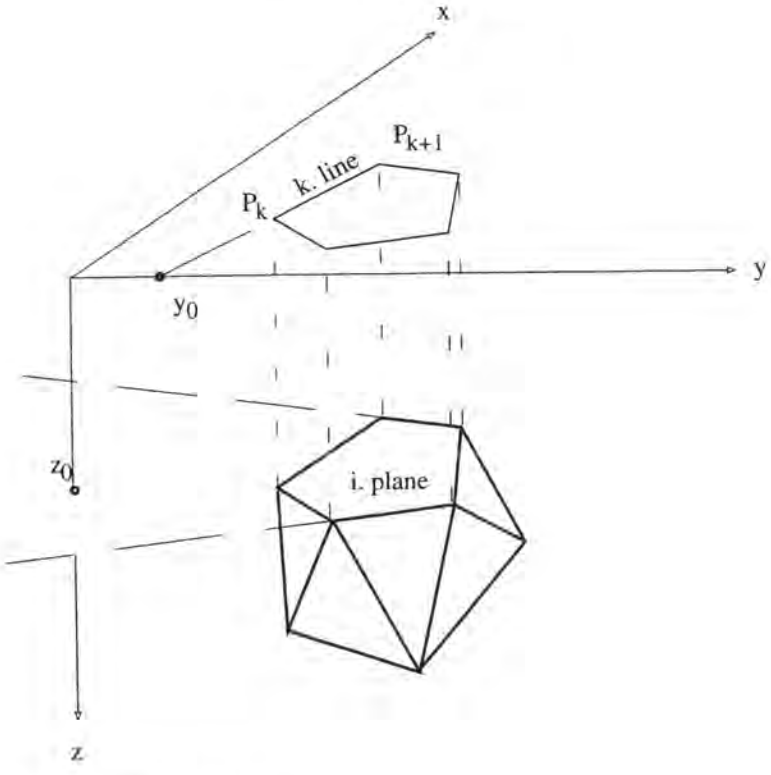

Fig 4.2 : polyhedron

with n : number of faces of the polyhedron
m_i : number of edges of the i. face
$z = z_0 + b\,x + c\,y$: plane equation of a face
$y = y_0 + a\,x$: line equation of an edge, projected to the (x,y)-plane

$$P = \frac{1}{\sqrt{1 + a^2 + (b + ca)^2}} \ln \frac{\dfrac{x_{k+1} + a y_{k+1} + (b + ca) z_{k+1}}{\sqrt{1 + a^2 + (b + ca)^2}} + \sqrt{x_{k+1}^2 + y_{k+1}^2 + z_{k+1}^2}}{\dfrac{x_k + a y_k + (b + ca) z_k}{\sqrt{1 + a^2 + (b + ca)^2}} + \sqrt{x_k^2 + y_k^2 + z_k^2}}$$

$$R = \frac{1}{1 + b^2 + c^2} \left(\arctan \frac{((b^2 + c^2 + 1) y_0 + (c - ba) z_0) x_{k+1} + (b y_0 - a z_0) z_0}{z_0 \sqrt{x_{k+1}^2 + y_{k+1}^2 + z_{k+1}^2}} - \right.$$

$$\left. - \arctan \frac{((b^2 + c^2 + 1) y_0 + (c - ba) z_0) x_k + (b y_0 - a z_0) z_0}{z_0 \sqrt{x_k^2 + y_k^2 + z_k^2}} \right)$$

For two dimensions, the exact calculation is much easier : The effect for a polygon can be expressed by :

$$(4.13)\quad T_z = \sum_{i=1}^{n} 2 \frac{x_{i+1} - x_i + a(z_{i+1} - z_i)}{1 + a^2} - \frac{a z_0}{1 + a^2} \log \frac{\sqrt{x_{i+1}^2 + z_{i+1}^2}}{\sqrt{x_i^2 + z_i^2}}$$

$$- 2 z_0 \left(\arctan \frac{x_{i+1} + a z_{i+1}}{z_0} - \arctan \frac{x_i + a z_i}{z_0} \right)$$

with n : number of sides of the polygon
$z = z_0 + a\,x$: line equation of a side

The volumes can be expressed explicitly by :

$$(4.14)\qquad V_e = \sum_{i=1}^{n} \sum_{k=1}^{m_i} \frac{b\,(x_{k+1} + x_k)(y_{k+1} x_k - y_k x_{k+1})}{6}$$

and the area of a polygon is given by :

(4.15) $$V_e = \sum_{i=1}^{n} \frac{x_{i+1} z_i - x_i z_{i+1}}{2}$$

If the densities ρ_e of the polyhedrons and the displacements are known, the gravity differences can be calculated and compared with the measured gravity values. Paragraphs 4.3 and 5 will emphasize on determination of the densities and displacements. Before that, some simpler estimates are calculated for a one-dimensional case with Bouguer slabs.
The effect of a Bouguer slab is given by

(4.16) $$g_{Bouguer} = 2 \pi \rho G h$$

with

$g_{Bouguer}$	: Bouguer effect
ρ	: Density
G	: Absolute gravitational constant
h	: Thickness of the plate

If the thickness h of plane changes, but the mass remains constant, it is easily verified, that the product ρ h is constant and with that also the Bouguer effect.

4.2 Correlation between Height and Gravity Changes

In chapter 4.1 we developed a relationship between gravity changes and crustal deformation. If there is only a constant extension of a Bouguer plate, we saw that the gravity change will be the free-air effect. This shall be our first assumption.

4.2.1 Factor between Gravity and Height Changes

To find out, whether the gravity changes are in fact only due to the free-air effect, we have to calculate the ratio between gravity and height changes. The obtained value will be the free-air gradient if our assumption is right.

(4.17) $$f = \frac{g_{sta}(t_2) - g_{sta}(t_1)}{h_{sta}(t_2) - h_{sta}(t_1)}$$

with

f	: factor between gravity and height changes
$g_{sta}(t)$	: absolute gravity value at the station sta at the time t
$h_{sta}(t)$	: orthometric height at the station sta at the time t

In Yellowstone National Park absolute precision gravity are not available, with only relative precision gravity measurements, and the heights as the results of the leveling can show an offset to their true heights, too :

(4.18)
$$h_{sta}(t) = h'_{base}(t) + dh_{sta}(t) + dh'_{base}(t)$$
$$g_{sta}(t) = g'_{base}(t) + dg_{sta}(t) + dg'_{base}(t)$$

with

$h'_{base}(t)$	: value introduced for the base station height for the time t
$dh_{sta}(t)$	: orthometric height difference between the station sta and the base station at the time t
$dh'_{base}(t)$	: difference between orthometric height and introduced height at the base station at the time t
$g'_{base}(t)$	: value introduced for the base station gravity for the time t
$dg_{sta}(t)$	: gravity difference between the station sta and the base station at the time t
$dg'_{base}(t)$	: difference between absolute gravity and introduced gravity at the base station at the time t

Let us assume that the height of the base station changed dh from t_1 to t_2. Then, according to (4.17), the gravity change at the base for the same period is $f \cdot dh$. If we fix the assumed height and the gravity values h'_{base} and g'_{base} over the time we get

(4.19)
$$h'_{sta}(t) = h'_{base} + dh_{sta}(t)$$
$$g'_{sta}(t) = g'_{base} + dg_{sta}(t)$$

with

$h'_{sta}(t)$	: height value for the station sta with h'_{base}
$g'_{sta}(t)$	: gravity for the station sta with g'_{base}

and, according to (4.18) for the base station :

$$dg'_{base}(t_2) - dg'_{base}(t_1) = f\,(dh'_{base}(t_2) - dh'_{base}(t_1)) \tag{4.20}$$

Applying (4.20) to (4.17) for other than the base station finally gives

$$f = \frac{g'_{sta}(t_2) - g'_{sta}(t_1)}{h'_{sta}(t_2) - h'_{sta}(t_1)}, \tag{4.21}$$

which is independent of the absolute heights and gravity.
Thus if there are both gravity and leveling measurements at the time t_1 and t_2 an estimate for f is obtained. There will be several stations with complete gravity and leveling measurements at two different times and hence there is again an over-determined problem with the only unknown f :

$$f = l_i + v_i \tag{4.22}$$

with

$$l_i = \frac{g'_{sta}(t_k) - g'_{sta}(t_j)}{h'_{sta}(t_k) - h'_{sta}(t_j)} = \frac{dg_i}{dh_i}$$

n : number of estimates for f

In the adjustment of the gravity and height measurements, the observations are presumed to be Gaussian distributed, and, therefore also the estimates g' and h' and finally the estimates l for f are Gaussian distributed. So the most probable value for f is obtained by minimizing $v^T P v$, with P equal to the inverse of the correlation matrix Q_{ll} of the estimates l, which is a non-diagonal matrix, because the adjusted gravity and especially the adjusted height values are correlated.
Generally, if y is linear dependent on x , so that y = Ax, the correlation matrix of y is given by $Q_{yy} = A Q_{xx} A^T$. Because the equation for l is not linear, we have to linearize it to get Q_{ll}. Further, the height changes $(h'_{sta}(t_2) - h'_{sta}(t_1))$ may become very small compared to the mean errors of the heights and, therefore, the term for l is non-linear. To reduce this non-linearity it is better to make an estimation for the arctan of f

$$f' = \arctan(l_i) + v'_i = l'_i + v'_i \tag{4.23}$$

Then the linearization for l' gives :

(4.24)a $$\Delta l' = \frac{dh}{dg^2+dh^2}\Delta g_2 - \frac{dh}{dg^2+dh^2}\Delta g_1 - \frac{dg}{dg^2+dh^2}\Delta h_2 + \frac{dg}{dg^2+dh^2}\Delta h_1$$

and in matrix writing :

(4.24)b $$\Delta l = A\,(\Delta g_2, \Delta g_1, \Delta h_2, \Delta h_1)^T = A\,x$$

The correlation matrix Q_{ll} is :

(4.25) $$Q_{ll} = A\,Q_{xx}\,A^T$$

Assuming that there is no correlation between the measurements of two different years and no correlation between gravity and height measurements the structure of equation looks like:

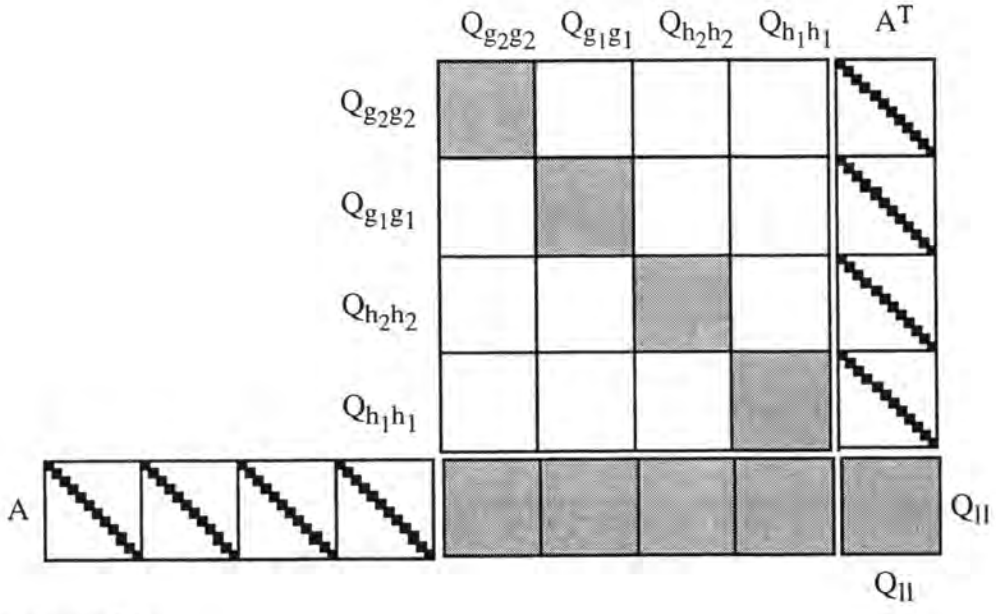

Fig 4.3 : Structure of Q_{ll}

The linearized observation equations become

(4.26) $$v = e\,f - l$$

with

$e^T = (1,1,...,1)$, a n - dimensional vector

and from this we get directly the value for f

(4.27) $$f = \frac{1}{e^T Q_{ll}^{-1} e} e^T Q_{ll}^{-1} l$$

If another value is obtained than the free air gradient for f, then our assumption of a contracting, respectively expanding Bouguer plate was wrong. If we still assume infinite Bouguer plates, but with mass changes, we have the following properties

	height decrease	**height increase**
f < -0.3 mgal/m	gain of mass	loss of mass
f = -0.3 mgal/m (free-air gradient)	no change of mass	
f > -0.3 mgal/m	loss of mass	gain of mass

4.2.2 Results

The upper results and formulas used for the Yellowstone gravity and leveling data give the following factors :

Time	**Factor** [mgal/m]	**Mass Change**
entire National Park		
77 - 87	-0.13± 0.11	increase
Canyon Junction - Fishing Bridge		
77 - 83	-0.17 ± 0.07	increase
77 - 86	-0.31 ± 0.11	-
86 - 87	-0.54 ± 0.15	increase
86 - 88	-0.24 ± 0.14	decrease
86 - 89	-0.24 ± 0.14	decrease
86 - 90	-0.20 ± 0.14	decrease
86 - 91	-0.27 ± 0.07	-
86 - 93	-0.33 ± 0.10	-

Table 4.1 : Factors between gravity and height changes

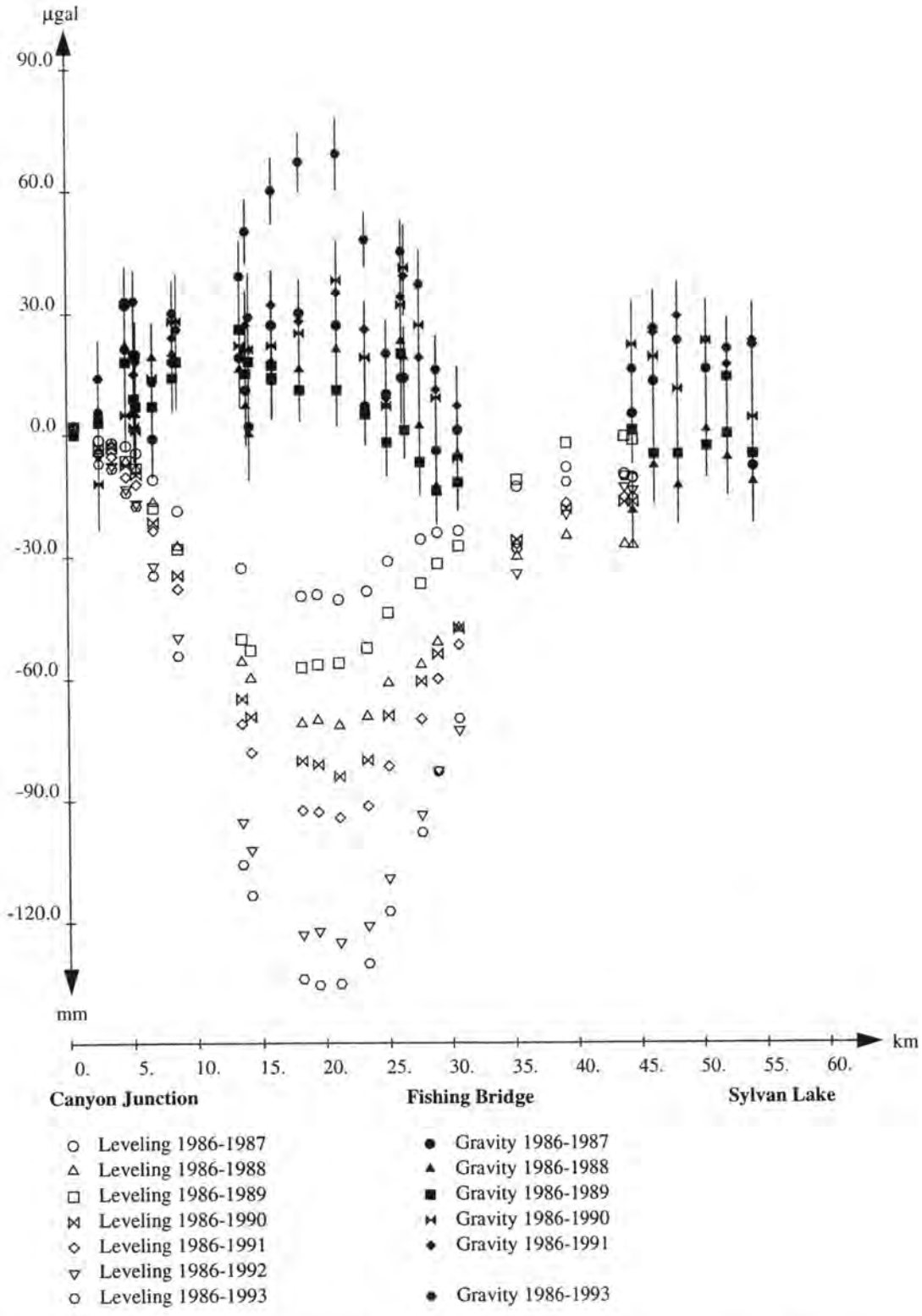

Fig. 4.4 Gravity versus height changes along the northern caldera crossing line. The vertical lines of the gravity changes show their mean errors. While the velocity of the height changes stayed more or less constant, with higher rates from 1986 to 1987 and from 1991 to 1992, the gravity changes occurred mainly from 1986 to 1987 and from 1991 to 1993.

The values of table 5.1 are rather inconsistent and strongly dependent on how the gravity values were obtained. Some rough errors can change the values significantly. Furthermore, for the factors for the time spans starting in 1977, the height data were measured from 1975 to 1977. It was assumed, that the heights remained constant until 1977, although this is probably not valid. A similar assumption was made for 1983, where the gravity changes were taken from this particular year. The height changes, however, were taken from the campaign 1984, because in 1983 no sufficient leveling data were available.

From the factors obtained, it looks as if a mass increase occurred during the uplift period from 1977 to 1983/84. This increase may have even continued until 1987. After that, a mass decrease took place in the period from 1987 to 1990, a time span with continuous height decrease and no significant gravity changes (fig 4.4). However, this is not significant. Furthermore, this increase seems to be compensated by 1993.

For other calderas the factor between height and gravity changes was calculated by Berrino et al (1992) and Rymer (1991). In some places, the measured gravity and height changes were about 10 times larger and therefore more significant values for the gravity-height relationship were obtained. During times of height increase, factors of -0.213 mgal/m (dh = 1.6 m) in Campo Flegrei (Italy), -0.216 mgal/m (dh = 1.8 m) at Rabaul (Papua New Guinea) and -0.250 mgal/m (dh = 0.8 m) at Krafla (Iceland) were obtained. During subsidence, the calculated factors were -0.120 mgal/m (dh = -0.5 m) in Campo Flegrei and -0.167 mgal/m (dh = -0.9 m) at Krafla. Thus there was generally mass increase during periods of uplift and mass decrease during subsidence. This corresponds just partly with the data found in the Yellowstone National Park (e.g. mass increase during subsidence from 1986 to 1987).

4.3 Density calculation

An important parameter for the gravity changes is the crustal density. Several relationships between the seismic velocity and the density of a material have been proposed, like e.g. Birch (1961).

A USGS data base with more than 600 gravity stations in the Yellowstone National Park area was used for the determinations of the gravity differences between the measured gravity values and the values found by different models in this chapter. The Yellowstone precision gravity network is part of the USGS data.

Evoy's (1978) density model based on both seismic velocity and gravity anomalies. The relationship he used between the p-wave velocity and the density was Birch's law :

(4.28) $v_p = a + b \cdot \rho$

with v_p : seismic compressional velocity

a,b : coefficients, depending on mean atomic weight of the rock

ρ : density of the rock

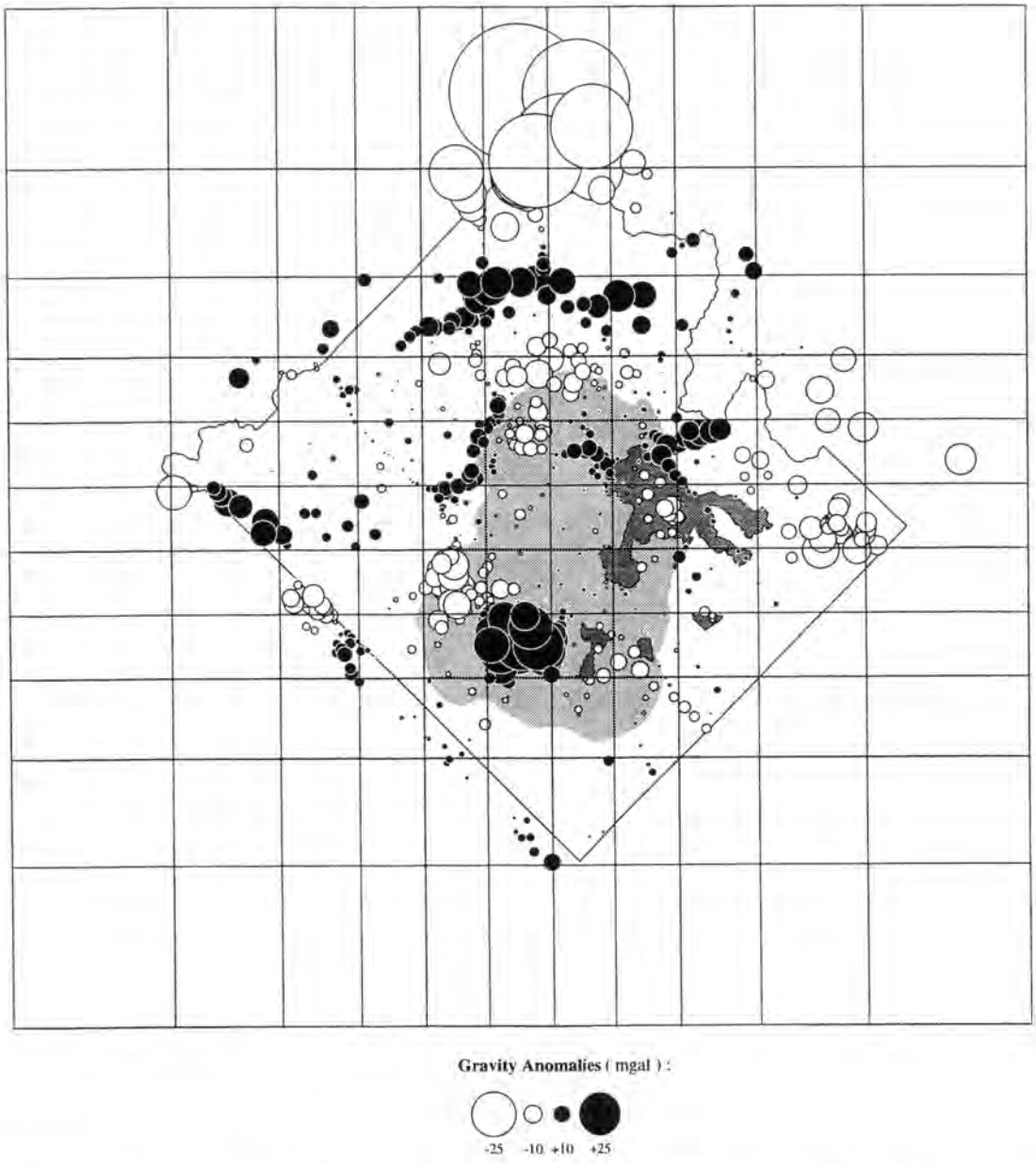

Fig. 4.5 : Gravity anomalies of Evoy's (1978) model with 4 layers down 100 km. There are probably some incorrect densities in some cells (large black or white dots).

This law is valid only for metamorphic rock samples, and not for sedimentary rocks. Evoy stated, that Birch's law may not be valid under resurgent domes. Figure 4.5 shows

the difference between the true gravity anomalies and the anomalies found by Evoy's density model. It may also be, that in some parts (e.g. near Old Faithful) some inconsistencies occurred. Furthermore, the model, that the density anomaly reaches down to 100 km is not proven by seismic results. Smith et al. (1982) show, that there are no special anomalies lower than 15 km.
15 km is also the border depth of the seismic velocity model of D. Miller (1994). In a first calculation, the gravity differences for the velocity model of D. Miller and Birch's law have been determined (fig. 4.6).

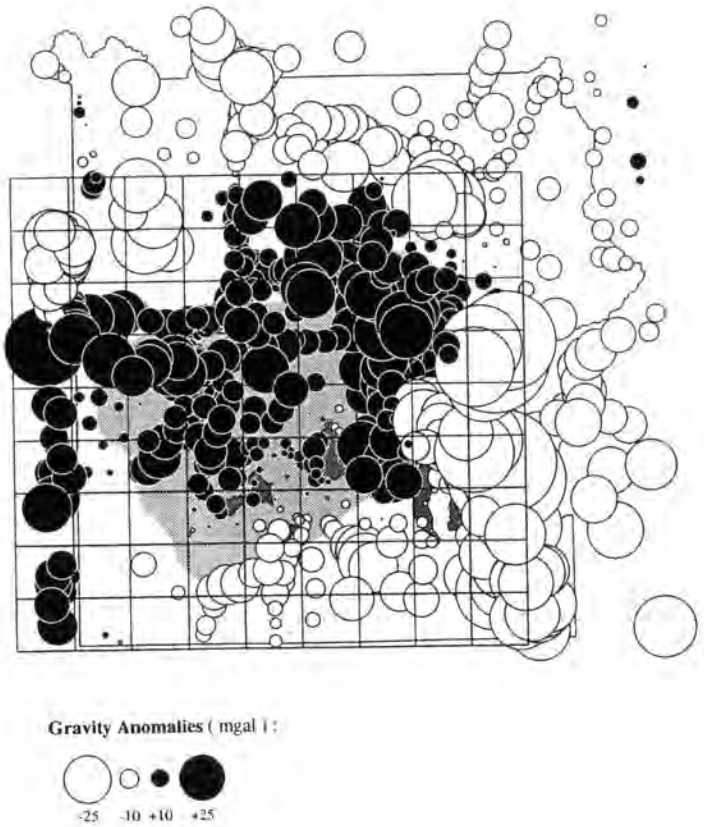

Fig 4.6 : Gravity anomalies calculated with seismic velocity model after Miller (1994) and Birch's Law. The anomaly within the Yellowstone caldera with its sediment filling cannot be modeled satisfyingly.

Next, a new density model was calculated, using the results of D. Miller and introducing the relationship between seismic velocities and density after Wyss (1993) as:

$$(4.29)\quad v_p = \begin{cases} 3\rho - 2.28 & \text{if } \rho > 2.876 \text{ g cm}^{-3} \\ -62.34+134.86\rho-104.08\rho^2+34.65\rho^3-4.13\rho^4 & \text{if } \rho < 2.876 \text{ g cm}^{-3} \end{cases}$$

with

v_p : p wave velocity [km s^{-1}]

ρ : density [g cm^{-3}]

Applying this model the results improve significantly (Fig. 4.8).

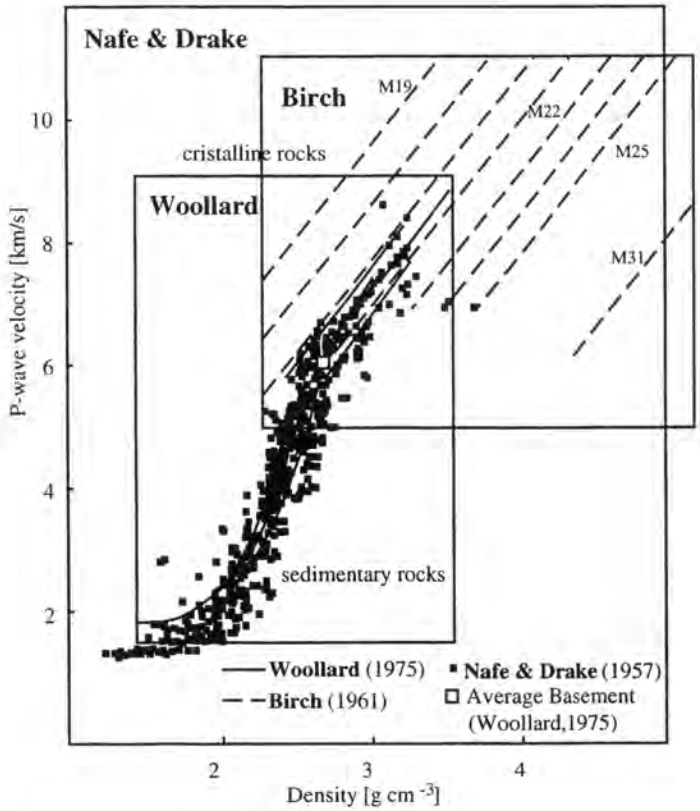

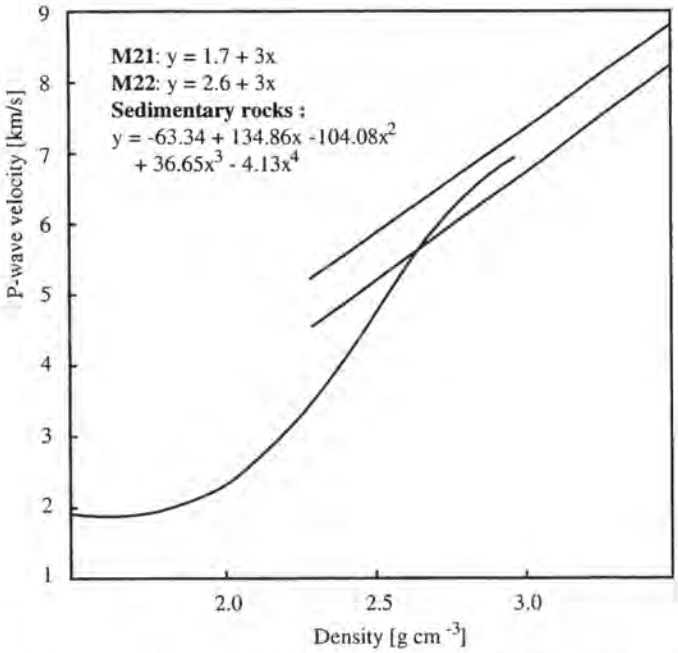

Fig. 4.7 : Density - seismic velocity relationship in rocks (Wyss (1994))

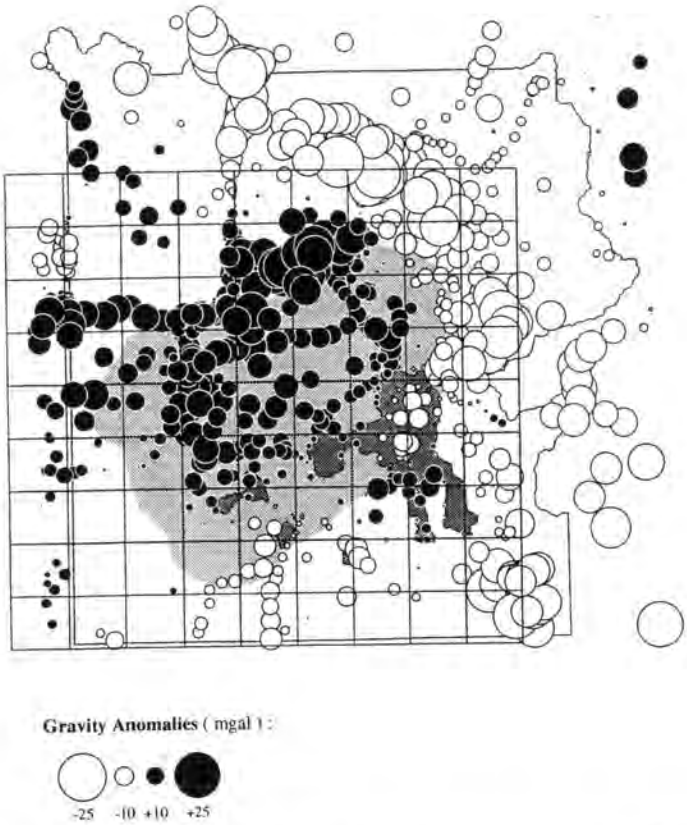

Fig 4.8 : Gravity anomalies calculated with seismic velocity model after Miller (1994) and Woollard's Law. The anomalies are significantly smaller than with Birch's Law.

Because there are some significant errors in the density-velocity relationships, these errors should also be introduced in the model for calculating the densities. This was done next. A 3-dimensional network of 8·8·8 blocks was introduced. The edges of the blocks are coincident with the nodes of the seismic velocity model (see table 4.2). The density of a single block was introduced with the mean velocity of the 8 nodes of the block and (4.29). Furthermore it was assumed, that one whole block has a constant density.

Origin : 44° 30' N, 110° 40' W , 0° rotation

x grid (E-W)[km]	-40	-30	-20	-10	0	10	20	30	40
y grid (S-N) [km]	-37	-28.75	-18.5	-9.25	0	9.25	18.5	28.75	37
z grid [km]	4*	0	-2	-4	-6	-8	-10	-12	-14

Table 4.2 : Definition of the blocks for gravity modeling

*This height cannot be introduced directly as the height of the top layer blocks. For a gravity observation at station j, it must be taken as the height of the station j to get a correct gravity model (see (4.30)).

The mean error of one observation of the density-velocity relationship was introduced as 0.2 g cm^{-3}, which is reasonable looking at the scatter of the curve of fig. 4.7 . Besides the velocity observations there are also the gravity observations on top of the surface layer. The observation equation for one gravity value is given by

$$(4.30)\quad g_j = g_{norm} - g_{f.a.} + 2\pi\rho_0\, G\, hg_{bouguer} - g_{topo} + \sum_i G\Delta\rho_i \int_{V_i} z\, r^{-3/2}\, dV + c$$

with

g_j : Measured absolute gravity value at station j

g_{norm} : Normal gravity for a latitude

$g_{f.a.}$: Free-air anomaly

$g_{bouguer}$: Bouguer plate anomaly = $2\pi\rho_0\, G\, h_j$

g_{topo} : Topographic correction = $\frac{\rho_0 + \Delta\rho_j}{\rho_0}\, g_{topo,\rho_0}$. The topographic correction for a density of 2.67 g cm^{-3} is taken from an USGS gravity data base of the Yellowstone National Park area and transformed for a density of ρ_0 *.

ρ_0 : Assumed density for the material above the geoid = 2.568 g cm^{-3}, corresponding to (5.29) for a velocity of 4.8 km s^{-1}

$\Delta\rho_j$: Density difference of the block the station j is lying on.

$\Delta\rho_i$: Density difference of the i. block.

V_i : Volume of the i. block

r : Distance to station j

z : Difference of z-co-ordinates to station j

c : Additional constant of the anomaly (regional anomaly)

* The assumption for the topography, to have a constant density, is not fully compatible with the rest of the model, where a separate density for each block is defined. However, most values of the topographic correction are smaller than 5 mgal and because the effect of the topography becomes smaller with the distance to the station, the error in the model is negligible.

An attempt was made to calculate the topographic corrections on the base of a 3"· 3" digital terrain model from 44° N to 45° N and from 110° W to 111° W. However, it turned out that there were large discrepancies between this digital terrain model and the

topographic map 1 : 125'000 of the Yellowstone Park. In some places the model is accurate, but in others there is a shift of several 100 m.
The gravity observations are assumed not to be correlated and to have a mean error of 5 mgal. Such a large value was taken due to local anomalies, which cannot be modeled by the block grid. The gravity differences between this model and the true gravity values can be seen in fig. 4.9. The improvements of the gravity values are much smaller than in Evoy's model. On the other hand, the modeled area is smaller.

Applied corrections : Some gravity stations were measured on the ice covered surface of the Yellowstone Lake. For these stations, a rough approximation of the anomalous effect of the water was calculated by a Bouguer plate having a thickness of the mean depth of the Lake near the station (table 4.3). This depth was taken from the topographic map 1:125'000.

Station	northern Latitude [deg]	eastern Longitude [deg]	depth [m]	gravity [mgal]
4687H073	44.5260	-110.3688	24	-1.68
4687H074	44.5263	-110.3445	60	-4.62
4687H075	44.5303	-110.3258	30	-2.10
4687H078	44.5107	-110.3113	75	-5.25
4687H079	44.5075	-110.3400	87	-6.09
4687H080	44.5067	-110.3965	45	-3.15
4687H083	44.4812	-110.3662	60	-4.20
4687H084	44.4803	-110.3268	84	-5.88
4687H089	44.4390	-110.3237	69	-4.83
4687H090	44.4405	-110.3473	45	-3.15
4687H091	44.4445	-110.3630	24	-1.68

Table 4.3 : Gravity effects of water for stations on the Yellowstone Lake for a density of -1.67 g cm^{-3}

As it could be expected from the fact, that closer masses have larger influence to the gravity, the improvements for the velocities in the top layer were maximal. This does not mean the velocity have to be corrected in Miller's model. The correction is only for value introduced in eq.(4.29). The corrections in the top layer were maximally 0.6 km/s, dropping below 0.3 km/s in the second layer. At the bottom, they are all smaller than 0.1 km/s. Positive and negative corrections are distributed evenly, so that no anomalous zone of eq.(4.29) can be found.

The density results (fig 4.10) show a low density zone from about 2 km to 12 km (below sea level) under the Yellowstone caldera. This corresponds with the low seismic velocity zone found by seismic results (Miller (1994), fig.3.11, and Smith et al (1982), fig.3.10).

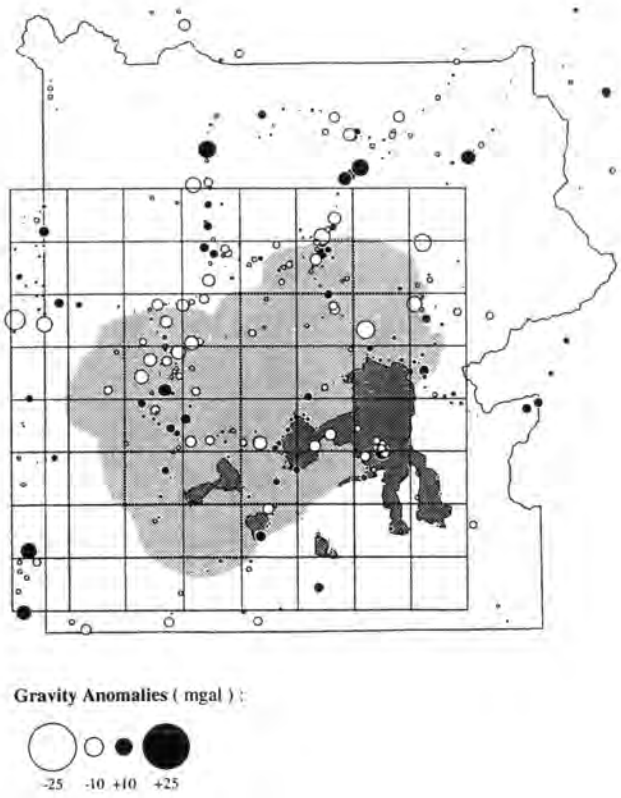

Fig 4.9 : Gravity Anomalies calculated with seismic velocity model after Miller (1994) and adjustment gives satisfying results all over the Yellowstone National Park

The figures 4.10 show the differences between the adjusted densities and the assumed density of the surroundings, within each layer.

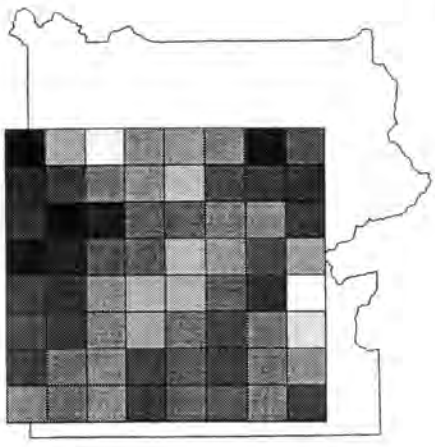

Layer from 2 km to 0 km
Assumed Density : 2.568

2.387	2.598	2.659	2.573	2.571	2.554	2.432	2.526
±.030	±.030	±.028	±.026	±.027	±.023	±.025	±.023
2.453	2.498	2.558	2.582	2.615	2.507	2.487	2.473
±.027	±.037	±.038	±.023	±.024	±.022	±.024	±.023
2.458	2.395	2.442	2.546	2.540	2.553	2.567	2.489
±.029	±.030	±.025	±.024	±.025	±.025	±.022	±.022
2.415	2.442	2.530	2.542	2.611	2.578	2.514	2.585
±.030	±.027	±.023	±.026	±.028	±.023	±.022	±.023
2.496	2.467	2.571	2.608	2.595	2.519	2.463	2.695
±.028	±.028	±.024	±.023	±.022	±.025	±.024	±.026
2.510	2.490	2.562	2.591	2.540	2.493	2.551	2.645
±.026	±.029	±.027	±.025	±.023	±.027	±.024	±.025
2.493	2.558	2.566	2.502	2.520	2.497	2.547	2.579
±.034	±.033	±.027	±.028	±.024	±.026	±.026	±.028
2.559	2.551	2.575	2.495	2.537	2.519	2.556	2.503
±.029	±.038	±.029	±.027	±.027	±.032	±.027	±.029

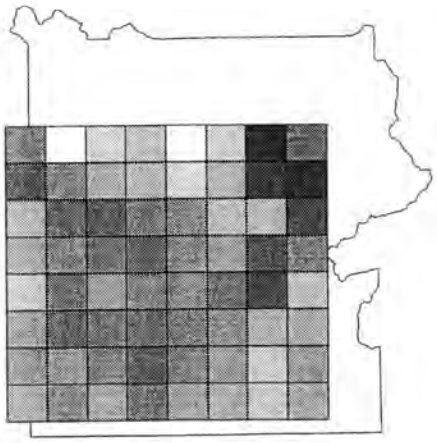

Layer from 0 km to -2 km
Assumed Density : 2.6013

2.596	2.718	2.670	2.650	2.693	2.654	2.500	2.582
±.036	±.042	±.039	±.037	±.039	±.037	±.036	±.036
2.571	2.610	2.632	2.641	2.665	2.629	2.535	2.514
±.035	±.038	±.038	±.036	±.037	±.036	±.036	±.036
2.634	2.582	2.578	2.598	2.600	2.645	2.643	2.547
±.036	±.036	±.035	±.036	±.036	±.037	±.037	±.036
2.625	2.607	2.587	2.582	2.604	2.615	2.557	2.596
±.037	±.037	±.035	±.036	±.036	±.036	±.035	±.036
2.652	2.591	2.619	2.610	2.602	2.574	2.548	2.649
±.037	±.036	±.036	±.036	±.036	±.035	±.035	±.037
2.620	2.583	2.598	2.594	2.595	2.605	2.639	2.632
±.037	±.037	±.036	±.036	±.036	±.036	±.036	±.037
2.613	2.619	2.604	2.577	2.592	2.615	2.659	2.621
±.037	±.038	±.037	±.036	±.036	±.036	±.038	±.037
2.622	2.605	2.625	2.598	2.617	2.626	2.653	2.624
±.037	±.038	±.037	±.036	±.037	±.037	±.038	±.038

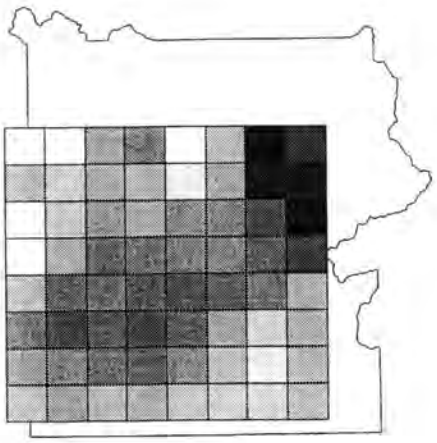

Layer from -2 km to -4 km
Assumed Density : 2.6626

2.795	2.887	2.683	2.665	2.772	2.698	2.519	2.578
±.050	±.072	±.041	±.039	±.047	±.041	±.037	±.037
2.704	2.727	2.693	2.701	2.746	2.678	2.527	2.536
±.041	±.043	±.041	±.041	±.044	±.039	±.037	±.037
2.800	2.722	2.679	2.700	2.669	2.664	2.621	2.528
±.050	±.043	±.039	±.041	±.039	±.039	±.038	±.037
2.765	2.702	2.652	2.665	2.661	2.668	2.635	2.615
±.047	±.041	±.038	±.039	±.039	±.039	±.038	±.038
2.713	2.651	2.655	2.639	2.633	2.640	2.657	2.704
±.042	±.039	±.038	±.038	±.038	±.038	±.039	±.041
2.649	2.623	2.636	2.627	2.637	2.688	2.737	2.697
±.039	±.038	±.038	±.038	±.038	±.040	±.043	±.041
2.679	2.660	2.643	2.635	2.665	2.712	2.747	2.702
±.040	±.040	±.039	±.038	±.039	±.042	±.044	±.041
2.709	2.683	2.701	2.698	2.715	2.726	2.735	2.712
±.042	±.041	±.041	±.041	±.042	±.043	±.044	±.042

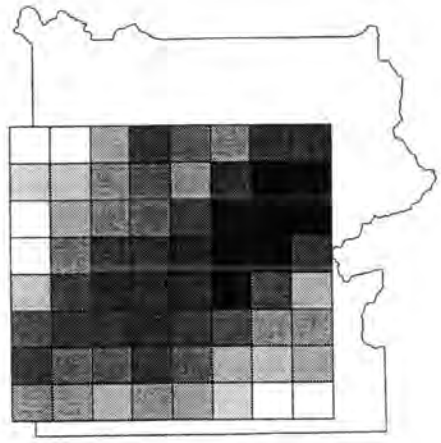

Layer from -4 km to -6 km
Assumed Density : 2.7379

2.875	2.927	2.758	2.660	2.709	2.727	2.634	2.644
±.072	±.075	±.046	±.040	±.042	±.043	±.039	±.039
2.798	2.789	2.740	2.709	2.741	2.628	2.507	2.585
±.051	±.051	±.045	±.042	±.044	±.038	±.038	±.038
2.878	2.761	2.731	2.713	2.657	2.592	2.506	2.541
±.073	±.047	±.043	±.042	±.039	±.038	±.037	±.037
2.829	2.724	2.663	2.654	2.620	2.585	2.575	2.654
±.058	±.043	±.040	±.039	±.038	±.038	±.037	±.039
2.784	2.675	2.622	2.635	2.614	2.581	2.676	2.779
±.049	±.040	±.038	±.039	±.038	±.037	±.040	±.049
2.681	2.660	2.644	2.632	2.643	2.677	2.739	2.735
±.041	±.040	±.039	±.038	±.039	±.040	±.044	±.044
2.671	2.711	2.699	2.660	2.696	2.765	2.783	2.759
±.040	±.043	±.042	±.040	±.041	±.047	±.049	±.046
2.731	2.751	2.772	2.749	2.752	2.806	2.847	2.845
±.044	±.046	±.048	±.045	±.046	±.053	±.063	±.063

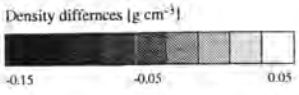

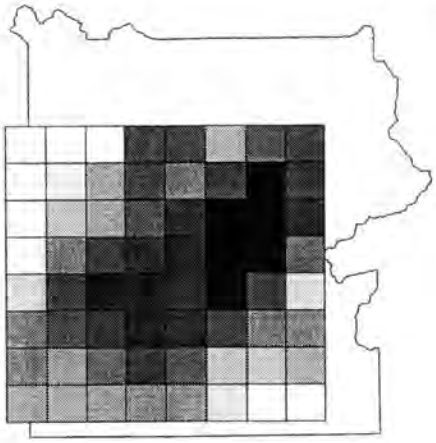

Layer from -6 km to -8 km
Assumed Density : 2.7599

2.953	2.942	2.864	2.704	2.701	2.797	2.716	2.699
±.075	±.075	±.070	±.042	±.042	±.052	±.043	±.042
2.874	2.843	2.781	2.711	2.748	2.679	2.569	2.689
±.073	±.062	±.050	±.042	±.045	±.041	±.038	±.041
2.917	2.811	2.787	2.731	2.654	2.589	2.529	2.661
±.075	±.055	±.050	±.044	±.040	±.038	±.038	±.040
2.847	2.768	2.708	2.673	2.647	2.604	2.610	2.740
±.064	±.048	±.042	±.040	±.039	±.038	±.038	±.045
2.834	2.704	2.640	2.651	2.657	2.616	2.701	2.840
±.060	±.042	±.039	±.039	±.040	±.038	±.042	±.061
2.752	2.716	2.679	2.642	2.653	2.697	2.751	2.770
±.046	±.043	±.041	±.039	±.040	±.042	±.046	±.048
2.752	2.777	2.733	2.686	2.723	2.812	2.816	2.792
±.046	±.049	±.044	±.041	±.043	±.055	±.056	±.051
2.786	2.790	2.779	2.766	2.770	2.840	2.893	2.886
±.050	±.051	±.049	±.048	±.048	±.061	±.075	±.076

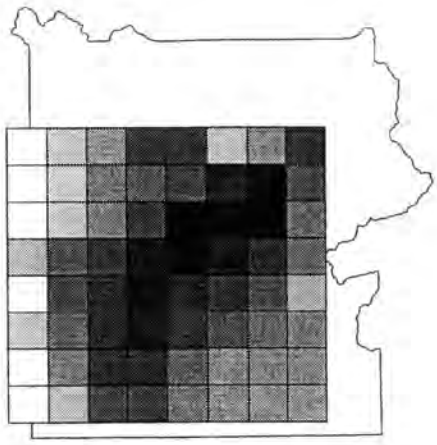

Layer from -8 km to -10 km
Assumed Density : 2.8155

2.929	2.873	2.832	2.747	2.744	2.872	2.814	2.734
±.076	±.074	±.060	±.046	±.045	±.073	±.055	±.044
2.920	2.883	2.816	2.791	2.754	2.689	2.632	2.778
±.076	±.076	±.056	±.051	±.046	±.041	±.039	±.049
2.945	2.873	2.826	2.753	2.659	2.608	2.617	2.805
±.076	±.074	±.058	±.046	±.040	±.038	±.039	±.054
2.851	2.786	2.750	2.689	2.663	2.688	2.720	2.798
±.065	±.050	±.046	±.041	±.040	±.041	±.043	±.052
2.903	2.772	2.710	2.683	2.703	2.731	2.775	2.844
±.076	±.049	±.043	±.041	±.042	±.044	±.049	±.063
2.862	2.793	2.720	2.689	2.727	2.767	2.791	2.807
±.069	±.052	±.043	±.041	±.044	±.048	±.051	±.054
2.911	2.810	2.716	2.721	2.784	2.817	2.815	2.817
±.076	±.055	±.043	±.043	±.050	±.056	±.056	±.056
2.954	2.856	2.767	2.762	2.799	2.814	2.821	2.829
±.076	±.067	±.048	±.047	±.053	±.055	±.057	±.059

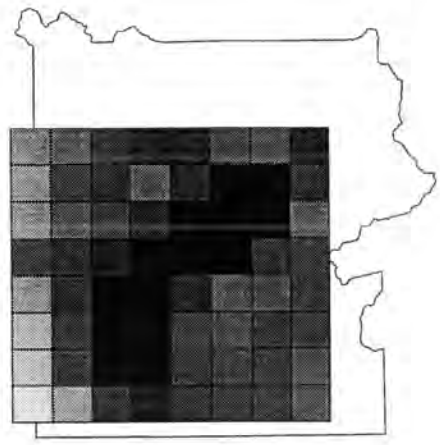

Layer from -10 km to -12 km
Assumed Density : 2.9038

2.894	2.872	2.810	2.776	2.770	2.833	2.843	2.779
±.076	±.074	±.055	±.049	±.048	±.060	±.063	±.050
2.907	2.842	2.805	2.867	2.774	2.677	2.690	2.806
±.076	±.063	±.054	±.071	±.049	±.041	±.041	±.054
2.902	2.865	2.837	2.780	2.693	2.630	2.703	2.871
±.076	±.070	±.061	±.050	±.042	±.039	±.042	±.073
2.835	2.805	2.780	2.723	2.696	2.739	2.814	2.846
±.061	±.054	±.050	±.044	±.042	±.045	±.056	±.064
2.909	2.811	2.739	2.734	2.789	2.869	2.862	2.833
±.076	±.055	±.045	±.044	±.051	±.072	±.069	±.060
2.942	2.837	2.743	2.751	2.840	2.864	2.830	2.837
±.076	±.061	±.045	±.046	±.062	±.070	±.059	±.061
2.953	2.843	2.752	2.750	2.829	2.840	2.831	2.865
±.076	±.063	±.046	±.046	±.059	±.062	±.060	±.070
2.975	2.922	2.819	2.782	2.822	2.833	2.838	2.867
±.076	±.076	±.057	±.050	±.057	±.060	±.061	±.072

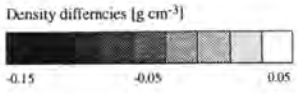

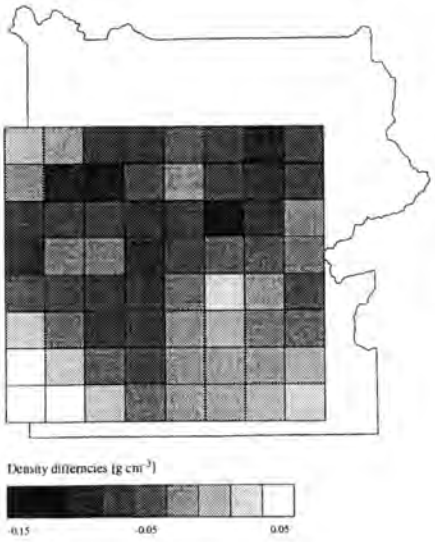

Layer from -12 km to - 14 km
Assumed Density : 2.9005

2.936	2.915	2.828	2.829	2.859	2.830	2.787	2.845
±.076	±.076	±.059	±.059	±.068	±.059	±.051	±.064
2.900	2.788	2.781	2.860	2.898	2.835	2.803	2.839
±.076	±.051	±.050	±.069	±.076	±.061	±.053	±.062
2.829	2.838	2.838	2.818	2.820	2.769	2.805	2.899
±.059	±.062	±.061	±.056	±.057	±.048	±.054	±.076
2.796	2.888	2.888	2.793	2.836	2.859	2.854	2.881
±.052	±.076	±.076	±.052	±.061	±.068	±.067	±.076
2.848	2.841	2.818	2.807	2.876	2.972	2.910	2.845
±.065	±.062	±.057	±.054	±.076	±.076	±.076	±.064
2.947	2.868	2.796	2.820	2.897	2.925	2.877	2.872
±.076	±.072	±.052	±.057	±.076	±.076	±.076	±.074
3.012	2.949	2.857	2.832	2.892	2.909	2.897	2.923
±.076	±.076	±.068	±.060	±.076	±.076	±.076	±.076
3.079	3.025	2.941	2.870	2.891	2.910	2.924	2.962
±.076	±.076	±.076	±.073	±.076	±.076	±.076	±.076

5 Finite-Element Modeling

If there is no mass diffusion, like e.g. groundwater changes, hydrothermal fluid movements or magma transport, the gravity changes must be an effect of mass movements and/or temperature dependent contraction or expansion within the earth. With the necessary physical laws and boundary conditions, it is possible to calculate the corresponding displacements. The physical laws are the ones for strain and for thermal expansion.
These two equations can be solved with given boundary conditions like known forces, displacements, temperature changes. In the Yellowstone National Park, the given boundary conditions are the displacements (by GPS and/or by leveling) and the gravity changes. The gravity changes are no common boundary condition. Therefore, parameters must be introduced such, that the solutions found fit the given gravity changes best.
A possibility to solve these problems is the Finite Element Method FEM.

5.1 Introduction into the Finite-Element Method

The finite-element method is a numerical technique for solving boundary problems of n-dimensional bodies. Given is a body with a certain structure, one or several conditions (normally physical laws) within the body and boundary conditions. A function d(x, y, z) of position is searched to describe the phenomena. Formulation of the method for problems typically involves seven steps :

1. Approximation of the body by a structure (mesh) of n components called elements. The elements are identified with integers, j = 1,2,...,n. Points where the elements are connected are referred with nodes. The nodes are also identified with integers.
   In mechanics, the body is characterized by a volume, which can be divided into a regular or irregular mesh of subvolumes
2. A function $d'_j(x, y, z)$ is chosen to approximate d(x, y, z) within the element j. The function d'_j is the 'assumed displacement field' for that element. The function d'_j is characterized by c_j unknown constants, a_{ij} , i = 1,2,..,c_j. Mostly, the function d'_j is a polynomial of the order depending on c_j. By this step, the problem is converted to find unknowns a_{ij}.
3. Mathematical formulation of the problem by physical laws.
4. Introducing the function d' into the functions found in step 3. The constants a_{ij} are expressed in terms of the given conditions and boundary conditions.
5. Solving for the primary unknowns (e.g. temperature, displacements).
6. Deduction of secondary unknowns (e.g. gravity values)
7. Conclusions

In crustal deformation we have several conditions like elasticity. In our problem the boundary conditions include orthometric height changes as well as gravity changes.
The modeling of the Yellowstone hot spot is divided into two parts. First, a two dimensional model will be developed for the specially active line from canyon Junction to Fishing Bridge to Sylvan Lake. Second, a three dimensional model will be constructed over the whole Yellowstone area. Both models will be calculated by means of the FEM.

5.2 Two Dimensional Model

1. Approximation of the structure by a mesh. The nodes are given on top of the model at the stations, where height changes were measured. The other nodes must be defined in a suitable way. The network chosen to connect the nodes is triangular. The nodes at the top are coincident with Yellowstone precision gravity stations. The nodes inside the mesh are distributed in such a way that

$$(5.1) \quad \sum_{i,j} \left(\alpha_{i,j} - \frac{\pi}{3} \right)^2 = \min.$$

with

i : 1,2, ..., n, n = number of triangles
j : 1,2,3 , corners of each triangle
α : angle

so that the angles tend to be equal to 60°. In all nodes, the primary unknowns are the displacements and the temperature changes. (fig. 5.1)

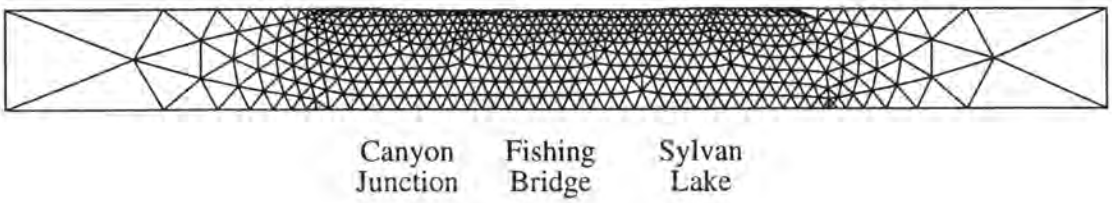

Fig 5.1 : 2-dimensional mesh along the northern caldera crossing line from Canyon Junction to Fishing Bridge to Sylvan Lake

2. The primary unknowns u*, v*, τ* (horizontal and vertical displacement, temperature difference) are approximated by the functions u(x, z), v(x, z), τ(x, z). For simplicity the

approximation is just shown for the displacements. For the temperature the procedure is very similar.

The functions are defined piecewise. Within each element, the components of the displacements are approximated by functions N_i :

$$(5.2) \quad \begin{pmatrix} u(x, z) \\ v(x, z) \end{pmatrix} = \sum_i N_i \begin{pmatrix} u_i \\ v_i \end{pmatrix} = \sum_i N_i \, \mathbf{a}_i = \mathbf{N}\,\mathbf{a}$$

with

i	: 1,2,..., number of nodes
u	: displacement in x-direction
v	: displacement in y-direction

The functions N_i have to be chosen such, that when introducing the co-ordinates of a node, the results are equal to the corresponding displacements, $N_i\,(x_i, z_i) = \begin{pmatrix} 1 \\ 1 \end{pmatrix}$, while if i $\neq$ j $N_i(x_j, z_j) = \begin{pmatrix} 0 \\ 0 \end{pmatrix}$. N_i are the so called shape functions and are normally formed by polynomial functions. If we want to use formula (4.13) for the calculation of the gravity changes, N_i must be piecewise linear within each element. Otherwise, numerical integration is necessary to calculate the gravity changes. For the temperature changes, higher degrees polynomial approximation functions may be introduced.

For piecewise linear integration, N_i are defined by linear functions within each element. It is shown easily, that N_i must be zero within each element e without the node i. Within an element e with the nodes i, j, k, N_i must be the identity matrix in i and zero in j and k. So $N_i = \begin{pmatrix} f_u(x, z) \\ f_v(x, z) \end{pmatrix}$ can be defined within the element e by

$$(5.3) \quad f_u(x, z) = c_{xu}\, x + c_{zu}\, z + c_u \qquad f_v(x, z) = c_{xv}\, x + c_{zv}\, z + c_v$$

The following steps are similar for f_u and f_v and therefore, only f_u is demonstrated.

V^e is defined by $\begin{vmatrix} x_i - x_k & x_j - x_k \\ z_i - z_k & z_j - z_k \end{vmatrix}$, which is twice the area of the triangle formed by the nodes i, j, k. If we define V_i^e by $\begin{vmatrix} x - x_k & x_j - x_k \\ z - z_k & z_j - z_k \end{vmatrix}$, then the function $\frac{V_i^e}{V^e}$ fulfills the upper conditions for N_i as can be easily proved.

Further, taking V_j^e as $\begin{vmatrix} x_i - x_k & x - x_k \\ z_i - z_k & z - z_k \end{vmatrix}$, $\frac{V_j^e}{V^e}$ = 1 in j and 0 in i and k. So N_i, N_j and N_k can be defined within the element e as :

$$(5.4)\quad N_i^e = \frac{V_i^e}{V^e} \qquad N_j^e = \frac{V_{e_j}}{V^e} \qquad N_k^e = 1 - \frac{V_i^e}{V^e} - \frac{V_j^e}{V^e}$$

These are the shape functions which will be introduced for the horizontal as well as for the vertical displacements and temperature changes.

3. Mathematical formulation of the problem

Strain

$$(5.5)\quad \varepsilon = \begin{pmatrix} \varepsilon_x \\ \varepsilon_y \\ \gamma_{xy} \end{pmatrix} = \begin{pmatrix} \frac{\partial u}{\partial x} \\ \frac{\partial v}{dy} \\ \frac{\partial u}{\partial y} + \frac{\partial v}{\partial x} \end{pmatrix} = \begin{bmatrix} \frac{\partial u}{\partial x} & 0 \\ 0 & \frac{\partial}{dy} \\ \frac{\partial}{\partial y} & \frac{\partial}{\partial x} \end{bmatrix} \begin{pmatrix} u \\ v \end{pmatrix} = \mathbf{S\,u = S\,N\,a = B\,a}$$

with descriptions after (6.2) and

ε : strain

With the shape function given in one element, the matrix B can be easily calculated. As these functions are piecewise linear, the strain remains constant within one element.

The two dimensional model of a crossing line of the Yellowstone caldera will be subjected to some initial strain due to temperature changes. The strain ε_0 can be expressed as

$$(5.6)\quad \varepsilon_0 = \begin{pmatrix} \alpha\tau \\ \alpha\tau \\ 0 \end{pmatrix}$$

with

α : linear thermal expansion coefficient

τ : mean temperature difference $T_2 - T_1$ at the nodes i, j, k $(= \frac{\tau_i + \tau_j + \tau_k}{3})$

I found hardly any data about thermal expansion coefficients. The only qualitative results are for some compounds like quartz, and some sandstone samples (fig. 5.2) in Somerton (1991). It shows, that the linear thermal expansion of sandstone is quite similar to the one of quartz. The coefficient remains constant at $2 \cdot 10^{-5}$ °C^{-1} for temperatures lower than 575 °C and is close to 0 °C^{-1} for higher temperatures.

Due to the lack of other data, the thermal expansion coefficient a was introduced with either $2 \cdot 10^{-5}$ °C^{-1} or 0 °C^{-1} for each element of the entire model.

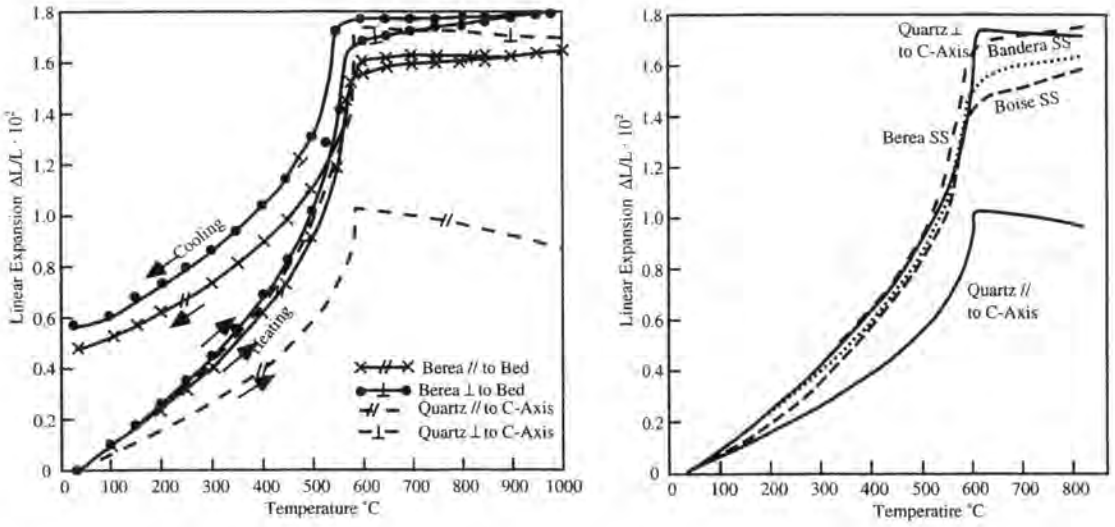

Fig. 6.2 : Linear thermal expansion of Berea sandstone and quartz parallel and perpendicular to bedding and C-axis, respectively, on heating and cooling cycles.(after Somerton)

Fig 6.3 Linear thermal expansion of three sandstones compared with quartz (after Somerton)

Furthermore, it was assumed that there is some initial stress σ_0 in the model.

$$(5.7) \quad \sigma = \mathbf{D}(\varepsilon - \varepsilon_0) + \sigma_0$$

with

$$(5.8) \quad \mathbf{D} = \frac{E}{1 - \nu^2}\begin{bmatrix} 1 & \nu & 0 \\ \nu & 1 & 0 \\ 0 & 0 & (1-\nu)/2 \end{bmatrix}$$

with

E : Young's modulus

ν : Poisson's constant.

Because no data are available for the initial stress, σ_0 is chosen as 0. Even if the initial stress is not 0, it does not influence the result significantly, because the geometry of the structure does not change very much. If the material is ideal elastic, E and ν are directly related to the p-wave and s-wave velocity, v_p, v_s as well as the density ρ of the material:

$$(5.9) \quad v_p = \sqrt{\frac{2\mu + \lambda}{\rho}} \qquad v_s = \sqrt{\frac{\mu}{\rho}}$$

with λ and μ equal the Lamé's constants and

(5.10) $E = \frac{\mu(3\lambda + 2\mu)}{\lambda + \mu}$ $\qquad \nu = \frac{\lambda}{2(\lambda + \mu)}$

v_p and v_s are known from seismic measurements (D. Miller, 1994) and the density was modeled in chapter 4.3. E, ν and **D** can be calculated.

Equivalent nodal forces

$\mathbf{q}^e = \begin{pmatrix} \mathbf{q}_i^e \\ \mathbf{q}_j^e \\ \mathbf{q}_k^e \end{pmatrix}$ define the nodal forces which are equivalent to the boundary stresses and distributed loads on the element e. $\mathbf{q}_i^e = \begin{pmatrix} U_i \\ V_i \end{pmatrix}$ must have the same number of components as $\mathbf{a}_i$. Further there is the body force $\mathbf{b} = \begin{pmatrix} b_x \\ b_y \end{pmatrix}$. Then, for one element e

(5.11) $\mathbf{q}^e = \int_{V_e} \mathbf{B}^T \sigma \, dV - \int_{V_e} \mathbf{N}^T \mathbf{b} \, dV$

is valid as can be seen in (Zienkievic, 1991). Further transformation leads to

(5.12) $\mathbf{q}^e = \mathbf{K}^e \mathbf{a}^e + \mathbf{f}^e$

with

(5.13) $\mathbf{K}^e = \int_{V_e} \mathbf{B}^T \mathbf{D} \mathbf{B} \, dV$

and

(5.14) $\mathbf{f}^e = - \int_{V_e} \mathbf{N}^T \mathbf{b} \, dV - \int_{V_e} \mathbf{B}^T \mathbf{D} \varepsilon_0 \, dV + \int_{V_e} \mathbf{B}^T \sigma_0 \, dV$

Taking all conditions of the elements into account leads to the equations for the unknowns u_i and v_i.

Thermal equations

In (5.6) the temperature difference τ is needed. It can be found by following means : Applying the Laplace operator on $\tau = T_2 - T_1$ gives

$$(5.15)\quad \Delta\tau = \Delta(T_2 - T_1) = c\frac{\partial T_2}{\partial t} - A_2(\mathbf{x}) - c\frac{\partial T_1}{\partial t} + A_1(\mathbf{x})$$

The thermal productivity $A(\mathbf{x})$ will not change significantly from t_1 to t_2 and so

$$(5.16)\quad \Delta\tau = c\frac{\partial T_2 - \partial T_1}{\partial t} = c\frac{\partial \tau}{\partial t}$$

Further simplification can be achieved, assuming that at any time t the temperature field is just a function of the boundary conditions and time independent. That is the case with slow temperature changes on the boundary, and

$$(5.17)\quad \Delta\tau = \frac{\partial^2\tau}{\partial x^2} + \frac{\partial^2\tau}{\partial z^2} = 0$$

This equation shall be solved with the Galerkin method :

$$(5.18)\quad \int_{V_e}\left(\frac{\partial^2\tau}{\partial x^2} + \frac{\partial^2\tau}{\partial z^2}\right)N_i\, dV = 0 \quad \text{for each node i}$$

Partial integration leads to

$$(5.19)\quad \int_{V_e}\left(\frac{\partial\tau}{\partial x}\frac{\partial N_i}{\partial x} + \frac{\partial\tau}{\partial y}\frac{\partial N_i}{\partial y}\right)dV - \int_{s_e} N_i\frac{\partial\tau}{\partial \mathbf{n}}\, ds = 0$$

where **s** is the border of the element and **n** the normal vector on s.
Introducing $\tau(x, z) = \sum_i N_i\, \mathbf{a}_i$, where $\mathbf{a}_i$ is a scalar value, leads to an equation system, which can be solved for the unknowns $\mathbf{a}_i$.

Boundary conditions

The boundary conditions must be chosen such, that they best fit the measured displacements as well as the gravity changes. For this, parameterized boundary conditions will be introduced. By this, the equation system can be found, which is only partly filled (see fig 5.3) Additionally the gravity and height changes can be expressed as functions of the displacements u, v, which give a normal equation system of a least squares problem.
The observations for the gravity differences look like

$$(5.20)\quad \Delta g_l = \sum_e g(x_i^e + u_i^e, z_i^e + v_i^e, x_j^e + u_j^e, z_j^e + v_j^e, x_k^e + u_k^e, z_k^e + v_k^e) - \sum_e g(x_i^e, z_i^e, x_j^e, z_j^e, x_k^e, z_k^e)$$

and for the height changes

$$(5.21)\quad \Delta h_l = v_l$$

The observation equation for the gravity changes (6.20) shows, that Δg_l is a function of all the displacements, and, therefore, the respective part of the matrix is filled completely. On the other hand, just one element is filled in each line of the part belonging to the height changes.
A Gaussian elimination algorithm can be applied to eliminate ε_0, the temperature and displacement variables. By that, a new normal equation system with the observed gravity changes and height changes as a function of the boundary condition parameters is found. The statistical model of the observations can be found from the Q_{xx}-matrices of each years gravity or leveling measurements, respectively (see also chapter 4.2). Solving this least squares problem leads to the values for the parameters of the boundary conditions with their mean errors and correlation. Further, displacements and temperature changes can be calculated and interpreted (points 4 to 7 of list at beginning of this chapter, see 5.2.1).

5.2.1 Yellowstone Caldera Two-Dimensional Models

It was assumed, that the Yellowstone height and gravity changes are due to pressure and/or temperature changes in a limited zone at a depth of 14 km (see fig 5.5). The displacements and temperatures of the border nodes outside this zone and not on the surface were fixed to 0. This assumption is plausible as a first approximation for the geology of a hot spot. Other boundary conditions with more free nodes on the border give worse results.
In a first step, the differences of the results of the GPS, leveling and gravity campaigns of 1987 and 1993 were examined. These results were taken, because the signals are maximal between these two campaigns. Models were calculated, where either a pressure change, or a temperature change, or both is active at a depth of 14 km . However no parametersgive satisfying results in modeling the measured leveling, gravity and GPS changes simultaneously. Looking at figures 5.6 is seen, that the calculated horizontal displacements are too large compared with the ones measured by GPS if the vertical

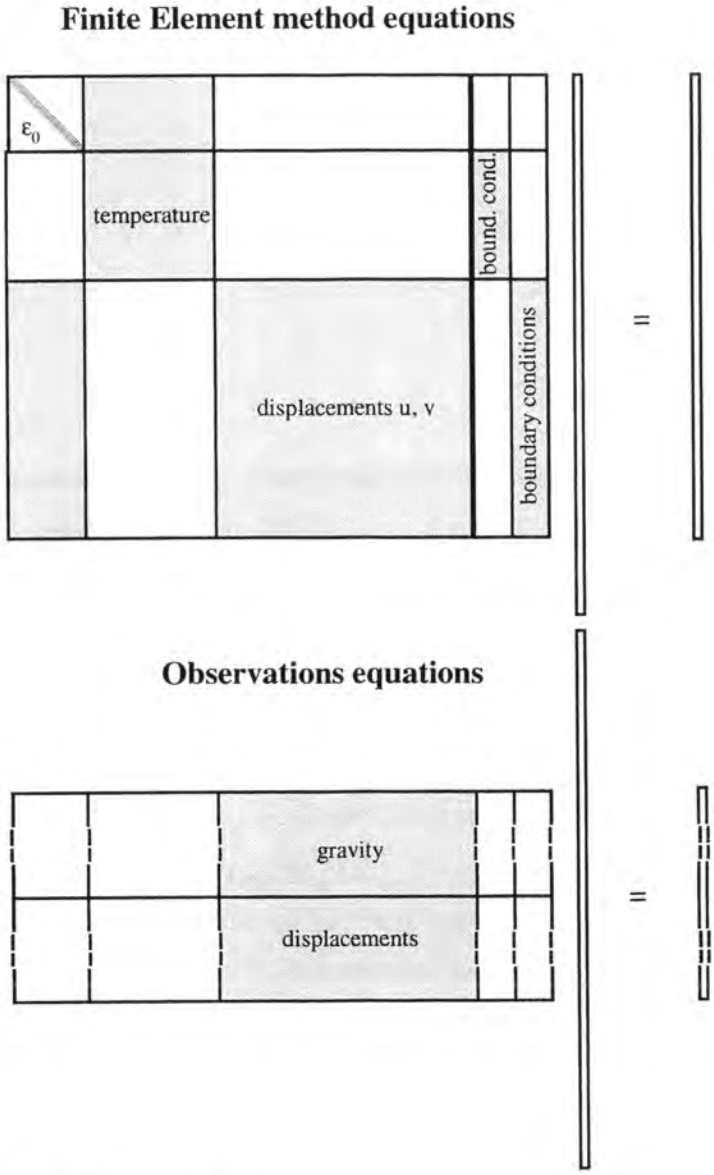

Fig 5.4 : Matrix scheme

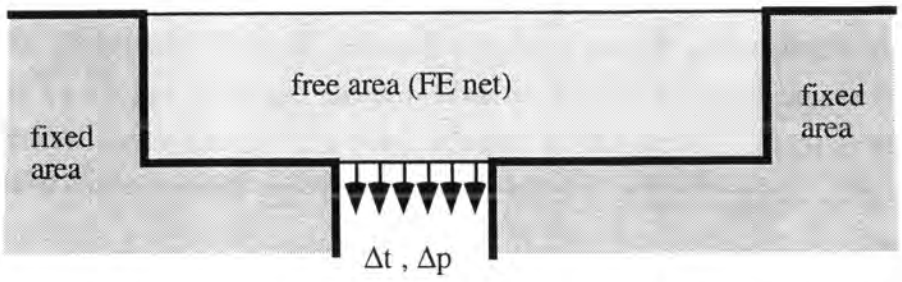

Fig. 5.5 : Schematic figure of the assumed structure of the Yellowstone Hot Spot

displacements found by leveling fit accurately. Vice versa, when the parameters are adjusted to fit the horizontal displacements found by GPS, the vertical displacements are too small. This discrepancy is true, independently of taking pressure or temperature or

both parameters to fit the measurements. Furthermore, the measured gravity changes are always significantly larger than the ones calculated.

	pressure [GPa]	**temperature bottom fixed** [K]	**temperature bottom free** [K]
fit for GPS	0.13	-1.21	-2.62
active zone [km]	7 - 28	15 - 20	15 - 18
rms	2.29	2.48	2.58
fit for leveling	0.32	-4.23	-4.45
active zone [km]	10 - 28	20 - 23	20 - 23
rms	2.00	2.37	2.38

Tab. 5.1 : Parameters to model the leveling, GPS and gravity data from 1987 to 1993

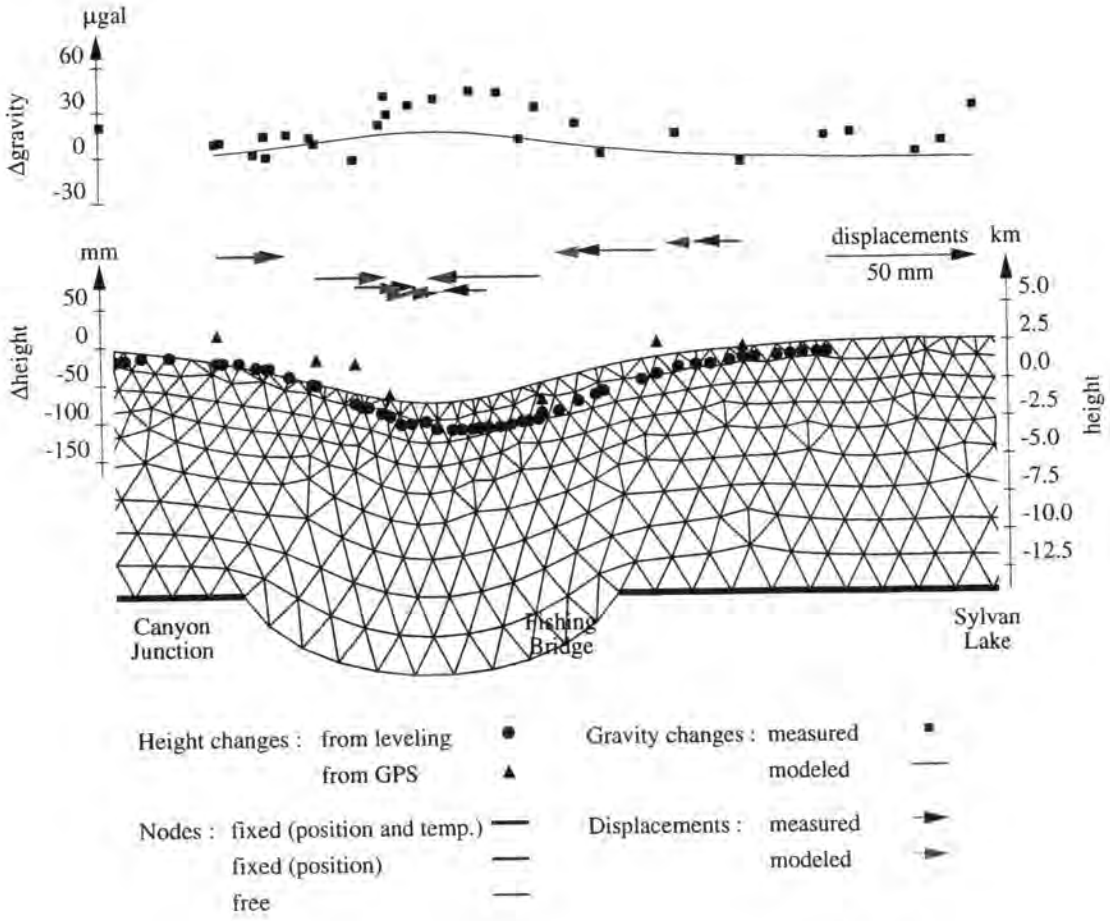

Fig. 5.6 a : Finite element model : Adjusted for GPS results : a pressure of 0.13 GPa is applied at a depth of 14 km with in the area of thin lines .

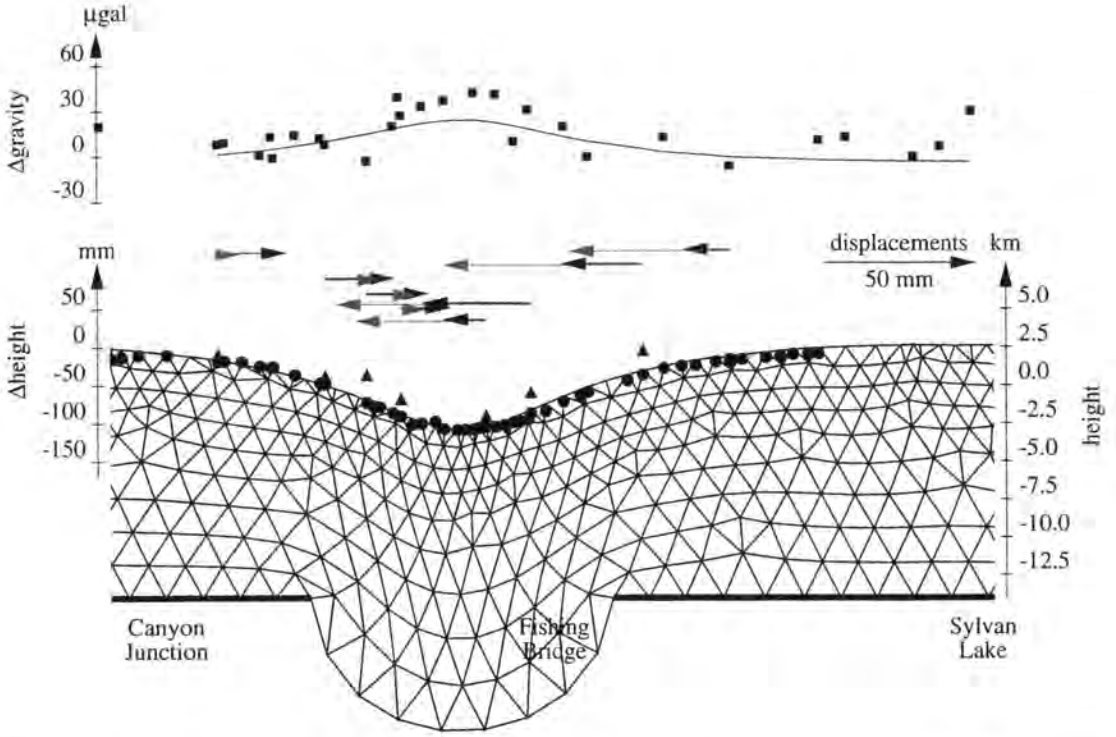

Fig. 5.6 b : Finite element model : Adjusted for leveling results : A pressure of 0.32 GPa is applied at a depth of 14 km with in the area of thin lines. Further description see Fig. 5.6 a

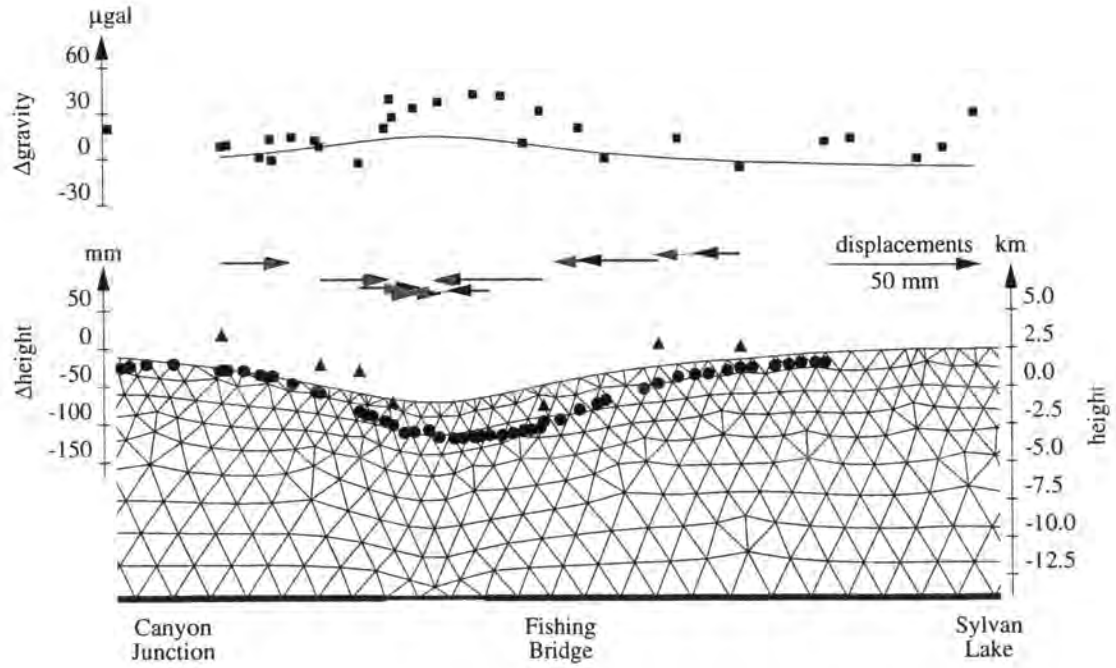

Fig. 5.6 c : Finite element model : Adjusted for GPS results : A temperature change of -1.21 K is applied at a depth of 14 km at the nodes fixed lying under the semi-bold line. Symbols see Fig. 5.6 a

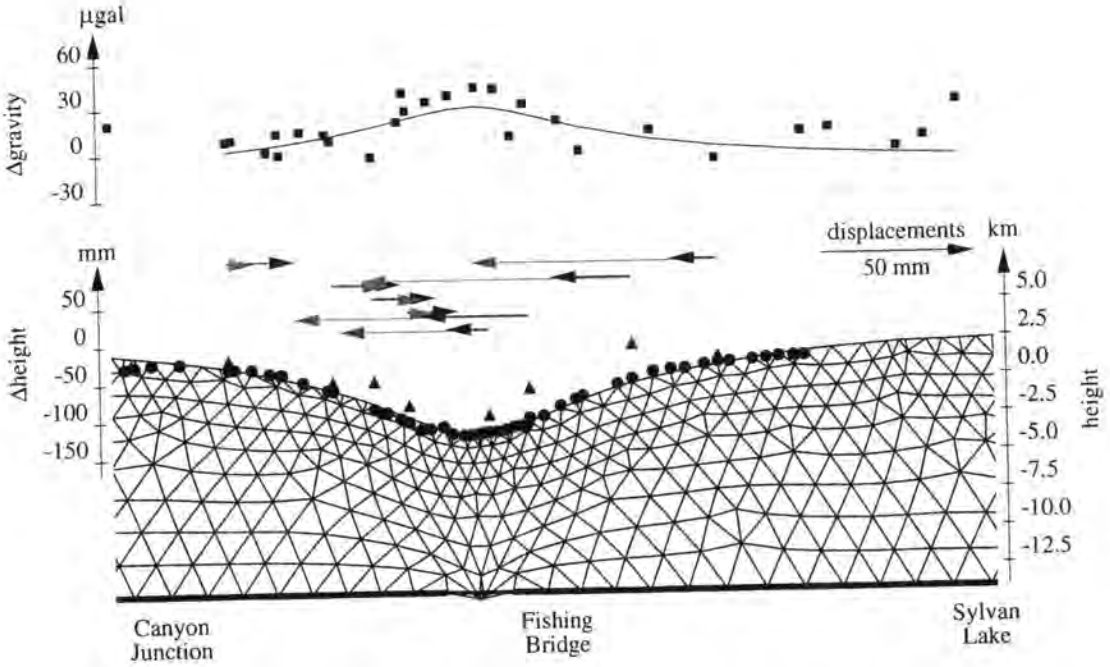

Fig. 5.6 d : Finite element model : Adjusted for leveling results : A temperature change of -4.23 K is applied at a depth of 14 km at the nodes fixed lying under the semi-bold line.

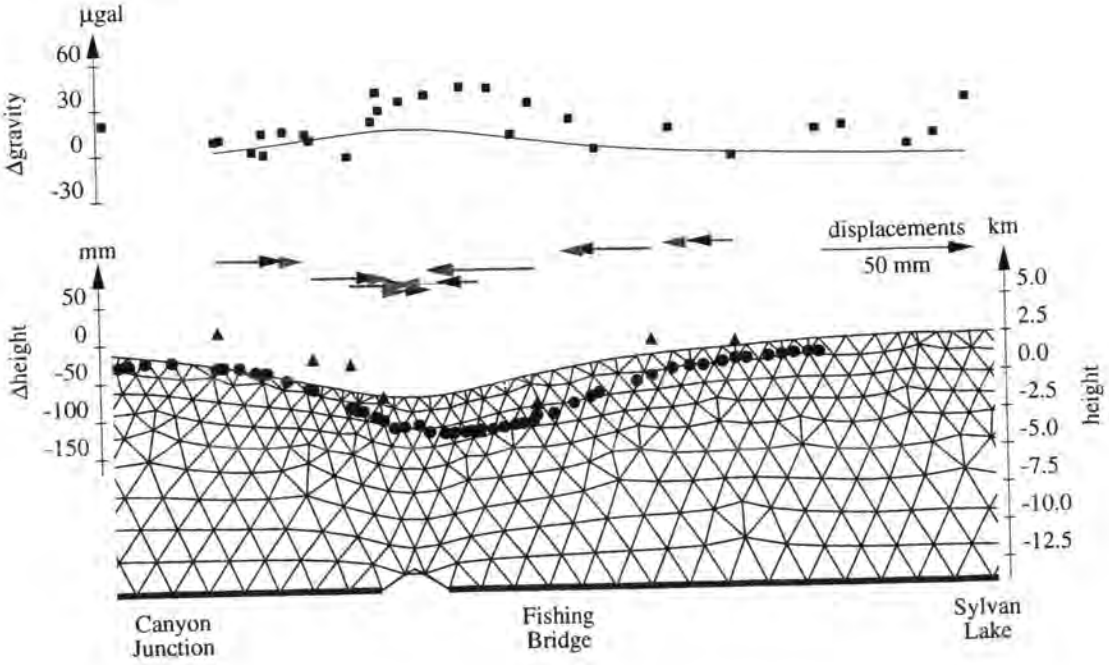

Fig. 5.6 e : Finite element model : Adjusted for GPS results : A temperature change of -2.62 K is applied at a depth of 14 km at the nodes lying under the thin line. Symbols see Fig. 5.6 a

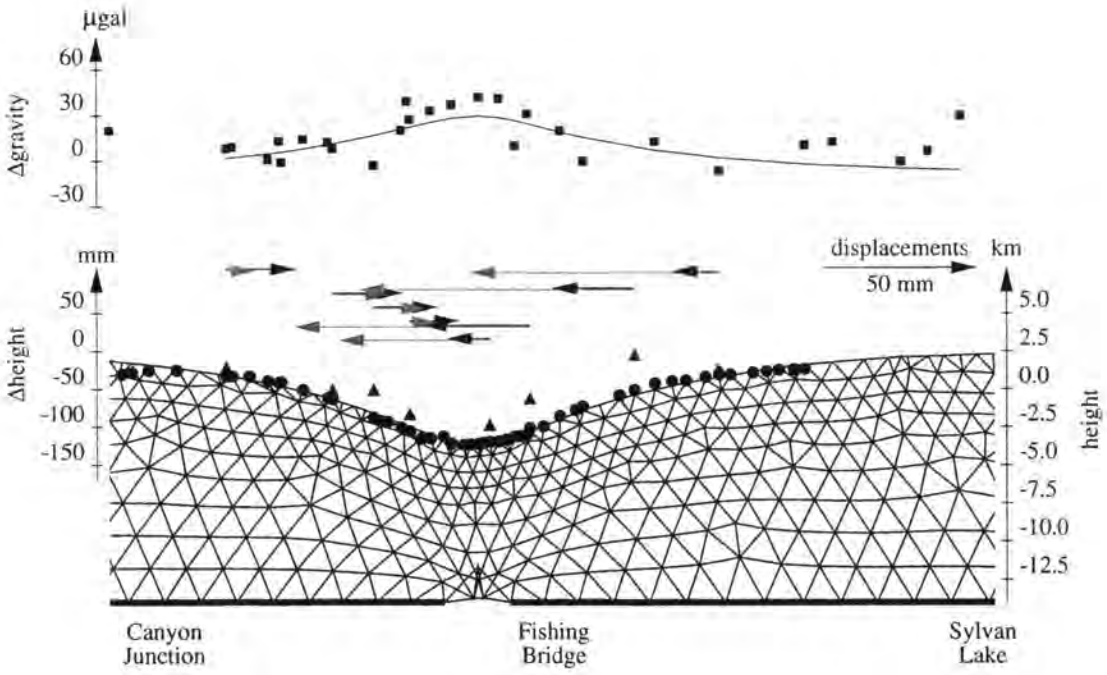

Fig. 5.6 f : Finite element model : Adjusted for leveling results : A temperature change of -4.645 K is applied at a depth of 14 km at the nodes lying under the thin line. Symbols see Fig. 5.6 a

This is an indication, that the Yellowstone caldera does not act like elastic material. Several probable reasons may cause this :

- Fault zones and the filling of the caldera with volcanic sediments are a probable cause for this. It is more likely, that in the upper part of the caldera the displacements from 1987 to 1993 are caused more by subsiding of separated blocks.
- The physical model chosen is time independent, which may be a non valid simplification of the problem. Perhaps, there is some significant elastic rebound.
- The cross section chosen is introduced as plane. However, in the line from Canyon Junction to Fishing Bridge to Sylvan Lake are some curves, which were not accounted for.

Furthermore, the calculated gravity changes due to deformed bodies are generally rather small (< 5 µgal). So the gravity changes are mainly due to the effect caused by the height changes (free-air gradient). That means, that most of the measured gravity changes different from the free-air gradient of the height changes are due to other effects. For one, this may be caused by groundwater table changes. The effect of a Bouguer slab of 1 m of groundwater in an area with an effective porosity of 0.25 causes 10 µgal of gravity changes. The effect of the groundwater can hardly be estimated in the Yellowstone area

due to the complicated geology. To reduce this problem, the Yellowstone gravity network was measured always in the same season, so effect of the water table remains about constant for the campaigns. Additionally, if there were gaps in the geologic structure of the caldera, they may get filled with material of different density (water -> rock). Another reason for observed gravity changes may still be systematic errors of the gravity meters. Another point is, that, if the displacements are due to temperature changes, the found offsets can be modeled best by limiting the temperature changes to a very small zone. This may be due to a convection in a magma chamber, bringing material of different temperature closer to the surface.

The difference between the calculated gravity changes are small for different kind of models (< 1 μgal for temperature, < 5 μgal for pressure). Thus the gravity changes can not help to reject one or the other model at the present stage of deformation. However, models with temperature changes (fig. 5.6 c-e) fit the gravity changes slightly better than pressure models (fig. 5.6 a, b).

For an interpretation of the changes between the other years, just the parameters of best fitting model were taken, that is a constant pressure applied at a depth of 14 km. Additionally, it is reasonable to keep the area of the pressure change constant to the one found in the model with 1987 and 1993. Looking at the results (tab. 5.2, figures 5.7), it shows, that an increasing pressure with time must be applied to fit the models best.

Independent of the correctness of the model parameters, this shows, that the force causing the deformations in the Yellowstone caldera was increasing from 1987 to 1993.

pressure [GPa] **rms of model**	1987	1989	1991	1993
1987	-	0.06	0.17	0.32
1989	1.5	-	0.10	0.26
1991	1.5	1.5	-	0.14
1993	2.0	2.9	1.6	-

Tab 5.2 : Calculated constant pressures (upper part) for different timespans at a depth of 14 km, from 10 km to 28 km (Canyon Junction : 0 km) with the calculated mean error of the model (lower part). Looking at 2 years time spans, it is seen, that the pressure is increasing.

5.3 Three dimensional model

The procedure for the three dimensional case is very similar

1. The net here is formed by tetrahedrons instead of triangles. The primary unknowns are the displacements in x, y and z direction and the temperature changes.

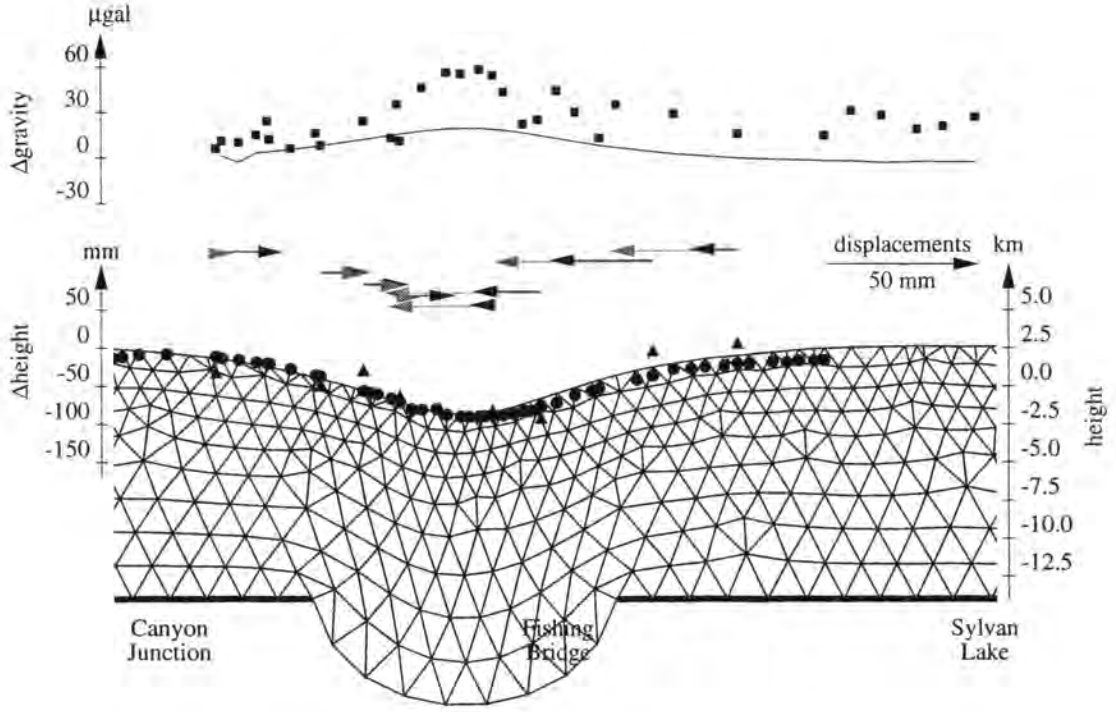

Fig. 5.7 a : Finite element model : Adjusted for leveling results 1989 - 1993: A pressure of 0.26 GPa is applied at a depth of 14 km at the area within thin lines. Further description see Fig. 5.6 a

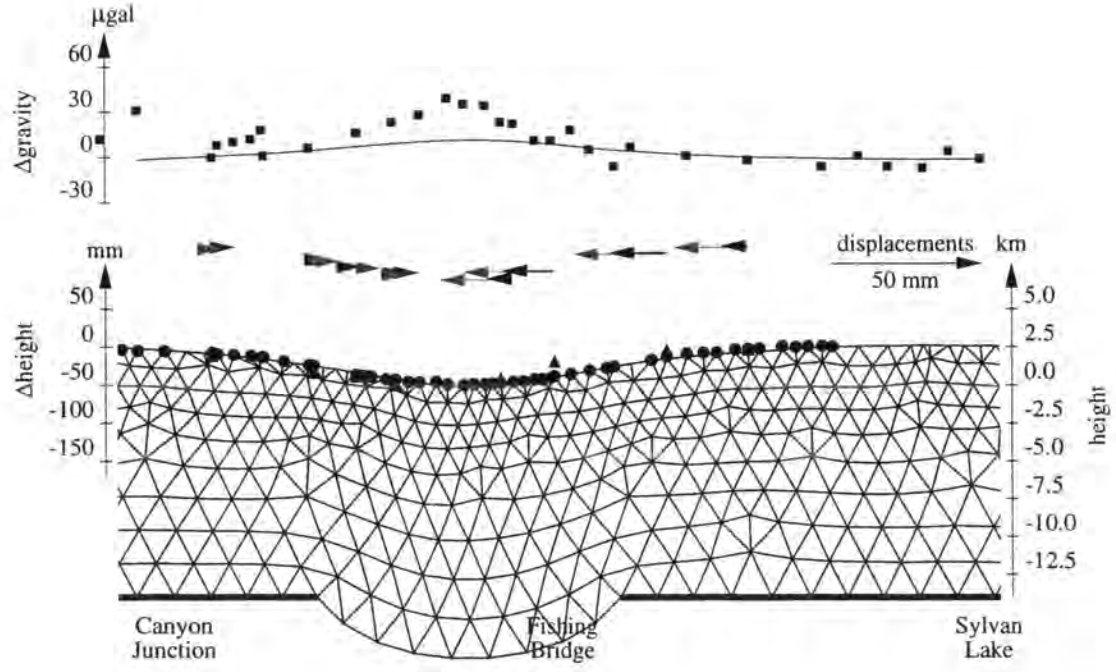

Fig. 5.7 b : Finite element model : Adjusted for leveling results 1991 - 1993: A pressure of 0.14 GPa is applied at a depth of 14 km at the area within thin lines. Further description see Fig. 5.6 a

- The spacing of the nodes horizontally is about 4 to 6 km.
- All GPS stations of the Yellowstone National Park are coincident with nodes (but w 367 and z 367, where the stations e 11a and 25 mdc respectively lay within 200 m).
- Precision gravity stations were used as much as possible to accomplish a regular net.
- Additional nodes were introduced in areas with neither GPS nor gravity stations in order to have a more or less equally spaced net.
- The nodes are connected by a triangular net that was achieved by Thyssen polygons.
- Two rings were added at the border of the area to enlarge it. One additional point was added for each two points of the previous border in each ring. So, the number of points is reduced in less interesting areas.
- The positions of the "free" nodes (neither GPS nor gravity stations) were adjusted so, that the sum of the squares of the horizontal distances to its neighbors is a minimum. The coordinates of the nodes of the outer ring were fixed in y-direction on the eastern and western border and in x-direction on the northern and southern border.
- The model consists of 9 layers that are horizontally equal spaced as the top layer. Vertically, the top nodes of the layer lie according to the topography and the ones of the bottom layer at a depth of 14 km. The nodes in between are spaced so, that the squares of the vertical distances to the neighboring nodes is a minimum. The distance from one layer to the next is about 2 km.
- In the rings, the number of layers is reduced to 5 and 3, respectively.

By these nodes and triangles, the structure can be subdivided in tetrahedrons. The Lamé constants, the thermal expansion coefficients and the density must be known within each tetrahedron. These values were determined as follows :
The values for v_p and v_s were interpolated for each node from the velocities found by D. Miller (1994). Outside the area of the velocity model, the velocities were chosen after tab 5.3. After that, the mean v_p and v_s velocities were linearly interpolated for each tetrahedron, and from that, the Lamé constants E an ν were found by (5.9) and (5.10).
In a first assumption, the expansion coefficients were chosen to constant = $2 \cdot 10^{-5}\ °C^{-1}$ (see also chapter 5.2, fig. 5.2).
The density values were interpolated for each node whenever possible according to the values found in chapter 4.3. Tab. 5.4 was used for nodes lying outside the modeled area.

2. The primary unknowns are u*, v*, w*, τ*. They were approximated by the functions u(x,y,z), v(x,y,z), w(x,y,z), τ(x,y,z). The application with the shape function is exactly the same as in the two-dimensional case.

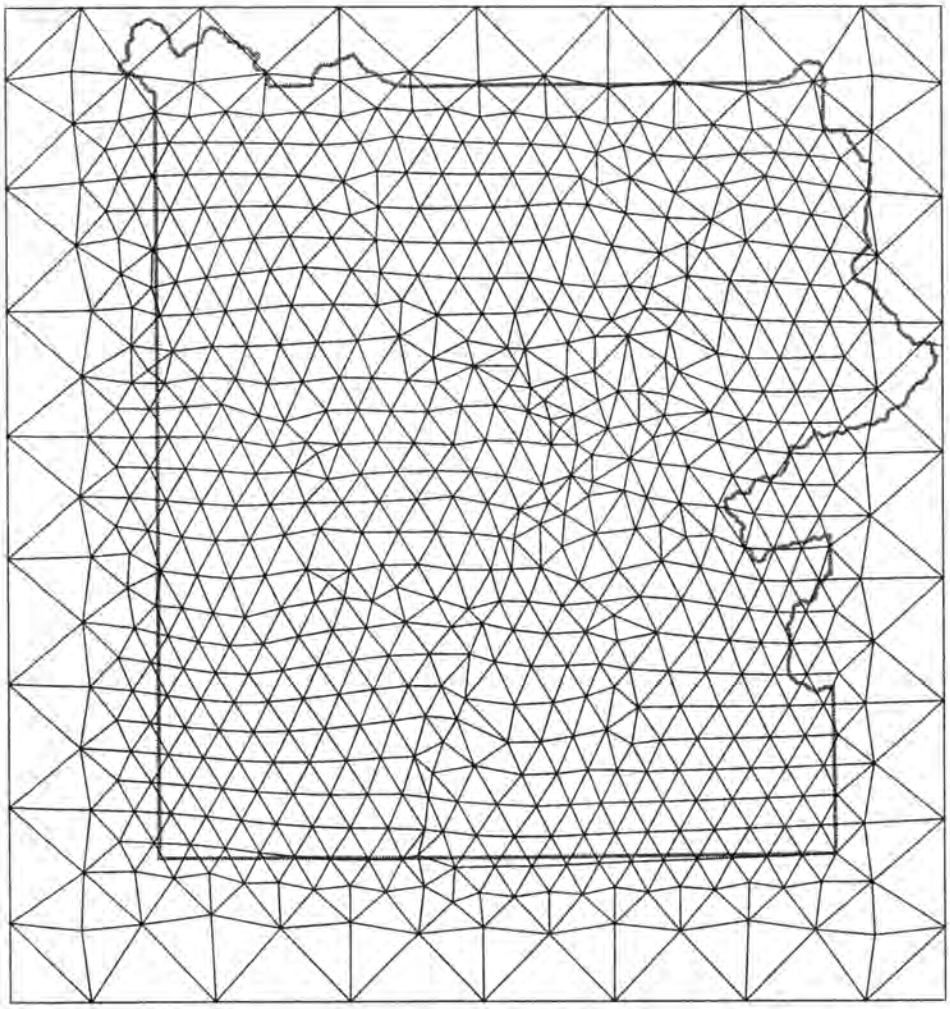

Fig 5.8 : Vertical view of the finite-element mesh over the Yellowstone National Park

height	v_p [km/s]	v_s [km/s]	ρ g cm^{-3}
4000.	4.80	3.00	2.568
2000.	4.80		2.584
0.	5.00		2.632
-2000.	5.36	3.19	2.698
-4000.	5.77		2.750
-6000.	5.88	3.56	2.785
-8000.	6.13		2.855
-10000.	6.43	3.90	2.900
-12000.	6.42		2.967
-14000.	6.82	4.13	

Tab. 5.4 : Assumed densities and seismic velocities outside the area of the velocity model of Miller (1994)

If we want to use formula (4.12) for the calculation of the gravity changes, N_i for the displacements must be again piece-wise linear within each element.

Here V^e is defined by $\begin{vmatrix} x_i - x_l & x_j - x_l & x_k - x_l \\ y_i - y_l & y_j - y_l & y_k - y_l \\ z_i - z_l & z_j - z_l & z_k - z_l \end{vmatrix}$, which is six times the volume of the tetrahedron formed by the nodes i, j, k, l. Then, with

$$V_i^e = \begin{vmatrix} x - x_l & x_j - x_l & x_k - x_l \\ y - y_l & y_j - y_l & y_k - y_l \\ z - z_l & z_j - z_l & z_k - z_l \end{vmatrix} \qquad V_j^e = \begin{vmatrix} x_i - x_l & x - x_l & x_k - x_l \\ y_i - y_l & y - y_l & y_k - y_l \\ z_i - z_l & z - z_l & z_k - z_l \end{vmatrix}$$

$$V_k^e = \begin{vmatrix} x_i - x_l & x_j - x_l & x - x_l \\ y_i - y_l & y_j - y_l & y - y_l \\ z_i - z_l & z_j - z_l & z - z_l \end{vmatrix}$$

, the linear shape functions in an element can be defined as

$$(5.22)\quad N_i^e = \frac{V_i^e}{V^e} \qquad N_j^e = \frac{V_j^e}{V^e} \qquad N_k^e = \frac{V_k^e}{V^e} \qquad N_l^e = 1 - \frac{V_i^e}{V^e} - \frac{V_j^e}{V^e} - \frac{V_k^e}{V^e}$$

3. Mathematical formulation of the problem

In three dimensions, the formulation for the stress-strain problem is more complicated :

$$(5.23)\quad \varepsilon = \begin{pmatrix} \varepsilon_x \\ \varepsilon_y \\ \varepsilon_z \\ \gamma_{xy} \\ \gamma_{yz} \\ \gamma_{zx} \end{pmatrix} = \begin{pmatrix} \frac{\partial u}{\partial x} \\ \frac{\partial v}{dy} \\ \frac{\partial w}{dz} \\ \frac{\partial u}{\partial y} + \frac{\partial v}{\partial x} \\ \frac{\partial v}{\partial z} + \frac{\partial w}{\partial y} \\ \frac{\partial w}{\partial x} + \frac{\partial u}{\partial z} \end{pmatrix} = \begin{bmatrix} \frac{\partial u}{\partial x} & 0 & 0 \\ 0 & \frac{\partial}{dy} & 0 \\ \frac{\partial}{\partial y} & \frac{\partial}{\partial x} & 0 \\ 0 & \frac{\partial}{\partial z} & \frac{\partial}{\partial y} \\ \frac{\partial}{\partial z} & 0 & \frac{\partial}{\partial x} \end{bmatrix} \begin{pmatrix} u \\ v \\ w \end{pmatrix} = \mathbf{S\,u = S\,N\,a = B\,a}$$

Piecewise linear shape functions lead again to constant strain within one element.

Stress

The three dimensional initial strain ε_0 due to temperature changes can be expressed as

$$(5.24)\quad \varepsilon_0 = \begin{pmatrix} \alpha\tau \\ \alpha\tau \\ \alpha\tau \\ 0 \\ 0 \\ 0 \end{pmatrix}$$

with

α : temperature expansion coefficient
τ : mean temperature difference $T_2 - T_1$ at the nodes i, j, k, l

The expression for the stress σ is given by :

$$(5.25)\qquad \sigma = \mathbf{D}(\varepsilon - \varepsilon_0) + \sigma_0$$

with

$$(5.26)\mathbf{D} = \frac{E(1-\nu)}{(1+\nu)(1-2\nu)} \begin{bmatrix} 1 & \nu/(1-\nu) & \nu/(1-\nu) & 0 & 0 & 0 \\ \nu/(1-\nu) & 1 & \nu/(1-\nu) & 0 & 0 & 0 \\ \nu/(1-\nu) & \nu/(1-\nu) & 1 & 0 & 0 & 0 \\ 0 & 0 & 0 & \frac{1-2\nu}{2(1-\nu)} & 0 & 0 \\ 0 & 0 & 0 & 0 & \frac{1-2\nu}{2(1-\nu)} & 0 \\ 0 & 0 & 0 & 0 & 0 & \frac{1-2\nu}{2(1-\nu)} \end{bmatrix}$$

with

E : Young's modulus
ν : Poisson's constant.

E and ν can be found in the same manner as in the two-dimensional case.
Expansion to three dimensions for the nodal and body forces can be easily formulated and equations (5.13) and (5.14) of the two-dimensional model are also valid here.

Thermal equations

Introduction of a third dimension leads to the conditions, that

$$(5.27)\quad \int_{V_e} \left(\frac{\partial\tau}{\partial x}\frac{\partial N_i}{\partial x} + \frac{\partial\tau}{\partial y}\frac{\partial N_i}{\partial y} + \frac{\partial\tau}{\partial z}\frac{\partial N_i}{\partial z} \right) dV - \int_{s_e} N_i \frac{\partial\tau}{\partial n}\, ds = 0$$

for each node i.

Boundary conditions

Also for the boundary conditions, the same thoughts as for the two dimensional case are valid. There are, however, additional observations, namely the horizontal displacements at the GPS stations, which of course will be also introduced in the least-squares part of the system.

5. A solution for the primary unknowns dT, dx, dy, dz could be found by an inversion of a matrix (see chapter 5.2). However, the model consists of more than 5000 nodes which gives more than 20000 unknown variables (in each node dx, dy, dz, and dT). An inversion of a matrix of this size is too slow and too large (size of inverted matrix : ≈ 400 mio. elements). Even for a Gaussian elimination method, the system is still too large. Therefore the equation system was solved numerically by a method close to Gauss-Seidel:

The Gauss Seidel Iterative Solution

We look for the solutions $\mathbf{x}$ of the linear equation system $A\mathbf{x} = \mathbf{f}$. If there are not too many unknowns $\mathbf{x}$ (≈ 1000), the matrix A can be inverted, and $\mathbf{x} = A^{-1}\mathbf{f}$. Faster and still accurate would even be the Gaussian elimination algorithm. However, if the system becomes too big, an inversion or an elimination algorithm becomes too large and too slow. For example, if we have 5000 nodes in a three-dimensional problem with the unknowns x, y, z and t, we get 20000 unknowns. In the matrix A, about 1 mio. elements will not be equal 0, which is quite large, but still manageable by reasonably large computers. However, the inverse A^{-1} would consist of 400 mio. elements. Using the symmetry of the matrix A and applying a Gaussian elimination algorithm reduces the number of elements, but it is still not enough that it could be used for practical calculations. Therefore, a method must be used, where the number of elements in the used matrices does not grow too large, or may stay even near the number of elements of A.
The Gauss-Seidel iteration is such a method. It is necessary to use an initial value for x, say $x^{(1)}$, which, if not known better, may be a null vector. Then we have for s = 1,2,...

$$(5.28)\quad x_i^{(s+1)} = a_{ii}^{-1}\left(f_i - \sum_{j=1}^{i-1} a_{ij}\, x_i^{(s+1)} - \sum_{j=i+1}^{n} a_{ij}\, x_i^{(s)} \right)$$

with

a_{ij} : elements of A
f_i : ith element of f
$x_i^{(s)}$: ith element of x of the sth iteration

The iteration is continued until the change in the current estimate of the displacement vector is small enough, i.e., until

$$\frac{|\mathbf{x}^{(s+1)} - \mathbf{x}^{(s)}|}{|\mathbf{x}^{(s+1)}|} < \varepsilon$$

where ε is the convergence tolerance. The number of iterations depends on the quality of the starting vector $\mathbf{x}^{(1)}$ and on the conditioning of the matrix A. Depending on A, it may also be that the iteration does not converge, especially if the diagonal elements are comparably "small" to the others. No further discussion about that shall be given here. Further, the rate of convergence can be increased using over-relaxation, in which case the iteration is

$$(5.29)\quad x_i^{(s+1)} = x_i^{(s)} + \beta\left(a_{ii}^{-1}\left(f_i - \sum_{j=1}^{i-1} a_{ij}\, x_i^{(s+1)} - \sum_{j=i+1}^{n} a_{ij}\, x_i^{(s)} \right) - x_i^{(s)} \right)$$

with

β : over-relaxation factor

The optimum value for β depends on A and is usually between 1.3 and 1.9.

6. The secondary unknowns of our system are the gravity values and the model parameters. The model parameters have to be adjusted such, that they fit the measured vertical, horizontal and gravity changes best. This can be achieved by a least-square approximation.
For that, the derivatives with respect to the parameters must be known. They are calculated numerically by introducing small changes in each one of the parameters and re-running the finite element system.
For the gravity changes, it turned out, that an exact calculation after (4.12) is too slow to allow efficient calculations. Therefore, only the differences of the effects of tetrahedrons lying closer than 15 km to each respective gravity station were determined accurately by

(4.12) (= dg_{exact}). The others were approximated by point masses (= $dg_{appr.}$), which is sufficient for the needed accuracy.

(5.30) $$dg_{exact} = \rho_{e_1} \frac{V_{e_1}}{V_{e_2}} T_{z,2} - \rho_{e_1} T_{z,1}$$

with T_z after (4.12), and

(5.31) $$dg_{appr.} = m_e U_{z,2} - m_e U_{z,1}$$

with

m_e : mass of tetrahedron e = $\rho_{e_1} V_{e_1}$

$U_z = \frac{z}{r^3}$

$P_s(x_s,y_s,z_s)$: Coordinates of the gravity station

$P_i(x_i,y_i,z_i)$: Coordinates of the edges of a tetrahedron e, i = 1,2,3,4

$\mathbf{r}_i$: vector from P_s to P_i $\quad$ r_i : length of vector $\mathbf{r}_i$

$$z = \sum_i \frac{z_i - z_s}{4} \qquad \mathbf{r} = \sum_i \frac{\mathbf{r}_i}{4}$$

For tetrahedrons of the typical size used for the finite elements,

$| dg_{appr.} - dg_{exact} | < 5 \cdot 10^{-5}$ µgal $\quad$ if r > 15 km

5.3.1 Yellowstone Caldera Three-Dimensional Models

For the 3-dimensional model, basically the same assumptions were taken as for the 2-dimensional model (see fig. 5.5). However, there are some more parameters to be found. In the 2-dimensional model, the left and the right border of the caldera and the pressure or the temperature change was unknown. For the 3 dimensional model, it makes sense to model the caldera as an elliptical cylinder. So the unknowns are the center of the ellipse, the lengths and the directions of the axes and again the temperature and/or pressure change.

With the data of 1987 and 1993, a model was calculated. It shows, that the displacements measured by GPS can be best modeled, if the nodes lying outside the elliptical cylinder are fixed (fig. 5.9 and 5.10). Even with the points fixed, the measured horizontal displacements are smaller than the ones modeled, if the vertical change is approximated best. This is more pronounced, when the leveled height changes are introduced in the adjustment additionally. The pressure found (0.15 GPa) is smaller than the one in the 2 dimensional model (0.32 GPa). This is due to the fact, that smaller axis of the elliptical cylinder, which corresponds to the active zone in 2 dimensional model, has a length of 36 km compared to 18 km in the two dimensions. This difference can be explained so,

that, first, the 2 dimensional model crosses not the entire active zone of the caldera and second, that there is an increase of the forces towards the middle of the caldera.
Basically the same discrepancies between the horizontal and vertical displacements are obtained by replacing constant pressure with a constant temperature change at a depth of 14 km.
From these results can be concluded, that the whole Yellowstone region does not behave like perfect elastic material. The probable reasons are the same as mentioned in results for the 2 dimensional model.

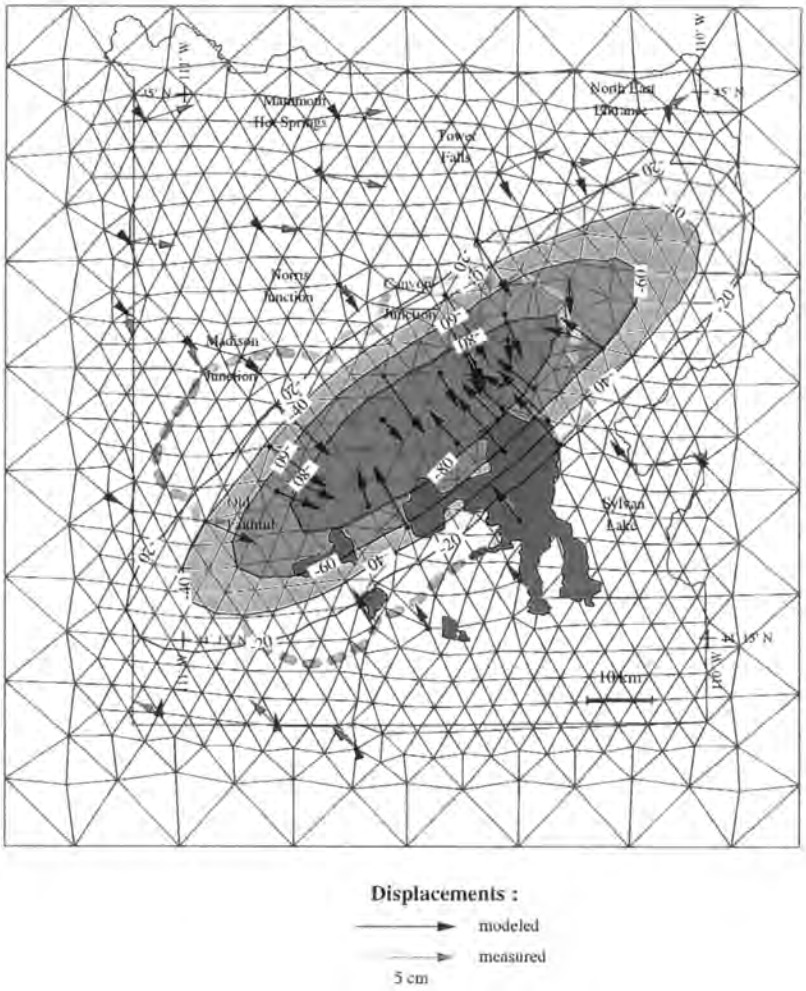

Fig. 5.9 : 3D Finite element model for 1987 to 1993: Points free outside elliptical cylinder. Calculated model and displacements of GPS results (see also fig 3.6)

Like in the 2 dimensional case, the development of the model from 1987 to 1993 was investigated. For this, the area of the elliptical cylinder was fixed to the one found for time span from 1987 to 1993. To model the measurements best, an increasing pressure with time must be applied at the bottom of the model. This is also coherent with the 2 dimensional model.

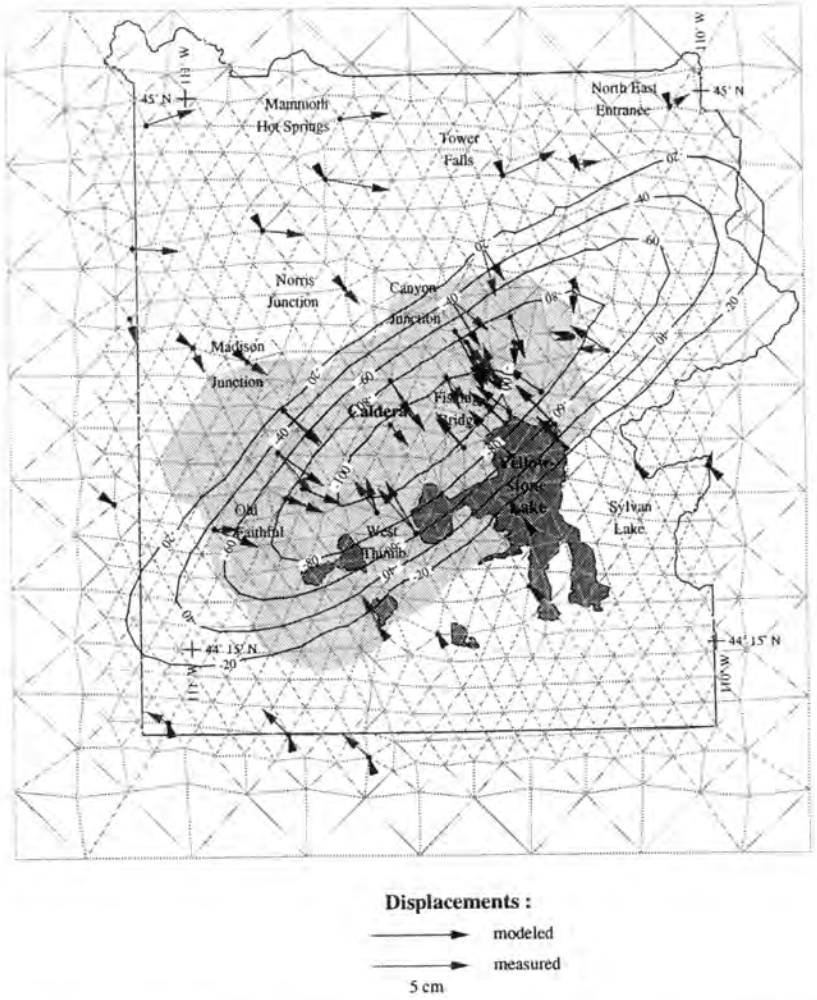

Fig. 5.9 : 3D Finite element model for 1987 to 1993: Points fixed outside elliptical cylinder. Calculated model and displacements of GPS results (see also fig 3.6)

pressure [GPa] **rms of model**	1987	1989	1991	1993
1987	-	0.032	0.079	0.15
1989	1.4	-	0.046	0.11
1991	1.4	1.4	-	0.069
1993	1.9	2.1	1.4	-

Tab. 5.5 : Calculated constant pressures for different time spans at a depth of 14 km, within an ellipse with semi axes of 70 km and 18 km, centered at 44°34.5' N, 110°29.0' W, azimuth of large semi axis 37°. The nodes outside the vertical elliptical cylinder were free.

6. Summary

Geodetic measurements confirm, that the Yellowstone caldera is a highly active region of contemporary crustal movements. From 1923 to 1984, uplift took place over the Yellowstone caldera with height changes of up to 0.8 m. This was measured by leveling. Additional evidence was contributed by the precision gravity network, installed in 1977. From 1977 to 1986, the gravity values decreased up to -60±12 µgal. After 1985, the heights in the caldera started to decrease with a rate of about 2 cm a^{-1}. The maximum height decrease was 14 cm until 1993. In the same time span, the gravity increased up to +65±12 µgal.

For the processing of the gravity data, systematic errors of the LaCoste and Romberg G and D-meters were estimated. It was found, that the circular error of the measuring screw of G-meters can be as large as 30 µgal. The factors of some instruments were calibrated on a USGS gravity calibration line near San Francisco, revealing that they can differ from the value given by LaCoste and Romberg up to 0.7 ‰.

In order to model the observed gravity, vertical and horizontal changes of the Yellowstone caldera, finite-element models were created. For that, some physical parameters had to be found from geophysical measurements : A density model of the Yellowstone area was calculated from a 3-D seismic p-wave velocity model and gravity anomalies. The Lamé coefficients, describing the elastic behavior of material, were calculated with the help of a model for p and s wave velocities.

A 2-dimensional model was established for a northern caldera crossing line with an active source at a depth of 14 km. Either a pressure decrease of 0.32 GPa within 18 km or a temperature decrease of -4 K was found to model the leveled height changes best. In both cases, the horizontal displacements modeled are about twice as large as the ones measured by GPS. It was also found, that the pressure increased in the period from 1987 to 1993.

A 3D model was constructed for the Yellowstone National Park region. It was shown, that the height changes can be best modeled applying a constant pressure of 0.15 GPa at a depth of 14 km within an ellipse with semi-axes of 70 km and 18 km and an azimuth of 37°. As for the 2-dimensional model the horizontal displacements calculated are too large. In the 2- as well as in the 3-dimensional models, the gravity changes do not significantly differ from the free-air effect (< 5 µgal), so that measured gravity changes were not used for the models.

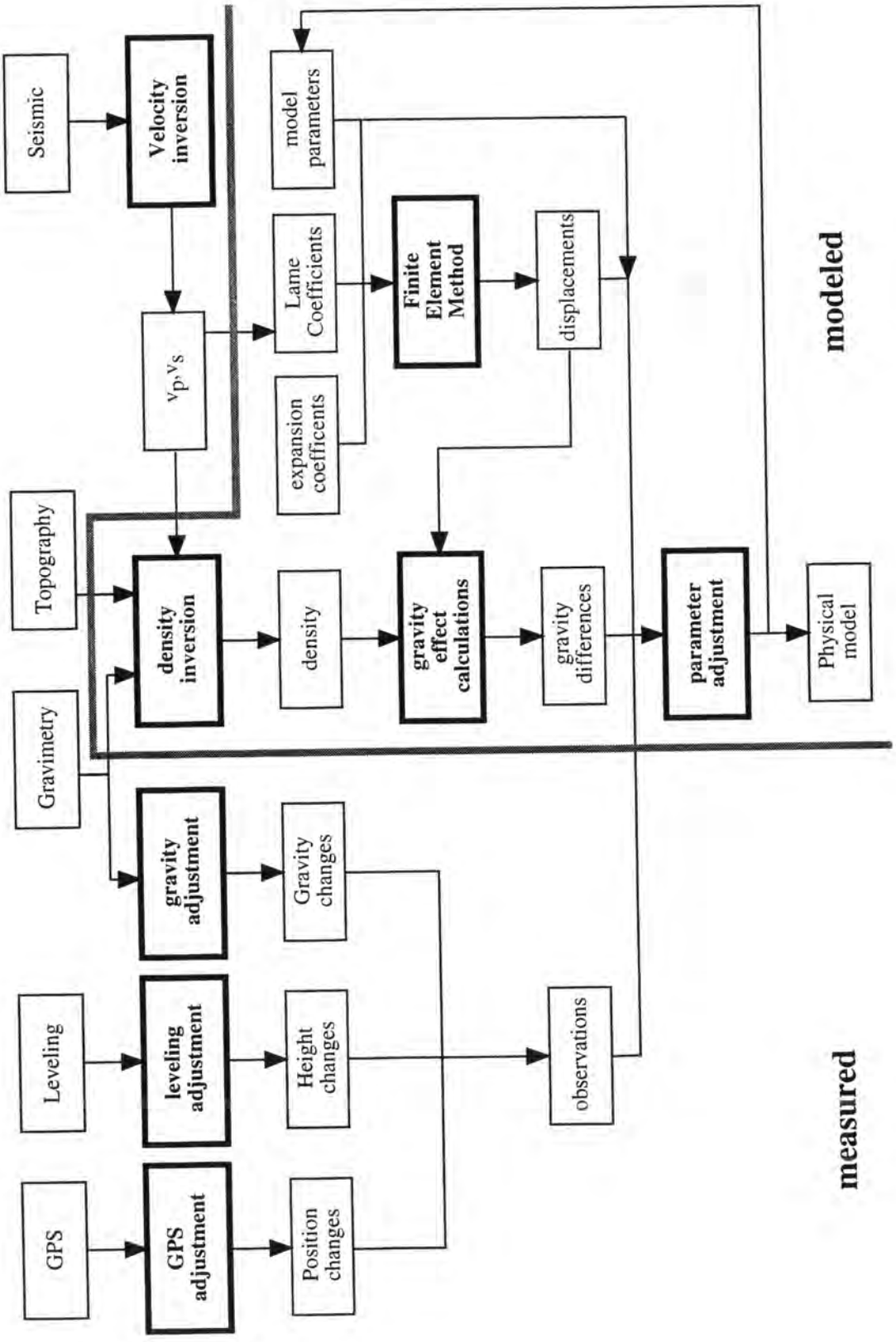

Fig. 6.1 : Flow chart of the computation procedure for models of the Yellowstone caldera

7. Conclusions

The Yellowstone caldera is one of the earth's most interesting and active geologic features. Although at the moment, the area is not imminently dangerous, huge eruptions 0.6 Ma and 1.2 Ma ago have shown the enormous power of the Yellowstone hotspot. Therefore it is of great interest to understand more about the tectonic processes and mechanics that are going on under the Yellowstone National Park.

Gravity, leveling and GPS networks cover the Yellowstone caldera. Leveling and GPS measurements allow to monitor the displacements at the surface with high accuracy. From this data it was detected, that uplift between 1923 and 1984 was followed by subsidence afterwards. Gravity and height changes in combination allow to obtain information about mass changes.

The main objective of this thesis was to analyze all available precision gravity data and to develop theoretical models that allow better understanding of the mechanics in the Yellowstone caldera.

The use of LaCoste and Romberg gravity meters permit to detect small non-tidal gravity changes that may be related to active geologic processes. One must be aware of the fact, that the gravity meters have significant circular errors, which have to be calibrated to arrive at reliable results. This can be done either with two model G-gravity meters, the results of which are compared during several years, or by calibrating it with a LaCoste and Romberg D-meter. The absolute factor of the gravity meters must be calibrated too, using either an absolute gravity line or by comparing the results with an instrument already calibrated.

However, even with correctly calibrated gravity meters, the mean errors of an instrument lie clearly below a value that can be expected to be the true one. This is one reason why the obtained gravity changes in the Yellowstone gravity network must be examined carefully. Furthermore, the reliability of the results of a gravity campaign depend on the measuring techniques applied. It is necessary to measure with at least two instruments and to carry out strengthened ladder loops with connections to all neighboring stations in order to obtain optimal results. In areas, where this cannot be done, e.g. in backcountry regions, the mean error of the calculated gravity value must be considered to be as high as some tenth of µgals. Compared with signals associated with the uplift and/or subsidence in the Yellowstone caldera, this is about 10 times higher than the annual rate.

The influences of the local effects of groundwater on the gravity cannot be determined. Estimations show, that they amount to some µgals, however, due to the complex geology of the Yellowstone region with its hot springs, the influences may be larger.

Static finite-element models with ideal elastic material and no fault zones were tested for the Yellowstone caldera. They cannot explain simultaneously the horizontal and vertical displacements measured. Compared to the height changes, the measured horizontal displacements are too small. Therefore, the upper part of the Yellowstone caldera cannot be considered as an elastic medium. It is of great interest to do more research in this direction. Time dependent models, that allow the introduction of fault zones and porous and plastic media would be steps to pursue. Unfortunately, this could not be done in this thesis.

At the present stage of deformation, the gravity changes determined are not significantly contributing to distinguish between different kind of models for the Yellowstone caldera, e.g., between a model with only temperature changes or one with active pressure. The displacements must be at least 5 to 10 times larger than those measured up to now, before the gravity changes can significantly contribute to reject or to sustain one of the models.

For the better understanding of the mechanics of the Yellowstone caldera it is necessary to continue with GPS campaigns on a regular base. The present status with measurements every two years is capable to monitor the trend of the displacements in the Yellowstone National Park accurately. In order to constrain the height changes in the most active areas, precision leveling is of good help, if not even necessary. At the present rate of deformations, it is sufficient to measure the gravity changes every five to ten years. However, when they are measured, it is necessary to take good care of the applied techniques to get usable results. The relative long time spans between the proposed gravity campaigns are a danger, that the gravity campaigns might get forgotten. Different persons in charge may set other priorities and so the gravity measurements, may get abandoned.

Anyway, the Yellowstone hot spot will continue to be active, with or without geodetic and geophysical measurements.

Acknowledgments

I want to thank my examiner **Prof. Dr. H.G.Kahle** that I could perform this PhD thesis of one of the most spectacular areas of the world with his guidance.

During several stays in the Yellowstone National park and in Salt Lake City, the "headquarters" of the Yellowstone geodynamics, I could profit from my co-examiner Prof. **Dr. R.B.Smith**, one of the best experts of the Yellowstone area. He was a great help, not only with his suggestions, but also with managing that I had all necessary equipment and data for a successful work.

For the analysis in Zurich, my other co-examiner **Prof. Dr. E.E.Klingelé** was always at hand to help me with his large knowledge about gravity and its related fields.

This thesis could not have been done without the work of many others I learned to know during my stays in the USA. Especially I want to thank **Dr. C. Meertens**, chief of the Yellowstone GPS campaigns, **D. Dzurisin** for his leveling data, and **D. Miller** for his seismic velocity models.

In the first period of my thesis, I was able to profit from stipends of the **Kanton St.Gallen** and the Swiss federal institute of technology, **ETH Zurich**. After that, I was able to work part time on my thesis with the help of the Swiss geophysical commission **SGPK**.

The field work in the Yellowstone National Park was supported by the **National Science Foundation** of the U.S.A.

References

Arnet, F. (1992) : POTENZ, ein Programmpaket zur Berechnung der Schwere und der ersten beiden Ableitungen von allgemeinen Polyedern konstanter Dichte. ETH Zürich

Arnet, F. (1993): Crustal Deformation Studies in the Yellowstone National Park, Part I: Levelling and Gravity Data. ETH Zürich

Bathe,K.J., E.Wilson (1976) : Numerical Methods in Finite Element Analysis. Prentice Hall.

Berrino, G. (1994) : Gravity changes induced by height-mass variations at the Campi Flegrei caldera. Journal of Volcanology and Geothermal Research 61,293-309.

Berrino, G.,H.Rymer,G.C. Brown, G.Corrado (1992): Gravity-height correlations for calderas at unrest. Journal of Volcanology and Geothermal Research 53,11-26.

Carle, S.F.,J.M.Glen, V.E. Langenheim, R.B.Smith and H.W.Oliver (1989): Isostatic gravity map and principal for 694 gravity stations in Yellowstone National Park and vicinity, Wyoming, Montana and Idaho, 1 over-sized sheet, scale 1:125'000 map, U.S.Geol.Survey, Open-file report 90-649A and B.

Dzurisin,D.,J.C.Savage,R.O.Fournier (1990): Recent crustal subsidence at Yellowstone Caldera, Wyoming. Bulletin of Volcanology,52:247-270, Springer Verlag.

Evoy,J.A. (1978) : Precision Gravity and Simultaneous Inversion of Gravity and Seismic Data for Subsurface Structure of Yellowstone. University of Utah.

Gallagher,R.H. (1975): Finite-Element-Analysis. Prentice Hall.

Hardman, W.L. (1991) : 1989 and 1990 Yellowstone Gravity Surveys with accompanying data from 1977-1990. University of Utah.

Hohldahl,S.R.,D.Dzurisin (1990) : Time Dependent Models of Vertical Deformation in the Yellowstone-Hebgen Lake Region for the Period 1923-1987. USGS

Hollis,J.R. (1988) : Precision Gravity Reobservation at Yellowstone National Park, Wyoming, 1977-1987. University of Utah.

Hughes,T. (1987): The Finite Element Method. Prentice Hall

Jachens, R.C., W. Thatcher, C.W.Roberts, R.S. Stein (1983) : Correlation of changes in gravity, elevation and strain in Southern California, Science, 219, 1215-1217.

Johnson, D.J. (1992) : Dynamics of magma storage in the summit reservoir of Kilauea Volcanoe, Hawaii, Journal of Geophysical Research, 97, pp 1807-1820

Johnson, D.J. (1995) Molten core model for Hawaiian rift zones, Journal of Volcanology and Geothermal Research, 66, pp 27-35.

Johnson, D.J. (1995) : Gravity changes on Mauna Loa Volcano in Mauna Loa revealed : Structure, composition, History and Hazards. Geophysical Monograph 92, edited

by J.M Rhodes and John P.Lockwood, pp 127-143, AGU (in press).

LaCoste, L. (1991):A new calbration method for gravity meters. Geophysics, Vol. 56, No. 5, pp. 701-704.

Kahle, H.G.,E.Klingelé (1995): Density Distribution within the Lithosphere. International Association of Geodesy, SSG 5.150.

Kahle, H.G., D.Werner (1980): A Geophysical Study of the Rhinegraben. II. Geophys. J. R. astr. Soc., Vol. 62, p. 631-716.

Kiviniemi, A. (1977) : The Finnish measurements at the Fennoscandian land uplift gravity lines. Proceedings of the Symposium on "Non-tidal graviy variations and their study" in Trieste, 1977. Boll. Geof. Teor. Appl. XX,80.

Marson,I., P.Baldi (1981): Gravity and Geodetic Networks for Study of Crustal Deformations in Seismic Area (Ancona). Bollettino di Geodesia e scienze affini, No.3.

Marson,I., M. Di Filippo, F.Palmieri, B.Toro, A.Rossi (1988): Microgravity Variations Observed in two Geothermal Fields in Italy. Bureau Gravimetric International, No.62.

Meertens,C.M.,R.B. Smith (1991): Crustal Deformation of the Yellowstone Caldera from First GPS Measurements : 1987-1989, University of Utah.

Mitchell,A.R.,R.Wait (1977): The Finite Element Method in Partial Differential Equations. J.Wiley&Sons.

Mogi, K. (1985) : Relations of eruptions of various volcanoes and the deformation of the ground surfaces around them. Bull. Earthquake Res. Univ. Tokyo, 39, 99-134.

Molbert,D.G.,W.T.Dewhurst (1990): The Yellowstone-Hebgen Lake Geoid obtained Through the Integerated Geodesy Approach. Submitted Journal of Geophysic Research.

Pelton,J.R., R.B.Smith (1979): The Analysis of Deformation - Included Variations in Orthometric Height and Gravity with an Application to Recent Crustal Movements in Yellowstone National Park.

Pelton, J.R., R.B.Smith (1979) : Recent crustal uplift in Yellowstone National Park. Science, 206, p 1179-1182.

Pelton,J.R.,R.B.Smith(1979) : Recent crustal Uplift in Yellowstone National Park. Science Reprint Series, Vol 206, pp 1179-1182.

Pelton,J.R.,R.B.Smith (1982): Contemporary Vertical Surface Displacements in Yellowstone National Park. Journal of Geophysic Research, Vol.87, p 2745-2761.

Peyton,S.L. (1988): Progress Report 1988 Yellowstone Precision Gravity Survey Processing and Results. University of Utah.

Rymer,H. (1989): A Contribution to Precision Microgravity Data Analysis Using Lacoste and Romberg Gravity Meters. Geophysical Journal, 97, p 311-322.

Rymer,H.,G.C.Brown (1987): Causes of Microgravity Change at Poasa Volcano Costa Rica: an Active but Non-Erupting system, Bulletin of Volcanology, 49: 389-398, Springer 1987

Rymer,H.,G.C.Brown (1986): Gravity Fields and the Interpretation of Volcanic Structures : geological Discrimination and Temporal Evolution. Journal of Volcanology and Geothermal Research, 27 p229-254.

Smith,R.B.,R.L.Christiansen (1980): Yellowstone Park as a Window on the Earth's Interior. Scientific American, 242, 2, p. 104-117.

Smith,R.B., R.E.Reilinger, C.M.Meertens, J.R.Hollis, S.R.Hohldahl, D.Dzurisin, W.K.Gross,E.E.Klingele (1989): What's Moving at Yellowstone; EOS, pp. 113-125.

Smith, R.B., L.W.Braile (1994) : The Yellowstone Hotspot. J.Volcanology and Geotherm. Research, eds. D.P. Hill, P. Gasparini, S. McNutt and H.Rymer, 61:121-188.

Somerton,W.H. (1992) : Thermal Properties and Temperature-related Behavior of Rock/Fluid Systems. Elsevier

Sylvester,A.G.,J.O.Byrd,R.B.Smith (1991): Aseismic Reverse Deplacement across the Teton Fault, Teton Range, Wyoming.

Valliant,H.D. (1991): Gravity meter calibration at LaCoste and Romberg. Geophysics, Vol. 56, No. 5, pp. 705-711.

Vasco, D.W. (1985) : Extremal inversion of vertical displacements, Long Valley caldera, California 1982/1983. J.Geophys. Res., 57, p 178-183.

Vasco, D.W., L.R. Johnson, and N.E.Goldstein (1988): Using surface displacements and strain observations to determine deformation at depth, with an application to Long Valley caldera, California. J. Geophys. Res., 93, 3232-3242

Vasco,D.W.,R.B.Smith,C.L.Taylor (1990) : Inversion for Sources of Crustal Deformation and Gravity Change at the Yellowstone Caldera. Journal of Geophysic Research, Vol 95., No B12, p 19839-19856.

Whitcomb, J.H.Franzen (1980): Time dependent gravity in Southern California. Journal of Geophysic Reasearch, Vol 85,p 4363-4373.

Williams,m D.L., G. Abrams,C.Finn, D.Dzurisin, D.J. Johnson, R.Denlinger (1987) : Evidence from gravity data for an intrusive complex beneath Mount St.Helens. Journal of Geophyscal Research, 92, pp 10207-10222

Zienkiewicz,O.C,Taylor,R.L. (1965): The Finite Element Method. McGraw-Hill, 1991

Zurmühl,R. : Praktische Mathematik, Springer Verlag.

Appendix A : Introduction into the Least-Squares Method

The following appendix gives a brief overview over the least squares method. It was applied in several sections, where unknown values were estimated, such as determining of the gravity values, densities, or model parameters of a Yellowstone crustal model.
The least-squares method can be used to find values of unknowns, like e.g. the height of a point or the co-ordinates x, y, h of a station. To determine this value, a functional model between known or given values and the unknowns must be formulated. For example, if the distance d between two points P_1, P_2 in a plane is measured, d can be expressed as :

$$d = \sqrt{(x_2 - x_1)^2 + (y_2 - y_1)^2}$$

All the equations belonging to the functional model form the set of observation equations. If these equations are non-linear, it would become complicated or impossible to find explicit formulations for the unknowns. Therefore, it is convenient to linearize the equations and to estimate a near solution x_{i0} for the unknowns x_i . So, e.g. $l = f(x_1,x_2)$ becomes

(A.1) $$l = f(x_{10} + dx_1, x_{20} + dx_2)$$

and by Taylor series expansion

$$l = f(x_{10}, x_{20}) + \frac{\partial f}{\partial x_1} dx_1 + \frac{\partial f}{\partial x_2} \text{ t.o.h.o } = l_0 + \frac{\partial f}{\partial x_1} dx_1 + \frac{\partial f}{\partial x_2} dx_2 + \text{t.o.h.o}$$

(t.o.h.o = terms of higher order, that are neglected)

Giving a set of an n-linear system of equations, if there are more observations than unknowns dx_i, produces an overdetermined problem. Then the least squares method can be applied by introducing improvements **v** to the observations **l** :

(A.2) $$\mathbf{v} = A\mathbf{x} - (\mathbf{l} - \mathbf{l}_0) = \mathbf{v} = A\mathbf{x} - \mathbf{f}$$

with

- **v** : vector of improvements
- **x** : vector of unknowns $(dx_1, dx_2, ...)$
- A : matrix achieved by linearizing the observation equations
- **l**, $\mathbf{l}_0$: observation, near solution

Equation (A.1) is called the functional model. Additionally to this, a statistical model must be introduced. Generally it is assumed, that the expected value of an element of **l**, l_i , has a

Gaussian distribution with a mean error σ_i and that the correlation with v_j, $j \neq i$, is known. By this, the correlation matrix Q_{ll} is known and P is the inverse of Q_{ll}. If the statistical and the functional models are corrected, then the most probable solution of the problem is obtained by minimizing $\mathbf{v}^T\mathbf{P}\mathbf{v}$. This leads to the equation for the unknowns

(A.3) $$\mathbf{x} = (A^TPA)^{-1}A^TP\mathbf{f}$$

If the observation equations have to be linearized, it is necessary to introduce the new solution as starting value in (A.1) calculate another solution and repeat this procedure, until the values for the unknowns are stable.

A.1 Some useful Formulas

The covariance matrix of the unknowns, **x**, is given by :

(A.4) $$Q_{xx} = (A^TPA)^{-1}$$

The diagonal elements of Q_{xx} are equal to the mean square errors σ_x^2 of x (a priori).
Other useful expressions are the covariance matrix of the residuals, v, called Q_{vv} :

(A.5) $$Q_{vv} = Q_{ll} - AQ_{xx}A^T$$

and the residuals v :

(A.6) $$\mathbf{v} = - Q_{vv}P\mathbf{f}$$

The i^{th} diagonal element of $Q_{vv}P$ further shows the grade of redundancy of the i^{th} measurement. In geodesy it turned out to be good if a redundancy of at least 0.3 is available to detect rough errors. The expected value of $\mathbf{v}_s^TP\mathbf{v}_s$, where s are special measurements (for example the measurements of one day or all the measurements with one instrument), is equal to the sum of the s. diagonal elements of $Q_{v_sv_s}P$ = red(s) (redundancy). Especially the expected value of $\mathbf{v}^TP\mathbf{v}$ of all measurements, if all the functional and statistical model assumptions are true, is given by :

(A.7) $$E(\mathbf{v}^TP\mathbf{v}) = n - u = \sum_{i=1}^{n} \text{diagonal elements of } Q_{vv}P$$

with

n : number of measurements

u : number of unknowns

The expression for the mean error a posteriori, $\hat{\sigma}_0$:

(A.8) $$\hat{\sigma}_0 = \sqrt{\frac{\mathbf{v}^T\mathbf{P}\mathbf{v}}{n - u}} \text{ (a posteriori)}$$

is t-distributed with a degree of freedom (n - u). So, e.g., the model assumptions can be rejected with a probability of 95%, if σ_0 is larger than $t_{n-u;95\%}$.

All the quotients $\sqrt{\frac{\mathbf{v}_s{}^T\mathbf{P}\mathbf{v}_s}{\sum_s \text{red(s)}}}$ are t - distributed with a degree of freedom = $\sum_s$ red(s).

Appendix B : Program *gravity*

In this appendix, a short introduction is given into the program *gravity*. Most of it was written especially for the reduction of the Yellowstone gravity measurements. However, its form is kept general enough, that all measurements with LaCoste&Romberg G and D gravimeters can be adjusted.

Data files

1. Format of the files of the measured values

```
       79- 9- 7   0  g461  1.000000
a 11    16 3  3401.046
11 mdc  1658  3418.083
a 11    1745  3400.966
11 mdc  1830  3418.008
a 11    1916  3400.922
11 mdc  2042  3417.976
a 11    2127  3400.930
11 mdc  2211  3418.023
a 11    2256  3400.982
11 mdc  2343  3418.084
       79- 9- 9   0  g461  1.000000
z 10    17 4  3400.318
a 11    1721  3401.049
30 mdc  1737  3397.736
b 11    18 8  3404.570
da 3c   1832  3407.890
27 mdc  1849  3407.576
30 mdc  2157  3397.650
b 11    2219  3404.531
da 3c   2239  3407.876
27 mdc  23 0  3407.632
z 10    1919  3400.314
```

with

Header (format (7x,i2,1x,i2,1x,,i2,2x,i1,2x,a4,2x,f8.6)) :
1. group : date (year, month, day) of the set
2. group : time offset between set time and Greenwich time
3. group : name of gravity meter
4. group : factor of gravity meter (multiplication factor for calibration table)

Measurements (format (a8,2i2,2x,f8.3)
1. group : station name
2. group : time (hour,m inutes)
3. group : reading

2. Format of the station file

```
base stations
11 mdc  44 44.17 -110 29.47   2413.19      888.130
free stations
hollis  44 43.32 -110 29.73   2395.47
j 11    44 43.18 -110 29.68   2377.69
1c 58   44 43.02 -110 30.27   2366.18
22 mdc  44 42.50 -110 30.12   2346.43
y 367   44 42.17 -110 30.35   2338.42
23 mdc  44 42.10 -110 30.30   2340.59
24 mdc  44 41.47 -110 29.95   2345.09
```

```
z 367   44 40.75 -110 29.30   2343.33
25 mdc  44 40.65 -110 29.12   2341.01
```

with

headers (format (a14)):
'base station' : followed by base stations with known gravity values
'free station' : followed by stations with unknown gravity values

base stations (format (a8,i3,f6.2,i5,f6.2,f10.2,f12.3)) :
1. group : station name
2. group : northern latitude (degrees, minutes)
3. group : eastern longitude (degrees, minutes)
4. group : height above sea (meters)
5. group : gravity value (in mgal)

free stations (format (a8,i3,f6.2,i5,f6.2,f10.2)) : same as base station but without gravity value

3. Format of the output file

```
 Gravity Measurements (version 4)

sigma0 a posteriori :   1.00  n :  171  u :  33   dof :  138

 estimations for mean errors of single measurements of meters

s(g461 )   a pr :  19.86   a po :  19.86  dof :  138.0   po/pr :  1.00

 factor of gravimeters

 circular errors of gravimeters

c(g461 )
 f[ 1] f la a pr :     -     fixed :   72.00
       f am a pr :     -     fixed :    6.69
       f ph a pr :     -     fixed :   0.326
 f[ 2] f la a pr :     -     fixed :   36.00
       f am a pr :     -     fixed :    7.60
       f ph a pr :     -     fixed :   1.097
 f[ 3] f la a pr :     -     fixed :   24.00
       f am a pr :     -     fixed :    2.86
       f ph a pr :     -     fixed :   2.102
 f[ 4] f la a pr :     -     fixed :   18.00
       f am a pr :     -     fixed :    1.24
       f ph a pr :     -     fixed :   6.179
 f[ 5] f la a pr :     -     fixed :   14.40
       f am a pr :     -     fixed :    4.39
       f ph a pr :     -     fixed :  -4.133

 adjusted values of the gravity stations

 base        value   gradi.          n. of  deg.of  sigma
             [mgal]  [mi/m]          meas.  free.   a post.

11 mdc      888.130    0.000           15    12.8    1.19
y 367       892.185    0.000   12.4
```

```
z 367        884.052    0.000    12.4
w 367        879.173    0.000    12.4
arbee        876.170    0.000    12.5
u 367        866.767    0.000     9.0

station       value    gradi.  m.err.  n. of  deg.of  sigma      max. corr.
              [mgal]   [mi/m]  [micro]  meas.  free.   a post.  name  corr.

j 11         886.746    0.000    11.9     4     2.9     0.46     0.47
22 mdc       892.141    0.000    12.0     4     2.9     0.76     0.47
23 mdc       891.483    0.000    12.0     4     2.9     0.43     0.47
24 mdc       885.357    0.000    11.9     4     2.9     1.85     0.47
25 mdc       884.288    0.000    11.9     4     2.9     1.03     0.47
f 11a        881.341    0.000    11.9     4     2.9     0.68     0.47
e 11a2       880.138    0.000    11.9     4     2.9     0.98     0.47
.
.
.

 stations measured, but not in the station-file

   none

  improvements (order by sets)


    gravimeter  :  g461    factor  :  1.000691  drift :   0.008

s :  1   code :      dof : 55.1   si :  0.97
const : 2748.477   0.008

station      time (GMT)     reading  height  volt   si    v       f     tide
         c  [y.m.d][h.m]    [ins.un]   [m]  [volt]                (v/si) [mgal]

a 11        79- 9- 7 2256  3400.982  0.000   -      1.0     2.5    0.1  -0.003
11 mdc      79- 9- 7 2343  3418.084  0.000   -      1.0    -4.7   -0.3  -0.035
z 10        79- 9- 9 1704  3400.318  0.000   -      1.0     7.3    0.4  -0.063
a 11        79- 9- 9 1721  3401.049  0.000   -      1.0     0.4    0.0  -0.058
30 mdc      79- 9- 9 1737  3397.736  0.000   -      1.0     1.7    0.1  -0.052
b 11        79- 9- 9 1808  3404.570  0.000   -      1.0     1.3    0.1  -0.040
da 3c       79- 9- 9 1832  3407.890  0.000   -      1.0     0.8    0.0  -0.031
27 mdc      79- 9- 9 1849  3407.576  0.000   -      1.0    44.7    2.5  -0.024
a 11        79- 9- 9 1907  3401.021  0.000   -      1.0   -10.2   -0.5  -0.017
z 10        79- 9- 9 1931  3400.258  0.000   -      1.0    17.0    0.9  -0.008
.

    gravimeter  :  g461    factor  :  1.000691  drift :   0.007

s :  2   code :      dof : 71.3   si :  0.92
const : 2748.532   0.007

station      time (GMT)     reading  height  volt   si    v       f     tide
         c  [y.m.d][h.m]    [ins.un]   [m]  [volt]                (v/si) [mgal]

38 mdc      79- 9-12 1615  3380.450  0.000   -      1.0     5.3    0.3   0.004
39 mdc      79- 9-12 1633  3393.438  0.000   -      1.0    -4.7   -0.3  -0.002
k 12        79- 9-12 1651  3394.854  0.000   -      1.0     9.7    0.6  -0.008
k 12        79- 9-12 1702  3394.841  0.000   -      1.0    26.9    1.6  -0.011
39 mdc      79- 9-12 1721  3393.467  0.000   -      1.0   -20.7   -1.2  -0.017
38 mdc    r 79- 9-12 1733  3380.379  0.000   -      1.0   104.9
z 10        79- 9-12 1816  3400.340  0.000   -      1.0    -3.7   -0.2  -0.030
z 10        79- 9-12 1943  3400.340  0.000   -      1.0     9.0    0.5  -0.042
k 12        79- 9-12 2025  3394.899  0.000   -      1.0    -0.4    0.0  -0.044
39 mdc      79- 9-12 2039  3393.445  0.000   -      1.0    31.9    1.9  -0.045
```

```
38 mdc      79- 9-12 2054  3380.509  0.000   -       1.0    -7.1  -0.4  -0.045
h 12        79- 9-12 2111  3385.594  0.000   -       1.0   -21.8  -1.3  -0.045
.


    gravimeter  :  g461    factor  :  1.000691  drift :    0.263

s :  3   code :      dof : 11.6   si :  1.49
const : 2748.498   0.263

station      time (GMT)     reading  height  volt   si     v       f     tide
         c  [y.m.d][h.m]   [ins.un]    [m]  [volt]                (v/si) [mgal]

31 mdc    r 79- 9-17 1454  3400.415  0.000   -       1.0   155.5
u7743       79- 9-17 1508  3399.230  0.000   -       1.0    29.2   1.9   0.038
32 mdc      79- 9-17 1527  3397.296  0.000   -       1.0     4.4   0.3   0.046
33 mdc      79- 9-17 1543  3396.110  0.000   -       1.0   -12.1  -0.8   0.053
d 12        79- 9-17 1606  3385.208  0.000   -       1.0    35.5   2.2   0.061
34 mdc      79- 9-17 1621  3392.177  0.000   -       1.0   -38.6  -2.4   0.066
.

  improvements (order by stations)


 base

11 mdc       888.130    0.000          ****      1.2

  meter : g461   d.o.f :   12.8   sigma :   1.19

g461      79- 9- 7 1658    -20.5    18.3    -1.1
g461      79- 9- 7 1830      2.7    18.4     0.1
g461      79- 9-11   27     -8.2    18.4    -0.4
g461      79- 9-13 2239    -17.1    18.7    -0.9
g461      79- 9-16 1834      6.4    18.5     0.3
g461      79- 9-17 2208     -6.4    18.0    -0.4
g461      79- 9-17 2322     11.8    17.1     0.7


j 11         886.746    0.000   11.9     4     2.9    0.46

  meter : g461   d.o.f :    2.9   sigma :   0.46

g461      79- 9-10 2219     -9.9    17.0    -0.6
g461      79- 9-10 2338     -5.0    17.0    -0.3
g461      79- 9-13 2259      5.5    17.0     0.3
g461      79- 9-16 1857      9.4    16.9     0.6


22 mdc       892.141    0.000   12.0     4     2.9    0.76

  meter : g461   d.o.f :    2.9   sigma :   0.76

g461      79- 9-10 2242     13.9    17.0     0.8
g461      79- 9-10 2352    -16.2    17.0    -0.9
g461      79- 9-13 2224     11.3    17.0     0.7
g461      79- 9-16 1818     -9.1    16.9    -0.5

.
.

            const.  m.err.   drift  m.err.  ...
            [mgal] [micro]   [mgal] [micro] ...

  1. set :  2748.477   7.8     0.008   3.0
  2. set :  2748.532   7.7     0.007   1.2
  3. set :  2748.498  12.4     0.263  51.2
```

Appendix C

Table C.1 : Gravity Station Coordinates

Yellowstone National Park

Name	Latitude [deg min]	Longitude [deg min]	Height [m]	Stamping
11 mdc	44 44.17	-110 29.47	2413	11 MDC 1976
d 367	44 44.17	-110 29.97	2403	D 367 1987
hollis	44 43.32	-110 29.73	2395	HOLLIS
j 11	44 43.18	-110 29.68	2377	J11 1923
lc 58	44 43.02	-110 30.27	2366	LC 58 1977
22 mdc	44 42.50	-110 30.12	2346	22 MDC 1976
y 367	44 42.17	-110 30.35	2338	Y 367 1987
23 mdc	44 42.10	-110 30.30	2340	23 MDC 1976
24 mdc	44 41.47	-110 29.95	2344	24 MDC 1976
z 367	44 40.75	-110 29.30	2343	Z 367 1987
25 mdc	44 40.65	-110 29.12	2341	25 MDC 1976
kaygee	44 39.83	-110 27.87	2344	KAYGEE 1987
f 11a	44 38.77	-110 27.48	2344	F11 A
w 367	44 38.52	-110 27.35	2351	W 367 1987
e 11a2	44 38.43	-110 27.25	2345	E11 A2
26 mdc	44 37.83	-110 26.48	2364	26 MDC 1976
arbee	44 37.85	-110 26.32	2361	ARBEE
27 mdc	44 37.10	-110 25.23	2351	27 MDC 1976
cv85222	44 36.67	-110 24.60	2350	CVO 85-222
da 3c	44 36.47	-110 23.25	2353	DA 3 1934
le hardy	44 35.95	-110 23.18	2362	LE HARDY
b 11	44 35.50	-110 23.05	2366	B11 1923
30 mdc	44 34.65	-110 22.73	2390	30 MDC 1976
u 367	44 34.15	-110 23.23	2390	U 367
a 11	44 34.07	-110 23.15	2375	A11 1923
cv8423	44 34.05	-110 23.05	2374	CVO 84-23
31 mdc	44 33.80	-110 22.32	2364	31 MDC 1976
u7743	44 33.50	-110 21.38	2361	USBPR7743
32 mdc	44 33.47	-110 20.10	2366	32 MDC 1976
cv8412	44 33.58	-110 19.38	2372	CVO 84-12
33 mdc	44 33.54	-110 18.47	2382	33 MDC 1976
d 12	44 33.37	-110 16.73	2437	D12 1923
34 mdc	44 33.24	-110 16.09	2412	34 MDC 1976
cv8417	44 32.93	-110 17.87	2358	CVO 84-17
cv8413	44 32.30	-110 17.37	2359	CVO 84-13
cv8424	44 31.00	-110 16.52	2361	CVO 84-24
35 mdc	44 30.59	-110 14.90	2493	35 MDC 1976
cv8421	44 30.20	-110 14.05	2547	CVO 84-21
36 mdc	44 30.12	-110 13.67	2546	36 MDC 1976
37 mdc	44 30.05	-110 12.45	2568	37 MDC 1976
37 ex	44 30.05	-110 12.45	2565	--
h 12	44 30.30	-110 11.57	2582	H 12 1923
38 mdc	44 29.45	-110 11.63	2630	38 MDC 1976
38 ex	44 29.45	-110 11.63	2620	
39 mdc	44 29.37	-110 10.42	2572	39 MDC 1976
k 12	44 28.72	-110 9.51	2565	K 12 1923
d 339	44 38.78	-110 51.53	2082	D339
40 mdc	44 37.90	-110 51.43	2143	40 MDC 1976
y 9	44 37.03	-110 51.37	2165	Y 9 1923
41 mdc	44 36.47	-110 50.70	2173	41 MDC 1976
u 366	44 36.18	-110 50.23	2180	U 366
z 9	44 35.88	-110 49.83	2181	Z 9 1923
42 mdc	44 35.07	-110 49.75	2183	42 MDC 1976
nperce	44 34.42	-110 49.13	2188	NEZ PERCE
da 1	44 34.38	-110 49.20	2188	DA 1 1934
43 mdc	44 33.30	-110 48.40	2211	43 MDC 1976
44 mdc	44 32.58	-110 48.63	2218	44 MDC 1976
45 mdc	44 31.97	-110 49.62	2208	45 MDC 1976
46 mdc	44 31.38	-110 49.75	2207	46 MDC 1976
thermal	44 30.97	-110 49.88	2206	THERMAL
da 3m	44 30.85	-110 49.83	2211	DA 3 1935
47 mdc	44 29.98	-110 50.35	2217	47 MDC 1976
u7273	44 28.98	-110 51.10	2217	USBPR 7273
48 mdc	44 28.13	-110 51.30	2222	48 MDC 1976
of 4	44 27.55	-110 50.65	2238	OF 4 1976
y 366	44 27.33	-110 50.00	2243	Y 366 1987
u7389	44 27.44	-110 49.30	2253	USBPR 7389
f 10	44 26.78	-110 48.28	2311	F 10 1923
f 367	44 26.77	-110 48.30	2308	F 367
g 367	44 26.23	-110 47.88	2363	G 367
49 mdc	44 26.15	-110 47.65	2379	49 MDC 1976
50 mdc	44 25.93	-110 46.55	2394	50 MDC 1976
h 10	44 25.92	-110 45.40	2415	H 10 1923
j 367	44 25.88	-110 44.83	2431	J 367
51 mdc	44 26.08	-110 44.05	2457	51 MDC
l 367	44 26.53	-110 43.03	2519	L 367
k 10	44 26.52	-110 43.07	2518	K 10 1937 R
l 10	44 26.87	-110 42.40	2443	L 10 1937 R
n 367	44 26.85	-110 41.88	2432	N 367
52 mdc	44 26.98	-110 41.45	2461	52 MDC 1976
n 10	44 26.92	-110 38.12	2536	N 10 1923
o 10	44 26.33	-110 37.50	2550	O 10 1923
p 10	44 25.67	-110 36.43	2508	P 10 1923
9107	44 26.77	-110 40.41	2550	
9106	44 25.93	-110 37.90	2530	
53 mdc	44 25.28	-110 35.50	2462	53 MDC 1976
s 367	44 25.29	-110 35.50	2466	S 367
54 mdc	44 25.00	-110 34.40	2378	54 MDC 1976
8 mdc7	44 25.81	-110 34.75	2387	8 MDC 1977
7 mdc7	44 27.05	-110 33.77	2387	7 MDC 1977
9105	44 26.86	-110 33.73	2393	
s 10a	44 28.03	-110 33.23	2360	S 10 A 1955
9104	44 27.66	-110 30.62	2370	
9103	44 27.57	-110 29.00	2370	
9102	44 28.25	-110 27.46	2365	
t 10	44 29.00	-110 32.33	2396	T 10 1923
u 10	44 30.17	-110 30.95	2569	U 10 1923
3 mdc7	44 31.00	-110 28.52	2430	3 MDC 1977
pit	44 31.20	-110 28.35	2423	PIT
w 10	44 31.47	-110 27.48	2391	W 10 1923
2 mdc7	44 31.88	-110 26.00	2364	2 MDC 1977
9101	44 32.11	-110 25.89	2364	
1 mdc7	44 32.69	-110 25.36	2368	1 MDC 1977
z 10	44 32.93	-110 24.03	2364	Z 10 RESET
ystone	44 33.13	-110 23.62	2360	YELLOWSTONE
9 mdc7	44 24.26	-110 33.98	2373	9 MDC 1977
9108	44 22.85	-110 34.43	2400	
9109	44 21.64	-110 34.82	2440	
h 13	44 22.13	-110 35.40	2429	H 13 1923
usbpr	44 19.04	-110 35.91	2374	USBPR NONE
9110	44 18.14	-110 36.29	2375	
10 mdc7	44 17.63	-110 36.75	2375	10 MDC 1977
lewis	44 16.05	-110 38.05	2353	LEWIS FALLS
n 13	44 15.90	-110 38.23	2359	N 13 1923
11 mdc7	44 13.87	-110 39.13	2347	11 MDC 1977
p 13	44 12.71	-110 39.96	2396	P 13 1923
9111	44 12.18	-110 39.56	2360	
q 13	44 11.46	-110 39.95	2306	Q 13 1923
12 mdc7	44 9.93	-110 39.93	2202	12 MDC 1977
s 13	44 8.15	-110 40.58	2098	S 13 1923
a 158	44 43.57	-110 42.13	2306	A 158 1960
z 157	44 44.30	-110 41.88	2278	Z 157 1960
x 157	44 45.15	-110 43.35	2292	X 157 1960
v 157	44 46.43	-110 44.12	2302	V 157 1960
u 157	44 47.22	-110 44.32	2294	U 157 1960
s 157	44 48.73	-110 43.80	2252	S 157 1960
r 157	44 50.02	-110 43.68	2243	R 157 1960
q 157	44 51.03	-110 44.17	2228	Q 157 1960
n 157	44 52.60	-110 44.15	2223	N 157 1960
m 157	44 53.30	-110 43.90	2220	M 157 1960
l 157	44 53.63	-110 44.07	2234	L 157 1960
10-17	44 55.80	-110 44.00	2220	10-17 1986
3 mdc5	44 56.00	-110 43.57	2212	3 MDC 1978
g 157	44 56.83	-110 42.80	2133	G 157 1960
4 mdc5	44 58.00	-110 42.38	2004	4 MDC 1975
c 157	44 58.20	-110 41.84	1935	C 157 1960
y 8	44 58.60	-110 41.98	1902	Y 8 1923
9 mdc	44 43.43	-110 31.40	2486	9 MDC 1976
7 mdc	44 42.82	-110 33.25	2482	7 MDC 1976
6 mdc	44 42.23	-110 34.75	2505	6 MDC 1976
4 mdc	44 42.48	-110 36.98	2446	4 MDC 1976
t 9	44 42.77	-110 38.75	2364	T 9 1923
1 mdc	44 43.64	-110 41.21	2281	1 MDC 1976
2 mdc5	44 42.90	-110 43.78	2269	2 MDC 1975
e 158	44 41.40	-110 44.69	2238	E 158 1960
g 158	44 40.65	-110 44.82	2225	G 158 1960
j 158	44 39.63	-110 44.90	2193	J 158
o 9	44 39.20	-110 46.18	2175	O 9 1923
m 158	44 38.98	-110 47.43	2122	M 158 1960
p 158	44 39.17	-110 49.27	2100	P 158 1960
q 158	44 38.96	-110 50.80	2103	Q 158 1960
u6802	44 38.47	-110 51.52	2074	USBPR 6802
harlq	44 38.40	-110 53.30	2070	HARLEQUIN

y 13	44 38.47	-110 53.70	2070	Y 13 1923	
z 13	44 38.80	-110 55.83	2061	Z 13 1923	
a 14	44 39.83	-110 57.87	2058	A 14 R 1958	
hull	44 39.62	-110 59.45	2051	HULL	
b 14	44 39.62	-110 59.47	2053	B 14 1923	
12 mdc	44 45.38	-110 28.78	2491	12 MDC 1976	
13 mdc	44 46.12	-110 27.28	2628	13 MDC 1976	
15 mdc	44 47.20	-110 27.10	2704	15 MDC 1976	
wburn	44 47.86	-110 26.03	3115	WASHBURN	
17 mdc	44 49.02	-110 26.98	2631	17 MDC 1976	
18 mdc	44 49.90	-110 26.77	2554	18 MDC 1976	
19 mdc	44 51.20	-110 24.97	2336	19 MDC 1976	
20 mdc	44 51.90	-110 23.78	2168	20 MDC 1976	
r 11	44 53.38	-110 23.33	2011	R 11 1923	
17 mdc7	44 54.87	-110 24.58	1913	17 MDC 1977	
cs6123	44 55.31	-110 24.02	1866	CHI SQ 6123	
cs6220	44 54.69	-110 22.38	1896	CHI SQ 6220	
39 vs	44 55.20	-110 19.07	1915	VS 39 1936	
1 gwm	44 54.85	-110 16.83	1992	1 GWM 1941	
2 gwm	44 54.20	-110 14.83	1999	2 GWM 1941	
3 gwm	44 53.10	-110 13.17	1997	3 GWM 1941	
u6580	44 52.23	-110 11.17	2006	6580.56	
4 gwm	44 52.40	-110 9.60	2027	4 GWM 1941	
u6684	44 53.33	-110 8.40	2038	6684.92	
5 gwm	44 54.23	-110 6.93	2073	5 GWM 1941	
u6902	44 55.23	-110 5.87	2104	6902.10	
u7008	44 56.67	-110 4.93	2137	7008.17	
6 gwm	44 58.47	-110 3.90	2208	6 GWM 1941	
u7194	44 59.47	-110 3.37	2194	7194	
u7302	45 0.34	-110 2.48	2227	7302	
u7348	45 0.29	-110 1.46	2241	7348	
8401	44 41.38	-110 25.63	2374		
8402	44 41.88	-110 22.69	2594		
8403	44 39.73	-110 22.46	2460		
bluff	44 39.72	-110 22.46	2458		
8404	44 37.77	-110 21.63	2560		
8405	44 35.59	-110 19.36	2539		
8406	44 34.55	-110 25.29	2670		
8406a	44 33.88	-110 28.17	2575		
spruce	44 33.11	-110 36.10	2481		
trout	44 36.94	-110 30.24	2431		
10 rds	44 36.72	-110 36.83	2498		
8407	44 38.15	-110 18.54	2655		
8408	44 37.45	-110 15.01	2450		
8409	44 39.84	-110 16.27	2511		
tern	44 40.07	-110 15.50	2506		
8410	44 40.41	-110 18.54	2499		
8412	44 42.52	-110 15.88	2511		
8413	44 44.22	-110 19.51	2478		
8415	44 35.07	-110 13.81	2425		
8416	44 41.69	-110 14.58	2545		
coneEDM	44 38.89	-110 11.56	2939		
pcone	44 38.88	-110 11.56	2939		

Table C.2 : Gravity Results

Gravity Results 1977

sigma0 a posteriori : 1.00 n : 980 u : 208 dof : 772

estimations for mean errors of single measurements of meters

s(g461) a pr : 10.59 a po : 10.59 dof : 364.5
s(d26) a pr : 15.44 a po : 15.44 dof : 407.5

factor of gravimeters

f(d26) a pr : 1.000921 a po : 1.000921 err (ppm) : 35.3

circular errors of gravimeters

c(g461)
f(1) f la a pr : - fixed : 72.00
f am a pr : - fixed : 6.69
f ph a pr : - fixed : 0.326
f(2) f la a pr : - fixed : 36.00
f am a pr : - fixed : 7.60
f ph a pr : - fixed : 1.097
f(3) f la a pr : - fixed : 24.00
f am a pr : - fixed : 2.86
f ph a pr : - fixed : 2.102
f(4) f la a pr : - fixed : 18.00
f am a pr : - fixed : 5.24
f ph a pr : - fixed : 6.179
f(5) f la a pr : - fixed : 14.40
f am a pr : - fixed : 4.39
f ph a pr : - fixed : -4.133

8417	44 40.42	-110 10.00	2569		
8418	44 44.76	-110 15.29	2560		
hspring	44 44.75	-110 15.32	2560		
8419	44 48.35	-110 13.63	2793		
8420	44 42.94	-110 10.82	2644		
8423	44 47.48	-110 17.21	2511		
8423a	44 50.19	-110 12.04	2426		
8424	44 49.92	-110 16.26	2792		
8438	44 47.61	-110 22.71	2697		
8439	44 45.31	-110 21.08	2658		
holmes	44 49.13	-110 51.35	3142		
toni	44 24.13	-110 57.35	2621		
p 12	44 29.42	-110 00.08	2100	P 12	
8450	44 32.04	-110 26.33	2358		
8437	44 30.87	-110 23.01	2359		
8426	44 27.14	-110 24.73	2371		
frank	44 25.50	-110 21.11	2358		
8427	44 24.81	-110 21.27	2358		
8428	44 23.02	-110 20.95	2358		
8429	44 21.85	-110 21.22	2362		
8430	44 21.01	-110 19.77	2359		
8431	44 18.36	-110 19.01	2360		
8432	44 23.55	-110 17.09	2377		

Absolute Gravity Line San Francisco

Name	Latitude [deg min]	Longitude [deg min]	Height [m]	Gravity -980000 [mgal]
a	37 27.34	-121 10.18	16.00	958.740
hc	37 19.55	-121 46.56	100.00	884.930
hcb	37 19.55	-121 46.56	100.00	885.061
hcc	37 19.55	-121 46.56	100.00	884.870
hd	37 20.55	-121 42.89	494.00	817.160
hdb	37 20.55	-121 42.89	494.00	817.130
he	37 19.42	-121 40.05	671.00	784.940
hea	37 19.42	-121 40.05	671.00	784.980
hf	37 20.47	-121 40.00	866.00	748.760
hg	37 20.36	-121 39.04	1114.00	697.720
hh	37 20.52	-121 38.49	1313.00	649.430
hha	37 20.52	-121 38.49	1313.00	649.104
aa	37 27.34	-121 10.18	16.00	

adjusted values of the gravity stations

base	value [mgal]	gradi. [mi/m]		n. of meas.	deg.of free.	sigma a post.
11 mdc	888.130	0.000		240	210.9	1.07
y 367	892.192	0.000	5.8			
z 367	884.067	0.000	6.3			
w 367	879.193	0.000	6.3			
arbee	876.209	0.000	8.0			
u 367	866.784	0.000	8.0			

station max.	value [mgal]	gradi. [mi/m]	m.err. [micro]	n. of meas.	deg.of free.	sigma a post.	name
j 11	886.744	0.000	4.6	8	6.9	0.71	-0.24
22 mdc	892.143	0.000	4.6	8	6.9	0.81	-0.24
23 mdc	891.491	0.000	4.6	8	6.9	0.99	-0.24
24 mdc	885.378	0.000	4.4	8	6.2	0.53	-0.26
25 mdc	884.303	0.000	5.5	6	4.7	0.97	-0.23
f 11a	881.358	0.000	5.6	6	4.5	0.75	-0.27
e 11a2	880.161	0.000	6.0	5	3.3	0.87	-0.30
27 mdc	877.043	0.000	6.8	4	2.7	1.16	-0.25
da 3c	877.282	0.000	6.8	4	2.7	0.88	-0.23
b 11	873.729	0.000	6.9	4	2.7	0.70	0.20
30 mdc	866.459	0.000	5.6	6	4.4	0.53	-0.27
31 mdc	869.562	0.000	6.9	4	2.7	0.64	0.21
u7743	868.168	0.000	7.0	4	2.6	1.44	0.21
32 mdc	866.094	0.000	2.8	28	25.0	1.04	-0.34
36 mdc	855.287	0.000	6.0	5	3.7	0.54	-0.39
37 mdc	854.982	0.000	7.7	4	2.9	0.56	-0.43
h 12	853.474	0.000	7.8	4	2.8	0.72	-0.45
38 mdc	848.074	0.000	7.8	4	2.8	0.56	-0.46
39 mdc	861.884	0.000	7.9	4	2.8	0.24	-0.47
k 12	863.406	0.000	7.9	4	2.8	0.24	-0.48
40 mdc	931.682	0.000	2.6	41	35.5	0.83	-0.31
y 9	923.486	0.000	7.0	4	2.8	0.89	-0.37

41 mdc	920.266	0.000	7.0	4	2.8	0.29	-0.37
z 9	919.212	0.000	7.0	4	2.8	0.63	-0.36
42 mdc	920.629	0.000	7.0	4	2.8	0.65	-0.36
da 1	918.272	0.000	7.0	4	2.8	0.73	-0.36
43 mdc	908.389	0.000	7.0	4	2.5	0.87	-0.30
44 mdc	905.935	0.000	7.6	4	2.6	1.54	-0.46
45 mdc	909.200	0.000	7.6	4	2.6	1.78	-0.46
da 3m	908.816	0.000	7.6	4	2.7	1.56	-0.49
48 mdc	900.008	0.000	6.8	4	2.8	1.74	-0.21
u7389	892.976	0.000	7.9	2	1.0	1.03	-0.19
49 mdc	867.449	0.000	6.8	4	2.8	0.66	-0.19
h 10	860.006	0.000	7.1	4	2.9	1.06	-0.49
l 10	852.468	0.000	7.3	4	2.9	0.76	-0.50
54 mdc	860.574	0.000	2.5	38	33.6	1.11	-0.32
8 mdc7	858.026	0.000	7.1	4	2.6	1.24	-0.38
s 10a	869.107	0.000	7.0	4	2.8	0.67	-0.30
2 mdc7	868.774	0.000	6.7	4	2.8	1.31	-0.30
z 10	869.192	0.000	6.7	4	2.7	0.94	-0.30
9 mdc7	860.371	0.000	6.9	4	2.9	1.43	-0.33
n 13	860.701	0.000	6.9	4	2.8	0.90	-0.32
11 mdc7	861.151	0.000	6.7	4	2.8	0.70	-0.22
12 mdc7	894.314	0.000	6.8	4	2.8	0.72	0.17
a 158	924.773	0.000	2.6	39	34.0	0.80	-0.35
z 157	932.676	0.000	4.8	8	6.9	0.47	-0.22
x 157	928.996	0.000	4.8	8	6.9	0.42	-0.23
v 157	928.488	0.000	7.1	4	2.6	0.54	-0.36
u 157	931.320	0.000	7.0	4	2.7	0.84	-0.36
s 157	942.291	0.000	7.0	4	2.7	1.57	-0.36
r 157	945.050	0.000	7.0	4	2.7	0.36	-0.35
q 157	950.628	0.000	7.0	4	2.7	0.96	-0.34
n 157	955.441	0.000	6.8	4	2.8	0.39	-0.30
l 157	956.313	0.000	6.8	4	2.8	0.65	-0.30
g 157	978.264	0.000	6.8	4	2.8	1.17	-0.28
4 mdc5	1005.091	0.000	11.1	1	0.0	0.00	-0.30
y 8	1023.754	0.000	11.1	1	0.0	0.00	-0.30
9 mdc	871.994	0.000	4.5	9	7.9	1.30	-0.21
7 mdc	878.277	0.000	4.6	8	6.9	1.39	-0.21
6 mdc	874.440	0.000	4.6	8	6.9	1.30	-0.20
4 mdc	891.619	0.000	4.6	8	6.9	1.07	-0.20
t 9	910.728	0.000	4.6	9	7.9	1.28	-0.20
1 mdc	930.558	0.000	4.8	8	6.9	1.12	-0.21
2 mdc5	927.629	0.000	6.8	4	2.8	1.05	-0.31
e 158	922.955	0.000	6.8	4	2.7	0.41	-0.31
g 158	924.770	0.000	6.8	4	2.7	0.78	-0.32
j 158	928.174	0.000	6.8	4	2.7	0.29	-0.32
o 9	931.559	0.000	6.9	4	2.8	0.50	-0.42
m 158	941.507	0.000	6.9	4	2.7	0.98	-0.32
p 158	945.187	0.000	6.8	4	2.7	0.47	-0.28
q 158	946.211	0.000	5.1	8	6.2	0.63	-0.32
y 13	953.804	0.000	7.0	4	2.7	1.04	-0.34
z 13	954.971	0.000	6.9	4	2.7	0.36	-0.34
b 14	969.437	0.000	7.0	4	2.6	0.82	-0.34
12 mdc	877.689	0.000	7.4	4	2.7	1.12	0.31
13 mdc	851.376	0.000	7.4	4	2.7	0.69	0.32
17 mdc	849.415	0.000	7.6	4	2.8	1.49	-0.34
18 mdc	866.120	0.000	7.4	4	2.7	0.13	-0.48
19 mdc	909.790	0.000	7.4	4	2.7	0.55	-0.48
20 mdc	947.298	0.000	7.6	4	2.8	0.45	0.34
r 11	988.799	0.000	7.7	4	2.8	0.88	0.34
17 mdc7	1015.260	0.000	7.8	4	2.8	0.59	-0.49
cs6123	1028.508	0.000	4.2	24	20.2	1.14	-0.46
cs6220	1023.508	0.000	7.8	4	2.8	0.71	-0.46
39 vs	1027.106	0.000	7.7	4	2.8	0.93	-0.43
1 gwm	1014.354	0.000	7.7	4	2.8	0.43	-0.40
2 gwm	1006.645	0.000	7.7	4	2.8	1.35	-0.36
3 gwm	1006.059	0.000	7.7	4	2.8	1.17	0.36
u6580	1002.792	0.000	7.4	4	2.9	0.82	-0.52
4 gwm	1000.686	0.000	7.4	4	2.9	1.04	-0.51
u6684	1001.213	0.000	8.1	4	2.7	1.44	0.40
5 gwm	996.793	0.000	7.4	4	2.9	0.60	-0.50
u6902	992.673	0.000	7.4	4	2.9	1.84	-0.49
u7008	987.833	0.000	7.4	4	2.9	1.41	-0.48
6 gwm	977.000	0.000	7.9	4	2.8	0.93	0.40
u7194	980.307	0.000	7.9	4	2.8	0.82	0.40
u7302	976.177	0.000	8.0	4	2.7	1.22	0.40
u7348	971.560	0.000	7.9	4	2.8	1.39	0.40
3 mdc5	962.745	0.000	6.8	4	2.8	1.13	-0.29
a 14	965.765	0.000	7.0	4	2.7	1.04	-0.34
33 mdc	864.800	0.000	5.2	8	6.5	0.68	-0.41
d 12	853.296	0.000	5.2	8	6.5	0.91	-0.40
34 mdc	860.630	0.000	5.3	7	5.6	0.93	-0.39
35 mdc	862.536	0.000	6.0	5	3.7	0.67	-0.39
1 mdc7	867.746	0.000	6.7	4	2.8	1.53	-0.30
w 10	864.681	0.000	6.7	4	2.7	0.30	-0.30
3 mdc7	856.026	0.000	6.7	4	2.6	0.71	-0.14
q 13	870.788	0.000	6.5	4	2.8	0.93	-0.11
p 13	849.808	0.000	6.5	4	2.8	0.90	0.12
h 13	850.774	0.000	6.6	4	2.9	0.24	-0.19
u 10	827.039	0.000	7.0	4	2.8	0.80	-0.30
t 10	862.463	0.000	7.0	4	2.8	0.34	-0.30
7 mdc7	859.795	0.000	7.0	4	2.8	1.02	-0.31
53 mdc	844.777	0.000	11.4	1	0.0	0.00	-0.30
p 10	837.792	0.000	7.1	4	2.7	0.94	-0.39
o 10	830.704	0.000	7.2	4	2.7	1.12	-0.39
n 10	835.037	0.000	7.2	4	2.7	2.13	-0.39
usbpr	859.997	0.000	7.3	3	1.9	0.49	-0.33
10 mdc7	859.170	0.000	6.9	4	2.8	1.03	-0.32
s 13	915.200	0.000	6.8	4	2.8	0.67	0.17
46 mdc	910.411	0.000	7.7	4	2.7	2.13	-0.49
u7273	901.897	0.000	7.6	4	2.7	0.99	-0.48
47 mdc	905.543	0.000	7.6	4	2.7	1.20	-0.48
15 mdc	833.406	0.000	7.5	4	2.6	1.02	0.32
26 mdc	875.608	0.000	7.2	4	2.2	1.31	-0.30
a 11	869.968	0.000	6.9	4	2.7	1.07	0.21
52 mdc	846.551	0.000	7.3	4	2.9	0.52	-0.50
k 10	836.973	0.000	7.3	4	2.9	0.48	-0.50
51 mdc	850.422	0.000	7.3	4	2.9	1.03	-0.49
50 mdc	864.198	0.000	7.3	4	2.9	0.65	-0.49
of 4	897.158	0.000	6.8	4	2.8	0.76	-0.20
f 10	881.321	0.000	6.8	4	2.8	0.98	-0.19

Gravity Results 1979

sigma0 a posteriori : 1.00 n : 171 u : 33 dof : 138

estimations for mean errors of single measurements of meters

s(g461) a pr : 19.86 a po : 19.86 dof : 138.0

factor of gravimeters

circular errors of gravimeters

```
c(g461 )
 f[ 1] f la a pr :    -      fixed :   72.00
       f am a pr :    -      fixed :    6.69
       f ph a pr :    -      fixed :   0.326
 f[ 2] f la a pr :    -      fixed :   36.00
       f am a pr :    -      fixed :    7.60
       f ph a pr :    -      fixed :   1.097
 f[ 3] f la a pr :    -      fixed :   24.00
       f am a pr :    -      fixed :    2.86
       f ph a pr :    -      fixed :   2.102
 f[ 4] f la a pr :    -      fixed :   18.00
       f am a pr :    -      fixed :    1.24
       f ph a pr :    -      fixed :   6.179
 f[ 5] f la a pr :    -      fixed :   14.40
       f am a pr :    -      fixed :    4.39
       f ph a pr :    -      fixed :  -4.133
```

adjusted values of the gravity stations

base	value (mgal)	gradi. (mi/mi		n. of meas.	deg.of free.	sigma a post.
11 mdc	888.130	0.000		15	12.8	1.19
y 367	892.185	0.000	12.4			
z 367	884.052	0.000	12.4			
w 367	879.173	0.000	12.4			
arbee	876.170	0.000	12.5			
u 367	866.767	0.000	9.0			

station max.	value (mgal)	gradi. (mi/mi	m.err. (micro)	n. of meas.	deg.of free.	sigma a post.	name
j 11	886.746	0.000	11.9	4	2.9	0.46	0.47
22 mdc	892.141	0.000	12.0	4	2.9	0.76	0.47
23 mdc	891.483	0.000	12.0	4	2.9	0.43	0.47
24 mdc	885.357	0.000	11.9	4	2.9	1.85	0.47
25 mdc	884.288	0.000	11.9	4	2.9	1.03	0.47
f 11a	881.341	0.000	11.9	4	2.9	0.68	0.47
e 11a2	880.138	0.000	11.9	4	2.9	0.98	0.47
26 mdc	875.569	0.000	11.9	4	2.9	0.94	0.47
27 mdc	876.985	0.000	10.0	6	4.9	1.86	0.50
da 3c	877.268	0.000	10.0	6	4.9	0.59	0.50
b 11	873.723	0.000	10.0	6	4.9	0.33	0.50
30 mdc	866.435	0.000	10.0	6	4.9	1.87	0.50
a 11	869.951	0.000	8.0	13	11.6	0.41	-0.61
31 mdc	869.516	0.000	13.6	3	2.0	0.22	-0.53
u7743	868.133	0.000	12.5	4	2.8	1.02	-0.57
32 mdc	866.059	0.000	12.4	4	2.8	0.62	-0.57
33 mdc	864.789	0.000	12.4	4	2.8	0.63	-0.56
d 12	853.255	0.000	12.3	4	2.9	1.58	-0.56
34 mdc	860.597	0.000	12.3	4	2.9	1.39	-0.56
35 mdc	862.516	0.000	12.3	4	2.9	0.48	-0.55
36 mdc	855.274	0.000	12.1	4	2.9	0.30	-0.55
37 mdc	854.983	0.000	12.1	4	2.9	0.54	-0.55
h 12	853.472	0.000	12.0	4	3.0	1.27	-0.53
38 mdc	848.078	0.000	13.3	3	2.0	0.33	-0.46
39 mdc	861.876	0.000	12.0	4	3.0	1.14	-0.53
k 12	863.386	0.000	12.0	4	3.0	1.35	-0.53
z 10	869.175	0.000	6.8	37	34.6	0.85	-0.76

Gravity Results 1983

sigma0 a posteriori : 1.00 n : 1060 u : 187 dof : 873

estimations for mean errors of single measurements of meters

```
s(g461 )   a pr :  15.68   a po :  15.68  dof :  250.1
s(g461a)   a pr :  43.92   a po :  43.92  dof :  165.7
s(g614 )   a pr :  27.31   a po :  27.31  dof :  434.7
s(g614o)   a pr :  22.08   a po :  22.08  dof :   22.5
```

factor of gravimeters

f(g614) a pr : 1.000037 a po : 1.000037 err [ppm] : 43.5

circular errors of gravimeters

```
c(g461 )
 f[ 1] f la a pr :    -      fixed :   72.00
       f am a pr :    -      fixed :    6.69
       f ph a pr :    -      fixed :   0.326
 f[ 2] f la a pr :    -      fixed :   36.00
       f am a pr :    -      fixed :    7.60
       f ph a pr :    -      fixed :   1.097
 f[ 3] f la a pr :    -      fixed :   24.00
       f am a pr :    -      fixed :    2.86
       f ph a pr :    -      fixed :   2.102
 f[ 4] f la a pr :    -      fixed :   18.00
       f am a pr :    -      fixed :    1.24
```

```
      f ph a pr :    -      fixed :   6.179
 f[ 5] f la a pr :    -      fixed :  14.40
      f am a pr :    -      fixed :   4.39
      f ph a pr :    -      fixed :  -4.133

c(g614 )
 f[ 1] f la a pr :    -      fixed :  72.00
      am a pr :   3.54   a po :   3.54   err [mgal] :  2.9
      ph a pr :   4.48   a po :   4.480  err [rad]  :  0.8
 f[ 2] f la a pr :    -      fixed :  36.00
      am a pr :  -3.84   a po :  -3.84   err [mgal] :  2.7
      ph a pr :  -1.35   a po :  -1.351  err [rad]  :  0.6
 f[ 3] f la a pr :    -      fixed :  24.00
      am a pr :  -5.83   a po :  -5.83   err [mgal] :  2.5
      ph a pr :   1.12   a po :   1.119  err [rad]  :  0.4
 f[ 4] f la a pr :    -      fixed :  18.00
      am a pr :   2.47   a po :   2.47   err [mgal] :  2.4
      ph a pr :   1.42   a po :   1.421  err [rad]  :  1.0
 f[ 5] f la a pr :    -      fixed :  14.40
      am a pr :   5.76   a po :   5.76   err [mgal] :  2.2
      ph a pr :  -4.87   a po :  -4.870  err [rad]  :  0.4
```

adjusted values of the gravity stations

base	value [mgal]	gradi. [mi/m]		n. of meas.	deg.of free.	sigma a post.
11 mdc	888.130	0.000		167	151.5	0.99
y 367	892.185	0.000	9.1			
z 367	884.060	0.000	9.0			
w 367	879.164	0.000	9.3			
arbee	876.190	0.000	8.5			
u 367	866.769	0.000	8.7			

station max.	value [mgal]	gradi. [mi/m]	m.err. [micro]	n. of meas.	deg.of free.	sigma a post.	name
j 11	886.733	0.000	8.7	8	6.7	0.91	-0.17
22 mdc	892.158	0.000	7.7	10	8.4	0.69	-0.17
23 mdc	891.483	0.000	8.7	9	7.6	0.91	-0.18
24 mdc	885.344	0.000	8.8	8	6.7	1.34	-0.17
25 mdc	884.296	0.000	8.5	9	7.5	0.78	0.13
f 11a	881.324	0.000	8.2	12	10.5	1.17	-0.21
e 11a2	880.137	0.000	8.9	8	6.7	0.50	-0.20
27 mdc	876.991	0.000	8.9	8	6.7	0.68	-0.20
da 3c	877.249	0.000	6.5	14	12.5	0.74	-0.28
b 11	873.714	0.000	6.9	12	10.4	1.13	-0.21
30 mdc	866.438	0.000	7.9	9	7.7	0.83	-0.21
31 mdc	869.549	0.000	8.9	8	6.7	0.99	-0.19
u7743	868.171	0.000	8.9	8	6.7	0.51	-0.19
32 mdc	866.077	0.000	4.5	46	41.4	1.03	-0.27
36 mdc	855.268	0.000	9.2	8	6.5	1.03	0.18
37 mdc	854.983	0.000	9.2	8	6.5	0.46	0.18
38 mdc	848.080	0.000	9.3	7	5.5	0.86	0.16
39 mdc	861.882	0.000	9.2	8	6.5	0.98	0.19
k 12	863.396	0.000	9.6	6	4.7	1.46	0.19
40 mdc	931.661	0.000	5.3	41	37.7	1.05	-0.59
y 9	923.480	0.000	9.7	8	6.4	1.36	-0.43
41 mdc	920.254	0.000	9.6	8	6.5	0.68	-0.43
z 9	919.186	0.000	9.7	8	6.5	0.68	-0.43
42 mdc	920.587	-0.001	9.6	8	6.5	1.41	-0.43
da 1	918.239	0.000	11.3	7	5.5	1.23	-0.36
43 mdc	908.351	0.000	9.7	8	6.5	0.76	-0.44
44 mdc	905.902	0.000	9.6	8	6.5	0.70	-0.43
45 mdc	909.207	0.000	9.6	8	6.6	0.36	-0.44
da 3m	908.771	0.000	7.4	16	14.1	0.98	-0.53
48 mdc	899.993	0.000	9.6	8	6.6	1.16	-0.38
u7389	892.947	0.000	9.4	8	6.5	1.15	-0.36
49 mdc	867.404	0.000	8.6	12	10.6	1.24	-0.38
h 10	859.982	0.000	9.1	8	6.8	0.87	-0.31
i 10	852.410	0.000	9.3	8	6.7	1.70	-0.31
54 mdc	860.546	0.000	5.2	26	23.2	1.01	0.25
8 mdc7	858.007	0.000	10.2	4	2.9	0.75	0.16
2 mdc7	868.763	0.000	10.2	4	2.7	0.12	0.14
z 10	869.189	0.000	10.2	4	2.7	0.51	0.13
9 mdc7	860.330	0.000	10.6	4	2.9	1.13	-0.31
n 13	860.685	0.000	10.6	4	2.9	0.76	-0.31
11 mdc7	861.150	0.000	10.7	4	2.9	0.41	-0.31
12 mdc7	894.293	0.000	10.8	4	2.8	1.10	-0.30
a 158	924.773	0.000	4.9	32	28.2	1.16	0.31
z 157	932.653	0.000	11.1	4	2.9	1.01	-0.38
x 157	928.981	0.000	11.1	4	2.9	0.28	-0.38
v 157	928.476	0.000	11.1	4	2.9	0.89	-0.38
u 157	931.318	0.000	11.1	4	2.9	1.07	-0.39
s 157	942.296	0.000	11.2	4	2.9	0.53	-0.39
r 157	945.040	0.000	11.2	4	2.9	1.39	-0.39
q 157	950.614	0.000	11.2	4	2.8	1.19	-0.39
n 157	955.418	0.000	8.4	8	6.4	0.83	-0.38
l 157	956.264	0.000	12.0	3	1.8	0.75	-0.42
g 157	978.235	0.000	11.5	4	2.7	0.81	-0.37
4 mdc5	1005.080	0.000	11.4	4	2.8	0.82	-0.34
y 8	1023.724	0.000	11.5	4	2.8	0.89	-0.32
9 mdc	871.994	0.000	14.8	5	3.7	0.86	-0.25
7 mdc	878.241	0.000	14.8	5	3.7	1.26	-0.25
6 mdc	874.436	0.000	14.9	5	3.7	1.06	-0.26
4 mdc	891.604	0.000	14.8	5	3.7	1.50	-0.27
t 9	910.663	0.000	15.0	5	3.7	0.85	-0.28
1 mdc	930.528	0.000	15.0	5	3.7	1.05	-0.28
2 mdc5	927.615	0.000	10.3	4	2.9	1.18	-0.28
e 158	922.955	0.000	10.3	4	2.9	0.86	-0.28
g 158	924.765	0.000	10.3	4	2.9	0.99	-0.28
j 158	928.160	0.000	10.3	4	2.9	0.36	-0.28
o 9	931.542	0.000	10.3	4	2.8	1.10	-0.27
m 158	941.512	0.000	7.7	8	6.6	1.07	-0.30
p 158	945.233	0.000	10.4	4	2.8	0.99	0.18
q 158	946.256	0.000	10.4	4	2.8	1.91	0.18
y 13	953.813	0.000	10.4	4	2.8	0.69	0.19
z 11	954.983	0.000	10.4	4	2.8	0.20	0.19
b 14	969.479	0.000	10.5	4	2.7	1.40	0.20
12 mdc	877.722	0.000	11.0	4	2.9	0.62	-0.45
13 mdc	851.365	0.000	11.0	4	2.9	0.61	-0.45
17 mdc	849.433	0.000	10.9	4	2.9	1.00	-0.44
18 mdc	866.115	0.000	10.9	4	2.9	1.51	-0.44
19 mdc	909.782	0.000	10.9	4	2.9	0.89	-0.43
20 mdc	947.304	0.000	8.1	8	6.7	0.88	-0.43
r 11	988.786	0.000	10.6	4	2.8	1.07	-0.21
17 mdc7	1015.245	0.000	10.5	4	2.9	0.66	-0.20
cs6123	1028.487	0.000	5.9	22	19.2	1.06	-0.32
cs6220	1023.486	0.000	11.4	4	2.8	0.90	-0.36
39 vs	1027.089	0.000	11.4	4	2.8	0.34	-0.37
1 gwm	1014.323	0.000	8.0	8	6.5	0.34	-0.31
2 gwm	1006.607	0.000	10.4	4	2.9	1.00	-0.26
3 gwm	1006.018	0.000	10.4	4	2.9	0.44	-0.26
u6580	1002.784	0.000	10.4	4	2.9	0.76	-0.25
4 gwm	1000.659	0.000	10.4	4	2.9	0.98	-0.25
u6684	1001.201	0.001	10.4	4	2.9	0.44	-0.25
5 gwm	996.769	0.000	10.4	4	2.9	0.91	-0.24
u6902	992.646	0.000	10.4	4	2.9	0.58	-0.24
u7008	987.808	0.000	10.5	4	2.8	0.79	-0.23
6 gwm	976.979	0.000	10.4	4	2.9	1.12	-0.24
u7194	980.287	0.000	10.4	4	2.9	1.59	-0.23
u7302	976.166	0.000	10.4	4	2.9	0.74	-0.24
u7348	973.549	0.000	10.5	4	2.8	0.47	-0.23
26 mdc	875.589	0.000	7.7	10	8.5	0.51	-0.20
a 11	869.953	0.000	7.7	10	8.5	0.71	-0.18
33 mdc	864.777	0.000	9.2	7	5.4	0.48	0.19
d 12	853.259	0.000	9.3	7	5.6	1.08	-0.18
34 mdc	860.581	0.000	9.0	8	6.3	0.82	-0.17
35 mdc	862.499	0.000	17.9	4	2.8	1.67	0.13
46 mdc	910.375	0.000	9.7	8	6.5	1.03	-0.44
47 mdc	905.490	0.000	9.4	8	6.6	1.00	-0.38
u7271	901.834	-0.001	9.5	8	6.6	1.18	-0.38
of 4	897.114	0.000	9.7	8	6.5	0.92	-0.38
f 10	881.277	0.000	9.5	8	6.4	0.99	-0.37
50 mdc	864.173	0.000	7.3	12	10.7	0.88	-0.43
51 mdc	850.396	0.000	9.1	8	6.8	0.76	-0.31
k 10	836.916	0.000	9.3	8	6.7	1.78	-0.32
52 mdc	846.528	0.001	9.2	8	6.7	1.23	-0.31
p 10	837.766	0.000	9.3	8	6.7	1.09	-0.32
53 mdc	844.723	0.000	9.3	8	6.7	1.17	-0.30
a 14	965.755	0.000	10.4	4	2.8	1.57	0.19
3 mdc5	962.724	0.000	11.3	4	2.8	0.68	-0.39
15 mdc	833.405	0.000	11.0	4	2.8	0.47	-0.45
o 10	830.672	0.000	10.3	4	2.9	1.08	-0.28
n 10	834.997	0.000	10.2	4	2.9	2.03	-0.28
t 10	862.430	0.000	10.2	4	2.9	0.66	0.16
u 10	827.018	0.000	10.4	4	2.8	0.97	0.14
3 mdc7	856.019	0.000	10.2	4	2.9	0.43	0.15
w 10	864.663	0.000	10.2	4	2.9	0.70	0.15
usbpr	859.996	0.000	10.6	4	2.9	0.71	-0.31
10 mdc7	859.140	0.000	10.6	4	2.9	0.72	-0.31
s 13	915.174	0.000	10.8	4	2.8	1.27	-0.30

Gravity Results 1984

```
sigma0 a posteriori :   1.00  n :  201  u :  57   dof :  144

 estimations for mean errors of single measurements of meters

s(g461 )   a pr :  12.01   a po :  12.01  dof :   66.2
s(g395 )   a pr :  17.23   a po :  17.23  dof :   77.8

 factor of gravimeters

f(g395 )   a pr : 1.000709   a po : 1.000709  err [ppm] :   66.7

 circular errors of gravimeters

c(g461 )
 f[ 1] f la a pr :    -      fixed :  72.00
      f am a pr :    -      fixed :   6.69
      f ph a pr :    -      fixed :   0.326
 f[ 2] f la a pr :    -      fixed :  36.00
      f am a pr :    -      fixed :   7.60
      f ph a pr :    -      fixed :   1.097
 f[ 3] f la a pr :    -      fixed :  24.00
      f am a pr :    -      fixed :   2.86
      f ph a pr :    -      fixed :   2.102
 f[ 4] f la a pr :    -      fixed :  18.00
      f am a pr :    -      fixed :   1.24
      f ph a pr :    -      fixed :   6.179
 f[ 5] f la a pr :    -      fixed :  14.40
      f am a pr :    -      fixed :   4.39
      f ph a pr :    -      fixed :  -4.133
```

adjusted values of the gravity stations

base	value [mgal]	gradi. [mi/m]		n. of meas.	deg.of free.	sigma a post.
11 mdc	888.130	0.000		54	49.5	1.05

station max.	value [mgal]	gradi. [mi/m]	m.err. [micro]	n. of meas.	deg.of free.	sigma a post.	name
32 mdc	866.078	0.000	5.6	8	6.8	1.17	-0.40
k 12	863.415	0.000	7.3	4	2.9	0.70	0.14
40 mdc	931.676	0.000	7.5	4	2.9	1.08	-0.31
54 mdc	860.555	0.000	7.6	4	2.9	1.65	-0.34
a 158	924.783	0.000	6.2	6	4.8	0.55	-0.31
9 mdc	871.985	0.000	10.1	2	1.0	0.96	-0.11
7 mdc	878.276	0.000	10.1	2	1.0	1.05	-0.11

6 mdc	874.445	0.000	10.1	2	1.0	0.73	-0.11
4 mdc	891.652	0.000	10.1	2	1.0	1.26	-0.11
t 9	910.720	0.000	10.1	2	1.0	0.22	-0.11
1 mdc	930.567	0.000	10.1	2	1.0	0.13	-0.11
cs6123	1028.493	0.000	7.9	4	2.5	0.40	-0.38
8403	856.378	0.000	10.1	2	1.0	1.69	0.11
8405	836.709	0.000	7.6	4	2.7	1.26	-0.19
8406a	829.807	0.000	10.2	2	1.0	0.59	-0.13
8408	854.591	0.000	10.5	2	0.9	1.12	-0.20
8410	845.904	0.000	10.2	2	1.0	0.82	0.10
8413	849.886	0.000	10.8	2	0.9	0.51	-0.20
8415	867.346	0.000	10.2	2	1.0	1.84	-0.12
8416	842.884	0.000	10.6	2	0.8	0.26	-0.21
8418	838.937	0.000	13.6	1	0.0	Inf	-0.47
8419	810.299	0.000	11.5	2	0.8	0.95	-0.45
8420	841.886	0.000	10.9	2	0.9	0.11	-0.22
8423	856.364	0.000	7.9	4	2.7	1.77	-0.21
8439	813.903	0.000	10.9	2	0.9	1.39	-0.21
8450	870.523	0.000	3.4	28	24.5	0.85	-0.41
8437	865.098	0.000	10.2	2	1.0	1.49	-0.23
8426	863.112	0.000	7.4	4	2.8	0.38	0.18
8427	873.507	0.000	7.4	4	2.8	0.53	0.18
8429	881.658	0.000	7.4	4	2.7	1.11	0.17
8430	883.315	0.000	7.5	4	2.6	1.07	0.16
8401	874.005	0.000	10.1	2	1.0	0.76	-0.11
8404	834.004	0.000	10.1	2	1.0	1.14	-0.12
8406	823.303	0.000	10.2	2	1.0	0.88	-0.14
8402	828.225	0.000	10.2	2	0.9	0.09	-0.13
8407	813.512	0.000	10.3	2	0.9	0.70	-0.16
8417	837.033	0.000	7.6	4	2.7	0.99	-0.17
8431	884.818	0.000	11.5	2	0.4	1.01	0.37
8428	889.748	0.000	10.6	2	0.8	1.30	0.16
8409	843.030	0.000	10.5	2	0.9	0.57	-0.20
8412	846.082	0.000	7.8	4	2.5	1.02	-0.19
8423a	902.667	0.000	10.7	2	0.9	0.22	-0.32
8424	813.243	0.000	10.8	2	0.9	0.59	-0.33
8438	816.355	0.000	10.9	2	0.9	0.30	-0.22

Gravity Results 1986

sigma0 a posteriori : 1.00 n : 435 u : 106 dof : 329

estimations for mean errors of single measurements of meters

s(g461) a pr : 11.60 a po : 11.60 dof : 69.3
s(g465) a pr : 26.91 a po : 26.91 dof : 259.7

factor of gravimeters

f(g465) a pr : 1.000291 a po : 1.000291 err [ppm] : 241.4

circular errors of gravimeters

c(g461)
f[1] f la a pr : - fixed : 72.00
f am a pr : - fixed : 6.69
f ph a pr : - fixed : 0.326
f[2] f la a pr : - fixed : 36.00
f am a pr : - fixed : 7.60
f ph a pr : - fixed : 1.097
f[3] f la a pr : - fixed : 24.00
f am a pr : - fixed : 2.86
f ph a pr : - fixed : 2.102
f[4] f la a pr : - fixed : 18.00
f am a pr : - fixed : 1.24
f ph a pr : - fixed : 6.179
f[5] f la a pr : - fixed : 14.40
f am a pr : - fixed : 4.39
f ph a pr : - fixed : -4.133

adjusted values of the gravity stations

base	value [mgal]	gradi. [mi/m]		n. of meas.	deg.of free.	sigma a post.
11 mdc	888.130	0.000		55	43.0	1.00
y 367	892.165	0.000	7.1			
z 367	884.044	0.000	7.6			
w 367	879.162	0.000	7.6			
arbee	876.169	0.000	7.8			
u 367	866.741	0.000	7.8			

station max.	value [mgal]	gradi. [mi/m]	m.err. [micro]	n. of meas.	deg.of free.	sigma a post.	name
j 11	886.729	0.000	6.2	8	6.0	1.45	-0.38
22 mdc	892.117	0.000	6.2	8	6.3	1.15	-0.39
23 mdc	891.463	0.000	6.2	8	6.3	1.04	-0.39
24 mdc	885.358	0.000	6.2	8	6.3	0.68	-0.40
25 mdc	884.280	0.000	7.0	6	4.6	1.45	-0.39
f 11a	881.322	0.000	7.0	6	4.6	1.03	-0.38
e 11a2	880.135	0.000	7.0	6	4.6	1.40	-0.39
27 mdc	876.973	0.000	7.0	6	4.2	0.54	-0.38
da 3c	877.229	0.000	6.3	8	6.0	1.32	-0.41
b 11	873.701	0.000	6.3	8	6.0	0.94	-0.41
30 mdc	866.432	0.000	6.3	7	5.5	1.25	-0.41
31 mdc	869.523	0.000	7.0	6	4.5	0.80	-0.38
u7743	868.158	0.000	7.1	5	3.6	0.90	-0.38
32 mdc	866.066	0.000	6.0	12	9.2	0.94	-0.37
36 mdc	855.247	0.000	7.2	6	4.2	0.52	-0.39
37 mdc	854.953	0.000	7.2	6	4.2	1.03	-0.39
h 12	853.446	0.000	7.0	7	5.1	1.10	-0.36
38 mdc	848.048	0.000	6.3	8	6.0	1.06	-0.40
39 mdc	861.860	0.000	7.1	6	4.5	1.04	-0.39
k 12	863.400	0.000	8.2	8	6.2	0.76	-0.39
40 mdc	911.655	0.000	9.3	34	26.0	1.18	-0.58
z 9	919.198	0.000	16.0	7	5.3	0.63	0.59
43 mdc	908.347	0.000	16.1	7	5.3	0.69	0.60
45 mdc	909.198	0.000	16.1	7	5.3	0.85	0.60
da 3m	908.776	0.000	16.1	7	5.3	0.89	0.60
48 mdc	899.963	0.000	16.5	7	5.3	0.84	0.62
u7389	892.932	0.000	16.4	7	5.2	0.59	0.63
49 mdc	867.399	0.000	19.5	7	5.2	1.06	0.73
h 10	859.996	0.000	20.8	7	4.9	0.78	0.78
1 10	852.408	0.000	21.9	7	5.2	0.90	0.79
46 mdc	910.359	0.000	16.1	7	5.3	0.69	0.60
47 mdc	905.498	0.000	16.2	7	5.3	1.25	0.60
u7273	901.856	0.000	16.4	7	5.3	0.41	0.61
of 4	897.116	0.000	16.8	7	5.4	1.05	0.62
f 10	881.262	0.000	17.6	7	5.2	0.79	0.69
50 mdc	864.185	0.000	19.9	7	5.2	1.18	0.75
51 mdc	850.384	0.000	22.4	7	4.9	0.95	0.78
52 mdc	846.508	0.000	22.9	7	5.1	1.23	0.80
p 10	837.704	0.000	24.7	7	5.3	0.50	0.84
o 10	830.679	0.000	26.1	7	5.3	1.51	0.84
n 10	834.993	0.000	25.3	7	5.4	0.75	0.83
53 mdc	844.706	0.000	24.4	6	4.5	0.87	0.81
54 mdc	860.555	0.000	20.2	8	6.0	0.98	0.78
9 mdc	871.964	0.000	13.0	7	5.3	0.43	0.36
7 mdc	878.285	0.000	12.7	7	5.3	0.92	0.36
4 mdc	891.624	0.000	12.6	7	5.3	0.71	0.32
t 9	910.697	0.000	13.6	7	5.0	1.17	0.47
1 mdc	930.541	0.000	16.4	7	5.3	1.16	-0.65
26 mdc	875.568	0.000	7.0	6	4.6	0.56	-0.39
a 11	869.925	0.000	6.2	8	6.4	0.96	-0.41

Gravity Results 1987

sigma0 a posteriori : 1.00 n : 1134 u : 204 dof : 930

estimations for mean errors of single measurements of meters

s(g264) a pr : 17.01 a po : 17.01 dof : 408.0 po/pr : 1.00
s(g461) a pr : 9.81 a po : 9.81 dof : 333.1
s(d86) a pr : 21.80 a po : 21.80 dof : 188.9

factor of gravimeters

f(d86) a pr : 0.999149 a po : 0.999149 err [ppm] : 98.1

circular errors of gravimeters

c(g264)
f[1] f la a pr : - fixed : 72.00
f am a pr : - fixed : -2.26
f ph a pr : - fixed : 3.865
f[2] f la a pr : - fixed : 36.00
f am a pr : - fixed : 1.74
f ph a pr : - fixed : 4.653
f[3] f la a pr : - fixed : 24.00
f am a pr : - fixed : 2.72
f ph a pr : - fixed : 1.815
f[4] f la a pr : - fixed : 18.00
f am a pr : - fixed : 4.14
f ph a pr : - fixed : 0.815
f[5] f la a pr : - fixed : 14.40
f am a pr : - fixed : 1.41
f ph a pr : - fixed : 1.184

c(g461)
f[1] f la a pr : - fixed : 72.00
f am a pr : - fixed : 6.69
f ph a pr : - fixed : 0.326
f[2] f la a pr : - fixed : 36.00
f am a pr : - fixed : 7.60
f ph a pr : - fixed : 1.097
f[3] f la a pr : - fixed : 24.00
f am a pr : - fixed : 2.86
f ph a pr : - fixed : 2.102
f[4] f la a pr : - fixed : 18.00
f am a pr : - fixed : 1.24
f ph a pr : - fixed : 6.179
f[5] f la a pr : - fixed : 14.40
f am a pr : - fixed : 4.39
f ph a pr : - fixed : -4.133

adjusted values of the gravity stations

base	value [mgal]	gradi. [mi/m]		n. of meas.	deg.of free.	sigma a post.
11 mdc	888.130	0.000		132	118.8	1.10
y 367	892.185	0.000	4.9			
z 367	884.062	0.000	4.6			
w 367	879.173	0.000	7.6			
arbee	876.196	0.000	5.7			
u 367	866.755	0.000	8.3			

station max.	value [mgal]	gradi. [mi/m]	m.err. [micro]	n. of meas.	deg.of free.	sigma a post.	name
hollis	886.040	0.000	4.7	8	6.3	1.13	-0.23
j 11	886.734	0.000	4.5	12	10.3	0.74	-0.36
22 mdc	892.149	0.000	4.5	12	10.3	0.72	-0.36
23 mdc	891.483	0.000	3.4	20	17.5	0.84	-0.36
24 mdc	885.357	0.000	7.3	5	3.8	0.97	-0.29
25 mdc	884.298	0.000	3.5	19	16.6	0.85	-0.32
kaygee	882.648	0.000	4.7	8	6.5	0.42	-0.23
f 11a	881.341	0.000	4.5	12	10.4	1.01	-0.36

e 11a2	880.137	0.000	3.8	14	12.2	0.86	-0.33
27 mdc	877.003	0.000	3.4	20	17.7	0.74	-0.36
da 3c	877.256	0.000	3.0	28	25.2	0.92	-0.30
n 11	872.708	0.000	4.5	12	10.5	0.67	-0.36
30 mdc	866.442	0.000	2.7	42	37.3	0.94	-0.38
u7743	868.154	0.000	5.0	11	9.3	1.26	0.24
32 mdc	866.067	0.000	4.8	11	9.2	1.43	0.24
cv8413	873.785	0.000	5.4	8	6.5	0.74	-0.24
cv8424	884.507	0.000	4.8	8	6.6	1.52	-0.27
36 mdc	855.252	0.000	5.1	11	9.2	0.81	-0.41
37 mdc	854.966	0.000	4.8	12	10.2	0.61	-0.40
38 mdc	848.064	0.000	4.8	12	10.3	0.62	-0.40
39 mdc	861.874	0.000	4.7	12	10.3	0.59	-0.40
k 12	863.392	0.000	6.2	6	4.6	0.83	-0.31
40 mdc	931.664	0.000	2.6	45	40.3	1.23	-0.46
41 mdc	920.241	0.000	4.6	9	7.6	0.99	-0.31
z 9	919.199	0.000	4.6	10	8.6	1.09	-0.31
42 mdc	920.606	0.000	4.6	10	8.6	1.36	-0.31
da 1	918.243	0.000	4.6	10	8.7	1.06	-0.31
43 mdc	908.374	0.000	4.6	10	8.7	0.89	-0.31
45 mdc	909.204	0.000	4.6	10	8.7	1.04	-0.31
da 3m	908.787	0.000	4.6	10	8.7	1.22	-0.31
48 mdc	899.995	0.000	6.1	5	3.9	1.25	-0.23
u7389	892.974	0.000	6.8	6	4.8	1.25	-0.55
49 mdc	867.420	0.000	5.5	12	10.6	0.76	-0.67
h 10	860.000	0.000	5.5	12	10.6	1.25	-0.67
l 10	852.442	0.000	5.6	12	10.6	0.84	-0.67
54 mdc	860.557	0.000	3.1	25	22.3	1.00	-0.36
8 mdc7	858.004	0.000	4.5	12	10.6	1.12	-0.38
s 10a	869.090	0.000	4.5	12	10.5	1.06	-0.38
pit	857.607	0.000	8.3	4	2.8	0.82	-0.54
z 10	869.171	0.000	5.0	9	7.6	0.99	-0.31
ystone	869.507	0.000	8.4	4	2.8	1.25	-0.54
9 mdc7	860.359	0.000	7.0	4	2.9	1.46	-0.49
n 13	860.699	0.000	7.0	4	2.9	0.78	-0.48
11 mdc7	861.140	0.000	7.3	4	2.8	0.79	-0.35
12 mdc7	894.279	0.000	7.0	4	2.9	1.23	-0.48
a 158	924.782	0.000	6.3	4	2.9	0.66	-0.13
z 157	932.663	0.000	6.3	4	2.9	0.32	-0.13
x 157	928.989	0.000	6.8	3	1.9	0.74	0.10
u 157	931.293	0.000	6.3	4	2.9	0.57	-0.14
s 157	942.281	0.000	6.4	4	2.9	0.90	-0.19
r 157	945.042	0.000	6.4	4	2.9	1.04	-0.19
q 157	950.598	0.000	6.4	4	2.9	1.55	-0.19
n 157	955.415	0.000	6.3	4	2.9	0.82	-0.14
m 157	958.074	0.000	9.2	3	1.8	0.97	-0.42
l 157	956.277	0.000	8.8	2	1.0	0.06	-0.15
c 157	1018.768	0.000	9.2	3	1.7	0.65	-0.43
y 8	1023.727	0.000	6.3	4	2.9	1.22	-0.14
9 mdc	871.983	0.000	6.2	6	4.7	0.85	-0.18
7 mdc	878.283	0.000	6.1	6	4.7	0.78	-0.18
4 mdc	891.642	0.000	6.1	6	4.7	1.31	-0.18
t 9	910.705	0.000	8.3	3	1.9	1.72	-0.13
2 mdc5	927.611	0.000	6.1	6	4.7	1.04	-0.15
g 158	924.768	0.000	6.1	6	4.7	0.84	-0.15
j 158	928.158	0.000	6.1	6	4.7	0.72	-0.16
o 9	931.538	0.000	6.1	6	4.7	0.78	-0.16
m 158	941.493	0.000	6.1	6	4.8	0.76	-0.16
p 158	945.178	0.000	6.1	6	4.8	0.48	-0.16
q 158	946.185	0.000	6.1	6	4.8	0.56	-0.16
u6802	950.392	0.000	6.4	4	2.9	0.44	-0.19
harlq	952.965	0.000	7.3	4	2.9	0.66	-0.55
y 13	953.791	0.000	6.4	4	2.8	0.52	-0.22
z 13	954.944	0.000	6.4	4	2.8	0.52	-0.24
bull	969.966	0.000	7.3	4	2.9	0.44	-0.55
b 14	969.434	0.000	6.8	4	2.8	0.74	-0.31
13 mdc	851.338	0.000	7.0	4	2.9	0.59	-0.30
wburn	726.895	0.000	7.8	4	2.7	1.61	-0.62
17 mdc	849.392	0.000	7.0	4	2.9	0.96	-0.30
18 mdc	866.107	0.000	7.0	4	2.9	0.50	-0.30
19 mdc	909.779	0.000	7.0	4	2.9	0.91	-0.30
20 mdc	947.297	0.000	7.0	4	2.9	0.61	-0.31
r 11	988.777	0.000	7.1	4	2.9	1.18	-0.32
cs6123	1028.496	0.000	3.5	21	18.6	1.13	-0.56
39 vs	1027.093	0.000	6.6	4	2.9	0.87	-0.39
1 gwm	1014.328	0.000	6.6	4	2.9	0.53	-0.39
2 gwm	1006.616	0.000	6.6	4	2.9	0.52	-0.39
3 gwm	1006.045	0.000	6.6	4	2.9	0.36	-0.39
u6580	1002.783	0.000	6.6	4	2.9	0.58	-0.39
4 gwm	1000.675	0.000	6.6	4	2.9	0.79	-0.39
u6684	1001.218	0.000	6.6	4	2.9	0.60	-0.39
5 gwm	996.783	0.000	6.6	4	2.9	0.81	-0.40
u6902	992.650	0.000	6.6	4	2.9	1.28	-0.40
u7008	987.815	0.000	6.6	4	2.9	0.64	-0.40
6 gwm	977.039	0.000	6.6	4	2.9	0.25	-0.40
u7194	980.305	0.000	6.5	4	2.9	0.46	-0.31
u7302	976.189	0.000	6.5	4	2.9	0.52	-0.31
u7348	971.565	0.000	6.5	4	2.9	0.25	-0.32
8403	856.381	0.000	8.7	2	1.0	0.48	-0.10
8405	836.701	0.000	8.7	3	1.7	1.66	-0.29
8406a	829.795	0.000	8.7	2	1.0	1.37	-0.11
10 rds	850.143	0.000	8.7	2	1.0	0.86	-0.11
8408	854.547	0.000	8.7	3	1.8	1.42	-0.29
tern	843.943	0.000	8.9	2	1.0	0.14	-0.21
8413	849.871	0.000	8.9	2	1.0	0.44	-0.21
coneEDM	748.217	0.000	9.3	2	0.9	0.66	-0.29
8418	838.938	0.000	8.7	3	1.7	1.57	-0.29
8420	841.870	0.000	8.7	2	1.0	1.24	-0.10
holmes	761.577	0.000	8.7	2	1.0	0.21	-0.10
toni	813.316	0.000	8.7	2	1.0	1.90	-0.10
8450	870.519	0.000	6.3	4	3.0	2.10	-0.20
frank	873.613	0.000	8.7	2	1.0	0.08	-0.14
a 14	965.747	0.000	6.8	4	2.9	0.97	-0.28
10 mdc7	859.158	0.000	7.0	4	2.9	0.80	-0.49
q 13	870.778	0.000	7.2	4	2.9	0.77	-0.32
p 13	849.798	0.000	7.2	4	2.9	0.16	-0.32
26 mdc	875.595	0.000	4.5	12	10.3	0.87	-0.37
a 11	869.939	0.000	5.3	9	7.3	0.90	0.24
3 mdc7	855.996	0.000	4.5	12	10.5	1.18	-0.38
t 10	862.444	0.000	5.0	9	7.6	0.84	-0.31
p 10	837.750	0.000	4.5	12	10.5	1.03	-0.38
o 10	830.689	0.000	4.5	12	10.5	1.14	-0.38
n 10	834.991	0.000	6.0	6	4.8	1.03	-0.29
46 mdc	910.380	0.000	5.0	9	7.7	0.99	-0.27
47 mdc	905.516	0.000	4.6	10	8.7	1.24	-0.31
f 10	881.298	0.000	5.5	12	10.6	1.21	-0.67
50 mdc	864.193	0.000	5.5	12	10.6	1.10	-0.67
51 mdc	850.408	0.000	5.6	12	10.6	0.92	-0.67
52 mdc	846.559	0.000	6.8	6	4.8	1.16	-0.54
8402	828.240	0.000	8.9	2	1.0	1.97	-0.21
8409	843.018	0.000	8.9	2	1.0	2.11	-0.20
8404	833.999	0.000	8.9	2	1.0	0.69	-0.20
8401	873.964	0.000	8.9	2	1.0	0.10	-0.19
pcone	748.426	0.000	9.3	2	0.9	0.93	-0.29
hspring	837.750	0.000	8.7	3	1.7	1.07	-0.29
8432	889.752	0.000	8.7	2	1.0	1.01	-0.15
8429	881.654	0.000	8.7	2	1.0	0.92	-0.15
8430	883.317	0.000	8.7	2	1.0	1.47	-0.14
8427	873.497	0.000	8.7	2	1.0	0.18	-0.14
8438	816.351	0.000	8.7	2	1.0	0.01	-0.10
nperce	918.304	0.000	7.1	4	2.9	0.92	-0.52
thermal	910.218	0.000	7.2	4	2.9	0.48	-0.52
p 12	931.051	0.000	8.0	4	2.8	0.95	-0.52
lewis	861.610	0.000	8.5	4	2.8	0.77	-0.55

Gravity Results 1988

sigma0 a posteriori : 0.84 n : 736 u : 86 dof : 650

estimations for mean errors of single measurements of meters

s(g264) a pr : 12.46 a po : 12.46 dof : 141.9
s(g461) a pr : 10.06 a po : 10.06 dof : 137.8
s(g615) a pr : 999.99 a po : 999.99 dof : 187.0
s(g721) a pr : 27.20 a po : 27.20 dof : 183.2

factor of gravimeters

f(g615) a pr : 1.000323 a po : 1.000323 err [ppm] : 4302.5
f(g721) a pr : 1.000622 a po : 1.000622 err [ppm] : 224.2

circular errors of gravimeters

c(g264)
f[1] f la a pr : fixed : 72.00
f am a pr : - fixed : -2.26
f ph a pr : - fixed : 3.865
f[2] f la a pr : fixed : 36.00
f am a pr : - fixed : 1.74
f ph a pr : + fixed : 4.653
f[3] f la a pr : + fixed : 24.00
f am a pr : - fixed : 2.72
f ph a pr : - fixed : 1.815
f[4] f la a pr : - fixed : 18.00
f am a pr : - fixed : 4.14
f ph a pr : - fixed : 0.815
f[5] f la a pr : - fixed : 14.40
f am a pr : - fixed : 3.41
f ph a pr : - fixed : 1.184

c(g461)
f[1] f la a pr : - fixed : 72.00
f am a pr : - fixed : 6.69
f ph a pr : - fixed : 0.326
f[2] f la a pr : - fixed : 36.00
f am a pr : - fixed : 7.60
f ph a pr : + fixed : 1.097
f[3] f la a pr : - fixed : 24.00
f am a pr : - fixed : 2.86
f ph a pr : - fixed : 2.102
f[4] f la a pr : - fixed : 18.00
f am a pr : - fixed : 1.24
f ph a pr : - fixed : 6.179
f[5] f la a pr : - fixed : 14.40
f am a pr : - fixed : 4.39
f ph a pr : - fixed : -4.133

adjusted values of the gravity stations

base	value [mgal]	gradi. [mi/m]	n. of meas.	deg.of free.	sigma a post
11 mdc	888.130	0.000	84	77.5	1.02

station max.	value [mgal]	gradi. [mi/m]	m.err. [micro]	n. of meas.	deg.of free.	sigma a post.	name
d 367	891.610	0.000	3.4	34	29.6	0.81	0.29
hollis	886.042	0.000	4.3	16	14.2	0.60	0.25
j 11	886.732	0.000	4.3	16	14.2	0.68	0.25
lc 58	891.680	0.000	4.5	15	13.2	0.58	0.24
22 mdc	892.139	0.000	4.9	14	12.1	0.72	0.23
y 367	892.170	0.000	4.3	16	14.1	0.49	0.25
23 mdc	891.468	0.000	4.9	10	8.5	0.80	0.21
24 mdc	885.377	0.000	6.0	8	6.6	0.76	-0.42
z 367	884.064	0.000	6.0	8	6.6	0.63	-0.42
25 mdc	884.298	0.000	6.0	8	6.6	0.83	-0.42
kaygee	882.622	0.000	3.2	32	28.7	0.89	0.37
f 11a	881.338	0.000	6.0	8	6.6	0.66	-0.42
w 367	879.169	0.000	6.0	8	6.6	0.60	-0.42
e 11a2	880.135	0.000	6.0	8	6.6	0.87	-0.42
arbee	876.187	0.000	3.4	27	24.2	0.85	0.35
27 mdc	876.989	0.000	5.9	8	6.7	0.74	-0.38
cv85222	877.030	0.000	6.0	7	5.8	1.01	-0.38
da 3c	877.250	0.000	3.2	30	27.3	0.88	0.36
le hardy	875.208	0.000	5.9	8	6.7	0.64	-0.39

b 11	873.707	0.000	5.9	8	6.7	0.56	-0.39
30 mdc	866.439	0.000	5.5	8	6.6	0.62	-0.40
u 367	866.764	0.000	2.6	66	61.3	0.83	-0.45
31 mdc	869.525	0.000	4.5	16	14.2	1.13	-0.44
u7743	868.145	0.000	4.6	15	13.3	1.31	-0.43
32 mdc	866.061	0.000	4.5	15	13.3	0.61	-0.44
cv8412	867.008	0.000	3.2	35	32.1	1.16	-0.43
cv8413	873.787	0.000	5.7	8	6.9	0.61	-0.25
cv8424	884.495	0.000	3.5	28	25.5	0.75	-0.43
cv8421	853.346	0.000	6.0	8	6.4	0.80	-0.23
36 mdc	855.226	0.000	5.7	8	6.8	0.42	-0.22
37 mdc	854.945	0.000	5.7	8	6.8	0.74	-0.22
h 12	853.433	0.000	5.1	9	7.8	0.84	-0.25
38 mdc	848.049	0.000	4.3	16	14.2	1.15	-0.33
39 mdc	861.854	0.000	5.7	8	6.9	0.35	-0.22
k 12	863.388	0.000	7.8	4	2.9	0.27	-0.16
d 339	949.899	0.000	21.8	11	9.4	0.21	-0.63
43 mdc	908.405	0.000	18.3	9	7.9	0.29	0.56
y 366	894.507	0.000	18.7	6	4.9	0.68	0.50
n 367	853.211	0.000	18.7	8	6.9	0.52	0.48
s 367	844.131	0.000	19.4	8	6.8	0.59	0.48
54 mdc	860.573	0.000	18.0	8	6.9	0.93	0.46
z 10	869.177	0.000	5.4	11	9.3	0.66	-0.46
ystone	869.499	0.000	4.6	16	13.9	0.91	-0.46
n 13	860.690	0.000	17.0	10	8.9	0.71	0.48
a 13	869.944	0.000	4.5	16	14.2	0.99	-0.44
26 mdc	875.581	0.000	6.0	8	6.6	0.62	-0.42

Gravity Results 1989

sigma0 a posteriori : 1.00 n : 979 u : 128 dof : 851

estimations for mean errors of single measurements of meters

s(g264) a pr : 13.15 a po : 13.15 dof : 446.5
s(g461) a pr : 8.07 a po : 8.07 dof : 404.5

factor of gravimeters

circular errors of gravimeters

c(g264)				
f[1]	f la a pr :	-	fixed :	72.00
	f am a pr :	-	fixed :	-2.26
	f ph a pr :	-	fixed :	3.865
f[2]	f la a pr :	-	fixed :	36.00
	f am a pr :	-	fixed :	1.74
	f ph a pr :	-	fixed :	4.653
f[3]	f la a pr :	-	fixed :	24.00
	f am a pr :	-	fixed :	2.72
	f ph a pr :	-	fixed :	1.815
f[4]	f la a pr :	-	fixed :	18.00
	f am a pr :	-	fixed :	4.14
	f ph a pr :	-	fixed :	0.815
f[5]	f la a pr :	-	fixed :	14.40
	f am a pr :	-	fixed :	3.41
	f ph a pr :	-	fixed :	1.184
c(g461)				
f[1]	f la a pr :	-	fixed :	72.00
	f am a pr :	-	fixed :	6.69
	f ph a pr :	-	fixed :	0.326
f[2]	f la a pr :	-	fixed :	36.00
	f am a pr :	-	fixed :	7.60
	f ph a pr :	-	fixed :	1.097
f[3]	f la a pr :	-	fixed :	24.00
	f am a pr :	-	fixed :	2.86
	f ph a pr :	-	fixed :	2.102
f[4]	f la a pr :	-	fixed :	18.00
	f am a pr :	-	fixed :	1.24
	f ph a pr :	-	fixed :	6.179
f[5]	f la a pr :	-	fixed :	14.40
	f am a pr :	-	fixed :	4.39
	f ph a pr :	-	fixed :	-4.133

adjusted values of the gravity stations

base	value [mgal]	gradi. [mi/m]	n. of meas.	deg.of free.	sigma a post.
11 mdc	888.130	0.000	72	68.5	1.12

station	value [mgal]	gradi. [mi/m]	m.err. [micm]	n. of meas.	deg.of free.	sigma a post.	max. name
d 367	891.613	0.000	3.4	12	10.9	0.91	-0.53
hollis	886.042	0.000	3.4	12	10.9	0.84	-0.53
j 11	886.732	0.000	3.4	12	10.9	0.77	-0.53
lc 58	891.685	-0.001	3.4	12	10.9	0.92	-0.53
22 mdc	892.135	0.000	3.4	12	10.9	0.79	-0.53
y 367	892.174	0.000	3.4	12	10.9	0.78	-0.53
23 mdc	891.470	0.000	4.4	6	5.0	0.52	-0.41
24 mdc	885.365	0.000	3.2	12	10.8	0.94	-0.41
z 367	884.058	0.001	3.2	12	10.8	0.75	-0.41
25 mdc	884.298	0.000	3.2	12	10.8	0.99	-0.41
kaygee	882.621	0.000	3.2	12	10.8	0.76	-0.41
f 11a	881.348	0.000	3.2	12	10.8	1.63	-0.41
w 367	879.177	0.001	3.2	12	10.8	1.08	-0.41
a 11a2	880.153	0.000	3.2	12	10.8	0.97	-0.41
arbee	876.183	0.000	4.3	6	4.9	0.72	-0.31
27 mdc	876.984	0.001	3.2	12	10.9	1.10	0.32
cv85222	877.025	0.001	3.2	12	10.9	0.78	0.32
da 3c	877.240	0.000	3.2	12	10.9	0.96	0.32
le hardy	875.205	0.001	3.2	12	10.9	0.61	0.32

b 11	873.706	0.001	3.2	12	10.9	1.04	0.32
30 mdc	866.430	0.000	3.2	12	10.9	0.78	0.32
u 367	866.761	0.001	2.0	60	54.7	0.93	-0.45
31 mdc	869.516	0.001	3.5	12	10.8	1.12	-0.45
u7743	868.144	0.001	3.5	12	10.8	1.15	-0.45
32 mdc	866.054	0.001	3.5	12	10.8	0.77	-0.45
cv8412	866.997	0.002	3.5	12	10.8	1.22	-0.45
cv8413	873.769	0.001	3.5	12	10.8	1.58	-0.45
cv8424	884.485	0.001	4.5	6	4.9	0.90	-0.35
36 mdc	855.248	0.002	3.8	12	9.7	1.19	0.44
37 mdc	854.948	0.002	3.8	12	9.9	1.17	0.44
h 12	853.441	0.001	3.8	12	10.1	0.78	0.44
38 mdc	848.045	0.002	3.8	12	10.3	0.63	0.44
39 mdc	861.860	0.002	3.8	12	10.3	0.63	0.44
k 12	863.395	0.001	4.7	6	4.7	0.87	0.36
40 mdc	931.655	0.004	5.2	27	23.5	0.86	-0.88
y 9	923.472	0.006	6.3	12	10.3	1.47	-0.85
41 mdc	920.231	0.005	6.3	11	9.3	1.86	-0.84
u 366	918.877	0.005	6.3	12	10.3	1.11	-0.85
z 9	919.196	0.006	6.3	12	10.5	0.68	-0.85
42 mdc	920.593	0.006	6.5	10	8.6	0.95	-0.83
da 1	918.246	0.006	7.0	5	3.8	1.51	-0.76
43 mdc	908.355	0.004	6.3	12	10.6	0.87	-0.85
45 mdc	909.188	0.004	6.3	12	10.6	0.62	-0.85
da 3m	908.779	0.004	6.3	12	10.6	0.57	-0.85
48 mdc	899.989	0.004	6.9	6	4.8	1.30	-0.77
u7389	892.939	-0.017	4.6	10	8.9	0.40	-0.74
f 367	881.502	-0.005	5.6	4	3.0	1.65	-0.49
g 367	870.884	-0.015	4.4	12	10.8	1.13	-0.76
49 mdc	867.404	-0.015	4.4	12	10.8	0.63	-0.76
j 367	856.143	-0.015	4.4	12	10.8	0.56	-0.76
l 367	837.265	-0.006	4.0	12	10.9	1.07	-0.70
l 10	852.420	-0.015	4.4	12	10.8	1.04	-0.76
n 367	853.134	-0.015	4.4	12	10.8	1.08	-0.76
54 mdc	860.546	-0.008	3.1	28	25.8	0.98	-0.76
8 mdc7	858.005	-0.001	5.5	4	2.9	0.79	-0.27
s 10a	869.077	-0.001	5.5	4	2.9	0.79	-0.27
z 10	869.171	0.001	4.3	6	5.0	0.61	0.24
ystone	869.499	0.001	3.2	12	10.9	1.07	0.32
9 mdc	871.954	0.000	3.9	8	6.9	0.93	-0.30
7 mdc	878.270	0.000	3.9	8	6.9	0.57	-0.30
4 mdc	891.618	0.000	3.9	8	6.9	1.11	-0.30
t 9	910.699	0.000	5.2	4	3.0	1.01	-0.23
2 mdc5	927.614	0.000	4.0	8	6.9	0.71	0.27
g 158	924.772	-0.001	4.0	8	6.9	1.07	0.27
j 158	928.149	0.000	4.0	8	6.9	1.06	0.27
o 9	931.534	-0.001	4.0	8	6.9	0.54	0.27
m 158	941.488	-0.001	4.0	8	6.9	0.28	0.27
p 158	945.168	-0.001	4.0	8	6.9	1.23	0.27
q 158	946.178	0.000	5.3	4	3.0	0.54	0.20
8403	856.408	0.011	7.3	2	0.9	0.60	-0.25
8405	836.727	0.003	7.3	2	1.0	0.11	-0.31
8406a	829.813	0.010	7.3	2	1.0	0.04	-0.26
8408	854.568	0.003	7.3	2	1.0	0.11	-0.31
tern	843.968	0.004	7.3	2	1.0	0.87	-0.30
8410	845.932	0.011	7.3	2	0.9	0.55	-0.25
8413	849.877	0.011	7.3	2	0.9	1.24	-0.25
8415	867.329	0.003	7.3	2	1.0	1.25	-0.31
8416	842.890	0.005	7.3	2	1.0	1.13	-0.30
coneEDM	748.233	0.004	7.3	2	1.0	0.01	-0.31
8450	870.513	-0.001	2.9	16	14.5	0.89	-0.31
8437	865.087	0.000	7.2	2	0.9	1.69	-0.22
11 mdca	888.187	0.000	3.4	12	10.5	1.07	-0.36
26 mdc	875.585	0.000	3.4	10	8.9	1.41	-0.39
a 11	869.926	0.002	3.5	12	10.8	0.82	-0.45
46 mdc	910.367	0.004	6.3	11	9.6	0.81	-0.84
47 mdc	905.500	0.004	6.3	11	9.6	1.97	-0.84
u7273	901.853	-0.019	6.1	4	2.9	0.68	-0.58
8412	846.095	0.004	7.3	2	1.0	0.38	-0.30
8406	823.311	0.010	7.3	2	0.9	1.33	-0.26
8404	833.978	0.010	7.3	2	0.9	1.98	-0.26
8407	813.532	0.011	7.3	2	0.9	0.14	-0.26
8426	863.037	0.000	7.2	2	0.9	1.09	-0.22
8427	873.494	0.000	7.2	2	0.9	0.28	-0.22
8429	881.664	0.001	7.2	2	0.9	0.16	-0.21
8430	883.297	0.000	7.2	2	1.0	0.26	-0.21
8432	889.749	0.000	7.2	2	1.0	0.15	-0.21
3 mdc7	855.997	-0.001	5.5	4	2.9	0.92	-0.27
t 10	862.446	-0.001	5.5	4	2.9	0.83	-0.27

Gravity Results 1990

sigma0 a posteriori : 1.00 n : 292 u : 57 dof : 235

estimations for mean errors of single measurements of meters

s(g264) a pr : 22.07 a po : 22.06 dof : 131.3
s(g461) a pr : 10.57 a po : 10.57 dof : 103.7

factor of gravimeters

circular errors of gravimeters

c(g264)				
f[1]	f la a pr :	-	fixed :	72.00
	f am a pr :	-	fixed :	-2.26
	f ph a pr :	-	fixed :	3.865
f[2]	f la a pr :	-	fixed :	36.00
	f am a pr :	-	fixed :	1.74
	f ph a pr :	-	fixed :	4.653
f[3]	f la a pr :	-	fixed :	24.00
	f am a pr :	-	fixed :	2.72
	f ph a pr :	-	fixed :	1.815
f[4]	f la a pr :	-	fixed :	18.00
	f am a pr :	-	fixed :	4.14
	f ph a pr :	-	fixed :	0.815
f[5]	f la a pr :	-	fixed :	14.40
	f am a pr :	-	fixed :	3.41

```
      f ph a pr :    -      fixed :   1.184

c(g461 )
 f[ 1] f la a pr :    -      fixed :   72.00
       f am a pr :    -      fixed :    6.69
       f ph a pr :    -      fixed :   0.326
 f[ 2] f la a pr :    -      fixed :   36.00
       f am a pr :    -      fixed :    7.60
       f ph a pr :    -      fixed :   1.097
 f[ 3] f la a pr :    -      fixed :   24.00
       f am a pr :    -      fixed :    2.86
       f ph a pr :    -      fixed :   2.102
 f[ 4] f la a pr :    -      fixed :   18.00
       f am a pr :    -      fixed :    1.24
       f ph a pr :    -      fixed :   6.179
 f[ 5] f la a pr :    -      fixed :   14.40
       f am a pr :    -      fixed :    4.39
       f ph a pr :    -      fixed :  -4.133
```

adjusted values of the gravity stations

base	value (mgal)	gradi. (mi/m)		n. of meas.	deg.of free.	sigma a post.
11 mdc	888.130	0.000		45	38.3	1.38

station max.	value (mgal)	gradi. (mi/m)	m.err. (micro)	n. of meas.	deg.of free.	sigma a post.	name
hollis	886.035	0.000	5.1	11	8.9	1.13	-0.35
j 11	886.717	0.000	4.9	12	10.2	1.46	-0.49
lc 58	891.665	0.000	5.7	8	6.5	1.34	-0.40
22 mdc	892.122	0.000	4.9	12	10.1	1.10	-0.49
y 367	892.167	0.000	5.0	11	9.2	0.68	-0.49
23 mdc	891.464	0.000	7.1	5	3.7	1.31	-0.37
24 mdc	885.372	0.000	5.5	8	6.5	0.74	-0.28
z 367	884.072	0.000	5.5	8	6.5	0.32	-0.27
25 mdc	884.308	0.000	5.6	8	6.6	0.81	-0.27
kaygee	882.624	0.000	6.2	6	4.7	0.76	-0.28
f 11a	881.344	0.000	5.5	8	6.7	0.68	-0.27
w 367	879.183	0.000	5.5	8	6.7	0.45	-0.27
s 11a2	880.156	0.000	5.5	8	6.7	0.78	-0.27
arbee	876.191	0.000	7.3	4	2.9	0.44	-0.21
cv85222	877.042	0.000	5.1	12	9.8	0.77	-0.51
27 mdc	876.998	0.000	5.8	10	8.1	1.18	-0.52
da 3c	877.267	0.000	5.1	12	9.9	1.00	-0.51
1e hardy	875.218	0.000	5.8	8	6.2	1.16	-0.42
b 11	873.720	0.000	5.0	12	10.2	0.98	-0.40
30 mdc	866.439	0.000	5.0	12	10.2	0.87	-0.40
u 367	866.773	0.000	5.0	12	10.3	0.57	-0.41
31 mdc	869.550	0.000	8.6	4	2.8	0.22	-0.41
u7743	868.167	0.000	8.6	4	2.8	0.55	-0.41
32 mdc	866.060	0.000	10.9	2	0.9	0.62	-0.32
cv8412	867.022	0.000	8.1	4	2.9	0.82	-0.53
cv8413	873.796	0.000	8.1	4	2.9	0.95	-0.53
cv8424	884.507	0.000	8.1	4	2.9	0.75	-0.53
36 mdc	855.269	0.000	8.1	4	2.9	0.86	-0.53
37 mdc	854.972	0.000	10.5	2	0.9	1.29	-0.41
h 12	853.457	0.000	7.8	4	2.9	0.32	-0.49
38 mdc	848.071	0.000	7.8	4	2.9	0.53	-0.49
39 mdc	861.874	0.000	7.8	4	2.9	0.36	-0.49
k 12	863.404	0.000	10.3	2	1.0	0.02	-0.37
ystone	869.518	0.000	6.3	6	4.6	1.04	-0.32
a 11	869.966	0.000	8.6	4	2.8	0.41	-0.40

Gravity Results 1991

sigma0 a posteriori : 1.00 n : 1435 u : 249 dof : 1186

estimations for mean errors of single measurements of meters

```
s(g264 )   a pr :   9.44   a po :   9.44  dof :  535.3
s(g461 )   a pr :  19.61   a po :  19.61  dof :  154.2
s(g461e)   a pr :  44.94   a po :  44.94  dof :   82.7
s(e839 )   a pr :  18.56   a po :  18.56  dof :  124.0
s(g839 )   a pr :  20.81   a po :  20.81  dof :  289.0
```

factor of gravimeters

```
f(e839 )   a pr : 1.001341   a po : 1.001341  err (ppm) :   408.0
f(g839 )   a pr : 1.000563   a po : 1.000563  err (ppm) :    47.6
```

circular errors of gravimeters

```
c(g264 )
 f[ 1] f la a pr :    -      fixed :   72.00
       f am a pr :    -      fixed :   -2.26
       f ph a pr :    -      fixed :   3.865
 f[ 2] f la a pr :    -      fixed :   36.00
       f am a pr :    -      fixed :    1.74
       f ph a pr :    -      fixed :   4.653
 f[ 3] f la a pr :    -      fixed :   24.00
       f am a pr :    -      fixed :    2.72
       f ph a pr :    -      fixed :   1.815
 f[ 4] f la a pr :    -      fixed :   18.00
       f am a pr :    -      fixed :    4.14
       f ph a pr :    -      fixed :   0.815
 f[ 5] f la a pr :    -      fixed :   14.40
       f am a pr :    -      fixed :    3.41
       f ph a pr :    -      fixed :   1.184

c(g461 )
 f[ 1] f la a pr :    -      fixed :   72.00
       f am a pr :    -      fixed :    6.69
       f ph a pr :    -      fixed :   0.326
 f[ 2] f la a pr :    -      fixed :   36.00
       f am a pr :    -      fixed :    7.60
       f ph a pr :    -      fixed :   1.097
 f[ 3] f la a pr :    -      fixed :   24.00
       f am a pr :    -      fixed :    2.86
       f ph a pr :    -      fixed :   2.102
 f[ 4] f la a pr :    -      fixed :   18.00
       f am a pr :    -      fixed :    1.24
       f ph a pr :    -      fixed :   6.179
 f[ 5] f la a pr :    -      fixed :   14.40
       f am a pr :    -      fixed :    4.39
       f ph a pr :    -      fixed :  -4.133
```

adjusted values of the gravity stations

base	value (mgal)	gradi. (mi/m)		n. of meas.	deg.of free.	sigma a post.
11 mdc	888.130	0.000		158	139.6	1.20

station max.	value (mgal)	gradi. (mi/m)	m.err. (micro)	n. of meas.	deg.of free.	sigma a post.	name
d 367	891.610	0.000	6.8	4	2.9	1.00	-0.44
hollis	886.048	0.000	5.1	8	6.4	1.32	-0.42
j 11	886.735	0.000	3.1	26	22.4	1.15	-0.51
lc 58	891.685	0.000	3.8	17	14.4	1.00	-0.54
22 mdc	892.138	0.000	5.4	9	7.2	0.79	-0.41
y 367	892.180	0.000	5.0	10	8.1	0.65	-0.42
23 mdc	891.481	0.000	6.8	4	2.8	1.13	-0.32
z 367	884.068	0.000	3.5	18	15.1	1.03	-0.43
kaygee	882.629	0.000	3.5	16	13.6	0.97	-0.37
w 367	879.189	0.000	3.9	12	9.9	0.93	-0.35
arbee	876.201	0.000	3.2	28	23.6	0.88	0.30
27 mdc	877.001	0.000	7.6	3	2.0	0.34	-0.49
cv85222	877.046	0.000	4.3	12	9.6	0.70	-0.23
da 3c	877.264	0.000	3.0	29	24.7	0.82	0.30
1e hardy	875.236	0.000	3.1	27	22.2	0.86	0.27
b 11	873.727	0.000	3.2	24	20.6	0.92	0.29
30 mdc	866.441	0.000	3.3	22	18.7	0.75	0.27
u 367	866.775	0.000	1.9	89	78.6	1.04	-0.43
31 mdc	869.542	0.000	7.6	3	2.0	0.59	-0.49
u7743	868.169	0.000	7.6	3	2.0	0.57	-0.48
32 mdc	866.073	0.000	7.7	2	1.0	0.49	-0.49
cv8412	867.025	0.000	4.0	13	11.1	0.73	-0.42
cv8413	873.797	0.000	4.0	14	11.8	1.02	-0.40
cv8424	884.503	0.000	3.2	20	18.2	1.09	-0.49
cv8421	853.385	0.000	4.1	12	10.7	1.15	-0.47
37 mdc	854.978	0.000	7.5	4	2.9	0.37	-0.48
h 12	853.475	0.000	4.1	12	10.7	0.94	-0.47
38 mdc	848.071	0.000	4.1	12	10.7	0.72	-0.47
39 mdc	861.877	0.000	7.6	3	2.0	0.94	-0.48
k 12	863.423	0.000	4.8	7	5.7	1.53	-0.35
d 339	949.869	0.000	5.1	8	6.6	1.21	-0.41
40 mdc	931.677	0.000	2.6	35	31.9	0.99	-0.29
y 9	923.485	0.000	4.5	10	8.7	0.69	-0.31
41 mdc	920.242	0.000	4.7	7	5.8	1.63	-0.27
u 366	918.902	0.000	4.7	8	6.8	0.42	-0.31
z 9	919.203	0.000	4.7	8	6.7	0.79	-0.27
42 mdc	920.616	0.000	4.7	8	6.8	0.57	-0.31
43 mdc	908.376	0.000	4.7	8	6.9	0.95	-0.21
45 mdc	909.212	0.000	4.7	8	6.9	0.70	-0.25
da 3m	908.790	0.000	4.7	8	6.9	0.67	-0.25
48 mdc	900.009	0.000	4.3	10	8.8	0.82	0.26
y 366	894.549	0.000	3.7	15	13.6	0.83	0.33
f 367	881.517	0.000	4.1	14	12.4	0.94	-0.40
g 367	870.925	0.000	5.2	8	6.8	0.63	-0.42
49 mdc	867.430	0.000	4.6	9	7.7	1.07	-0.34
j 367	856.177	0.000	4.9	8	6.7	1.19	-0.32
l 367	837.283	0.000	4.9	7	5.7	1.20	0.25
l 10	852.457	0.000	4.9	8	6.7	0.70	-0.32
n 367	853.174	0.000	4.4	10	8.1	1.39	-0.30
9107	828.163	0.000	7.4	4	2.9	0.75	-0.56
9106	833.356	0.000	7.4	4	2.9	0.55	-0.56
s 367	844.074	0.000	2.6	43	38.0	1.05	0.35
54 mdc	860.551	0.000	4.3	13	10.9	0.92	-0.39
8 mdc7	858.021	0.000	5.1	8	6.5	0.84	-0.24
9105	858.753	0.000	7.4	4	2.9	0.72	-0.56
s 10a	869.103	0.000	5.1	8	6.3	0.80	-0.26
9104	864.015	0.000	7.4	4	2.9	1.54	-0.56
9103	863.347	0.000	7.4	4	2.9	1.08	-0.57
9101	869.275	0.000	7.4	4	2.9	0.83	-0.57
z 10	869.191	0.000	6.9	4	2.8	0.88	-0.27
ystone	869.517	0.000	5.1	8	6.3	1.19	-0.37
9 mdc7	860.353	0.000	7.0	4	2.9	1.03	0.24
9108	854.140	0.000	8.2	2	1.0	0.64	-0.39
9109	848.228	0.000	8.2	2	1.0	0.33	-0.39
9110	859.651	0.000	8.2	2	1.0	0.93	-0.39
n 13	860.676	0.000	5.1	9	7.4	1.22	-0.42
11 mdc7	861.138	0.000	5.0	10	8.3	1.12	-0.39
9111	855.568	0.000	8.2	2	1.0	0.78	-0.39
12 mdc7	894.284	0.000	5.0	7	5.5	0.79	-0.30
a 158	924.772	0.000	2.9	31	28.6	1.12	-0.35
x 157	928.996	0.000	5.0	6	5.0	0.67	0.26
y 157	928.469	0.000	4.7	8	6.9	0.57	-0.28
u 157	931.308	0.000	4.9	7	6.0	0.74	0.26
s 157	942.272	0.000	4.7	8	6.9	1.28	-0.28
r 157	945.030	0.000	4.8	8	6.9	0.57	0.27
q 157	950.596	0.000	4.7	8	6.9	1.40	-0.28
n 157	955.419	0.000	4.8	8	6.9	1.51	0.27
m 157	958.055	0.000	5.7	5	3.9	0.95	0.25
g 157	978.250	0.000	5.2	8	6.9	0.45	-0.41
4 mdc5	1005.074	0.000	5.0	8	6.9	0.90	0.30
c 157	1018.749	0.000	5.2	8	6.9	0.72	-0.40
y 8	1023.736	0.000	5.1	8	6.9	1.04	-0.36
9 mdc	871.992	0.000	5.2	8	6.7	1.01	-0.53
7 mdc	878.296	0.000	4.8	8	6.7	0.69	-0.37

6 mdc	874.444	0.000	5.2	8	6.7	0.77	-0.53
4 mdc	891.627	0.000	4.8	8	6.7	0.93	-0.37
t 9	910.710	0.000	5.2	8	6.7	1.05	-0.53
2 mdc5	927.634	0.000	5.2	7	5.8	1.09	0.29
g 158	924.783	0.000	4.9	8	6.7	0.97	-0.34
o 9	931.553	0.000	5.1	8	6.7	0.82	0.30
m 158	941.497	0.000	4.9	8	6.7	0.83	-0.34
p 158	945.197	0.000	5.1	8	6.8	0.62	0.30
q 158	946.208	0.000	5.5	6	4.8	0.64	-0.25
harlq	952.973	0.000	7.0	4	2.9	1.13	-0.45
y 13	953.806	0.000	5.1	8	6.6	1.30	-0.41
z 13	954.974	0.000	5.9	4	2.9	0.83	-0.44
hull	969.970	0.000	9.2	2	0.9	0.26	-0.34
b 14	969.440	0.000	5.7	8	4.7	0.50	-0.43
12 mdc	877.685	0.000	6.7	4	2.9	0.70	-0.40
13 mdc	851.346	0.000	6.7	4	2.9	0.63	-0.40
17 mdc	849.393	0.000	5.6	6	4.7	0.96	-0.43
18 mdc	866.093	0.000	6.7	4	2.9	0.80	-0.40
19 mdc	909.761	0.000	5.7	5	3.9	1.17	-0.43
20 mdc	947.291	0.000	6.7	4	2.9	0.90	-0.39
x 11	988.775	0.000	6.7	4	2.8	1.40	-0.39
17 mdc7	1015.235	0.000	6.2	6	4.3	1.73	-0.27
cs6123	1028.495	0.000	2.7	40	35.3	1.01	-0.44
19 vc	1027.103	0.000	4.6	10	8.4	1.12	-0.37
1 gwm	1014.339	0.000	4.7	10	8.3	0.66	-0.32
2 gwm	1006.637	0.000	5.4	7	5.6	0.57	-0.32
3 gwm	1006.043	0.000	6.4	4	3.0	0.82	-0.30
4 gwm	1000.663	0.000	6.2	6	4.6	0.82	-0.26
5 gwm	996.791	0.000	5.6	8	6.2	0.99	-0.34
u6902	992.643	0.000	4.5	11	9.2	1.00	-0.44
u7008	987.799	0.000	4.9	8	6.9	0.94	-0.46
6 gwm	977.019	0.000	4.9	8	6.7	0.98	-0.45
u7194	980.310	0.000	5.1	6	4.9	0.88	-0.46
u7302	976.195	0.000	4.9	8	6.7	0.66	-0.45
u7348	973.572	0.000	5.6	5	3.8	0.68	-0.37
8403	856.412	0.000	9.9	2	1.0	0.31	-0.21
bluff	856.691	0.000	9.9	2	1.0	0.24	-0.20
8405	836.757	0.000	10.5	2	0.9	0.04	-0.48
8406a	829.828	0.000	9.8	2	1.0	0.45	-0.18
10 rds	950.176	0.000	9.8	2	1.0	1.78	-0.18
8408	854.594	0.000	10.1	2	0.9	0.06	-0.28
tern	843.941	0.000	10.1	2	0.9	0.74	-0.29
8410	845.947	0.000	10.5	2	0.9	0.78	-0.48
8413	849.873	0.000	10.1	2	0.9	1.12	-0.30
8415	867.329	0.000	10.7	1	0.0	0.00	-0.48
8416	842.895	0.000	10.5	2	0.9	0.93	-0.48
coneEDM	748.240	0.000	10.7	1	0.0	0.00	-0.48
8418	838.952	0.000	7.5	3	1.7	0.34	-0.39
8419	810.290	0.000	10.1	2	1.0	0.70	-0.41
8420	841.879	0.000	10.2	2	0.9	1.28	-0.32
8423	856.365	0.000	10.5	2	0.9	0.81	-0.48
8439	813.901	0.000	10.5	2	0.9	1.20	-0.48
8437	865.112	0.000	9.6	2	0.8	0.42	-0.44
a 11	869.964	0.000	7.4	4	2.8	0.94	-0.45
usbpr	859.996	0.000	7.1	4	2.9	1.10	-0.49
10 mdc7	859.147	0.000	7.0	4	2.9	0.95	0.24
8427	873.517	0.000	9.6	2	0.8	1.42	-0.44
8430	883.305	0.000	10.5	1	0.0	0.00	-0.44
8426	863.070	0.000	9.6	2	0.8	0.51	-0.44
8407	813.539	0.000	10.5	2	0.9	0.20	-0.48
8423a	902.652	0.000	7.7	4	2.9	1.47	-0.54
8424	813.213	0.000	10.4	1	0.0	0.00	-0.42
8406	823.348	0.000	10.0	1	0.0	0.00	-0.17
trout	861.212	0.000	9.8	2	1.0	1.80	-0.19
8402	828.258	0.000	9.9	2	1.0	0.86	-0.20
8404	833.987	0.000	10.1	1	0.0	0.00	-0.21
8412	846.075	0.000	10.1	2	0.9	0.37	-0.30
hspring	837.733	0.000	10.2	2	0.9	2.08	-0.31
9102	864.974	0.000	7.4	4	2.9	1.46	-0.57

Gravity Results 1993

sigma0 a posteriori : 1.00 n : 1769 u : 208 dof : 1561

estimations for mean errors of single measurements of meters

s(g264) a pr : 7.75 a po : 7.75 dof : 750.1
s(g461) a pr : 11.20 a po : 11.20 dof : 810.9

factor of gravimeters

circular errors of gravimeters

c(g264)
f[1] f la a pr : - fixed : 72.00
f am a pr : - fixed : -2.26
f ph a pr : - fixed : 3.865
f[2] f la a pr : - fixed : 36.00
f am a pr : - fixed : 1.74
f ph a pr : - fixed : 4.653
f[3] f la a pr : - fixed : 24.00
f am a pr : - fixed : 2.72
f ph a pr : - fixed : 1.815
f[4] f la a pr : - fixed : 18.00
f am a pr : - fixed : 4.14
f ph a pr : - fixed : 0.815
f[5] f la a pr : - fixed : 14.40
f am a pr : - fixed : 3.41
f ph a pr : - fixed : 1.184

c(g461)
f[1] f la a pr : - fixed : 72.00
f am a pr : - fixed : 6.69
f ph a pr : - fixed : 0.326
f[2] f la a pr : - fixed : 36.00
f am a pr : - fixed : 7.60
f ph a pr : - fixed : 1.097
f[3] f la a pr : - fixed : 24.00
f am a pr : - fixed : 2.86
f ph a pr : - fixed : 2.102
f[4] f la a pr : - fixed : 18.00
f am a pr : - fixed : 1.24
f ph a pr : - fixed : 6.179
f[5] f la a pr : - fixed : 14.40
f am a pr : - fixed : 4.39
f ph a pr : - fixed : -4.133

adjusted values of the gravity stations

base	value (mgal)	gradi. (mi/m)		n. of meas.	deg.of free.	sigma a post.	
11 mdc	988.130	0.000		139	132.8	1.09	
station max.	value (mgal)	gradi. (mi/m)	m.err. (micro)	n. of meas.	deg.of free.	sigma a post.	name
d 367	891.615	0.000	4.7	4	3.0	1.19	-0.19
hollis	886.048	0.000	2.5	16	14.5	1.02	-0.27
j 11	886.743	0.000	2.5	16	14.6	1.01	-0.22
lc 58	891.695	0.000	2.5	16	14.5	1.11	-0.27
22 mdc	892.150	0.000	4.7	4	3.0	0.55	-0.19
y 367	892.198	0.000	2.5	16	14.6	0.68	-0.22
23 mdc	891.482	0.000	4.8	4	2.8	0.52	-0.27
24 mdc	885.371	0.000	4.7	4	2.9	0.96	-0.18
z 367	884.074	0.000	2.5	16	14.5	0.84	-0.27
25 mdc	884.306	0.000	4.7	4	2.9	0.58	-0.17
kaygee	882.645	0.000	2.5	16	14.6	0.84	-0.22
f 11a	881.361	0.000	4.7	4	2.9	1.07	-0.16
w 367	879.212	0.000	2.4	18	16.5	0.81	-0.28
e 11a2	880.164	0.000	4.6	4	2.9	0.59	-0.19
arbee	876.229	0.000	2.6	16	14.5	1.00	-0.28
27 mdc	877.040	0.000	2.5	16	14.6	0.89	-0.26
cv85222	877.080	0.000	2.6	16	14.5	0.88	-0.28
da 3c	877.298	0.000	2.5	16	14.6	1.21	-0.27
le hardy	875.259	0.000	2.6	16	14.5	0.89	-0.28
b 11	873.749	0.000	2.5	16	14.6	1.01	-0.27
30 mdc	866.452	0.000	2.6	16	14.5	1.05	-0.28
u 367	866.786	0.000	1.2	109	103.9	1.05	-0.36
31 mdc	869.560	0.000	4.6	4	3.0	1.10	-0.14
u7743	868.174	0.000	4.6	4	3.0	0.95	0.12
32 mdc	866.067	0.000	2.9	12	10.9	1.31	-0.33
cv8412	867.032	0.000	2.4	16	14.7	0.79	-0.24
cv8413	873.798	0.000	2.5	16	14.8	0.66	-0.32
cv8424	884.501	0.000	2.4	16	14.7	0.66	-0.24
cv8421	853.379	0.000	2.5	16	14.7	0.71	-0.28
36 mdc	855.263	0.000	2.8	12	10.8	0.79	0.21
37 mdc	854.979	0.000	2.5	16	14.8	0.65	-0.25
37 ex	855.779	0.000	3.5	8	6.9	1.22	0.19
h 12	853.469	0.000	2.3	20	18.6	0.85	0.26
38 mdc	848.064	0.000	2.5	16	14.8	1.01	-0.25
38 ex	851.819	0.000	3.5	8	6.9	0.79	0.19
39 mdc	861.881	0.000	2.5	16	14.7	0.79	-0.25
k 12	863.422	0.000	2.6	14	12.7	1.06	0.22
d 339	949.867	0.000	3.4	8	6.9	0.36	-0.27
40 mdc	931.676	0.000	1.7	46	43.9	1.15	-0.41
y 9	923.489	0.000	2.8	12	10.8	0.72	-0.28
41 mdc	920.253	0.000	2.9	12	10.9	1.05	-0.37
u 366	918.910	0.000	2.8	12	10.8	1.25	-0.28
z 9	919.212	0.000	2.9	12	10.9	1.05	-0.26
42 mdc	920.615	0.000	2.9	12	10.8	1.37	-0.29
da 1	918.271	0.000	6.5	2	1.0	0.98	-0.15
43 mdc	908.374	0.000	2.9	12	10.8	0.95	-0.32
44 mdc	905.944	0.000	2.9	12	10.8	0.82	-0.27
45 mdc	909.215	0.000	2.9	12	10.7	0.71	-0.28
da 3m	908.803	0.000	3.0	11	9.9	0.76	-0.27
48 mdc	900.016	0.000	2.9	12	10.7	0.87	-0.28
y 366	894.557	0.000	2.2	22	20.5	0.67	-0.35
u7389	892.986	0.000	6.6	2	1.0	1.38	-0.18
f 367	881.517	0.000	2.6	16	14.7	1.17	-0.34
g 367	870.928	0.000	2.9	12	10.8	0.95	-0.31
49 mdc	867.421	0.000	3.0	12	10.8	1.29	-0.38
h 10	860.025	0.000	2.9	12	10.8	1.02	-0.35
j 367	856.178	0.000	3.0	12	10.8	0.86	-0.39
l 367	837.298	0.000	2.6	16	14.7	1.03	-0.37
l 10	852.473	0.000	3.0	12	10.9	0.94	0.33
n 367	853.186	0.000	3.0	12	10.9	1.13	0.33
9107	828.177	0.000	3.0	12	10.9	1.20	0.33
9106	833.362	0.000	3.0	11	9.9	0.80	0.33
s 367	844.101	0.000	1.8	40	45.9	0.98	-0.45
54 mdc	860.583	0.000	3.5	8	6.9	0.41	0.28
8 mdc7	858.039	0.000	3.4	8	6.8	0.96	-0.24
9105	858.777	0.000	3.4	8	6.8	0.75	-0.25
z 10a	869.113	0.000	3.4	8	6.8	1.42	-0.18
9104	864.031	0.000	3.4	8	6.8	0.94	-0.22
9103	863.362	0.000	3.4	8	6.8	0.75	-0.18
pit	857.645	0.000	4.6	5	3.9	1.31	-0.22
2 mdc7	868.769	0.000	4.8	4	2.9	1.11	-0.24
9101	869.289	0.000	3.4	8	6.8	0.80	-0.22
z 10	869.202	0.000	3.4	8	6.8	0.93	-0.18
ystone	869.533	0.000	3.4	8	6.8	0.62	-0.22
9 mdc7	860.381	0.000	4.7	4	3.0	0.42	0.21
9108	854.154	0.000	3.5	8	7.0	0.70	0.28
9109	848.233	0.000	3.5	8	6.9	0.42	0.28
9110	859.677	0.000	3.5	8	6.9	0.85	0.28
n 11	860.700	0.000	3.6	8	6.9	0.44	0.28
11 mdc7	861.161	0.000	3.5	8	6.9	0.85	0.28
9111	855.570	0.000	3.6	8	6.9	0.69	0.28
12 mdc7	894.272	0.000	4.0	6	4.9	0.44	0.25
a 158	924.776	0.000	1.9	29	27.0	1.20	-0.33
z 157	932.647	0.000	6.6	2	0.9	0.32	-0.25
x 157	928.983	0.000	3.5	8	6.7	1.46	-0.24
v 157	928.469	0.000	3.4	8	6.7	0.94	-0.23
u 157	931.299	0.000	3.5	8	6.7	0.63	-0.24
s 157	942.274	0.000	3.4	8	6.7	1.24	-0.23

r 157	945.026	0.000	3.5	8	6.7	1.29	-0.26
q 157	950.609	0.000	3.4	8	6.8	0.97	-0.26
n 157	955.421	0.000	3.5	8	6.7	0.65	-0.26
m 157	958.058	0.000	3.4	8	6.8	1.01	-0.20
l 157	956.284	0.000	3.5	8	6.8	0.85	-0.24
10-17	961.457	0.000	3.4	8	6.8	0.99	0.15
g 157	978.264	0.000	3.5	8	6.6	0.65	-0.24
4 mdc5	1005.068	0.000	3.5	8	6.8	0.65	0.16
t 157	1018.758	0.000	2.5	16	14.5	1.51	-0.23
y 8	1023.724	0.000	3.4	8	6.8	1.03	-0.17
9 mdc	871.992	0.000	3.3	8	6.9	1.06	-0.22
7 mdc	878.309	0.000	3.4	8	6.9	1.33	-0.26
6 mdc	874.452	0.000	3.3	8	6.9	1.07	-0.22
4 mdc	891.628	0.000	3.4	8	6.9	0.67	-0.26
t 9	910.709	0.000	3.3	8	6.9	1.30	-0.22
1 mdc	930.542	0.000	4.7	4	3.0	1.37	-0.19
2 mdc5	927.638	0.000	3.4	8	6.9	1.57	-0.23
e 158	922.990	0.000	3.4	8	6.9	0.85	-0.23
g 158	924.791	0.000	3.4	8	6.9	0.67	-0.22
j 158	928.179	0.000	3.8	6	4.9	0.43	-0.22
o 9	931.558	0.000	3.4	8	6.9	1.11	-0.24
m 158	941.491	0.000	3.4	8	6.9	0.70	-0.22
p 158	945.191	0.000	3.4	8	6.9	0.85	-0.24
q 158	946.197	0.000	3.4	8	6.9	0.45	-0.22
u6802	950.409	0.000	6.5	2	1.0	0.39	-0.14
harlq	952.982	0.000	3.4	8	6.9	1.24	-0.25
y 13	953.809	0.000	3.4	8	6.9	1.05	-0.27
z 13	954.962	0.000	3.4	8	6.9	1.26	-0.25
hull	969.951	0.000	3.9	6	4.9	0.76	-0.27
b 14	969.430	0.000	3.4	8	6.9	1.01	-0.33
12 mdc	877.716	0.000	3.4	8	6.7	1.11	-0.20
13 mdc	851.358	0.000	3.4	8	6.8	0.83	-0.23
17 mdc	849.402	0.000	3.4	8	6.7	1.10	-0.23
wburn	726.895	0.000	4.1	5	4.0	1.84	-0.16
18 mdc	866.099	0.000	3.4	8	6.7	0.60	-0.21
19 mdc	909.771	0.000	3.4	8	6.7	1.04	-0.23
20 mdc	947.301	0.000	3.4	8	6.7	0.74	-0.21
r 11	988.779	0.000	3.4	8	6.7	0.80	-0.24
17 mdc7	1015.243	0.000	3.4	8	6.7	0.98	-0.23
cs6123	1028.511	0.000	2.2	24	22.4	1.22	-0.39

cs6220	1023.474	0.000	3.4	8	6.9	1.32	-0.33
39 vs	1027.119	0.000	3.4	8	6.9	1.09	-0.33
1 gwm	1014.342	0.000	3.4	8	6.9	1.16	-0.33
2 gwm	1006.629	0.000	3.4	8	6.8	0.81	-0.26
3 gwm	1006.038	0.000	3.4	8	6.9	1.39	-0.33
u6580	1002.788	0.000	3.4	8	6.9	0.86	-0.33
4 gwm	1000.668	0.000	3.4	8	6.9	0.86	-0.33
u6684	1001.209	0.000	3.4	8	6.9	1.01	-0.33
5 gwm	996.786	0.000	3.1	10	8.8	1.13	-0.33
u6902	992.658	0.000	3.4	8	6.8	0.93	-0.26
u7008	987.807	0.000	3.4	8	6.8	0.90	-0.26
6 gwm	977.039	0.000	3.4	8	6.8	1.01	-0.26
u7194	980.307	0.000	3.4	8	6.8	0.84	-0.26
u7302	976.185	0.000	3.4	8	6.8	1.19	-0.26
u7348	973.568	0.000	3.9	5	4.9	0.82	-0.25
8403	856.448	0.000	6.7	2	1.0	1.43	-0.21
bluff	856.709	0.000	6.7	2	1.0	0.60	-0.21
8405	836.775	0.000	6.5	2	1.0	3.15	0.10
8406a	829.858	0.000	6.5	2	1.0	0.04	0.10
spruce	853.836	0.000	6.7	2	1.0	0.92	-0.22
10 rds	850.194	0.000	6.6	2	1.0	0.73	-0.13
8408	854.622	0.000	6.5	2	1.0	2.42	0.10
tern	843.997	0.000	6.5	2	1.0	0.54	0.10
8410	845.939	0.000	6.5	2	1.0	0.01	0.10
8413	849.902	0.000	6.5	2	1.0	0.23	0.10
8415	867.343	0.000	6.5	2	1.0	0.21	0.10
8416	842.930	0.000	6.5	2	1.0	0.48	0.10
8418	838.966	0.000	6.5	2	1.0	1.03	0.10
coneEDM	748.267	0.000	6.5	2	1.0	1.27	0.10
8419	810.305	0.000	6.5	2	1.0	0.44	0.10
8420	841.896	0.000	6.5	2	1.0	0.20	0.10
8423	856.379	0.000	6.5	2	1.0	0.96	0.10
8439	813.918	0.000	6.5	2	1.0	0.13	0.10
holmes	761.585	0.000	6.6	2	1.0	1.71	-0.13
toni	813.352	0.000	6.6	2	1.0	0.31	-0.13
8450	870.548	0.000	6.9	2	0.9	2.23	0.37
8437	865.100	0.000	5.6	4	2.7	0.43	-0.53
frank	873.631	0.000	5.6	4	2.7	1.50	-0.53

Table C.3 : Removed measurements

station	c	time (GMT) (y.m.d) (h.m)	reading [ins.un]	height [m]	volt [volt]	si	y
e 158	r	77- 8- 1 1613	3444.115	0.000	-	1.0	-65.2
40 mdc	r	77- 8- 1 1726	3450.540	0.000	-	1.0	-53.7
40 mdc	r	77- 8- 1 1734	3450.535	0.000	-	1.0	-53.2
e 11a2	r	77- 8- 5 1729	3402.850	0.000	-	1.0	-610.2
54 mdc	r	77- 8-31 2010	3384.892	0.000	-	1.0	-36.4
11 mdc	r	77- 9- 9 1422	3410.982	0.000	-	1.0	32.8
38 mdc	r	79- 9-12 1733	3380.379	0.000	-	1.0	104.9
z 10	r	79- 9-12 2229	3400.268	0.000	-	1.0	89.4
z 10	r	79- 9-16 1642	3400.156	0.000	-	1.0	115.6
31 mdc	r	79- 9-17 1454	3400.415	0.000	-	1.0	155.5
27 mdc	r	83- 6-23 1643	3416.493	0.000	-	1.0	-187.9
33 mdc	r	83- 6-24 1649	3404.679	0.000	-	1.0	181.0
38 mdc	r	83- 6-25 1722	3389.021	0.000	-	1.0	146.9
k 12	r	83- 6-25 1801	3403.404	0.000	-	1.0	133.0
11 mdc	r	83- 7- 8 1631	3426.740	0.000	-	1.0	52.9
11 mdc	r	83- 7- 8 1644	3426.658	0.000	-	1.0	133.1
11 mdc	r	83- 7-12 2341	3426.965	0.000	-	1.0	-108.8
11 mdc	r	83- 7-15 127	3426.991	0.000	-	1.0	-63.0
da 1	r	83- 9- 3 2302	3455.572	0.000	-	1.0	-94.3
25 mdc	r	83- 9- 6 1628	3423.421	0.000	-	1.0	69.1
d 12	r	83- 6-24 1737	3387.576	0.000	-	1.0	81.4
k 12	r	83- 6-25 39	3397.863	0.000	-	1.0	-68.2
32 mdc	r	83- 6-25 1850	3400.269	0.000	-	1.0	-89.2
40 mdc	r	83- 6-29 1711	3464.400	0.000	-	1.0	121.9
11 mdc	r	83- 7- 8 1711	3421.837	0.000	-	1.0	297.9
11 mdc	r	83- 7- 8 1729	3421.950	0.000	-	1.0	176.3
11 mdc	r	83- 7-12 202	3422.240	0.000	-	1.0	140.0
l 157	r	83- 7-15 2226	3489.082	0.000	-	1.0	-94.6
8418	r	84- 9-11 1316	3370.541	0.000	-	1.0	141.0
11 mdc	r	86- 9- 6 31	3431.840	0.000	-	1.0	178.7
h 12	r	86- 9- 7 1954	3399.478	0.000	-	1.0	-106.9
11 mdc	r	86- 9-10 1926	3431.960	0.000	-	1.0	59.1
40 mdc	r	86- 8-15 2221	3470.535	0.000	-	1.0	134.6
40 mdc	r	86- 8-22 1846	3470.685	0.000	-	1.0	387.9
u7743	r	86- 9- 6 1849	3410.507	0.000	-	1.0	165.3
30 mdc	r	86- 9- 7 1731	3408.932	0.000	-	1.0	116.2
11 mdc	r	86- 9- 7 2202	3429.785	0.000	-	1.0	92.3
l 157	r	87- 7-20 2141	3496.641	0.000	-	1.0	-59.9
x 157	r	87- 7-23 1756	3470.501	0.000	-	1.0	178.6
cv8413	r	87- 8-26 1733	3418.395	0.000	-	1.0	58.0
32 mdc	r	87- 8-26 2203	3411.175	0.000	-	1.0	-69.2
54 mdc	r	87- 8-27 2007	3405.968	0.000	-	1.0	-62.2
30 mdc	r	87- 9- 4 1511	3411.315	0.000	-	1.0	78.0
11 mdc	r	87- 9- 5 1554	3432.023	0.000	-	1.0	-80.9
cs6123	r	87- 7-14 1912	3561.605	0.000	-	1.0	49.2
l 157	r	87- 7-20 2135	3493.602	0.000	-	1.0	78.6
25 mdc	r	87- 8-24 1738	3425.960	0.000	-	1.0	-99.2
da 3c	r	87- 8-24 2124	3419.303	0.000	-	1.0	-65.9
24 mdc	r	87- 8-25 11	3427.014	0.000	-	1.0	-57.5
11 mdc	r	87- 8-26 1417	3429.670	0.000	-	1.0	-86.1
u7743	r	87- 8-26 1632	3410.844	0.000	-	1.0	-63.3
30 mdc	r	87- 9- 4 1522	3409.104	0.000	-	1.0	-51.9
36 mdc	r	87- 9- 4 1712	3398.572	0.000	-	1.0	-57.4
11 mdc	r	87- 9- 5 1600	3429.580	0.000	-	1.0	-133.8
46 mdc	r	87- 9- 9 2127	3450.488	0.000	-	1.0	-88.6
c 157	r	87- 9-14 2145	3552.155	0.000	-	1.0	179.3
m 157	r	87- 9-14 2211	3495.414	0.000	-	1.0	-124.3
11 mdc	r	87- 9-14 2307	3429.612	0.000	-	1.0	-28.1
41 mdc	r	87- 8-31 2335	147.697	0.000	-	1.0	147.3
z 10	r	88- 9- 8 1518	3415.319	0.000	-	1.0	-57.9
u7743	r	88- 9- 8 1731	3414.159	0.000	-	1.0	75.7
cv8412	r	88- 9- 8 1840	3413.108	0.000	-	1.0	47.1
d 367	r	88- 9- 9 1718	3436.377	0.000	-	1.0	52.2
lc 58	r	88- 9- 9 1831	3436.424	0.000	-	1.0	56.9
arbee	r	88- 9-12 1659	3322.862	0.000	-	1.0	386.7
30 mdc	r	88- 9-12 2237	3313.355	0.000	-	1.0	88.9
d 367	r	88- 9-14 1731	3341.065	0.000	-	1.0	261.5
11 mdc	r	88- 9-14 1745	3337.644	0.000	-	1.0	279.3
11 mdc	r	88- 9-14 1843	3337.601	0.000	-	1.0	302.4
y 366	r	88- 9-19 1810	3343.823	0.000	-	1.0	-106.7
d 339	r	88- 9-19 1849	3397.939	0.000	-	1.0	-112.2
43 mdc	r	88- 9-19 1917	3357.465	0.000	-	1.0	-152.2
y 366	r	88- 9-19 1938	3343.968	0.000	-	1.0	-221.9
cv85222	r	88- 9-12 2018	3410.623	0.000	-	1.0	-105.2
32 mdc	r	88- 9-13 1548	3399.785	0.000	-	1.0	111.5
26 mdc	r	89- 8-17 1740	3422.034	0.000	-	1.0	83.8
40 mdc	r	89- 8-31 1639	3475.133	0.000	-	1.0	53.9
46 mdc	r	89- 8-31 1813	3454.970	0.000	-	1.0	46.4
da 1	r	89- 9- 4 1815	3462.595	0.000	-	1.0	-62.7
42 mdc	r	89- 9- 4 1839	3464.814	0.000	-	1.0	-71.3
41 mdc	r	89- 9- 4 1947	3464.453	0.000	-	1.0	-64.0
47 mdc	r	89- 9- 5 1725	3450.450	0.000	-	1.0	49.5
26 mdc	r	89- 8-17 1732	3420.326	0.000	-	1.0	84.9
42 mdc	r	89- 9- 4 1744	3462.772	0.000	-	1.0	37.0
lc 58	r	90- 9- 6 2143	3438.173	0.000	-	1.0	-61.6
y 367	r	90- 9-15 1823	3438.329	0.000	-	1.0	87.4
11 mdc	r	90- 9-17 1855	3434.582	0.000	-	1.0	78.1
11 mdc	r	90- 9-18 1813	3434.539	0.000	-	1.0	68.0
hollis	r	90- 9- 6 1613	3431.343	0.000	-	1.0	-54.4
lc 58	r	90- 9- 6 1743	3436.611	0.000	-	1.0	-78.9
23 mdc	r	90- 9- 7 2037	3436.333	0.000	-	1.0	74.6
27 mdc	r	90- 9-11 2228	3422.801	0.000	-	1.0	83.3
11 mdc	r	90- 9-15 1420	3498.166	0.000	-	1.0	49.8
27 mdc	r	90- 9-17 1459	3488.355	0.000	-	1.0	-360.5
11 mdc	r	90- 9-17 1844	3498.520	0.000	-	1.0	-110.8
11 mdc	r	90- 9-18 1804	3498.336	0.000	-	1.0	80.9
u 367	r	91- 9- 4 1541	3404.216	0.000	-	1.0	-35.4
11 mdc	r	91- 7-14 1932	3500.385	0.000	-	1.0	191.5
da 3c	r	91- 7-22 1605	3491.649	0.000	-	1.0	118.9
11 mdc	r	91- 7-22 1843	3502.113	0.000	-	1.0	-139.9
40 mdc	r	91- 7-26 2212	3542.944	0.000	-	1.0	166.5
cv8412	r	91- 7-27 2145	3482.028	0.000	-	1.0	175.1
12 mdc7	r	91- 8-13 1532	3507.285	0.000	-	1.0	591.1
n 13	r	91- 8-13 1622	3476.030	0.000	-	1.0	227.5
11 mdc	r	91- 8-14 1440	3501.598	0.000	-	1.0	412.8
17 mdc	r	91- 8-14 1509	3465.446	0.000	-	1.0	132.6
19 mdc	r	91- 8-14 1531	3522.200	0.000	-	1.0	123.2
2 gwm	r	91- 8-14 2134	3613.300	0.000	-	1.0	72.0
5 gwm	r	91- 8-16 2312	3603.937	0.000	-	1.0	73.3
u7194	r	91- 8-21 2026	3587.937	0.000	-	1.0	399.5
u7348	r	91- 8-21 2043	3581.762	0.000	-	1.0	237.9
u7194	r	91- 8-21 2059	3588.207	0.000	-	1.0	130.9
m 157	r	91- 8-22 2138	3567.335	0.000	-	1.0	67.1
x 157	r	91- 8-23 1725	3540.082	0.000	-	1.0	-82.5
8415	r	91- 9- 4 2018	3482.110	0.000	-	1.0	-289.7
coneEDM	r	91- 9- 4 2029	3370.164	0.000	-	1.0	-290.4
k 12	r	91- 9- 6 2059	3478.043	0.000	-	1.0	134.8
11 mdc	r	91- 9- 7 1352	3501.308	0.000	-	1.0	202.3
8406	r	91- 9- 7 1534	3440.254	0.000	-	1.0	299.6
11 mdc	r	91- 7-15 1432	3411.000	0.000	3.478	1.0	53.3
23 mdc	r	91- 7-15 1642	3411.000	0.000	0.237	1.0	97.2
11 mdc	r	91- 7-16 1416	3411.000	0.000	1.630	1.0	141.8
11 mdc	r	91- 7-16 1812	3411.000	0.000	3.562	1.0	89.5
u 367	r	91- 7-31 1836	3391.179	0.000	-	1.0	67.6
41 mdc	r	91- 8- 2 1510	3443.663	0.000	-	1.0	-66.8
u 367	r	91- 8- 3 1354	3391.128	0.000	-	1.0	75.0

1 367 r 91- 8- 3 2029 3362.982 0.000 - 1.0 -76.4
49 mdc r 91- 8- 3 2051 3392.557 0.000 - 1.0 -93.5
1 mdc5 r 91- 8- 8 1553 3451.325 0.000 - 1.0 -72.4
19 mdc r 91- 8-14 1538 3433.903 0.000 - 1.0 -90.5
2 gwm s 91- 8-14 1950 3528.720 0.000 - 1.0 104.9

a 158 s 93- 8-30 1750 3458.398 0.000 - 1.0 34.0
11 mdc r 93- 8- 7 1401 3506.282 0.000 - 1.0 -46.1
9106 s 93- 8-24 1436 3454.717 0.000 - 1.0 47.8
11 mdc r 93- 9- 1 1248 3506.402 0.000 - 1.0 46.7

C 4 : Determinations of the gravity differences of neighboured stations in the Hayden Valley

					Δg [mgal]	σ [µgal]
26 mdc - arbee						
1988	875.581	6.0	876.187	3.4	0.606	6.9
1989	875.585	3.4	876.183	4.3	0.598	5.5
average					**0.601**	**3.5**
z 367 - 25 mdc						
1988	884.064	6.0	884.298	6.0	-0.236	8.5
1989	884.058	3.2	884.298	3.2	-0.240	4.5
1990	884.072	5.5	884.308	5.5	-0.236	7.8
1993	884.074	2.5	884.306	4.7	-0.232	5.3
average					**-0.236**	**3.0**
y 367 - 23 mdc						
1988	892.170	4.3	891.468	4.9	0.702	6.6
1989	892.174	3.4	891.470	4.4	0.704	5.5
1990	892.167	5.0	891.470	4.4	0.704	5.5
1991	892.180	5.0	891.481	6.8	0.699	8.4
average					**0.702**	**3.5**
u 367 a 11						
1988	866.764	2.6	869.944	4.5	-3.180	5.5
1990	866.773	5.0	869.966	8.6	-3.193	10.0
1991	866.775	1.9	869.964	7.4	-3.189	7.6
average					**-3.184**	**4.0**
f 11 a - w 367						
1988	881.338	6.0	879.169	6.0	2.169	8.5
1989	881.348	3.2	879.177	3.2	2.171	4.5
1990	881.344	5.5	879.183	5.5	2.161	7.8
1993	881.361	4.7	879.212	2.4	2.149	5.3
average					**2.162**	**3.0**
e 11 a2 - w 367						
1988	880.135	6.0	879.169	6.0	0.966	8.5
1989	880.152	3.2	879.177	3.2	0.986	4.5
1990	880.156	5.5	879.183	5.5	0.973	7.8
1993	880.164	4.6	879.212	2.4	0.952	5.3
average					**0.971**	**3.0**

Lebenslauf

Personalien

Name	Arnet
Vornamen	Felix Karl
Geburtsdatum	28. November 1965
Geburtsort	St. Gallen
Bürgerort	Kriens LU
Staatszugehörigkeit	Schweiz
Zivilstand	ledig

Schulausbildung

1972 - 1978	Primarschule in St. Gallen
1978 - 1980	Sekundarschule in St. Gallen
1980 - 1984	Kantonsschule in St. Gallen (Typus C)
1985 - 1989	Studium an der Abteilung VIII der ETH Zürich (Studienrichtung Vermessung)
Dez. 1989	Abschluss des Studiums als dipl. Verm. Ing. ETH
1990	Wissenschaftlicher Mitarbeiter bei Prof. Dr. H.G. Kahle am Institut für Geodäsie und Photogrammetrie der ETH Zürich
1991	Austauschstudent bei Prof. Dr. R.B.Smith am Departement of Geophysics an der University of Utah, Salt Lake City, USA
seit 1992	Wissenschaftlicher Mitarbeiter bei Prof. Dr. H.G. Kahle am Institut für Geodäsie und Photogrammetrie der ETH Zürich und Angestellter der Schweizerischen Geophysikalischen Kommission SGPK.